Understanding the mechanisms involved in *Escherichia coli* decay during wastewater treatment in High Rate Algal Ponds

A thesis presented in partial fulfilment of the requirements for the degree of

Doctor of Philosophy

in Environmental Engineering

At Massey University, Palmerston North, New Zealand

Paul Chambonnière

2019

Abstract

Little is known about the mechanisms and magnitude of pathogen disinfection in High Rate Algal Ponds (HRAPs). However, maturation ponds are used worldwide for wastewater disinfection, and pathogens can experience similar environmental conditions in maturation ponds and HRAPs. The literature suggests that pathogen removal in maturation ponds is primarily supported by sunlight-mediated mechanisms (direct DNA damage, endogenous photo-oxidation, and exogenous photo-oxidation), and a range of poorly characterized "dark" mechanisms. Based on this evidence, and knowing HRAPs are specifically designed to optimize light supply into the broth, there is reason to believe sunlight mediated disinfection mechanisms should be significant in HRAPs. This thesis therefore aimed at identifying and quantifying the mechanisms responsible for *Escherichia coli* (*E. coli*) decay in HRAPs under the hypothesis that understanding the mechanisms involved in disinfection during wastewater treatment in HRAPs can provide the scientific foundation needed to optimize the design and operation for this critical wastewater treatment service. *E. coli* was selected for being an established indicator of the removal of faecal contamination during wastewater treatment.

Two pilot scale HRAPs (0.88 m^3) were commissioned and monitored over 1-2 years, showing a mean *E. coli* decay coefficient of 11.90 d^{-1} (std = 24.05 d^{-1}, N = 128), equivalent to a mean *E. coli* log removal of 1.77 (std = 0.538, N = 128) when operated at a hydraulic retention time (HRT) of 10.3 d (std = 2.01 d, N = 139). Hourly monitoring showed high daily variations of *E. coli* log removal (up to 2.6 $\log_{10}$ amplitude) during the warmest summer days, with the lowest *E. coli* cell counts observed in the late afternoon, when the broth pH, dissolved oxygen concentration, and temperature typically reached peak values in the HRAP. No mechanisms driving *E. coli* removal in HRAP could be identified during the monitoring of pilot scale HRAPs so a mechanistic study of *E. coli* decay was performed at laboratory and bench scale to individually quantify potential mechanisms.

At laboratory scale under various conditions (e.g. darkness vs sunlight exposure, neutral pH vs alkaline pH, RO water vs filtered HRAP broth), direct DNA damage, endogenous photo-oxidation, and high-pH toxicity were identified as the main mechanisms contributing to *E. coli* decay. Exposure to potentially toxic algal metabolites and exogenous photo-oxidation were not found to be significant under the conditions tested. Natural decay (i.e. decay in conditions identified not to be detrimental to *E. coli* survival) was never significant. The impact of predation could not be investigated due to technical challenges although pilot scale observations suggested this mechanism may be significant in certain conditions.

Subsequent bench-scale tests conducted in HRAP broth indicated that temperature-dependent uncharacterized dark decay (i.e. decay in conditions not known to be detrimental to *E. coli* survival) was likely to be the dominant mechanism of *E. coli* removal under conditions relevant to full-scale operation. Temperature-dependent high-pH toxicity was confirmed to further increase *E. coli* decay at pH levels commonly reached in HRAPs. The contribution of sunlight mediated mechanisms was however not significant. Exposure to toxic algal metabolites was suspected to cause significant *E. coli* decay at times of extreme photosynthetic activity, but more research is needed to confirm this mechanism and its true significance.

Results from laboratory scale and bench scale experiments enabled the development of a model capable of predicting *E. coli* decay in HRAP broth according to pH, temperature, and sunlight intensity distribution. A model predicting HRAP broth temperature and pH according to design and weather data was also developed and validated against data from the pilot scale HRAPs monitored during this study for temperature (average absolute error of predictions 1.35°C, N = 25,906) and pH (average absolute error of predictions 0.501 pH unit, N = 23,817). Coupling the *E. coli* decay model with the environmental model enabled long term predictions of *E. coli* removal performances in HRAP for various weather conditions, design, and operational regimes. Simulations predicted that a 3-HRAPs series would sustain average yearly *E. coli* log-removal of 3.1 in Palmerston North, New Zealand when operated in conditions similar to the pilot scale HRAPs used in the present study. Such performance would deliver year round compliance with local microbial quality guidelines. Disinfection performance could be further improved by increasing the hydraulic retention time, lowering the depth, or collecting the effluent once daily in the late afternoon while letting HRAP depth fluctuate.

Overall, this research challenges the common belief that sunlight mediated disinfection mechanisms contribute the most to pathogen removal in HRAPs. Instead, uncharacterized dark decay was predicted to cause 87% of the total *E. coli* decay over one year simulation. High-pH toxicity may significantly contribute to overall *E. coli* decay in specific conditions (e.g. low depth where high-pH toxicity was predicted to account for 33% of total yearly *E. coli* decay), while sunlight mediated disinfection was limited under all simulated designs and operations (highest contribution predicted being 16% of total yearly *E. coli* decay). Because this study also confirmed the potential of HRAP to achieve sustained wastewater disinfection, further research is needed to better characterize dark decay mechanisms (for *E. coli* and other key indicators) as this knowledge has the potential to further improve HRAP design and operations for wastewater disinfection.

Acknowledgements

I would first like to thank my supervisor Professor Benoit Guieysse, for giving me the opportunity to accomplish this thesis, and for his enthusiastic guidance over the last four years. I will always remember Benoit's relentless search for improvements which I hope I can keep getting inspired from in the future. I would also like to thank Professor John Bronlund for his wise and smart supervision, always finding the right words of reassurance. Thanks to John for helping me keeping my sanity at critical times!

I would like to thank Quentin Béchet who first ignited my spark for research 6 years ago, and without whom I would probably not be writing these words today.

A big thank you goes to Maxence Plouviez, for all his help, not only in our common projects, but also for his unofficial supervision and constant encouragements; to Esther Posadas Olmos "la chica Segoviana", for all her cheerful work on the pilot scale HRAP and helping me to get my PhD on the best tracks. To Romain Lebrun, Zane Norvill, and Andrea Hom Díaz for their work on the pilot scale HRAP, to Zoe Foreman for her great contribution to my thesis through her 4th year project, to Quentin Chataigner and Natalien Carlier for their kind hand.

I would like to thank all the technicians I came to work with at Massey University, in particular John Sykes for bearing with my constant checks of the IC machine status, John Edwards for his smart hands-on solutions, Ann-Marie Jackson, Julia Good, Kylie Evans, and Haoran Wang for their help in the microlab, Anthony Wade, Morio Fukuoka, and Ian Thomas at the workshop. I also wish to thank the administrative staff, in particular Glenda Rosoman and Dilantha Punchihewa for making our lives as post-grads significantly easier.

I am infinitely grateful to the team at the Palmerston North City Council wastewater treatment plant, and I wish to thank Mike Monaghan, Mike Sahayam and their team for letting us carry out this research on their site. I wish them all the best with the coming upgrade of the wastewater treatment plant.

I wish to thank all my post-grads colleagues within our research group Maxence Plouviez, Zane Norvill, Roland Schaap, Matthew Sells, Aidan Crimp, and all the visiting interns for the good times, and I extend these acknowledgements to everyone at the SEAT that made the work environment so enjoyable. A special thank you goes to Greg Frater for his help, kindness, and wise advices on how to catch trout (which has to bring me to address my gratitude to New Zealand trouts, for their forgiveness, their wild beauty, and the wild places they pushed me to visit).

And finally, I dedicate this thesis to my family for their endless support despite the distance, to my old friends for the memorable meet-ups, to all the friendly faces I met in Palmerston North whether in hiking boots, in soccer boots, on a surfboard, or behind a drink, to Ángela: you all contributed to make my PhD a very special time in my life, and I cannot thank any of you enough for this.

TABLE OF CONTENTS

List of Illustrations

List of Tables

Introduction

Gotaas et al. (1954) first reported the possibility of using algae in wastewater treatment systems. Their rationale was to take advantage of the oxygen produced by algae to boost the growth of heterotrophic bacteria breaking down organic pollutants, which in turn provides the carbon dioxide necessary for algae growth. Algal technology was therefore thought to further enhance the traditional activated sludge system. Gotaas et al. (1954) also reported the possibility of harvesting algal biomass in order to reclaim some of the then wasted organic matter and inorganic nutrients. These preliminary results led to the development of High Rate Algal Ponds (HRAPs) in the early 1960s (Buhr and Miller, 1983) in order to combine wastewater treatment with maximal algal recovery. Since then, HRAPs have repeatedly been shown to achieve high removal of BOD, TSS, nitrogen, phosphorus, and metals (Hoffmann, 1998).

However, little is known about the disinfection potential of HRAPs treating wastewater. This is surprising as other pond technologies have consistently shown good disinfection performances (Maynard et al., 1999). Maturation ponds in particular have been developed for the purpose of disinfection, with design guidelines specified for the removal of coliform bacteria (Mara, 2005), a commonly used indicator of faecal contamination. Based on the effectiveness of maturation ponds for disinfection and the similarities in operational conditions between HRAPs and maturation ponds, we postulated that HRAPs can achieve good disinfection performances. This study aimed at verifying this assumption and at providing a deeper understanding of the mechanisms causing pathogen removal in algal ponds. By uncovering new relationships between pathogen removal and design and operational parameters (e.g. working depth, hydraulic retention time, mixing), we hypothesized that this knowledge may also provide a foundation for optimizing disinfection in HRAPs treating wastewater.

Glossary

BOD	Biochemical oxygen demand
CBS	Carbonate buffer saline solution
CFU	Colony forming unit
CI_{95}	Confidence interval at the 95% confidence level
COD	Chemical oxygen demand
DO	Dissolved oxygen
DOC	Dissolved organic carbon
DN	Dissolved nitrogen
DNA	Deoxyribonucleic acid
E. coli	*Escherichia coli*
FP	Facultative pond
HRAP	High rate algal pond
HRT	Hydraulic retention time
IC	Inorganic carbon
IN	Inorganic nitrogen
IP	Inorganic phosphorous
MP	Maturation pond
MPN	Most probable number
NIWA	National Institute of Water and Atmospheric Research
PAR	Photosynthetically active radiation
PBS	Phosphate saline buffer solution
PC	Polycarbonate
PE	Photosynthetic efficiency
PET	Polyethylene terephtalate
PNCC	Palmerston North City Council
PPCO	Polypropylene copolymer
PS	Polystryrene
RE	Removal efficiency
RNA	Ribonucleic acid
RO	Reverse osmosis
ROS	Reactive oxidative species
RPM	Rotation per minutes
RMSE	Root mean square error
sCOD	Soluble chemical oxygen demand
SRT	Solid retention time
TC	Total carbon
TKN	Total Kjeldahl nitrogen
TOC	Total organic carbon
TN	Total nitrogen
TSS	Total suspended solids
US EPA	United State Environmental Protection Agency
UV	Solar ultraviolet radiation (100 – 400 nm)
UV-A	Solar ultraviolet A radiation (320 – 400 nm)
UV-B	Solar ultraviolet B radiation (280 – 320 nm)
UV-C	Solar ultraviolet C radiation (100 – 280 nm)
VIS	Solar visible radiation (400 – 800 nm)
VSS	Volatile suspended solids
WHO	World Health Organization
WSP	Waste stabilization ponds

Chapter 1: Literature review

Motivated by the similarities in environmental conditions between High Rate Algal Ponds (HRAPs) and conventional maturation ponds (MPs), this study aims at 1) demonstrating HRAPs can achieve good wastewater disinfection, 2) improving our understanding of disinfection mechanisms in relation to HRAP design and environmental parameters, to provide solutions for optimization of HRAP operation.

With that in mind, this Chapter outlines findings from a review of the literature. A definition of disinfection for domestic wastewater relevant to the study of HRAPs is identified in section 1.1. The HRAP technology, as well as existing results of the disinfection performance of HRAPs, will be described in section 1.2. and compared with results from studies of maturation ponds. Finally, the potential disinfection mechanisms in algal ponds and their relationship to design and environmental parameters of HRAPs are reviewed in section 1.3.

1.1. PATHOGENS IN WASTEWATER

Domestic wastewater can be contaminated with a range of pathogenic organisms, originating from the guts of humans and animals. Hence the presence of pathogens in wastewater is often referred to as faecal contamination. Pathogens include organisms such as bacteria, viruses, protozoan parasites, and worm parasites (Metcalf and Eddy Inc., 2003). Examples of pathogenic organisms found in wastewater are given in Table 1 - 1. The diseases resulting from their absorption are generally minor and short-lived but in some cases, pathogenic organisms can pose a serious threat to lives of infected individuals, or result in debilitating effects on health (Ministry for the Environment, 2003). The risk of infection depends upon the pathogenic agent, the dose received, as well as the immune status of the individual absorbing the pathogen (World Health Organization, 2011). The average infectious dose depends on the pathogens, examples of which are also provided in Table 1 - 1.

Table 1 - 1: Categories of pathogenic micro-organisms encountered in domestic wastewater (Davies-Colley, 2005) presented with their effect and infective dose (Bitton, 2014; Christensen and Li, 2014)

Category of pathogen	Example of organism	Illness caused	Infectious dose[1]
Bacteria	*Salmonella spp.*	Salmonellosis	10^{4-7}
	Shigella spp.	Bacterial dysentery	10^{1-2}
	Vibrio cholera	Cholera	10^{6}
	Escherichia coli	Diarrhoea	10^{6-8}
	Campylobacter jejuni	Campylobacteriosis	~ 500
Viruses	Polioviruses	Paralysis, meningitis	1 – 10
	Enteroviruses	Meningitis, respiratory infection	
	Hepatitis A	Hepatitis	
	Norwalk types	Gastroenteritis and Dysentery	
	Rotavirus		
Protozoan parasites	*Giardia spp.*	Giardasis	1 – 10
	Cryptosporidium	Cryptosporidiosis	1 – 30
	Entamoeba spp.	Amoebic dysentery	10 – 100
Worm parasites	Tapeworms (e.g. *Taenia spp.*)	Parasitism	1 – 10
	Roundworms (e.g. *Ascaris spp.*)		
	Hookworms (e.g. *Necator americanus*)		

[1] Infectious dose as defined by Christensen and Li, (2014) in number of ingested cells

Due to the human health risks associated with pathogenic organisms, a key process in wastewater treatment is disinfection, i.e. deactivating pathogenic organisms in wastewater to provide safe effluent after treatment. In order to evaluate the efficiency of disinfection, operators need to monitor pathogenic organisms or trace any faecal contamination in the wastewater. Being often difficult to monitor, dangerous to manipulate, and only sporadically present in wastewater, pathogenic organisms are almost never measured directly. To avoid these difficulties, microbiologists monitor indicator species instead. The World Health Organization, (2011) refers to indicators as “reference pathogens” since indicators are generally groups of pathogens presenting characteristics convenient for monitoring. This study will particularly focus on faecal indicators since faecal contamination is the main concern for pathogenicity in domestic wastewater. The removal of faecal indicators is used as evidence of disinfection, avoiding the need to monitor the diversity of pathogenic species on a case-by-case basis (Ministry for the Environment, 2003). To ensure that the pathogenicity indicator monitored is efficiently assessing the pathogenicity of the wastewater and the efficiency of the disinfection treatment with no risk, an ideal indicator should satisfy the criteria summarized in Table 1 - 2[1].

[1] Adapted from Davies-Colley (2005), Ashbolt et al. (2001), and Sinclair et al. (2012)

Table 1 - 2: List of criteria for an ideal indicator

Criterion	Rationale
Ubiquitous enteric organism	Always present in faecally contaminated wastewater
Always present in the presence of enteric pathogens	So that presence of indicator warns of risk of disease
More common than the pathogen	Easier to detect and monitor
More resistant than the pathogen	Pathogen will not be present if the indicator is not detected
Does not multiply in the environment	So that contamination is not falsely detected
Easily detected by inexpensive methods	So on-going routine monitoring is affordable
Non pathogenic	No danger to laboratory personnel

In particular, an indicator displaying higher resistance than potential pathogens (Criterion 4) is critical to assess the disinfection of a process. Because of the diversity of pathogens, one indicator will have limited representativeness for some pathogens in a given process (World Health Organization, 2011). Examples of breaches to the criteria of Table 1 - 2 for commonly used indicators are presented in Appendix 1.

Despite also displaying such limitations, organisms of the coliform bacteria group, and *Escherichia coli* (*E. coli*) in particular, are commonly used to control wastewater bacterial quality and treatment efficiency. Hence, our review of 49 studies dealing with pathogen removal in algal systems or natural water systems found 27 studies dealing directly with *E. coli* decay and 20 other studies dealing with species from the coliform group. While 21 of the studies dealing with species of the coliform group also studied the decay of faecal indicators from other groups (e.g. viruses, helminths), only two studies were found to focus on species outside the coliform group (*Cryptosporidium parvum* and poliovirus respectively) without any research on species from the coliform group. This focus on the coliform group, and *E. coli* specifically, is reflected in the guidelines used to determine microbial quality of water. For example, according to the New Zealand Microbiological Water Quality Guidelines for Marine and Freshwater Recreational Areas, *E. coli* is the preferred indicator in New Zealand (Ministry for the Environment, 2003). The guidelines prescribe *E. coli* as a suitable indicator for the potential risk posed by any pathogenic bacteria, viruses, and protozoa but should not be used in the case of an outbreak alert of waterborne disease in a community. The US EPA (U.S. Environmental Protection Agency, 1987) recommends the use of different organisms to test for bacterial, viral, and protozoan contamination. Bacterial contamination is tested using *Klebsiella terrigena*, a common coliform, as an indicator, but the report still proposed *E. coli* as a good substitute.

Several proven techniques are available and routinely used for *E. coli* counting (methods used by this study are described in Chapter 2), and non-pathogenic strains of *E. coli* suitable for laboratory scale experiments were available in our facility (e.g. *E. coli* ATCC® 10536™). Being a widely-used model organism, mechanisms of *E. coli* decay can be evaluated using specific mutants of the bacteria. For instance, Fisher and Nelson (2014) used *E. coli* mutants unable to scavenge particular reactive oxidative species (ROS) in order to determine the susceptibility of *E. coli* to different ROS.

Based on these considerations, *E. coli* was selected for this study as indicator for studying pathogen decay in HRAPs.

1.2. WASTEWATER DISINFECTION IN ALGAE-BASED WASTEWATER TREATMENT TECHNOLOGIES

This section describes the design of various algae-based wastewater technologies and the environmental conditions prevailing in these systems. The disinfection efficiency achieved in these systems is then reviewed, analysing available data for HRAPs in the light of the disinfection performances of MPs.

1.2.1. BIOLOGY AND ENVIRONMENTAL CONDITIONS OCCURRING IN ALGAL PONDS TREATING WASTEWATER

Algal ponds are a complex broth in which both algal and bacterial activities drive numerous mechanisms involved in the treatment of wastewater (Pearson, 2005). These mechanisms, by which wastewater treatment is achieved, are discussed in the following and summarized in Figure 1 - 1.

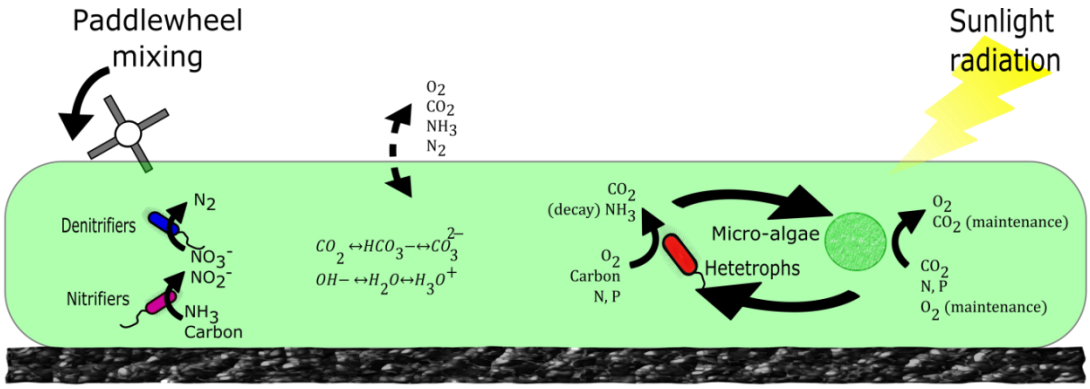

Figure 1 - 1: Summary of the main biological, chemical, and physical processes driving HRAP environmental conditions

1.2.1.1. Algal activity

Phototrophic organisms such as micro-algae grow through photosynthesis, a biological process during which microorganisms convert sunlight energy to produce biomass from carbon dioxide and available nutrients. The growth process of phototrophs is summarized by Equation 1 - 1.

$$Cells + Light + CO_2 + Nutrients \rightarrow New\ cells + O_2 \quad (1 - 1)$$

Oppositely, phototrophic biomass gradually decays in a process similar to heterotrophic biomass decay and described by Equation 1 - 3.

1.2.1.2. Heterotrophic bacterial activity

Aerobic heterotrophic bacteria grow by deriving energy from organic substrate using O_2 as electron donor. The organic substrate is also used as the carbon source for the synthesis of new cells (Metcalf and Eddy Inc., 2003). Aerobic heterotrophic biomass growth can be summarized by Equation 1 - 2.

$$Heterotrophs + O_2 + Organic\ matter + Inorganic\ Nutrients \rightarrow New\ cells + CO_2 \quad (1 - 2)$$

A fraction of the aerobic heterotrophic biomass also decays, a process in which O_2 is consumed and CO_2 is produced as summarized by Equation 1 - 3.

$$Cells + O_2 \rightarrow CO_2 + Inorganic\ Nutrients \quad (1 - 3)$$

1.2.1.3. Dissolved oxygen and pH in algal ponds

As shown by Equation 1 - 1, intense photosynthetic activity during the day may lead to high levels of dissolved oxygen (DO), despite the counter-effects of heterotrophic bacterial growth, and algal and bacterial decay. Concentrations consistently above 20 mg $O_2.L^{-1}$ have thus been reported in HRAPs (Craggs et al., 2004; García et al., 2006; Park et al., 2011; Paterson and Curtis, 2005; Pearson, 2005). Conversely, due to both bacterial activity and algae respiration during the night in the absence of photosynthetic activity, DO levels can drop as low as 0.0 mg of $O_2.L^{-1}$ by the end of a night (García et al., 2006).

In parallel, the consumption of CO_2 through phototrophic growth forces the consumption of H^+ by the action of the carbonate system equilibrium (Equation 1 - 4) which raises the pH significantly.

$$CO_2 + H_2O \leftrightarrow H_2CO_3^* \leftrightarrow HCO_3^- + H^+$$
$$HCO_3^- \leftrightarrow CO_3^{2-} + H^+ \quad (1 - 4)$$

Hence, pHs above 10 were reported in HRAPs by Craggs et al. (2012). Such high pHs are reached despite the moderation from heterotrophic bacterial growth, and algal and bacterial decay, which all release carbon dioxide in the broth thus lowering the pH.

For both pH and DO concentration, effects may be moderated by aeration of the liquid broth due to the absorption/desorption of O_2 and CO_2 respectively from the atmosphere. Aeration occurs naturally at the air-water interface and depends largely on the pond design as well as the presence of an aeration system (e.g. bubbling, paddlewheel). While CO_2 bubbling was reported to lower both pH and DO concentration of the algal broth (Ruas et al., 2017), there has been no investigation on how the paddlewheel speed effects these parameters in HRAPs.

1.2.1.4. Nitrogen removal

Nitrogen is present in domestic wastewater, mostly as a component of organic pollutants, but also in the form of free ammonia in significant concentrations (12 – 45 $mg.L^{-1}$, Metcalf and Eddy Inc. 2003). As a result, nitrification/denitrification is known to occur in algal ponds (Pearson, 2005): these biological mechanism sequentially convert ammonium into nitrite and nitrate, then reduce nitrate (or nitrite) into N_2 which can escape by volatilisation. Nitrogen is also known to volatilize in the form of ammonia gas (Pearson, 2005). Because ammonia formation is favoured by very high pH, this process is likely to be significant in HRAPs. Gas volatilization may be more significant in HRAPs than MPs due to the paddlewheel mixing.

Finally, some nitrogen is assimilated by biomass growing in algal ponds as shown by Equations 1 - 1 and 1 - 2.

1.2.1.5. Algal ponds ecology

Algal species in HRAPs were reported to differ from the species typically found in MPs because non-motile species, which are disadvantaged for light acquisition in maturation or facultative ponds, are competitive in HRAPs (Pearson, 2005). Hence, *Chlorella* and *Scenedesmus* species were found to dominate HRAPs (Hoffmann, 1998). The same author pointed out a relatively low diversity of algae species in HRAPs ($\leq$ 12 genera on a year cycle).

More recently, a two-year study of small scale HRAPs found seasonal variations in the dominance of 5 different species in the algal broth (e.g. domination from *Pediastrum* in the winter months) and a potential change of dominance due to species blooming in the influent over extended periods of time (Cho et al., 2017). The same study also suspected that predatory pressure from protozoa (e.g. *giardia*) influenced algal diversity. In any case, it was

concluded that algal diversity facilitated stable biomass productivity in HRAPs against variation in HRAP conditions.

While little research has been dedicated to algal species in algal ponds, even less is known of bacteria species inhabiting such systems. Results from Cho et al. (2017) indicated a share of bacterial biomass below 10% of the total biomass (algal + bacterial), falling regularly below 1% in pilot scale HRAPs (100L).

1.2.1.6. Other mechanisms influencing water quality in algal ponds

As for nitrogen, phosphorous removal is known to occur in algal ponds through biomass assimilation, but also through precipitation with chemicals in water e.g. calcium (Pearson, 2005).

Numerous biological and physical phenomena take place in algal ponds, some with detrimental impact on the global performance of ponds: for instance, algae can release compounds inhibiting bacterial activity (Muñoz and Guieysse, 2006), and algal growth can also be limited by the presence of grazing micro- and macro- organisms (Hoffmann, 1998). Seasonal and diurnal variations in biological and environmental parameters are expected in HRAPs because the biological, physical, and chemical mechanisms described above are dependent on meteorological variables, (e.g. sunlight intensity).

Because all the mechanisms described in this section are interrelated and affect the efficiency of pathogen removal in algal ponds, the study of wastewater disinfection using HRAPs as intended in this work should ideally study all aspects of the behaviour of HRAPs[2] and how they relate to disinfection.

1.2.2. COMPARISON OF HRAPS AND MATURATION PONDS CHARACTERISTICS

In this section, the maturation pond and HRAP technologies are presented. The physical and environmental characteristics of both are summarized in Table 1 - 3.

1.2.2.1. Maturation ponds

Maturation ponds (MPs) are ponds operated with depths[3] around 1–1.5 m with no mechanically-induced mixing, and typically fed with secondary effluents poor in organic material. Due to this low input of organic pollutants, no anaerobic zones are expected and

[2] i.e. environmental conditions in the algal broth, water quality in terms of secondary wastewater treatment, and ecology of the pond.
[3] There is currently a trend to design MPs of depth as shallow as 0.4 m (Dias and Von Sperling, 2017)

MPs typically operate fully aerobically. MPs are used as a polishing step before the release of wastewater into receiving water and are primarily designed for disinfection (Shilton and Walmsley, 2005). Marais (1974) proposed the design of MPs based on coliform removal assuming coliform decay follows a first order decay coefficient, and assuming a steady state and well mixed pond (Equation 1 - 5).

$$N_e = \frac{N_i}{1 + k_B.\theta} \quad (1 - 5)$$

In Equation 1 - 5, N_e is the concentration of total coliforms in the effluent, N_i is the concentration of total coliforms in the influent, k_B is the first order decay coefficient (d^{-1}) given by Equation 1 - 6 as developed by Marais (1974), and θ is the MP hydraulic retention time (HRT).

$$k_B = 2.6 \cdot 1.19^{T-20} \quad (1 - 6)$$

In Equation 1 - 6, T is the pond temperature in °C.

The design HRT can be easily calculated from Equations 1 - 5 and 1 - 6, and is based on the requirements of effluent quality with regards to the total coliform concentration. MPs are often designed as series of smaller ponds or as one single baffled pond to avoid short circuiting favoured by the lack of mechanical mixing.

MPs are designed with variable HRTs (generally 5 – 15 days although Von Sperling (1999) reported ponds with HRTs over 100 days). These ponds have been repeatedly shown to achieve good disinfection performances as displayed in Table 1 - 4 although they are known for delivering inconsistent effluent quality (Craggs et al. 2012; Hickey et al. 1989).

MPs experience diurnal variations in their physico-chemical characteristics due to algal activity. pH, for example, is known to reach levels as high as 10 during the day (cf. Table 1 - 3).

1.2.2.2. High Rate Algal Ponds

The HRAP technology was developed in California 50 years ago (Gotaas et al., 1954) and is based on the use of shallow (0.1 – 0.5 m depth) raceways mixed by one or several paddlewheels (Buhr and Miller, 1983) which enhances the efficiency of sunlight use by algal cells. HRAPs are operated at lower HRT than MPs, typically 1–14 days, minimizing biomass loss by decay. Due to the mixing and shallower depth, HRAPs are characterized by higher algal densities than MPs.

The intense algal activity has many effects on the behaviour of HRAPs despite the general overall process being the same as MPs. For instance, the physical and chemical conditions of

HRAPs are similar to MPs but were found to present more extreme diurnal variations: pH as high as 11 and DO concentration as high as 30 $mg.L^{-1}$ or below 2 $mg.L^{-1}$ were reported (see Table 1 - 3).

HRAP ecology differs from that of conventional algal ponds, as flagellate species lose their edge in HRAPs due to mixing. Non-motile species are thus known to develop large colonies in these systems (Pearson, 2005).

Finally, HRAPs are often supplied with CO_2 used to prevent carbon limitation and improve algal productivity (Park et al., 2011), as well as to mitigate high values of pH, which are known to inhibit algal growth (Craggs et al., 2012).

Table 1 - 3: General characteristics of maturation ponds versus HRAPs adapted from Norvill et al. (2016)

Parameter	Maturation Pond	High Rate Algal Pond (HRAP)
Depth	1-1.5 m	0.1-0.5 m
HRT	3-15 days	1-14 days
SRT	3-15[2] days	1-28 days
Biomass conc. (VSS)	0.03-0.07 $g.L^{-1}$	0.1-0.3 $g.L^{-1}$
Typical microbiology type present[1]	Phototrophs; Aerobic chemotrophs	Phototrophs; Aerobic chemotrophs
pH	6.5 – 10.6 with diurnal fluctuation	7 – 11 with diurnal fluctuation or controlled at 7 – 8
Dissolved Oxygen (DO)	Fully aerobic to supersaturated during daytime (>15 $mg.L^{-1}$ DO possible). Pond may be anoxic at night.	Aerobic to supersaturated during daytime (>30 $mg.L^{-1}$ possible). Pond may be anoxic at night.
BOD loading	NA (not designed for BOD removal)	Up to 35 $g\ m^{-2}\ d^{-1}$ (Up to 0.12 $kg\ m^{-3}\ d^{-1}$ for a 0.3 m deep pond)
Mixing/ Aeration	Inlet momentum; Wind	Paddlewheel; May include CO_2 addition
References	Archer and Mara (2003); Craggs et al. (2003); Moreira et al. (2009); Sheludchenko et al. (2016)	Craggs et al. (2003); El Hamouri et al. (2003); Craggs et al., 2012); Muñoz and Guieysse (2006); Park et al. (2013); Posadas et al. (2015)

[1] Phototrophs use light as an energy source, chemotrophs use organic carbon as an energy source;

1.2.3. COMPARISON OF DISINFECTION PERFORMANCES ACHIEVED BY MATURATION PONDS AND HRAPS

1.2.3.1. Disinfection performance of maturation ponds

Because maturation ponds are directly designed for wastewater disinfection, a lot of research has been performed to determine the disinfection performance of these systems. Examples of removal efficiencies of pathogen indicators from the coliform group are given in Table 1 - 4.

When possible, first order decay coefficients associated were provided calculated as $\frac{1}{HRT} \cdot \left(\frac{C_{IN}}{C_{OUT}} - 1\right)$. This expression is derived from Equation 1 - 5 assuming a well-mixed steady state, unless stated otherwise. While the well-mixed assumption was verified in our pilot scale HRAPs (see Appendix 2), a dispersed flow model should be preferred for maturation ponds (Von Sperling, 2005) and large scale HRAPs. As a consequence, decay coefficients reported in Table 1 - 4 are likely to be overestimated (Von Sperling, 1999).

As shown in Table 1 - 4, efficient removal of pathogen indicators can be achieved using MPs. For example, Papadopoulos et al. (2014) reported removal efficiencies (RE) for *E. coli* above 99.99%. Due to the long retention time needed to reach such RE, the decay coefficients reported being all below 0.77 d^{-1}.

Table 1 - 4 also illustrates the poor consistency of disinfection performance reported in MPs. The lowest removal efficiency reported is 51.5% (Moeller and Calkins, 1980), while values under the 90% mark (i.e. 1 log-removal) were frequently found.

Table 1 - 4: Maturation pond coliform removal performances reported in the literature

References	Type of pond	Organisms studied	Position / Number of ponds in the series	First order coefficients (d^{-1})	Removal efficiency (%)[1]
Huang et al. (2017)[2,3]	MP	*E. coli*	1/1	$1.4x10^{-4}$ – $5.6x10^{-3}$	92.1 – 99.9
Dahl et al. (2017)[4,5]	MP	*E. coli*	1/1	0.21 – 3.8	99.2
(Buchanan, 2014)	MP	*E. coli*	1/3	3.87	99.1
			2/3	1.99	95.0
			3/3	0.28	71.2
Papadopoulos et al. (2014)[5]	MPs (Algal ponds)	*E. coli*	3 (considered as one system)	0.03 – 0.29	99.4 – 99.99
	MPs (Duckweed pond)			0.06 – 0.22	99.4 – 99.7
Ansa et al. (2012a)[4]	MP - Top layer	Faecal coliforms	1/4	3.3	94.3
			2/4	7.2	97.3
			3/4	7.4	97.4
			4/4	1.7	89.5
	MP – midpoint		1/4	6.0	96.8
			2/4	9.2	97.9
			3/4	4.8	96.0
			4/4	2.1	91.3
	MP Bottom		1/4	1.8	90.0
			2/4	0.9	81.8
			3/4	2.4	92.3
			4/4	0.5	71.4
Moreira et al. (2009)[5]	Secondary FP – deep	Faecal coliforms	1/4	0.056	81.48
	Primary MP – deep		2/4	0.038	81.60
	Secondary MP – deep		3/4	0.025	76.09
	Tertiary MP – deep		3/4	0.027	86.36
García et al. (2008)	MP (pilot scale)	Total coliforms	1/1	4.0 – 144	99.87 – 99.96
		Faecal coliforms		4.9 - 228	99.00 – 99.98
Reinoso et al. (2008)	FP	Total coliforms	1/1	0.074	84.82
		E. coli		0.40	96.81
Fernandez et al. (1992)	MP	Total coliforms	1/4	0.09	39.3
			2/4	0.25	50.3
			3/4	0.13	18.1
			4/4	1.15	66.7
		Faecal coliforms	1/4	0.03	18.1
			2/4	0.12	33.0
			3/4	0.60	50.3
			4/4	1.15	66.7
Polprasert et al. (1983)	MP (pilot scale)	Total coliforms	2 (considered as one system)	0.45 – 56.3	77.14 – 99.86
		Faecal coliforms		1.25 - 104	80.00 – 99.85
Moeller & Calkins (1980)	MP	Total coliforms	1/4	–	51.5
			2/4		70.0
			3/4		67.2
			4/4		66.7
		Faecal coliforms	1/4	–	56.3
			2/4		77.4
			3/4		69.3
			4/4		62.94

[1] Calculated as $\frac{C_{IN}-C_{OUT}}{C_{IN}} \cdot 100$;

[2] Arctic ponds;

[3] The decay coefficient provided is calculated as $\frac{\ln\left(\frac{C_{Initial}}{C_{end}}\right)}{t_{end}-t_{initial}}$ i.e. first order decay coefficient assuming a batch reactor behaviour;

[4] Found by fitting a first order decay coefficient model to field data;

[5] Decay coefficient calculated using dispersed model as performed by the authors

1.2.3.2. Disinfection performance of HRAPs

HRAPs are not initially intended for disinfection and therefore only a few studies have reported evaluation of disinfection performance for this technology. All the published data currently available on HRAP disinfection performances to the best of our knowledge are gathered in Table 1 - 5.

As expected at the start of this study from the similar environmental conditions between MPs and HRAPs (cf. Table 1 - 3), high efficiencies for removal of pathogen indicators were consistently reported in the literature.

While poor removal efficiencies in MPs were reported in some instances, REs above 90% were reported by every author for all types of indicators investigated except *Aeromonas spp*. REs above 99% (2 log-removal) are not rare.

Table 1 - 5: HRAP disinfection performances reported in the literature

References	Organisms studied	Disinfection coefficient (d^{-1})[1]	Removal efficiency (%)[2]
Fallowfield et al. (2018)	*E. coli*	9.34	97.6
	F-RNA bacteriophage	35.4[3]	99.4
	Aerobic spore forming bacteria	0.09	28.7
Ruas et al. (2017)	*E. coli*	99.8	99.8
	Total coliforms	33.1	99.4
	Enterococci	14.1	98.6
	Pseudomonas aeruginosa	49.8	99.6
Young et al. (2016)	*E. coli*	26.8	99.3
	F-RNA bacteriophage	7.6	97.4
Buchanan (2014)	*E. coli*	4.60 – 22.0	97.0 – 99.3
Craggs et al. (2012)	*E. coli*	5.7 – 38.0	98.0 – 99.7
El Hamouri (2009)	Faecal coliforms	3.05	93.8
García et al. (2008)	Total coliforms	16.9 – 23.3	94.1 – 99.4
	Faecal coliforms	4.7 – 22.3	97.9 – 99.6
	Faecal streptococci	4.58 – 4.91	97.9 – 98.0
	Staphylococci	1.45 – 1.60	93.5 – 94.1
	Clostridium perfringens	3.14 – 4.37	96.9 – 97.8
Araki et al. (2001)	*Cryptosporidium parvum*	4.90 – 11.2	97.1 – 98.0
Bahlaoui et al. (1998)	Faecal coliforms	7.76	98.4
	Faecal Streptococci	9.80	98.7
	Aeromonas spp.	1.13	90.0
Bahlaoui et al. (1997)	Total coliforms	0.234 – 3.91	58.6 – 96.9
	Faecal coliforms	0.306 – 13.8	64.1 – 99.1
	Faecal streptococci	0.829 – 17.7	78.9 – 99.3
Fallowfield et al. (1996)	*E. coli*	0.35 – 2.34	NA

[1] Calculated as $\frac{1}{HRT} \cdot \left(\frac{C_{IN}}{C_{OUT}} - 1\right)$ derived from Equation 1 - 5 i.e. assuming a well-mixed steady state;

[2] Calculated as $\frac{C_{IN} - C_{OUT}}{C_{IN}} \cdot 100$ (expressed as a percentage of removal);

[3] A second HRAP following the first described in this table had an average disinfection rate for F-RNA bacteriophage of 0.65 d^{-1} (76.6 % RE)

The context in which data of HRAP disinfection performances were collected for each study in Table 1 - 5 was investigated and is reported in Table 1 - 6. Most of these results originate from prospective and relatively short term studies at pilot scale, or not primarily dedicated to wastewater disinfection. Only the data reported from Young et al., (2016) was derived from experiments performed at large scale, over a long term period and primarily dedicated to disinfection.

Table 1 - 6: Characteristics of the studies presented in Table 1 - 5

References	HRAP surface	Number of samples tested	Duration of the study	Study dedicated to wastewater disinfection	Outdoor	Type of wastewater
Fallowfield et al. (2018)	200 m^2	40	3 months	Yes	Yes	Domestic wastewater
Ruas et al. (2017)	1.2 m^2	8	25 days (x2)	Yes	No (greenhouse)	Domestic wastewater
Young et al., (2016)	200 m^2	62	10 months	Yes	Yes	Domestic wastewater
Buchanan (2014)	200 m^2	> 200	2 years	No	Yes	Septic tank effluent / facultative pond effluent
Craggs et al. (2012)	5 ha	Unknown	15 months	No	Yes	Primary settled wastewater
El Hamouri (2009)	790 m^2	Unknown	Unknown	No	Yes	Domestic wastewater post upflow anaerobic reactor
García et al. (2008)	1.54 m^2	Unknown	2 years	Yes	Yes	Primary settled domestic wastewater
Araki et al. (2001)	1.54 m^2	2	10 days	Yes	Yes	Urban wastewater
Bahlaoui et al. (1998)	48.2 m^2	Unknown	2 years	Yes	Yes	Post primary pond wastewater
Bahlaoui et al. (1997)	48.2 m^2	105	2 years	Yes	Yes	Post primary pond wastewater
Fallowfield et al. (1996)	13.1 m^2	33	4 days batch	Yes	Yes	Synthetic medium + *E. coli* suspension

The good disinfection performances reported in the literature, despite the lack of dedicated studies, confirmed the rationale of the present study that HRAPs are a viable alternative to achieve wastewater disinfection.

1.3. MECHANISMS LEADING TO MICROBIAL DEATH IN HRAPS

Little knowledge is available on the mechanisms causing microbial death in algal ponds. Identifying the disinfection mechanisms would help to:

1. better understand how the disinfection performances given in Table 1 - 4 and Table 1 - 5 could be reached in algal ponds,
2. relate decay coefficients with process and environmental parameters thus enabling optimization of the disinfection process in HRAPs,

Potential pathways of microbial death are presented in section 1.3.1. The mechanisms identified as relevant in algal ponds by the literature are then reviewed (section 1.3.2.) before finishing with the dependence of such mechanisms on environmental and process parameters (section 1.3.3.).

1.3.1. MECHANISMS OF MICROBIAL DEATH

Park Talaro (2008) defined the death of a single-cell organism as the loss of its ability to multiply. This raises the question of the "viable but non-culturable state" discussed in the literature when cells that do not multiply in laboratory can be reactivated under certain conditions. This issue is not addressed in this study and microbial death will be assumed when *E. coli* is not detected through the counting method used (see Chapter 2).

Antimicrobial agents have a range of cellular targets. Non-selective agents have a wide range of action while selective agents only target one cellular component and only affect a narrow range of microbes. Examples of cellular targets include (Park Talaro, 2008):

- The cell wall
- The cell membrane
- Cellular synthetic processes (i.e. alteration of proteins and nucleic acid synthesis)
- Proteins (i.e. alteration of protein functions)

The mechanisms possibly affecting each cellular target and their consequences are shown in Table 1 - 7.

Table 1 - 7: Cell-level mechanisms leading to death of microbial pathogenic organisms

Target	Mechanism	Consequences	Example
Cell wall	• Block synthesis • Digest • Break down	• Cell lysis	• Penicillin • Detergents • Alcohols
Cell membrane	• Break the selective permeability mechanisms	• Loss of vital chemicals • Entry of damaging chemicals	• Surfactants
Cellular synthetic process	• Inhibit protein formation • Inhibit the replication of nucleic acid • Change the genetic code of nucleic acids	• Lack of proteins required for growth and metabolism • No or wrong replication of DNA meaning no possibility for transcription in growing cells	• High frequency electromagnetic waves (UV, X-ray, gamma radiation) • Formaldehyde
Proteins	• Break the bonds maintaining the structure of proteins	• Denature vital proteins	• Moist heat • Strong organic solvents • Phenolics

1.3.2. MECHANISMS OF PATHOGEN DECAY IN ALGAL PONDS

Research on disinfection in algal ponds has focused on linking measurable parameters (e.g. sunlight, temperature) with disinfection performance. Such results provided design guidelines at given climatic conditions. While many studies give numerical relationships between decay rates of indicators and process/environmental parameters, studies dedicated to the mechanisms behind these relationships have only emerged recently.

Following Davies-Colley et al. (1999) who identified three sunlight-mediated mechanisms leading to pathogen death (as presented in 1.3.2.1.), most of the research focused on sunlight-mediated mechanisms while research on non-sunlight-mediated mechanisms remained marginal (such mechanisms will be referred to as “dark mechanisms” in the following).

1.3.2.1. Sunlight-mediated mechanisms

Direct damage

Many studies have evidenced strong positive correlation between the decay rates of indicator pathogens and sunlight intensity (Ansa et al., 2008; Benchokroun et al., 2003; Canale et al., 1993; Curtis et al., 1992; Davies-Colley et al., 1994; Davies-Colley et al., 1999; Maïga et al., 2009a; Maraccini et al., 2016a; Maraccini et al., 2016b; Mayo, 1995; Moreira et al., 2009; Nguyen et al., 2015; Schultz-Fademrecht et al., 2008; Silverman and Nelson, 2016; Sinton et

al., 2002; Xu et al., 2002). UV radiations such as UV-C and UV-B are known to kill bacteria by damaging the DNA of the cell (Maynard et al., 1999). The relevance of UV-C action can be dismissed given the near absence of UV-C radiation reaching the Earth surface (U.S. Environmental Protection Agency, 2010).

The killing effect of UV-B on indicator organisms has been demonstrated repeatedly (Curtis et al., 1992; Maraccini et al., 2016b; Maraccini et al., 2016a; Ouali et al., 2015; Silverman and Nelson, 2016; Sinton et al., 2002). Curtis et al. (1992) found that, when exposing indicator bacteria to sunlight radiation, the shorter the wavelength, the higher the bacterial decay. Several studies reported significant dark regrowth following exposure to low light radiation but little to no regrowth following high irradiance, suggesting DNA damage can be repaired following low-dose exposures (Davies-Colley et al., 1999; Schultz-Fademrecht et al., 2008; Zhang et al., 2015). However, UV-B intensity is low at the Earth surface and is rapidly attenuated in algal ponds (Maïga et al., 2009b). UV-Bs role in algal pond disinfection may therefore be limited. It was also found that wild strains of bacteria such as *E. coli* and enterococci have a better resistance to UV-Bs than lab cultured bacteria (Fisher and Nelson, 2014; Silverman and Nelson, 2016). Indeed, lab cultured bacteria may have lost resistance to sunlight as there was no incentive to keep this trait in successive lab cultured generations.

All these results indicate that direct damage by sunlight is likely to be of limited significance for disinfection in HRAPs. Nevertheless, other sunlight-mediated mechanisms have been discussed in the literature.

Evidence for sunlight-mediated disinfection from indirect damage

Davies-Colley et al. (1994) found that the decay rates of faecal coliforms and enterococci were dependent on pond depth and correlated to 360 nm light radiation attenuation (UV-A), indicating a lower impact of UV-B than UV-A. Visible light radiation (VIS) was also found to inactivate bacteria by Curtis et al. (1992), who reported a clear killing effect on faecal coliforms with wavelengths up to 700 nm. Similarly, Dias and Sperling (2017) found significant sunlight-dependent decay rates of *E. coli* in maturation ponds, even at a depth of 0.8 m, where only visible radiation is expected to be present. Yet UV-A and VIS are not known to directly damage cells, suggesting their contribution involves indirect photo-damage mechanisms. Furthermore, while direct DNA damage from sunlight should only depend on sunlight intensity, the influence of other parameters on sunlight-induced death rates of faecal indicators has been frequently reported.

The impact of light on pathogen removal was shown to be strongly enhanced by pH, with studies repeatedly showing a positive correlation between decay rates and pH when

pathogens are exposed to sunlight (Ansa et al., 2008; Curtis et al., 1992; Davies-Colley et al., 1999; Maynard et al., 1999; Moreira et al., 2009). The combined effect of light and pH was found to depend on the wavelength: Curtis et al. (1992) found an impact on the decay rate of pathogens for wavelengths above 500 nm only at high pH.

The impact of light on pathogen removal was also found to be enhanced with increasing dissolved oxygen concentration (Ansa et al., 2008; Curtis et al., 1992; Davies-Colley et al., 1999; Khaengraeng and Reed, 2005; Maynard et al., 1999; Muela et al., 2002) while no decay was reported in low dissolved oxygen conditions despite sunlight exposure (Benchokroun et al., 2003; Curtis et al., 1992).

Finally, the levels of potential photosensitizers such as humic acids have been repeatedly shown to negatively impact on the survival of pathogens (Benchokroun et al., 2003; Curtis et al., 1992; Davies-Colley et al., 1999; Fisher et al., 2012; Maraccini et al., 2016c; Maraccini et al., 2016a). Likewise, adding oxidative-specie scavengers has been shown to lower decay rates under exposure to sunlight (Benchokroun et al., 2003; Khaengraeng and Reed, 2005). Fisher and Nelson (2014) even proposed a Fenton-like process for pathogen light-induced decay, showing that iron could act as a powerful photosensitizer at the intracellular level.

All these results strongly suggest that disinfection in algal ponds is largely dependent on indirect photo-oxidation processes.

Proposed mechanisms

Following Curtis et al. (1992), who hypothesized the existence of endogenous and exogenous sensitizers involved in the generation of reactive oxidative species (ROS), Davies-Colley et al. (1999) identified three mechanisms of solar-induced decay as detailed below:

- Mechanism 1: direct absorption of solar UV-B by DNA resulting in DNA damage. All organisms can be affected although, at low dose, bacteria are able to repair the damaged DNA.
- Mechanism 2: photo-oxidation of key cellular biomolecules by reactive oxygen species (ROS) generated by endogenous photosensitizers (i.e. photosensitizers existing within the organism) reacting with UV light. Internal targets, notably DNA, can thus be damaged by the activated species. This mechanism is mainly caused by solar UV-B, as light absorption by potential endogenous photosensitizers is only significant for the shortest wavelength, but UV-A radiations may be involved in this mechanism. High DO concentration would favour this mechanism as O_2 molecules may become a powerful oxidiser when activated by sunlight.

- Mechanism 3: photo-oxidation of key cellular biomolecules by ROS generated by exogenous photosensitizers. Humic substances are notorious photosensitizers, which absorb a wide wavelength range (the efficiency of energy transfer increases when wavelength decreases). Exogenous ROS damage the external structures of microorganisms (e.g. cell membrane). High DO concentration would favour this mechanism, as O_2 molecules may become a powerful oxidiser when activated by sunlight. High pH would also favour this mechanism as damaged membranes would become more sensitive to unfavourable conditions.

These mechanisms have been widely accepted and relayed in the more recent literature (Benchokroun et al., 2003; Boehm et al., 2009; Dias and Von Sperling, 2018; Fisher et al., 2012; Maraccini et al., 2016c; Maraccini et al., 2016b; Maraccini et al., 2016a; Muela et al., 2002; Nguyen et al., 2015; Ouali et al., 2015; Sinton et al., 2002; Young et al., 2016).

The sunlight mechanisms identified and their relevance to the present study are summarized in Table 1 - 8.

Table 1 - 8: Sunlight-mediated mechanisms inducing *E. coli* decay in algal ponds

Mechanism	Mechanism description	Potential relevance
Direct UV-B damage	UV-B radiation can damage DNA, thereby suppressing the pathogens ability to replicate (UV-C is negligible at the Earth surface and their impact was dismissed).	UV-B represents 0.15% of the solar light intensity reaching the Earth surface and is rapidly absorbed in ponds (Davies-Colley et al., 1994). UV-B irradiance in HRAPs is therefore significant only to very shallow depths. However, due to the mixing conditions of HRAPs, every *E. coli* cell may experience significant UV-B exposure so that this mechanism cannot be disregarded at this stage and its precise impact in HRAPs should be assessed.
Endogenous photo-oxidative damage	The absorption of UV radiation (mainly UV-B) by bacterial cellular constituents can result in the formation of ROS with high oxidative potential. These ROS can oxidize cell constituents and cause death of bacteria.	This mechanism was shown to be significant for *E. coli* in WSPs (Davies-Colley et al., 1999). As in the case of direct UV-B damage, the radiation involved should only affect a minor volume of the HRAP but the mixing conditions of HRAPs require the precise quantification of this mechanism's relevance.
Exogenous photo-oxidative damage	UV-A and B, as well as certain visible wavelengths, can be absorbed by photosensitizers present outside bacterial cells. This may result in the formation of ROS capable of damaging cell constituents and causing death of bacteria.	This mechanism is frequently suggested to be highly significant in maturation ponds given the involvement of longer wavelengths in the UV and even in the visible part of sunlight spectrum (Benchokroun et al., 2003; Davies-Colley et al., 1999; Ouali et al., 2015). However, gram-negative bacteria (e.g. *E. coli*, *Campylobacter jejuni*) were reported to show strong resistance to this mechanism (Maraccini et al., 2016c).

1.3.2.2. Dark mechanisms

While few targeted studies have been reported, a wide range of potential dark mechanisms have been proposed in the literature. These suspected mechanisms are detailed in the following, and summarized in Table 1 - 9.

Competition with biomass

HRAPs are a complex environment where diverse microbial communities are coexisting. The survival of indicators is therefore expected to be affected by competition for nutrients (Ansa et al., 2008; Barcina et al., 1997; Decamp and Warren, 1998).

Mayo and Noike (1996) cultured a mix of heterotrophic bacteria and *Chlorella vulgaris* in batch reactors and found unexpectedly low bacteria density at 30°C. This suggested that, due to the rapid algal growth at such temperatures, bacteria may have had to compete against *Chlorella vulgaris* for glucose. Both Maynard et al. (1999) and Moreira et al. (2009) also reported that coliforms were outcompeted by other bacteria.

However, other studies did not show BOD loading was affecting coliform survival (Maynard et al., 1999; Mayo, 1995; Xu et al., 2002) suggesting that nutrient availability is unlikely to be a factor in indicator survival in algal ponds. Nevertheless, few studies have been carried out on this phenomenon (Maynard et al., 1999) and no quantitative data was found to assess the potential relevance of this mechanism.

Predation

Although little research has been carried out to specifically assess the quantitative impact of predation on pathogen removal, the literature provides evidence that it may be an important mechanism (Ansa et al., 2012b; Decamp and Warren, 1998; Nørgaard and Roslev, 2016).

The presence of ciliates was cited as a dominant factor for bacterial decay in aerobic wastewater treatment by Decamp and Warren (1998), who also suggested that a variety of *in situ* parameters could affect the grazing ability of ciliates. Ansa et al. (2012a) found a strong positive correlation between faecal coliform counts and ostracod numbers at the surface of duckweed ponds where algae are scarce (such a relationship was not found in algal ponds) indicating that the main source of energy for ostracods was bacteria instead of algae. In general, a predator-prey pattern between faecal coliforms and ostracods was evidenced in this study. John and Rose, (2005) measured higher *E. coli* decay in soils when native bacteria were present than when native bacteria were absent. Adding nutrients reduced *E. coli* decay and this effect was linked to attenuated or inhibited predation from native bacteria.

The possibility of an influence of potential predators on pathogen decay rate in HRAPs is obvious in the light of the literature. However, predicting predation in algal ponds is challenging. Algae may protect bacteria from predators by attachment (see below), however the predation of faecal indicators may be enhanced if the algae-protecting pathogens are themselves grazed (Ansa et al., 2012b).

To conclude, predation is likely to be a significant mechanism of pathogen removal in algal ponds but quantifying the impact of this poorly studied mechanism is challenging.

Toxicity

Algal toxicity

The generation of algal toxins harmful to bacteria was suggested as early as 1964 (Maynard et al., 1999). Cyanobacteria were reported to be toxic to *E. coli*, and *Chlorella spp.* was suspected to be toxic to *Vibrio cholerae* (Mezrioui et al., 1994). But while repeatedly mentioned in literature (Ansa et al., 2008; Auer and Niehaus, 1993; Mayo and Noike, 1996; Moreira et al., 2009; Xu et al., 2002), the impact of algal toxicity on pathogens has never been investigated to the best of our knowledge.

Chemical toxicity

It is likely that some of the chemicals present in algal ponds are toxic to indicators of faecal contamination (Barcina et al., 1997; Decamp and Warren, 1998).

Ammonia is a known antiseptic, likely to occur in HRAP effluents, that has been proposed as a potent toxicant (Maynard et al., 1999) although Davies-Colley et al. (1999) reported no effect. To the best of our knowledge, no work has been conducted to extensively identify and study such removal mechanisms in algal ponds. In the literature from other fields, Deal et al. (1975) reported a toxic effect of ammonia on *E. coli* at high concentrations (0.1 M) and high pH (9.5), although it was unclear if the heightened decay rate of *E. coli* was related to the effect of ammonia or the effect of pH. Conversely, Müller et al. (2006) found *E. coli* to be highly resistant to ammonium. They too noticed an impaired growth at high concentration, which they attributed to osmotic pressure on bacteria cells.

Finally, pH is known to contribute to inactivation with improved decay rates at higher pH even in the dark (Benchokroun et al., 2003; Curtis et al., 1992; Mayo and Noike, 1996; Mendonca et al., 1994; Parhad and Rao, 1974), but specific investigations on this mechanism are scarce.

Settling and attachment onto solids

Indicator species such as *E. coli* or helminths can attach to suspended solids and subsequently settle with them (Dias et al., 2017). Studies have reported high contents of indicator species in sludge (Nelson et al., 2004), biofilms (Schultz-Fademrecht et al., 2008), or even suspended solids (Auer and Niehaus, 1993; Parker and Darby, 1995) suggesting settling may be an important pathogen removal mechanism. Settling is in fact the only identified removal mechanism of intestinal parasite cysts in maturation ponds (Maynard et al., 1999) and because these organisms have a long survival period in sludge (Maynard et al., 1999), sludge disturbance in algal ponds should be carefully avoided.

Virus removal was associated with solids removal (Maynard et al., 1999), suggesting significant virus attachment onto solids. Sobsey and Cooper (1973) found that 25% of polioviruses were adsorbed by pond solids after only 3 minutes of contact.

While attachment is an identified pathway for pathogen removal, it may also shield pathogens from light radiation (Blaustein et al., 2013; Parker and Darby, 1995), predation, or oxidation by chemicals in solution (Qualls et al., 1983). No investigations of this possibility were found.

In situ conditions (e.g. pH, conductivity, DO) greatly influence the adsorption potential of solids. As an example, coliphages were reported to be adsorbed in aerobic conditions but desorbed in anaerobic conditions.

Finally, attachment may bias pathogen counting: if microorganisms form aggregates around one single particle, counting methods such as plate counts (Ansa et al., 2012b) or Quanti-Tray® will count these aggregates as one single organism.

Because this study focuses on HRAPs, pathogen removal by settling will be assumed to be negligible due to the mixing provided by the paddlewheel. Quantifying attachment of pathogens to particles (e.g. algae, inert solids) and its impact on counting results will still be necessary.

Heat inactivation

Human pathogens are generally mesophilic organisms for which optimal growth temperature is around 37°C. Higher temperatures cause the denaturation of vital proteins, and microorganisms are inhibited and then killed above certain thresholds (e.g. 48°C for *E. coli* according to Madigan and Martinko, 2006). However, such temperatures are not expected in HRAPs. A direct killing effect of temperature on human pathogens would therefore be highly unexpected.

Table 1 - 9: Dark mechanisms inducing *E. coli* decay in algal ponds

Mechanism	Mechanism description	Potential relevance
Natural decay: Starvation, competition with biomass, cell-programmed death.	Pathogens may have to compete against other microorganisms for substrate acquisition. If too much competition is present, pathogens may starve and die at a rate higher than 'natural'. The concept of "cell apoptosis" for bacteria suggests the existence of self-regulated death mechanisms of bacterial cells (Bayles, 2014).	Since *E. coli* are assumed to have no activity outside of their host, competition with biomass for nutrients is not expected to have an impact on decay in algal ponds. However, *E. coli* were reported to grow in tropical environments (Ashbolt et al., 2001), probably stimulated by gut-like temperatures. Therefore, HRAPs characterized by lower depth and potentially higher temperatures might support *E. coli* regrowth. In such cases, both food availability and the number of competing microorganisms might influence *E. coli* decay. This mechanism has received little attention and, if occurring, is most likely accounted for as part of a general "dark decay" mechanism. The rate of 'dark' decay, including cell-apoptosis, will be quantified using dark controls during every experiment. Unless these rates are inexplicably high, there will be no further investigation on cell programmed death.
Predation	Algal ponds hold significant quantities of grazers and bacterivores. Bacterivores may directly affect *E. coli* survival while grazers may digest algae that may have previously adsorbed *E. coli* (indirect effect).	This mechanism has received little attention in the literature and its importance is hard to assess in light of the data available. Existing studies have shown a potentially significant impact. (Ansa et al., 2012b). This mechanism cannot be dismissed and requires further investigation.
Algal toxicity	Some algae may produce toxins or antibiotics that could affect *E. coli* survival.	This mechanism is potentially significant but it has not yet been investigated. As this mechanism has not been evidenced in the literature, it is not expected to be significant and will not be an initial focus of the investigation.
Chemical toxicity	Algal ponds harbour chemical species that may be toxic to *E. coli*.	Chemical toxicity is potentially significant as the concentrations of NH_3 (a recognized antiseptic) can reach inhibitory levels at pH above 11 (which can occur in HRAPs). However, although frequently discussed, the occurrence of harmful chemicals in HRAPs and their effect on bacteria such as *E. coli* have never been investigated. This mechanism is not expected to be significant in light of the literature. It would need further investigation if laboratory results on other key mechanisms cannot match the disinfection performance measured on pilot scale HRAPs. Elevated pH has been reported to enhance the decay of some indicators (e.g. pH > 9.4 for *E. coli*, Parhad and Rao, 1974). pH toxicity will therefore be investigated by this study.
Attachment onto solids	Bacteria can be adsorbed and desorbed by suspended solids (including algal biomass) in algal ponds.	Attachment onto solids has potentially antagonistic outcomes: 1. Several cells adsorbed to the same particle may be 'counted' as one cell only (e.g. plate count and Quanti-Tray®) lowering the apparent number of pathogens 2. Attachment may shield pathogens from biocide agents (e.g. sunlight direct damage) 3. Attachment may enhance certain removal

Mechanism	Mechanism description	Potential relevance
		mechanisms (e.g. settling, predation through algal grazing, exposure to algal toxins) Therefore, the significance of attachment on counting method results will be investigated. It is however dismissed as a relevant *E. coli* removal mechanism until any result should suggest otherwise.

1.3.3. EFFECT OF ENVIRONMENTAL AND PROCESS PARAMETERS ON PATHOGEN DECAY IN ALGAL PONDS

Now that identified mechanisms of pathogen removal have been reviewed, this section lists the important design and environmental parameters for indicator decay linking them to the previously identified mechanisms.

The conclusions reached about the impact of each parameter on mechanisms of *E. coli* decay and their relevance to this study are summarized in Table 1 - 10 (sunlight-mediated mechanisms) and Table 1 - 12 (dark mechanisms), and results from studies testing the survival of pathogens in controlled conditions are provided in Table 1 - 11 (investigation on sunlight-mediated decay), Table 1 - 13 (investigation of dark mechanisms), and Table 1 - 14 (compilation of dark control results from studies targeting light-mediated mechanisms)[4].

1.3.3.1. Broth temperature

Amid the many parameters thought to influence pathogen removal in HRAPs, temperature has long been considered to be best correlated to pathogen indicator decay in algal ponds (Auer and Niehaus, 1993; Dias et al., 2017; Maynard et al., 1999). For this reason, the first model of disinfection in algal ponds predicted bacterial removal as having constant first order decay kinetics (Marais and Shaw, 1961) and was later improved by including an empiric temperature dependence factor (Marais, 1974). This approach was widely used in the following decades and further refined, being the basis for design guidelines of maturation ponds (Davies-Colley, 2005) as seen in Equation 1 - 6 presented in 1.2.2.1.

Temperature was still viewed as a key factor in more recent studies (Ouali et al., 2015; Xu et al., 2002) but other authors identified temperature as being insignificant (Ansa et al., 2012a;

[4] To be included in these tables, the study had to have been undertaken in a microcosm with known and relatively stable conditions of light intensity, pH, DO, algal concentration, temperature, and broth optical conditions. The study had to specify the indicator species used and provide the initial and final counts in the reactor (or alternatively the percentage of die-off during the experiment) as well as the duration of the experiment so that a consistent decay coefficient could be calculated. The decay coefficients were calculated as first order decay coefficients, thus comparable to some extent to the values of decay coefficient obtained in studies of algal ponds and given in Table 1 - 4 and Table 1 - 5.

Auer and Niehaus, 1993; Sukias et al., 2001). However, no study reported in Table 1 - 13 and Table 1 - 14 specifically investigated the effect of temperature while keeping other parameters constant. Only Kapuscinski and Mitchell (1983), who investigated the influence of temperature on sunlight-mediated decay in seawater, gave a temperature dependent decay rate, but their results did not reach a clear conclusion since sunlight intensity varied between experiments. This lack of specific results reflects either a lack of research or a lack of significant results due to publication bias.

Temperature is closely coupled to solar light intensity and solar intensity drives the variations of many other pond parameters (e.g. pH and dissolved oxygen). These parameters, including solar intensity, are known to have a significant impact on pathogen decay mechanisms. Hence, temperature may only be a proxy for other parameters of more direct impact, explaining why temperature dependent models provide reasonable accuracy despite controversy on the exact effect of temperature.

Due to the influence of temperature on chemical reactions and microbial kinetics, temperature is expected to be a secondary parameter of critical importance for faecal indicator decay (Ouali et al. 2015).

1.3.3.2. Sunlight intensity

Sunlight has been widely identified as the main parameter for disinfection in algal ponds since it is the driver of the most prominent removal mechanisms.

As previously shown in 1.3.2.1., sunlight radiation can cause direct disinfection (mechanism 1) through UV-B radiation although the significance of this pathogen removal mechanism can be questioned in algal ponds. Sunlight radiation is also implicated in indirect photo-oxidation involving the excitation of photosensitizers from endogenous (mechanism 2) and exogenous (mechanism 3) origin, supporting the production of ROS. Both indirect mechanisms are wavelength dependent and may be enhanced/inhibited by environmental conditions (e.g. pH and DO). In addition, sunlight drives algal activity and temperature variations, both of these parameters having been identified as influencing pathogen removal mechanisms.

Sunlight intensity is a critical parameter for pathogen removal in HRAP, if not the most critical, as reflected by the amount of publications tackling sunlight-mediated decay (see Table 1 - 11). Sunlight radiations influence different mechanism so its role as a parameter has to be assessed cautiously.

1.3.3.3. Wavelengths

As can be interpreted from results shown in Table 1 - 11, wavelengths significantly affect the decay rates of pathogen indicators.

UV-B radiation has repeatedly been shown to induce rapid decay of faecal indicators (Curtis et al., 1992; Maraccini et al., 2016b; Maraccini et al., 2016a; Ouali et al., 2015; Silverman and Nelson, 2016). UV-B radiation can damage DNA in cells (Maynard et al., 1999). Using a sunlight simulator, Maraccini et al. (2016a) showed that reducing UV-B intensity by 84% (from its natural sunlight level) would reduce the decay rate of 8 indicator species by 72 to 95% (90 and 92% for two *E. coli* strains) indicating that UV-B is the major source of decay under natural sunlight. However, the experiment was carried out in beakers filled with saline water, thus with little light scattering compared with normal HRAP broth.

UV-A and VIS, while not known to induce direct damage, have also been shown to induce decay of faecal indicators (Curtis et al., 1992; Davies-Colley et al., 1994; Dias and Von Sperling, 2018) due to indirect photo-oxidation processes. However, UV-A radiation are believed to have a small role in endogenous photo-oxidation, which would still mostly rely on UV-B radiation (Maraccini et al., 2016a).

VIS is not known to induce any endogenous photo-oxidation although this result remains unclear (Dias et al., 2017). VIS was, however, shown to have an impact on pathogen removal through exogenous photo-oxidation (Curtis et al., 1992).

1.3.3.4. Photosensitizers

In algal ponds, sunlight-dependent decay of pathogen indicators has been found to be enhanced in the presence of chemicals known as photosensitizers (Benchokroun et al., 2003; Curtis et al., 1992; Davies-Colley et al., 1999; Fisher et al., 2012; Maraccini et al., 2016c; Maraccini et al., 2016a). When excited by radiation of appropriate wavelength, photosensitizers generate ROS that destroy pathogen cells through oxidative damage (Curtis et al., 1992; Maynard et al., 1999). Maynard et al. (1999) reported that humic substances can absorb sunlight and transfer its energy to oxygen, forming powerful oxidizers (e.g. singlet oxygen, peroxide) capable of killing both bacteria and algae. The positive effect of photosensitizers and negative effect of ROS scavengers appears in several results displayed in Table 1 - 11.

Maraccini et al. (2016c) studied the reaction of eight indicator species when exposed to sunlight in the presence of artificial and naturally occurring photosensitizers. They noticed that, while each different photosensitizer could affect all the tested bacteria, there was a significant resistance to exogenous photo-oxidation by gram-negative bacteria (*E. coli* and

Campylobacter jejuni). Naturally occurring photosensitizers were even found to not influence or even lower the decay rate of such bacteria, (probably due to light scattering accompanied by no exogenous photo-oxidation). Hence, the presence of photosensitizers in water can have both a constructive and a destructive effect on the system disinfection performance.

In HRAPs, the concentration of photosensitizers and ROS scavengers are likely to significantly influence faecal indicator decay. Despite humic substances being often cited as photosensitizers involved in exogenous photo-oxidation, there is little knowledge on the photosensitizers commonly found in algal ponds.

In conclusion, while many studies support the existence of exogenous photo-oxidation, further investigations are needed to determine which chemicals occurring in HRAPs are potential photosensitizers, and to assess their impact on pathogen removal.

1.3.3.5. pH

Several studies report a lethal pH threshold for pathogenic indicators (Benchokroun et al., 2003; Mayo and Noike, 1996; Mendonca et al., 1994; Parhad and Rao, 1974). Maynard et al. (1999) cited a wide group of studies reporting the lethal level to be between 9 and 9.5 for bacteria. Benchokroun et al. (2003) found *E. coli* populations significantly decreased in the dark at pH above 8.4 while Parhad and Rao (1974) identified the lethal threshold to be 9.4. Such levels are common in HRAPs as was shown in Table 1 - 3.

High pH has been consistently shown to have an impact on faecal coliform removal in algal ponds (Ansa et al., 2012a; Benchokroun et al., 2003; Maïga et al., 2009a; Maynard et al., 1999; Mayo, 1995; Moreira et al., 2009; Ouali et al., 2015), but in many cases the correlation between pH and pathogen decay was poor in algal ponds (Maynard et al., 1999; Mayo, 1995), suggesting other mechanisms were involved. Hence, light-induced decay was shown to strongly interact with pH through mechanism 3 (Ansa et al., 2008; Curtis et al., 1992; Davies-Colley et al., 1999). While the coupled effect of pH with sunlight radiation was investigated on several occasion (as shown in Table 1 - 11), the impact of pH alone on indicator species was investigated only by Parhad and Rao (1974). These authors found a lethal pH threshold of 9.4 for *E. coli*, regardless of the buffer used to increase pH, and associated the mortality of *E. coli* in the presence of growing micro-algae to the increase of pH above this threshold. The results of this study are not displayed in Table 1 - 11 as the experiment would not fit the criteria described in introduction of 1.3.3.

High pH is widely accepted as critical with regards to pathogen decay in algal ponds. However, pH's exact influence, both as a direct and indirect parameter, remains unclear. In

addition, pH is known to reach higher levels in HRAPs than in MPs as shown by Table 1 - 3, meaning conclusions from MPs may be limited for HRAPs. Therefore, the impact of pH on pathogen removal needs to be thoroughly investigated.

1.3.3.6. Dissolved oxygen

Dissolved oxygen (DO) concentration has been positively correlated to pathogen decay in numerous studies (Ansa et al., 2012a; Benchokroun et al., 2003; Curtis et al., 1992; Davies-Colley et al., 1999; Khaengraeng and Reed, 2005; Maïga et al., 2009a; Moreira et al., 2009). The bactericidal effect of sunlight was repeatedly reported to be significantly enhanced at high DO concentration (Ansa et al., 2008; Benchokroun et al., 2003; Curtis et al., 1992; Davies-Colley et al., 1999; Khaengraeng and Reed, 2005; Ouali et al., 2015) as displayed in Table 1 - 11.

However, high DO concentration with no variation from any other parameter was consistently reported to not damage bacteria (Benchokroun et al., 2003; Curtis et al., 1992; Maynard et al., 1999; Mayo and Noike, 1996), and some studies even found no effect of sunlight in anaerobic conditions (Benchokroun et al., 2003; Curtis et al., 1992). These results strongly suggest that the impact of DO on pathogen removal is only through indirect photo-oxidation processes.

As shown in Table 1 - 3, DO concentration in HRAPs is larger than in MPs. As for pH, the impact of DO concentration on pathogen removal needs to be thoroughly investigated.

Table 1 - 10: Sunlight-mediated mechanisms for pathogen decay and their link to environmental and design parameters

	Direct UV-B damage	Endogenous photo-oxidative damage	Exogenous photo-oxidative damage
Sunlight intensity	Sunlight intensity should correlate with decay rate in any light-limited system		
Photosensitizer / quencher content of the pond	No	No	Photosensitizers enhance the formation of ROS. Quenchers react with ROS before they reach pathogens. The presence of these species should critically affect disinfection performance in HRAPs.
Wavelength	Only UV-B are relevant since UV-C radiation is negligible at the earth surface	UV-B radiation is commonly considered as critical although UV-A might have a significant impact.	Due to the large variety of potential photosensitizers, all radiations are potentially involved.
pH	No effect expected	Unknown	Elevated pH is known to damage the membranes of cells and increase vulnerability to exogenous ROS. Thus high pHs, as encountered in HRAPs, are known to affect this mechanism.
DO	No	DO concentration may influence the rate (and type) of ROS intracellular formation. The influence of DO on sunlight-mediated mechanisms is commonly associated with endogenous-photo-oxidation in the literature.	DO concentration is positively associated with exogenous photo-oxidative damage as dioxygen molecules are themselves photosensitizers.
Temperature	No effect expected	Effect is likely as higher temperatures are associated with accelerated rates of ROS generation and reaction. This parameter deserves attention in lab tests.	Effect is likely, this parameter deserves attention in laboratory tests.
Pond depth	At constant HRT, a shallower depth will result in higher average light intensity received by pathogens. In addition, lower depths are associated with higher temperature.		
SRT	In well-mixed HRAPs, the average SRT equates to the average HRT. Increasing SRT at constant depth would result in a higher contact time and a high SRT should improve the rates of the three mechanisms considered. However, a higher SRT means a higher algal concentration thus lower light penetration. The impact of the SRT remains unclear and deserves investigation.		

Table 1 - 11: Decay coefficients under sunlight exposure of various pathogens measured in microcosms in which different parameters were controlled

Reference	Indicator species	Light	pH	DO ($mg.L^{-1}$)	Algae in the broth	Duration of experiment	Temperature	Broth	Optical change	First order decay coefficient (d^{-1})
Dias and Sperling (2017)	*E. coli* (wild)	Sun – Morning	7.53 – 8.04	1.47 – 5.59	HRAP broth	4h	18.40 – 25.90	Pond effluent	10 cm HRAP depth	10.8
		Sun – Afternoon	7.65 – 8.41	2.94 – 14.32			20.50 – 27.90		10 cm HRAP depth	11.5
		Sun – Morning	2.01 – 10.97	2.01 – 10.97			19.10 – 25.20		20 cm HRAP depth	9.35
		Sun – Afternoon	7.63 – 8.75	4.51 – 14.49			21.20 – 29.00		20 cm HRAP depth	6.72
		Sun – Morning	7.63 – 8.44	2.72 – 8.18			18.60 – 24.50		30 cm HRAP depth	7.44
		Sun – Afternoon	7.66 – 8.50	8.19 – 15.68			20.10 – 27.60		30 cm HRAP depth	6.72
Maraccini et al. (2016c)[5]	*E. coli* K12	400 W/m2 solar simulator + 290 nm cut-off filter	7.64	Unknown	-	Unknown	15°C	Carbonate buffer saline solution (CBS)	-	130
									SRNOM	22.1
									Rose Bengal	110
									Nitrite	102
									Methylene Blue	245
									Isolated DOM	47.0
	E. coli 0157:H7								-	120
									SRNOM	17.7
									Rose Bengal	82.0
									Nitrite	85.7
Maraccini et al. (2016b)[6]	*E. coli* sewage sourced	400 W/m2 solar simulator	Unknown	Unknown	-	Unknown	15°C		Natural Saline Water	272
									Natural Freshwater	78.1
Maraccini et al. (2016a)[7]	*Bacteroides thetaiotaomicron*	Solar simulator 400 $W.m^{-2}$ + UV-B cut-off filter	7.64	Unknown	-	3.5h	15°C	CBS	200 $mg.L^{-1}$ nitrite	167
									0.5 µmol.L^{-1}	198

[5] Decay coefficients calculated using the mean of the decay coefficients of all the replicates for the first order law (see Table S3 in the publication)
[6] Decay coefficients calculated using the first order values (see Table S3 in the publication)
[7] Decay coefficients calculated using the means of the decay coefficients of all the replicates for the first order law (see Table S1 in the publication)

Reference	Indicator species	Light	pH	DO ($mg.L^{-1}$)	Algae in the broth	Duration of experiment	Temperature	Broth	Optical change	First order decay coefficient (d^{-1})
									rose Bengal	
									20 mg $C.L^{-1}$ river natural organic matter	78.3
	Campylobacter jejuni								200 $mg.L^{-1}$ nitrite	75.1
									0.5 µmol.L^{-1} rose Bengal	1515
									20 mg $C.L^{-1}$ river natural organic matter	123
									None	67.9
	Enterococcus faecalis								0.5 µmol.L^{-1} methylene blue	1178
									200 $mg.L^{-1}$ nitrite	52.0
									0.5 µmol.L^{-1} rose Bengal	200
									20 mg $C.L^{-1}$ river natural organic matter	8.98
									20 mg $C.L^{-1}$ wetland dissolved organic mater	20.3
									None	11.5
	E. coli K12								0.5 µmol.L^{-1} methylene blue	88.9
									200 $mg.L^{-1}$ nitrite	25.6
									0.5 µmol.L^{-1} rose Bengal	12.2
									20 mg $C.L^{-1}$ river natural organic matter	6.68
									20 mg $C.L^{-1}$ wetland dissolved	8.52

Reference	Indicator species	Light	pH	DO ($mg.L^{-1}$)	Algae in the broth	Duration of experiment	Temperature	Broth	Optical change	First order decay coefficient (d^{-1})
									organic mater	
									None	10.8
	E. coli O157:H7								200 $mg.L^{-1}$ nitrite	19.8
									0.5 µmol.L^{-1} rose Bengal	8.98
									20 mg C.L^{-1} river natural organic matter	4.61
									None	11.5
	Salmonella enterica								200 $mg.L^{-1}$ nitrite	26.9
									0.5 µmol.L^{-1} rose Bengal	12.2
									20 mg C.L^{-1} river natural organic matter	9.21
									None	11.3
	Staphylococcus aureus								200 $mg.L^{-1}$ nitrite	65.6
									0.5 µmol.L^{-1} rose Bengal	264
									20 mg C.L^{-1} river natural organic matter	43.5
									None	52.0
	Streptococcus bovis								200 $mg.L^{-1}$ nitrite	40.3
									0.5 µmol.L^{-1} rose Bengal	83.8
									20 mg C.L^{-1} river natural organic matter	14.3
									None	13.6
Silverman and Nelson (2016)	*E. coli* NCM 4236	Solar simulator (1000 7.5 W/m2)		~9	-	Up to 48h	20	Phosphate buffer saline solution	Atmospheric filter	173
									Cut off < 305 nm	125

Reference	Indicator species	Light	pH	DO ($mg.L^{-1}$)	Algae in the broth	Duration of experiment	Temperature	Broth	Optical change	First order decay coefficient (d^{-1})
								(PBS)	Cut off < 320 nm	94.5
									Cut off < 335 nm	74.6
									Cut off < 345 nm	52.5
									Cut off < 390 nm	9.39
									Cut off < 455 nm	~0
									Cut off < 515 nm	~0
		0							Dark	~0
	E. coli (isolated from wastewater)	Solar simulator (1000 W/m2)							Atmospheric filter	24.9
									Cut-off < 305 nm	19.9
									Cut-off < 320 nm	12.7
									Cut-off < 335 nm	7.74
									Cut-off < 345 nm	6.63
									Cut-off < 390 nm	1.11
									Cut-off < 455 nm	~0
									Cut-off < 515 nm	~0
		0							Dark	~0
Kadir and Nelson (2014)	*Enterococcus faecalis*	332 W/m2 UV-B block. sim. sunlight	7.5	1	-	Unknown	20	PBS	-	10.6
	E. coli									1.68
	Enterococcus faecalis			9						38.7
	E. coli									7.60
	Enterococcus faecalis			17						51.8
	E. coli									8.29
	Enterococcus faecalis			1				MP effluent		48.8
	E. coli									0.48

Reference	Indicator species	Light	pH	DO ($mg.L^{-1}$)	Algae in the broth	Duration of experiment	Temperature	Broth	Optical change	First order decay coefficient (d^{-1})
	Enterococcus faecalis			9						103
	E. coli									4.37
	Enterococcus faecalis			17						106
	E. coli									6.68
	Enterococcus faecalis	313 W/m2 full spect. sim. sunlight		1				PBS		18.2
	E. coli									25.8
	Enterococcus faecalis			9						51.6
	E. coli									49.7
	Enterococcus faecalis			17						80.2
	E. coli									49.3
	Enterococcus faecalis			1				MP effluent		80.6
	E. coli									15.2
	Enterococcus faecalis			9						114
	E. coli									16.3
	Enterococcus faecalis			17						116
	E. coli									19.8
Fisher et al. (2012)[8]	*E. coli* K12	Natural sunlight	6.5 – 7.5	-	-	3h	-	PBS	PET bottle	56.6
								PBS + 100 mg Na_2CO_3 + 100 mg citric acid	PET bottle	40.5
								PBS + 100 mg Na_2CO_3 + 100 mg ascorbic acid + 20 µg $CuSO_4$	PET bottle	47.4
								PBS	Tritan® bottle	52.7
								PBS	PC bottle	98.8
								PBS	PS bottle	161
								PBS	PPCO bottle	85.0
								PBS + 100 mg Na_2CO_3 + 100 mg citric acid	PPCO bottle	404

[8] PET: polyethylene terephthalate; PC: polycarbonate; PS: polystyrene; PPCO: polypropylene copolymer

Reference	Indicator species	Light	pH	DO ($mg.L^{-1}$)	Algae in the broth	Duration of experiment	Temperature	Broth	Optical change	First order decay coefficient (d^{-1})
								PBS + 100 mg Na_2CO_3 + 100 mg ascorbic acid + 20 µg $CuSO_4$	PPCO bottle	272
	Wastewater *E. coli*							PBS	PET bottle	24.4
								PBS + 100 mg Na_2CO_3 + 100 mg citric acid	PET bottle	21.9
								PBS + 100 mg Na_2CO_3 + 100 mg ascorbic acid + 20 µg $CuSO_4$	PET bottle	23.7
								PBS	Tritan® bottle	38.2
								PBS	PC bottle	55.3
								PBS	PS bottle	93.0
								PBS	PPCO bottle	57.3
								PBS + 100 mg Na_2CO_3 + 100 mg citric acid	PPCO bottle	68.6
								PBS + 100 mg Na_2CO_3 + 100 mg ascorbic acid + 20 µg $CuSO_4$	PPCO bottle	155
	Enterococci faecalis							Phosphate buffered saline (PBS) solution	PET bottle	58.0
								PBS + 100 mg Na_2CO_3 + 100 mg	PET bottle	50.7

Reference	Indicator species	Light	pH	DO ($mg.L^{-1}$)	Algae in the broth	Duration of experiment	Temperature	Broth	Optical change	First order decay coefficient (d^{-1})
								citric acid		
								PBS + 100 mg Na_2CO_3 + 100 mg ascorbic acid + 20 µg $CuSO_4$	PET bottle	55.9
								PBS	Tritan® bottle	59.4
								PBS	PC bottle	92.1
								PBS	PS bottle	84.5
								PBS	PPCO bottle	54.1
								PBS + 100 mg Na_2CO_3 + 100 mg citric acid	PPCO bottle	195
								PBS + 100 mg Na_2CO_3 + 100 mg ascorbic acid + 20 µg $CuSO_4$	PPCO bottle	98.1
	Wastewater *Enterococci*							PBS	PET bottle	26.5
								PBS + 100 mg Na_2CO_3 + 100 mg citric acid	PET bottle	25.3
								PBS + 100 mg Na_2CO_3 + 100 mg ascorbic acid + 20 µg $CuSO_4$	PET bottle	30.8
								PBS	Tritan® bottle	42.6
								PBS	PC bottle	59.4
								PBS	PS bottle	89.9
								PBS	PPCO bottle	32.2
								PBS + 100 mg Na_2CO_3 + 100 mg	PPCO bottle	110

Reference	Indicator species	Light	pH	DO ($mg.L^{-1}$)	Algae in the broth	Duration of experiment	Temperature	Broth	Optical change	First order decay coefficient (d^{-1})
								citric acid		
								PBS + 100 mg Na_2CO_3 + 100 mg ascorbic acid + 20 µg $CuSO_4$	PPCO bottle	65.8
	MS2 Coliphage							PBS	PET bottle	5.07
								PBS + 100 mg Na_2CO_3 + 100 mg citric acid	PET bottle	6.68
								PBS + 100 mg Na_2CO_3 + 100 mg ascorbic acid + 20 µg $CuSO_4$	PET bottle	4.14
								PBS	Tritan® bottle	8.75
								PBS	PC bottle	14.5
								PBS	PS bottle	40.3
								PBS	PPCO bottle	122
								PBS + 100 mg Na_2CO_3 + 100 mg citric acid	PPCO bottle	96.9
								PBS + 100 mg Na_2CO_3 + 100 mg ascorbic acid + 20 µg $CuSO_4$	PPCO bottle	37.3
Ansa et al. (2008)[9]	*Faecal coliforms*	+	8	6	0	7d	Unknown	Unknown	Unknown	1.15
		-	8	6	0					0.69
		+	9	8	1199 mug/L chl-a					2.30

[9] Approximate reading of values on figures

Reference	Indicator species	Light	pH	DO ($mg.L^{-1}$)	Algae in the broth	Duration of experiment	Temperature	Broth	Optical change	First order decay coefficient (d^{-1})
		-	8	7	1199 mug/L chl-a					0.69
		+	9	8	1653 mug/L chl-a					0.92
		-	8	8	1653 mug/L chl-a					0.46
		+	9	8	6734 mug/L chl-a					1.61
		-	8	7	6734 mug/L chl-a					0.92
		+	9	7	17464 mug/L chl-a					1.38
		-	8	6	17464 mug/L chl-a					0.92
		+	8.5	6	33892 mug/L chl-a					1.61
		-	8	5	33892 mug/L chl-a					0.92
Benchokroun et al. (2003) [10]	*E. coli*	6.7 MJ/m2	7	8.2	-	300 min	29°C	Sterilized wastewater	-	11.0
		-	7							0
		6.7 MJ/m2	7.7							11.0
		-	7.7							0
		6.7 MJ/m2	8.4							33.2
		-	8.4							11.0
		6.7 MJ/m2	9.5							49.7
		-	9.5							22.1
		7.32 MJ/m2	8.3	9.2		360 min	30°C	Sterilized wastewater		7.83
		-		9.2						0
		7.32 MJ/m2		0						0.09
		-		0						0.09
		7.5 MJ/m2	8.2	0		Not said, assumed 6h	30°C	Sterilized wastewater		0
				3						4.14
				7						7.60
				12						10.59
				23						12.89

[10] Decay coefficients at pH 7 in the dark were assumed equal to 0 d^{-1}.

Reference	Indicator species	Light	pH	DO ($mg.L^{-1}$)	Algae in the broth	Duration of experiment	Temperature	Broth	Optical change	First order decay coefficient (d^{-1})
		7.32 MJ/m2: I have high doubts about if the fact that these reactors were actually exposed to sunlight	8.2	8.6		240 min	29°C	Sterilized wastewater		1.84
								Sterilized wastewater + H2O2		11.8
								Sterilized wastewater + H2O2 + pyruvate		0.23
								Sterilized wastewater + H2O2 + catalase		0
		-	8.2	8.4		Not said, assumed 6h	30°C	Sterilized wastewater		0.28
		7.6 MJ/m2						Sterilized wastewater		2.76
								Sterilized wastewater + pyruvate		0
								Sterilized wastewater + catalase		0
Muela et al. (2002)	*E. coli* CECT 471	Artificial light (see publication for detail of light bulbs) 10 W.m-2 PAR	Unknown (likely neutral – phosphate buffered)	Anaerobic	-	96h	25°C	Saline solution	-	0.85
		6 W.m-2 UV-A								1.27
		0.1 W.m-2 UV-B								0.94
		10 W.m-2 PAR		Aerobic						1.38
		6 W.m-2 UV-A								3.25
		0.1 W.m-2 UV-B								1.73
		10 W.m-2 PAR	Unknown	Anaerobic				River water		0.90
		6 W.m-2 UV-A								1.38
		0.1 W.m-2 UV-B								3.45
		10 W.m-2 PAR		Aerobic						1.36
		6 W.m-2 UV-A								1.38
		0.1 W.m-2 UV-B								3.45

Reference	Indicator species	Light	pH	DO ($mg.L^{-1}$)	Algae in the broth	Duration of experiment	Temperature	Broth	Optical change	First order decay coefficient (d^{-1})
Sinton et al. (2002)	Faecal coliforms (WSP)	Sunlight summer (7 – 26 $MJ.m^{-2}$)	Unknown	Unknown	-	8h	14°C	River freshwater	-	6.29
		Sunlight winter (7 – 15 $MJ.m^{-2}$)								3.29
		Dark								0.39
	Faecal coliforms (Raw sewage)	Sunlight summer (7 – 26 $MJ.m^{-2}$)								16.74
		Sunlight winter (7 – 15 $MJ.m^{-2}$)								7.18
		Dark								0.16
	E. coli (WSP)	Sunlight summer (7 – 26 $MJ.m^{-2}$)								6.01
		Sunlight winter (7 – 15 $MJ.m^{-2}$)								2.72
		Dark								0.41
	E. coli (RS)	Sunlight summer (7 – 26 $MJ.m^{-2}$)								16.7
		Sunlight winter (7 – 15 $MJ.m^{-2}$)								8.01
		Dark								0.55
	Enterococci (WSP)	Sunlight summer (7 – 26 $MJ.m^{-2}$)								18.4
		Sunlight winter (7 – 15 $MJ.m^{-2}$)								3.82
		Dark								0.41
	Enterococci (RS)	Sunlight summer (7 – 26 $MJ.m^{-2}$)								8.63
		Sunlight winter (7 – 15 $MJ.m^{-2}$)								4.37
		Dark								0.30
	Somatic coliphages (WSP)	Sunlight summer (7 – 26 $MJ.m^{-2}$)								4.77
		Sunlight winter (7 – 15 $MJ.m^{-2}$)								1.80
		Dark								0.18
	Somatic coliphages (RS)	Sunlight summer (7 – 26 $MJ.m^{-2}$)								6.65
		Sunlight winter (7 –								2.65

Reference	Indicator species	Light	pH	DO ($mg.L^{-1}$)	Algae in the broth	Duration of experiment	Temperature	Broth	Optical change	First order decay coefficient (d^{-1})
		15 $MJ.m^{-2}$)								
		Dark								0.02
	F-RNA phages (WSP)	Sunlight summer (7 – 26 $MJ.m^{-2}$)								4.14
		Sunlight winter (7 – 15 $MJ.m^{-2}$)								2.00
		Dark								0.35
	F-RNA phages (RS)	Sunlight summer (7 – 26 $MJ.m^{-2}$)								4.42
		Sunlight winter (7 – 15 $MJ.m^{-2}$)								290
		Dark								0
Curtis et al. (1992)	Total coliforns	6.03 MJ/m2	8.9	?	-	170 min	Unknown	Buffered pond water	> 300 nm	Unlnown[11]
									> 430 nm	1.74
									> 525 nm	6.68
									> 575 nm	5.07
									> 700 nm	0
	E. coli	9.19 MJ/m2	9.4			200 min		Distilled water	> 300 nm	> 66.3
									> 430 nm	~ 0
									> 575 nm	~ 0
									> 700 nm	~ 0
								Filtered and unfiltered pond water (similar results)	> 300 nm	> 66.3
									> 430 nm	49.7
									> 575 nm	24.9
									> 700 nm	8.29
	Faecal coliforms	4.52 MJ/m2	8.9	8.8		255 min		Pond water		21.9
		0								~ 0
		7.83 MJ/m2	8.8	0		136 min				0.32
				1						2.30
				3						6.45
				5						9.67
				7						23.5
				10						27.4

[11] All cells were found inactivated while no initial concentration was given

Reference	Indicator species	Light	pH	DO ($mg.L^{-1}$)	Algae in the broth	Duration of experiment	Temperature	Broth	Optical change	First order decay coefficient (d^{-1})
				16						35.5
				18						41.4
				19						41.4
		6.12 MJ/m2	7.5	2.8		83 min				15.9
		0	7.5							~ 0
		6.12 MJ/m2	8							28.1
		0	8							~ 0
		6.12 MJ/m2	8.25							28.1
		0	8.25							~ 0
		6.12 MJ/m2	8.5							47.9
		0	8.5							12.0
		6.12 MJ/m2	9							99.9
		0	9							40.1
		6.12 MJ/m2	9.5							5.07
		0	9.5							19.8
		7.83 MJ./m2	7.7	?		226 min			> 300 nm	5.07
			8.8							19.8
			7.7						> 430 nm	5.07
			8.8							16.1
			7.7.						> 525 nm	~ 0
			8.8							10.4
			7.7.						> 575 nm	~ 0
			8.8							10.4
			7.7.						> 700 nm	0.67
			8.8							5.76
Kapuscinski and Mitchell (1983)	*E. coli*	+	Unknown	Unknown	-	Unknown	10	Filtered coastal seawater	-	108
		-								0.60
		+					15			119
		-								0.51
		+								68.6
		-								0.28
		+					23			161
		-								1.22

Reference	Indicator species	Light	pH	DO ($mg.L^{-1}$)	Algae in the broth	Duration of experiment	Temperature	Broth	Optical change	First order decay coefficient (d^{-1})
Parhad and Rao (1974)[12]	*E. coli* (isolated from wastewater)	Artificial light	7.5 – 8.5	Unknown	-	8 days	26 – 33	Sterilized wastewater	-	No decay
			9.5 – 10.5		Growing chlorella	8 days				5.30
			9 – 10		Growing Scenedesmus	8				5.30
			10		Growing Synechocystis	8				5.30
			10		Growing chlorella					4.03
			7.5		Growing chlorella					0
			9.5 – 10.5		-	4		Sterilized wastewater + alkali species		9.21

[12] pH, *E. coli* cell count: approximate reading of values on figures

1.3.3.7. Algal activity

As discussed in 1.2.1., algal activity in HRAPs results in an increase of pH and dissolved oxygen in the broth. As both parameters are believed to significantly contribute to pathogen decay in algal ponds (cf. 1.3.3.5. and 1.3.3.6.), algal activity is likely to be a critical driver of pathogen removal in algal ponds. In addition, algal activity would be linked to algal toxicity if this mechanism is significant (cf. 1.3.2.2), further supporting algal activity as a means of pathogen removal in algal ponds.

No precise results linking algal activity to decay coefficients have been reported (see Table 1 - 11) probably because algal activity cannot be separated from sunlight intensity and, to a lesser extent, pH and DO concentration, as a driver of pathogen removal.

1.3.3.8. Cell and hydraulic retention time

In well-mixed systems, the hydraulic retention time (HRT) represents the average duration of pathogen exposure to potentially harmful conditions, and is therefore expected to affect faecal indicator decay significantly. Surprisingly, Maynard et al. (1999) reported that the HRT impact on pathogen removal in maturation ponds, although crucial, was not a widely studied subject. The HRT is also crucial to settling, with longer HRT being associated with higher settling rates in MPs. Due to the mixing from the paddlewheel however, settling is not relevant for the HRAP technology and was assumed to be negligible in this study.

The potential impact of HRT on pathogen removal requires extra caution in the design of ponds. Short circuiting due to e.g. sludge accumulation or thermal stratification as reported by Maynard et al. (1999) and Nelson et al. (2004) are thus likely to have significant consequences on the pond disinfection capacity by lowering the pond HRT.

1.3.3.9. Depth

A negative correlation between pond depth and pathogen decay has been widely described in the literature for maturation ponds (Ansa et al., 2012b; Davies-Colley et al., 1994; Dias and Von Sperling, 2018; Maïga et al., 2009a; Maynard et al., 1999; Von Sperling, 2005). At constant HRT and broth optical properties, lesser depth results in higher mean sunlight intensity experienced by pathogens. This could explain the observations of Maïga et al., (2009b) who found appreciably higher decay coefficients during warmer months in shallow microcosms than during colder months, while seasonal variations in deeper microcosms were not significant.

As described in Table 1 - 3, the depth of HRAPs is generally significantly less than for MPs, suggesting the impact of sunlight-mediated mechanisms will be enhanced. However, HRAPs

are also characterized by higher biomass concentration and are therefore more opaque, which may counter-balance the effect of the lesser depth on pathogen removal performance. Hence, the exact impact of depth needs further investigation as it is likely that an optimal depth can be reached between algal productivity and average sunlight intensity in the broth.

1.3.3.10. Paddlewheel mixing

The paddlewheel mixing first ensures a recirculation of algae from the bottom to the upper layer and sufficient linear velocity to prevent settling of algae from the top to the bottom layers. As a result, algal growth in HRAPs is significantly higher than in MPs (illustrated in Table 1 - 3 by significantly higher VSS in HRAPs than in MPs). As discussed in 1.3.3.7., algal activity is likely to positively contribute to pathogen removal in HRAPs, leading to the same conclusion for the effect of paddlewheel mixing.

The paddlewheel mixing also serves as an aeration system; the transfer between the atmosphere and the liquid broth of O_2 and CO_2 affects DO concentration and pH respectively. DO and pH having been identified as critical to pathogen removal (see 3.3.5 and 3.3.6), paddlewheel mixing is possibly crucial to HRAPs disinfection performance.

The impact of paddlewheel mixing on pathogen decay in HRAPs comes from the influence of this factor on several characteristics of HRAPs. Its impact is therefore likely to be complex. For instance, higher speed would result in higher algal biomass concentration (to some extent), and thus higher pathogen removal. At the same time, higher paddlewheel speed would result in a higher mass transfer of gases from the atmosphere to the pond, resulting in lower DO concentration and pH during the afternoon peak, thus lower decay rates. The impact of paddlewheel speed on pathogen removal has not yet been studied.

1.3.3.11. CO_2 bubbling

Bubbling of CO_2 has been applied to HRAPs in order to ensure a sufficient supply of inorganic carbon to support algal growth and moderate pH conditions. In addition, CO_2 bubbling improves mixing conditions.

Only one study was found assessing the impact of CO_2 bubbling on pathogen removal. No significant difference between bubbling and non-bubbling was found on *E. coli* and enterococci survival, but it was suspected to positively influence *Pseudomonas aeruginosa* removal (Ruas et al., 2017).

66 Table 1 - 12: Dark mechanisms for pathogens decay and their link to environmental and
67 design parameters

	Natural death	Predation	Chemical toxicity	Algal toxicity	Attachment onto solids
Sunlight intensity	Possible influence, particularly by indirect effect on temperature	Sunlight may have an impact on predation activity	Sunlight intensity will influence temperature, pH, and therefore the rates of toxicant formation and removal (e.g. NH_3).	As this mechanism has not been investigated to our knowledge, no assumptions on the impact of individual parameters were made. However, it can be safely assumed that any parameter promoting algal activity should promote any algal toxicity	No direct effect is expected but the impact of sunlight on temperature may result in indirect effects
pH	Probable influence by promoting or eliminating other species or *E. coli* itself	pH may have an impact on predation activity	pH is likely to influence toxic chemical toxicity (e.g. NH_3).		Unknown
DO	Probable influence by promoting or eliminating other species	DO concentration is expected to have an impact on predation activity (beneficially or negatively)	Unknown		Unknown
Temperature	Probable influence by promoting or eliminating other species or *E. coli* itself	Temperature will probably influence the metabolism of predators, either accelerating or inhibiting their growth	Hard to predict as both toxicity and detoxification mechanisms could be enhanced by temperature.		Unknown
Pond depth	Unknown	No direct effect is expected but the impact of depth on other parameters (e.g. average sunlight in the HRAP, temperature) could generate indirect effects	No direct effect is expected but the impact of depth on other parameters (e.g. average sunlight in the HRAP, temperature) could generate effects		No direct effect is expected but the impact of depth on other parameters (e.g. average sunlight in the HRAP, temperature) could generate effects
HRT	Longer HRT would result in possible starvation of microbial species, particularly pathogens	The higher the HRT, the higher the chances for a single cell to encounter a predator. However, in a predator/prey equilibrium, a higher HRT seems likely to result in a lower density of predators resulting in no change in the relative impact of predation	Higher HRT increases contact time with harmful chemicals and is expected to favour this mechanism		Higher HRT increases contact time with suspended solids and is expected to favour this mechanism

Table 1 - 13: Decay coefficient in darkness of various pathogen indicators measured in microcosms in which different parameters were controlled

Reference	Bacteria	pH	DO ($mg.L^{-1}$)	Algal concentration	Duration of experiment	Temperature	Broth	First order decay coefficient (d-1)
Müller et al. (2006)	*E. coli* MG1655	Unknown	Unknown	-	400 min?	Unknown	Addition of $(NH_4)_2SO_4$ 50 – 375 mM	No effect
Mendonca et al. (1994)[1]	*E. coli* O157:H7	9	Unknown	-	15 min	37°C	$NaHCO_3$/NaOH buffer	~0[2]
		10						884
		11						2304[3]
		12						Instant inactivation
	Salmonella enteriditis	9						~ 0
		10						55.3
		11						3,979
		12						Instant inactivation
	Listeria monocytogenes	9						~ 0
		10						110
		11						221
		12						221

[1] The authors studied decay coefficients for temperatures up to 45°C. While no data is shown, the authors acknowledged an improved decay with higher temperature;
[2] Values calculated from figure readings, and therefore imprecise;
[3] Decay coefficient from measurement performed following a 5 minutes incubation period. Decay coefficient was reported to slow afterward

Table 1 - 14: Decay coefficient in darkness of various pathogen indicators: dark control results of studies investigating the effect of light on pathogens

Reference	Bacteria	pH	DO ($mg.L^{-1}$)	Algal concentration	Duration of experiment	Temperature	Broth	First order decay coefficient (d-1)
Silverman and Nelson (2016)	*E. coli* NCM 4244	7.5	~17	-	Up to 48h	28°C	PBS	~ 0
	E. coli (isolated from wastewater)	7.5	~26			37°C		~ 0
Ansa et al. (2008)	Faecal coliforms	8	6	0		Unknown	Unknown	0.69
			7	1199 mug/L chl-a				0.69
			8	1653 mug/L chl-a				0.46

Reference	Bacteria	pH	DO ($mg.L^{-1}$)	Algal concentration	Duration of experiment	Temperature	Broth	First order decay coefficient (d-1)
			7	6734 mug/L chl-a				0.92
			6	17464 mug/L chl-a				0.92
			5	33892 mug/L chl-a				0.92
Benchokroun et al. (2003)	*E. coli*	7	9.2	-	301 min	29°C	Sterilized wastewater	0
		7.7	11.2		303 min			0
		8.4	13.2		305 min			11.1
		9.5	15.2		307 min			22.1
		8.3	9.2		361 min			0
		8.3	0		363 min			0.09
		8.2	8.4		Not said, assumed 6h	30°C		0.28
Sinton et al. (2002)	Faecal coliforms (WSP)	Unknown	Unknown	-	8h	14°C	River freshwater	0.39
	Faecal coliforms (Raw sewage)							0.16
	E. coli (WSP)							0.41
	E. coli (RS)							0.55
	Enterococci (WSP)							0.41
	Enterococci (RS)							0.30
	Somatic coliphages (WSP)							0.18
	Somatic coliphages (RS)							0.02
	F-RNA phages (WSP)							0.35
	F-RNA phages (RS)							0

Reference	Bacteria	pH	DO ($mg.L^{-1}$)	Algal concentration	Duration of experiment	Temperature	Broth	First order decay coefficient (d-1)
Curtis et al. (1992)	Faecal coliforms	8.9	8.8	-	256 min	Unknown	Pond water	~ 0
		7.5	2.8		84 min			~ 0
		8	2.8		86 min			~ 0
		8.25	2.8		88 min			~ 0
		8.5	2.8		90 min			~ 0
		9	2.8		92 min			12.0
		9.5	2.8		94 min			40.1
Kapuscinski and Mitchell (1983)	*E. coli*	Unknown	Unknown	-	Unknown	10°C	Filtered coastal seawater	0.60
						15°C		0.51
						15°C		0.28
						23°C		1.22

1.4. CONCLUSION

The literature review confirmed similarities in behaviour between MPs and HRAPs. The main differences between both systems are shorter HRTs and significantly smaller depths for HRAPs from a design point of view, which translates to larger magnitudes in the variation of key environmental parameters such as algal density, pH, and DO concentration. As a result, and as expected, the decay rates of faecal indicators in HRAPs were reported to be similar and often higher than in MPs despite a lack of dedicated research. This demonstrates the importance of this study which may confirm HRAPs as an effective and robust alternative to MPs for wastewater disinfection characterized by lower HRTs.

Due to the wide utilization of *E. coli* as a pathogen decay indicator in wastewater treatment technology, and since methods for its monitoring were readily available in our facilities, *E. coli* was retained as the indicator to monitor for the purpose of this thesis.

Because a parametric study of *E. coli* decay rate in HRAPs would provide only limited information on the disinfection potential of HRAPs, emphasis was put on researching disinfection mechanisms relevant to HRAPs. Sunlight-mediated mechanisms were reported to be most likely to drive much of the *E. coli* decay in HRAPs, although it is not clear if this effect originates from direct UV-B effects, or from indirect photo-oxidation. In addition, despite their potential importance, very little is known on dark mechanisms partly due to the extreme environment presented by HRAPs.

Chapter 2: Research strategy & materials and methods

This Chapter starts by outlining the general research strategy developed to improve the understanding of the mechanisms and parameters involved in wastewater disinfection in HRAPs. Following this introduction, the detailed methodology used in this study is described.

2.1. OVERALL RESEARCH STRATEGY

As discussed previously, current knowledge on disinfection in maturation ponds showed that several disinfection mechanisms are likely to take place in HRAPs (section 1.3.2.), and numerous environmental and process parameters can influence the rate of these mechanisms (section 1.3.3.). Unfortunately, we do not currently know which mechanisms and parameters quantitatively drive disinfection performance in HRAPs. Under the hypothesis that such knowledge would provide the scientific foundation for improving the design and operation of HRAP for the purpose of disinfection, the following 4-steps strategy was proposed:

1. Collect field data from pilot scale HRAPs in order to i) quantify long-term HRAP disinfection performance under relevant conditions (outdoor, real wastewater, pilot scale) and ii) validate or invalidate findings from laboratory and bench scale experiments (see step 2). This monitoring is needed because only a few studies have hitherto reported disinfection performance in HRAPs often based on a few samples without consideration of daily or seasonal variability (see Table 1 - 5 and Table 1 - 6).
2. Conduct laboratory experiments (<1 L) aiming to quantitatively identify significant disinfection mechanisms and the impact of selected parameters on these mechanisms. This step is needed because it is difficult to identify/dissociate the disinfection mechanisms that are potentially involved due to the high daily and seasonable variability of the parameters involved under real-life conditions (e.g. light irradiance, pH, DO, temperature, influent composition, ecology).
3. Conduct bench experiments (i.e. 1 – 5 L scale) to test (‘recalibrate’) findings from laboratory experiments (step 2) under conditions more relevant to field operation. These experiments are needed to provide more relevant data, especially for

parameters that are very difficult to scale-down, while still allowing some level of control in order to 'isolate' key mechanisms.

4. Develop a predictive model to translate findings from laboratory and bench scale experiments and, if validated, optimize the design and operation of HRAPs for disinfection. This will be done by quantifying the accuracy of the model predictions against experimental data (generated in step 1) and testing the ability of the model to identify conditions (environmental and/or operational) associated with high performance.

A rationale for the need for laboratory to pilot scale step-up is listed in Table 2 - 1.

Table 2 - 1: Main features of experiments used in HRAP research

Scale	Typical characteristics	Advantages	Disadvantages
Laboratory (mL)	Short-term batch assays conducted indoors or outdoors	Experimental conditions are controlled and reproducible when performed indoors, economical, suitable for high throughput screening.	Limited representativeness by design (e.g. when a specific mechanism is isolated against others) and due to scale factors (e.g. small volume and high area/volume ratio often means overheating while light supply and mass transfer limitations are not experienced)
Bench (L)	Short-term batch conducted outdoors	Experimental conditions are controlled and reproducible; introduces a step between laboratory and full-scales.	While more relevant than laboratory scale, still suffers from lack of representativeness, small area/depth ratio compared to full sale, small volume outdoor inducing overheating
Pilot and Full (m^3)	Long term continuous (or semi-continuous) conducted outdoors	Representativeness	Potentially costly, difficult to control and reproduce due to exposure to outdoor conditions.

2.2. MATERIAL AND METHODS

This section describes the material and methods used during experimental work, and is organized based on the first three strategic steps defined above: 1) Pilot monitoring (section 2.2.1.); 2) Laboratory experiments (section 2.2.2.); 3) Bench experiments (section 2.2.3.).

2.2.1. PILOT SCALE HRAP MONITORING

2.2.1.1. HRAPs set up and operation

Two pilot scale HRAPs (henceforth named HRAP A and HRAP B) were set up at the wastewater treatment plant of Palmerton North City Council (PNCC), New Zealand

(Latitude: 40° 23′ 7” S; Longitude: 175° 34′ 47” E). These ponds were made of a 0.25 m deep[13] concrete trough equipped with a central concrete wall to create a raceway path (as shown in Figure 2 - 1 and Figure 2 - 2). The total working volume of each pond was calculated to be 0.86 m^3 (3.42 m^2 of free surface). Mixing was provided by a paddlewheel operated at about 10 rpm, generating a linear fluid velocity[14] of 23 $cm.s^{-1}$. Because the timescale of the mixing of the pilot scale HRAP broth which was found to be significantly lower than the timescales of the different processes governing physical, chemical, and biological conditions in the algal broth (see Appendix 2), the pilot scale HRAPs were assumed to be well mixed. Wastewater was pumped from the outlet channel of the primary settler of Palmerston North wastewater treatment plant and continuously supplied to the ponds to reach an average HRT of 5 to 10 d[15].

HRAP A was started prior to the beginning of this study (16/12/2014; Hom-Diaz et al. 2017) and HRAP B was started on 07/07/2016. The regular monitoring of pathogen decay was conducted from July 2015 to the end of May 2017. HRAP A was seeded using an algal/bacterial broth obtained from a maturation pond located in Rongotea, New Zealand (Latitude: 40° 17′ 40.6” S; Longitude: 175° 24′ 47.8” E). HRAP B was seeded using half of the volume from HRAP A and both ponds were gradually filled with wastewater on the same day.

From September 2015, the ponds were typically visited for maintenance, in situ measurements, and sampling for laboratory measurements twice per week. Maintenance of the ponds included inlet tubing cleaning, pump speed adjustment, paddlewheel speed control, outlet cleaning, and power reset in case of electric outage. Influent flowrate was measured by letting the influent pipe fill up a graduated cylinder for two minutes: this method was calibrated using a tipping-bucket flow meter as described in Appendix 3. The flow rate was first measured before any other action was taken (to measure the actual influent flowrate at the time of sampling) and after maintenance (to maintain the targeted HRT). Prior to September 2015, the actual flowrate at the time of sampling was assumed to equal the targeted flow rate after maintenance. The paddlewheel speed (measured in revolutions per minute) was routinely measured and adjusted from June 2016.

Temperature, pH, and dissolved oxygen (DO) concentration in the HRAP broths were measured during each visit at the time of sampling (Multimeter Thermo Scientific™ Orion Star™ A326). From December 2015, these parameters were nearly continuously recorded by setting up a Multimeter Thermo Scientific™ Orion Star™ A326 logging data every 15

[13] Within the typical depth of 0.1 – 0.5 m for HRAPs (see. Table 1 - 3)
[14] Within the typical range of 15 – 30 $cm.s^{-1}$ (Craggs et al. 2014)
[15] Within the typical range of 1 – 14 d, see Table 1 - 3

minutes. Hourly sunlight radiant energy data was obtained from the National Institute of Water and Atmospheric Research Ltd (NIWA) database (Palmerston North, location agent number 21963).

As the pilot scale HRAPs could only be visited twice a week, several issues were encountered:

- Inlet clogging leading to insufficient influent flow.
- Outlet clogging leading to increased working pond depth.
- Paddlewheel malfunction leading to biomass settling
- Power failure causing the stopping of the paddlewheel and the inlet flow.

Measurements made at days when such issues were recorded were excluded for analysis.

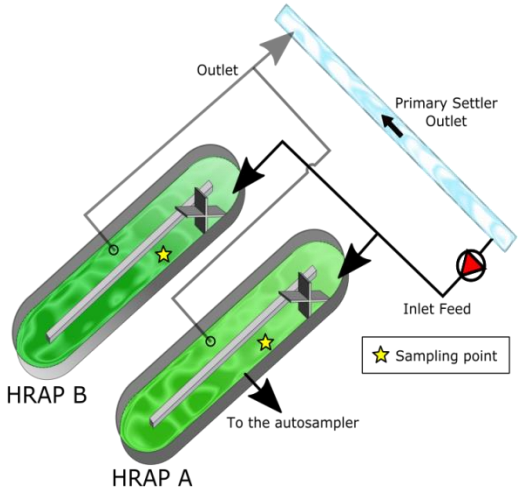

Figure 2 - 1: Pilot scale schematic HRAPs set up

Figure 2 - 2: Pilot scale HRAPs A and B (picture taken on 01/12/2016)

2.2.1.2. Sampling

During each visit, 250 mL grab samples were withdrawn from HRAPs and the wastewater feed. The HRAPs samples were collected downstream from the paddlewheel to ensure a maximum mixing (as depicted in Figure 2 - 1). The wastewater sample was drawn by letting the inlet tubing directly fill the sampling bottle. This was done prior to cleaning the inlet tubing to prevent solids from the detached biofilm to spoil the inlet sample. Aliquots of 1.5 mL were also saved in Eppendorf tubes for *Escherichia coli* (*E. coli*) counts in the laboratory.

Since the literature showed *E. coli* decay was likely to be maximized by the co-action of high pH, high DO concentration, and high sunlight intensity (Davies-Colley et al., 1999), *E. coli* cell count in the HRAPs was suspected to be consistently lower in the afternoon than in the morning when routine monitoring was performed (9 A.M.). A refrigerated autosampler (ISCO 6712FR) was therefore used to grab 200 mL samples every hour from 9 A.M. to obtain the 'daily profiles' of important parameters. These samples were withdrawn downstream from the paddlewheel approximately 5 cm below the surface. All samples were stored at 4°C in the refrigerated chamber of the autosampler until collection the next day at the time of the routine visit. All analyses were conducted within the day of collection.

As the generation of daily profiles was very time demanding, 6 tests were performed across 3 seasons[16] before being replaced by the collection of a single HRAP sample on the day before the maintenance/monitoring visit. This 200 mL grab sample was withdrawn in the afternoon at a fixed hour (ranging from 3:00 PM in winter to 5:00 PM in summer) in an attempt to sample when pH and DO concentration peaked. An aliquot of 1.5 mL from this sample was transferred in an Eppendorf tube and brought back to the laboratory for *E. coli* cell count measurement.

2.2.1.3. Analysis

The concentration of total suspended solids (TSS) was quantified via dry weights measurements following the standard method 2540.D using GF/C™ grade (General Electric®) fiberglass filters (Eaton et al., 1998). The filtrate was used to quantify the concentrations of chloride, nitrite, nitrate, sulphate, and phosphate by ion chromatography (IC) system described by Hom-Diaz et al. (2017), as well as the concentration of ammonium via colorimetry (Thermo Scientific™ Orion™ AQUAfast™ AQ3700 , tests Ammonia TT LR and HR, or colorimeter Hach™ DR3900™, tests TNT plus™ vial tests ammonia ULR

[16] Tests performed on 30/09 – 01/10/2015, 29 – 30/10/2015, 16 – 17/11/2015, 03 – 04/02/2016, 10 – 11/02/2016, and 16 – 17/03/2016.

and HR). The methods used are described in the Thermo Scientific™ Orion™ AQUAfast™ AQ3700 user guide (methods 6.5 and 6.6) and the Hach™ datasheet method 10205.

The concentrations of total and dissolved organic carbon (TOC and DOC), total carbon (TC), and total and dissolved nitrogen (TN and DN) were quantified both in the raw and filtrated samples using a Shimadzu TOC-L analyser (Shimadzu, Japan) equipped with an autosampler and TBM-L unit from the same manufacturer. Standard solutions of total organic carbon (500 mg-C.L^{-1} – 1.0624 g.L^{-1} Potassium Hydrogen Phthalate) and total nitrogen (100 mg-N.L^{-1} – 0.72196 g.L^{-1} Potassium Nitrate) were injected during each analysis in order to verify the accuracy of the measurements. A magnetic stirrer was inserted in each vial containing an unfiltered sample.

The concentrations of chemical oxygen demand (COD) and its soluble fraction (sCOD) were measured via colorimetry (Thermo Scientific™ Orion™ AQUAfast™ AQ3700 colorimeter, tests COD TT, or colorimeter Hach™ DR3900™, tests TNT plus™ vial tests COD HR). The methods used are described in the Thermo Scientific™ Orion™ AQUAfast™ AQ3700 user guide (methods 1.3.0, 1.3.1, and 1.3.2), or the Hach™ datasheet method 10236.

The total cell counts of coliforms and *E. coli* were quantified using the IDEXX Quantitray® Colilert-18® method. Wastewater influent and HRAP samples were diluted 20 000 and 1 000 times, respectively, in distilled water, using glassware cleaned with detergent and thoroughly rinsed with distilled water prior each measurement. The detailed procedure for *E. coli* cell counting is described in Appendix 5.

All samples were immediately stored in the fridge upon arrival to the laboratory. Dry weight, colorimetry, and bacterial counts analyses were conducted as soon as samples arrived at the laboratory (i.e. all analyses were finished within 4 hours after sampling). Ammonia and COD concentrations were quantified weekly while IC and TOC analyses were carried out every two weeks. For this purpose, both filtered and unfiltered samples were frozen after filtration and thawed the day of analysis.

2.2.2. LABORATORY EXPERIMENTS

The mechanisms of decay identified in the literature review were investigated at laboratory scale through experiments aimed at isolating and quantifying their impact individually. The experiments performed are summarized in Table 2 - 2 (sunlight-mediated mechanism), and Table 2 - 3 (dark mechanisms) also showing the parameters reported to impact the respective actions of each mechanism.

The impact of predation was not assessed as a suitable assay could not be developed during the timeframe of this study. No investigation of the impact of DO concentration on sunlight disinfection was performed however impact of DO concentration on overall decay was investigated during bench experiments. No studies involving the addition of known photosensitizers or ROS scavengers were carried out as it was believed to artificially inflate (respectively mitigate) exogenous photo-oxidation and therefore over-represent the significance of this mechanism compared to full scale HRAPs[17].

Table 2 - 2: Sunlight-mediated mechanisms screening experiments performed at laboratory scale

Mechanism	Experiment to determine the potential of the mechanism	Parameters of interest
Sunlight-mediated mechanisms: - **Direct UV-B damage** - **Endogenous photo-oxidative damage** - **Exogenous photo-oxidative damage**	Direct exposure of *E. coli* to sunlight of known spectrum. Because exposition to different part of the spectrum is known to help identify the origins of the decay, reactors were exposed to: 1- Full solar spectrum 2- Solar spectrum minus UV-B radiations The experiment were conducted in transparent culture medium (or RO water), and filtrated wastewater or HRAP broth in order to mix *E. coli* with potential photosensitizers.	- Suspended and dissolved matter - Wavelength of the light source - Incident sunlight intensity - DO (not controlled for practical reasons) - pH - Temperature (not controlled for practical reasons) - Photosensitizers

Table 2 - 3: Dark mechanisms screening experiments performed at laboratory scale

Mechanism	Experiment to determine the potential of the mechanism	Parameters of interest
Predation	Not investigated	NA
Chemical toxicity	*E. coli* decay was recorded in RO water, sometimes after addition of ammonium chloride to reach different concentrations representative of HRAPs chemistry. Tests at different pH and temperature were performed to investigate the toxic impact of pH. Tests in basic pH were also performed in presence of NH_4^+/NH_3 salt to force the equilibrium toward NH_3	Temperature pH NH_3 concentration
	E. coli decay was recorded when inoculated in wastewater filtrate in darkness over several days	Temperature pH
Algal toxicity	*E. coli* decay was recorded inoculated in filtrates from algal pure cultures and pilot scale HRAP	Temperature pH
Natural death	Dark controls performed in every experiments served to quantify natural decay	

[17] Such experiments would however be of great value if supported by ROS concentration measurements in the experimental broth and measurements of ROS content in real HRAP broth.

All experiments included a suite of 'standard steps' aiming to 1) cultivate *E. coli*: 2) prepare the experimental broths; 3) inoculate *E. coli* cells in the experimental broths; and 4) incubate the test cultures under specific conditions. Experiments investigating 'dark mechanisms' were conducted indoor in darkness in 150 mL covered E-flasks while experiments investigating 'light-mediated mechanisms' were conducted outdoor (laboratory rooftop) in opened 100 mL beaker (outdoor dark controls were conducted in 150 mL E-flasks covered with aluminium foil).

2.2.2.1. *E. coli* pure strain selection and maintenance

A non-pathogenic strain *E. coli* ATCC® 10536™ was initially selected to minimize risks. It was however later thought that this strain, which had been cultivated in the laboratory for several decades, might have lost some phenotypic characteristics and thus not be a relevant model organism[18]. Hence, 'wild' *E. coli* strains were isolated from samples of positive Quanti-Tray wells performed on the pilot scale HRAP (see 2.1.3) serially diluted in 5 $mg.L^{-1}$ peptone water. These serial dilutions were immediately spread-plated on Brain Heart agar and grown overnight. Single colonies with aspects consistent to *E. coli* colonies were subsequently plated on brain heart agar and grown overnight. Four strains were thus isolated and plating on Eosin Methylene Blue agar confirmed two of these bacteria were *E. coli*. These are henceforth referred to as *E. coli* #1 and *E. coli* #2.

For long term conservation at 4°C, colonies of each strain (ATCC® 10536™, #1, and #2) were plated and grown overnight on brain heart agar typically every third month. Cultures grown overnight in liquid brain heart broth were used as back-up in case *E. coli* cells from plates were dead, which occurred on one occasion. In this occurrence, the liquid culture was serially diluted, and the dilutions were spread-plated. Each time the stock cultures were renewed, a colony isolated from the "old" plates was tested on Eosin Methylene Blue agar to confirm the presence of *E. coli*.

Before each experiment, the strain to be tested was inoculated in 25 mL of liquid brain heart broth and grown overnight at 37°C in an incubator. The liquid culture was then stored in the fridge until the day of the experiment. On the day of the experiment, the liquid culture was centrifuged at 4,400 rpm for 10 minutes (Eppendorf® centrifuge 5702). The liquid medium was immediately discarded and the cells were re-suspended in 30 mL of reverse osmosis (RO) water. The resuspension was left to rest for 30 minutes as early tests showed *E. coli* ATCC® 10536™ counts were impacted immediately after centrifugation before quickly recovering. Although strain ATCC® 10536™ was likely to be more sensitive to centrifugation than the wild strains, this protocol was used during the entire study. Then, 2

[18] Professor Steve Flint, Massey University, is gratefully acknowledged for this important suggestion.

mL from the resuspension (mixed before sampling) was aseptically inoculated into the test flasks consistently resulting in an initial cell count between $2.0 \cdot 10^7$ and $2.0 \cdot 10^8$ CFU.mL^{-1}.

2.2.2.2. Experiment protocols

The glassware used was autoclaved or thoroughly washed with detergent prior to the experiment to avoid any contamination interfering with the results. Following inoculation, the cultures were continuously agitated at 200 rpm using an orbital shaker (IKA® KS 260 control) and incubated under the targeted conditions. Samples were withdrawn at pre-decided intervals relevant to the expected[19] decay coefficient. The shortest feasible time interval to perform the counting procedure on every assay (up to 12 reactors for one experiment) was about 30 minutes.

Sunlight direct damage:

E. coli cells were introduced in distilled water (to prevent the presence of exogenous photosensitizers) in open beakers exposed to direct sunlight. The *E. coli* decay coefficients calculated from the cell count reduction recorded in these tests is henceforth reported as 'sunlight direct damage' caused by direct DNA damage and/or endogenous photo-oxidation, most likely caused by UV-Bs (see Chapter 1 section 1.3.3.3.). This experiment was repeated at pH 10 using the buffer described in Table 2 - 4. Dark controls were conducted in 150 mL E-flasks covered with foil.

UVA and visible radiation damage:

Open beakers were incubated outdoor and covered with optical filter (Schott® WG320, see specification in Appendix 6) to prevent transmissions of radiations below 320 nm to the media. Distilled water was again used as medium to prevent exogenous photo-oxidation. Only endogenous photo-oxidation related to longer wave radiation was therefore expected to contribute to *E. coli* decay in these trials (see Chapter 1 section 1.3.3.3.). Dark controls were conducted in 150 mL E-flasks covered with foil.

Exogenous photo-oxidation:

E. coli decay was assessed in open beakers incubated outdoor using wastewater or HRAP filtrates as experimental broths in order to introduce natural photosensitizers. This experiment was repeated at pH 10 by adding carbonate buffer to the HRAP filtrate (see Table 2 - 4). The specific contribution of UVA and visible wavelengths (VIS) to exogenous photo-oxidation was also investigated by covering beakers filled with HRAP filtrates with the optical filters Schott® WG320. Dark controls were conducted in covered 150 mL E-flasks to quantify the impact of the filtrates on *E. coli* survival.

[19] e.g. previously recorded in preliminary experiment

pH-mediated toxicity:

E. coli decay was assessed in 150 mL E-flasks filled with different pH-buffers[20] (see Table 2 - 4) ranging from pH 7 to 10.8[21], pre-incubated for 30 min at the desired temperature before inoculation. The flasks were then inoculated and incubated (incubator Contherm® Digital Series Five) at constant temperature ranging from 5 to 35°C[22] and continuous agitation.

Table 2 - 4: pH buffers recipe (from Dawson et al., 1986)

Buffer Formula	pH expected (25°C)
20 mL 0.2 M KH_2PO_4 30 mL 0.2 M Na_2HPO_4	7.0
2.5 mL 0.2 M KH_2PO_4 47.5 mL 0.2 M Na_2HPO_4	8.0
45 mL 0.1 M $NaHCO_3$ 5 mL 0.1 M Na_2CO_3	9.2
25 ml 0.1 M $NaHCO_3$ 25 mL 0.1 M Na_2CO_3	9.9
5 mL 0.1 M $NaHCO_3$ 45 mL 0.1 M Na_2CO_3	10.8

Ammonia toxicity:

The impact of ammonium/ammonia on *E coli* decay was assessed in 150 mL E-flasks filled with 50 mL of either pH buffer (see Table 2 - 4 above) or pure distilled water, and 1 mL of ammonium chloride stock solution (3.7 mM or 109 mM) to reach a final total ammonium + ammonia concentration of 1 or 30 mg $N\text{-}NH_3$/L at pH of 8 to 10 (distilled water was used a control). These concentrations were selected as being representative of the typical ammonium/ammonia concentrations found in HRAP effluent and primary wastewater, respectively (see Chapter 3 section 3.1.2. and 3.2.2.). The pH was varied as ammonium is converted into ammonia at high pH (pKa = 9.25).

The post experiment check for ammonia concentration generally found levels were lower than expected. Reactors projected to hold 30 mg $N\text{-}NH_3.L^{-1}$ were controlled between 25.7 and 29.4 mg $N\text{-}NH_3.L^{-1}$ with one exception measured at 31.8 mg $N\text{-}NH_3.L^{-1}$. The ammonia in two reactors projected to hold 0.5 mg $N\text{-}NH_3.L^{-1}$ was below the detection of the colorimetric test[23] despite one reactor prepared in the same conditions resulting in a 1.8 mg $N\text{-}NH_3.L^{-1}$. Finally, two reactors prepared in different conditions projected to hold 50 mg $N\text{-}NH_3.L^{-1}$ were controlled with 11.8 and 13.8 mg $N\text{-}NH_3.L^{-1}$. The reason for this shift is unknown but possible explanations are ammonia volatilization (not expected to be significant as the flasks were not actively aerated), ammonium assimilation by *E. coli* (unlikely as the absence of other essential nutrients prevented growth), or experimental error. Nevertheless, measurements from all reactors were included in the analysis, and the impact of NH_3 on *E. coli* decay was studied by separating results by NH_3 levels (wastewater or

[20] The buffers were not autoclaved in order to prevent change in equilibrium properties affecting pH
[21] Representative range for HRAP broth, see Table 1 - 3 and Chapter 3 section 3.2.3.
[22] Representative range for HRAP broth, see Table 1 - 3 and Chapter 3 section 3.2.3.
[23] 0.02 mg $N\text{-}NH_3.L^{-1}$

HRAP level) from projected concentrations, rather than based on the measured concentrations.

Toxicity of algal metabolites and wastewater constituents:

The potential impact of extracellular algal metabolites was investigated by exposing *E. coli* to filtrates from algal cultures. For this purpose, 2×100 mL of HRAP A culture was mixed with 2×25 mL of primary-treated wastewater (Palmerston North wastewater treatment plant) in 2×250 mL E-flasks (samples collected on the same day 28 June 2016, process repeated on 30 June 2016). The E-flasks were then incubated (incubator INFORS HT Minitron, at 25°C, 2% CO2-enriched atmosphere, continuous illumination at 14W.m^{-2} of photosynthetically active radiation as described by Béchet et al. 2015) until the day of the experiment. This 'algae cultivation' step was used to enhance the content in potentially toxic compound excreted by the algae (and/or other organisms present). On the day of experiment, algal solutions were filtered through GF/C™ grade (General Electric®) fiberglass filters and added to foil-covered 150 mL E-flasks. The filtrates were not autoclaved to avoid the deactivation of potentially toxic compounds. Sampling was performed 2, 3, and 7 days after inoculation. Similar tests were carried out using centrifuged or filtrated wastewater as experimental broths.

Heat inactivation:

Because HRAP broth temperature can be expected to rise above 30°C potentially boosting natural decay with increasing temperature (Pachepsky et al., 2014), the natural decay of *E. coli* in distilled water or tap water was tested at 25 to 40 °C using a water bath. Dark controls in distilled water at temperatures ranging from 5 to 35°C when testing for pH toxicity also contributed to this investigation.

Starvation:

Because HRAPs broth may limit nutrients availability for growth and maintenance of *E. coli* cells, an analysis was performed using data from dark controls conducted with different substrates (i.e. RO water, buffered water, wastewater filtrates, HRAP filtrates). Certain dark controls were incubated up to 1 week aiming to force *E. coli* cells into starvation.

2.2.2.3. Experimental analyses

Microbial counting was performed using the pour plate method according to Eaton et al. (1998)[24]. Briefly, 1 mL samples were collected from tested reactors and serially diluted in

[24] The use of advanced molecular tools for *E. coli* cell counts (e.g. qPCR) was considered for laboratory experiments study, but plate counting was preferred since the capacity for advanced molecular analysis was not available in our laboratory and developing the capacity or subcontracting such analysis was prohibitively expensive for our unfunded PhD.

buffered peptone water (Eaton et al., 1998, method 9050C) under aseptic conditions. 1 mL of diluted sample was then poured into a petri-dish and mixed with standard count agar. The dishes were finally left to solidify and incubated 48 hr at 37°C. When possible, only the results of plates showing 20-200 colonies are presented. A more detailed protocol can be found in Appendix 7.

When necessary (e.g. pH tests, temperature tests, and rooftop experiments where overheating could be an issue), pH and temperature (Multimeter Thermo Scientific™ Orion Star™ A326) where recorded at the time of the last sampling. When testing the effect of ammonia, ammonium/ammonia concentration was checked at the time of the last counting (same method as described in section 2.2.1.3.), as well as in test reactors prior to the beginning of the study[25].

2.2.2.4. Data analysis

Laboratory experiment in darkness:

E. coli decay was observed to follow first order kinetics in stable harmful conditions. Assuming no *E. coli* growth in the tested conditions[26], *E. coli* decay coefficient was therefore determined as the slope of the linear regression between the natural logarithm (ln) of the cells counts and the time of sampling when three or more time points were obtained from a single experiment as commonly done in the literature (Blaustein et al., 2013; Kadir and Nelson, 2014; Kapuscinski and Mitchell, 1983). If only two points were available, or if the linear regression was poor, the decay coefficient was simply calculated as $\frac{\ln\left(\frac{C_0}{C}\right)}{t-t_0}$ where C_0 and C are the values of the cell counts at the initial and second (or latest suitable) times of samplings, respectively, and t_0 and t are the respective times of samplings (Dias and Von Sperling, 2018). When the decay was too fast to be quantified (i.e. no viable cells left at the time of the second sampling), the decay coefficient was reported as being greater than $\frac{\log(C_0)}{t-t_0}$ where t_0 is the time of the initial sampling and t is the time of the second sampling.

Rooftop experiments under natural sunlight irradiation:

Due to exposure to variable sunlight intensity and/or temperature, a linear regression over the data recorded was not meaningful. Hence, the decay coefficient was calculated between

[25] Such reactors were prepared similarly to the experimental broths, only for the purpose of checking ammonia concentration, and were thus not inoculated with *E. coli*.

[26] The absence of growth of indicators outside a host is a critical assumption for the use of a pathogen removal indicator (Table 1 - 2). This is valid in particular for *E. coli* (Edberg et al., 2000) meaning no growth was expected during laboratory scale (as well as bench scale and pilot scale) experiments. In addition, the monitoring of *E. coli* cell count in filtrates, therefore in presence of organic material and nutrients readily available to support *E. coli* growth never evidenced an increase in cell count further confirming the validity of this assumption.

each consecutive data point recorded following the calculation method used for dark experiment with only two points available. Data for light intensity was obtained from the National Institute of Water and Atmospheric Research Ltd (NIWA) database (Palmerston North, location agent number 21963)

2.2.3. BENCH EXPERIMENTS

2.2.3.1. Set-up

Rather than seeking to isolate a specific disinfection mechanism as done for laboratory experiments, bench experiments were aimed at recreating relevant but controllable conditions to confirm and refine findings from laboratory experiments. Bench scale experiments were therefore conducted outdoor (natural sunlight) under conditions 'as relevant as possible' to the conditions experienced by *E. coli* cells in HRAPs. For this purpose, two column reactors (3.8 and 5.0 L working volume, 25 cm deep, 14 and 16 cm diameters) mixed using a vertical propeller (RW 20 Janke & Kunkel, IKA Werk, Staufen, Germany) were set-up and operated at Palmerston North, New Zealand (40°23'15"S 175°37'08"E). The sides of the reactors were covered with opaque tape up to the 25 cm mark so that sunlight could reach the algae only from the liquid surface. The propeller speed was adjusted to match the liquid-gas mass transfer coefficient experienced in the pilot scale HRAP. The mixing performance of the propeller at the corresponding speed was deemed satisfactory based on colorimetric visual assay[27]. The reactors were also equipped with a bubbler (flat spiral coil shaped). When the bubbler was in use (see below), the propeller was removed since aeration also provided mixing.

2.2.3.2. Experiments start-up

The experimental broth consisted of HRAP broth collected on the morning of the experiment. Although *E. coli* was present in this broth, *E. coli #1* was seeded in each reactor prior to the start of each experiment in order to obtain a consistent initial *E. coli* cell count[28]. Hence, 50 mL *E. coli* #1 liquid culture was centrifuged 10 min at 4,400 rpm (Eppendorf® centrifuge 5702) on the day of the experiment, the liquid medium was discarded, and the cells were resuspended in ca. 30 mL of tap water. Then, 0.2 mL of the resuspension was injected in each reactor leading to initial *E. coli* cell densities similar to the natural levels reported in the pilot scale HRAPs.

[27] The reactor was filled with distilled water and a few drops of bromothymol blue. Addition of 0.1 M HCl or NaOH solutions would change the broth colour from yellow to blue. The mixing was found to provide a uniform colour in the reactor within 20 second after addition of the acidic or basic solution.

[28] Wild type *E. coli* was used as it was the strain available being the most representative of field conditions.

Figure 2 - 3: Bench experiment full set up during light assay.
Gas bubbling is visible in the reactor on the right

Figure 2 - 4: Bench experiment full set up during dark assay

2.2.3.3. Experimental conditions tested

The set of conditions listed in Table 2 - 5 were tested in bench experiments covering the range of conditions that could be observed in HRAP. When needed, the concentration of DO was reduced below 2 $mg.L^{-1}$ by bubbling N_2 gas and the pH was kept neutral by adding either 0.1 M HCl or 0.1M NaOH during the experiment. Temperature was not controlled. The effect of high DO concentration and/or high pH in darkness was assessed by reseeding the reactors with *E. coli* #1 at the end of an experiment (when the values of DO and/or pH were at their peak values), and by covering the reactors with cardboard (Figure 2 - 4).

Table 2 - 5: Set of conditions tested during bench experiments

DO concentration	pH	Light
High	High (> 10)	Sunlight
Low	High (> 10)	Sunlight
High	Neutral	Sunlight
Low	Neutral	Sunlight
High	High (> 10)	Dark
Low	High (> 10)	Dark
High	Neutral	Dark
Low	Neutral	Dark

2.2.3.4. Sampling and analysis

The reactors were sampled every 30 minutes to 1h, a single experiment lasting 2h as it was the interval deemed necessary to trigger significant *E. coli* decay in batch conditions. Samples were diluted in distilled water by a factor 10^2 or 10^3 depending on the decay expected by pipetting respectively 1 or 0.1 mL of sample into a 100 mL volumetric flask. *E. coli* cell count was quantified using the IDEXX Quantitray® Colilert-18® assays described in 2.1.3. pH, DO, and the temperature was logged during experiments using multimeters Thermo Scientific™ Orion Star™ A326 (probes visible in Figure 2 - 3).

Due to the time available to complete experiments, two sunlit experiments and one experiment in the dark were performed in this order for each day of experiment.

2.2.3.5. Data analysis

Influence of environmental parameters on E. coli decay coefficient

Decay coefficients were calculated from two consecutive samplings as defined in 2.2.4. for rooftop laboratory scale experiment.

E. coli decay coefficients and/or log removal measured from bench experiments were studied according to the ranges of the different parameters studied (i.e. sunlight radiation intensity, pH, dissolved oxygen, and temperature). Data were regrouped into the following clusters:

- Per quartile of sunlight radiant energy

- Low (< 2 $mg.L^{-1}$) and high (> 8 $mg.L^{-1}$) DO concentration
- Low pH (< 8) and high pH (> 9.4)

As pH, DO concentration, and temperature experienced mild variations over a sampling period, the values used were evaluated as the averaged logged in between two samplings from which the decay coefficient was calculated.

Comparison of bench experiments results with laboratory experiments results

The *E. coli* decay coefficients measured during bench experiments were compared with decay coefficients expected following laboratory experiments. Based on the differences observed, relationships between environmental parameters and intensity of *E. coli* decay mechanisms developed at laboratory scale were recalibrated from bench scale results (because it was deemed more representative of HRAPs, see section 2.1). Remaining differences following the recalibration of results would highlight remaining knowledge gaps.

Chapter 3: Disinfection performance in HRAPs

While the disinfection potential of maturation ponds has been widely studied, specific data on HRAP is still scarce as highlighted in Chapter 1 section 1.2.3. The study of two pilot scale outdoor HRAPs was therefore carried out providing much needed data. This Chapter displays, analyses, and discusses the data obtained from this study. The set-up and measurements performed were extensively described in Chapter 2 section 2.2.1.

The conditions to which the HRAPs were subjected (i.e. weather and influent characteristics) are first presented giving context to the ponds' operations. The general HRAP performances in terms of environmental parameters and secondary wastewater treatment performance are then provided, in order to demonstrate that the HRAP was functioning consistently with expectations thus giving credibility to the later generalization of the measurements obtained. *E. coli* removal performances are then shown, with results presented from regular monitoring and analysed in light of the measured pond parameters, to explore the mechanisms of disinfection that are potentially involved. An analysis is then performed on "daily profiles", investigating the consequences on *E. coli* removal of the diurnal variations in the HRAP environment.

3.1. CONDITIONS EXPERIENCED BY THE HRAPS

The following section presents the weather conditions which the HRAPs were experiencing during the study (07/2015 –06/2017) as well as the characteristics of the wastewater fed to the HRAPs, thus providing context to the results presented in this Chapter.

3.1.1. CLIMATIC CONDITIONS

Weather data was obtained from the NIWA database for the Palmerston North weather station (agent number 21963) for the period of study of the pilot scale HRAPs, and is shown in Figure 3 - 1. As these results show, Palmerston North has a temperate climate, characterized by mild temperatures (rare frost and temperate summers) and significant rainfall. Summers were warm and tended to be dry, while winters showed high rainfalls and little sunshine.

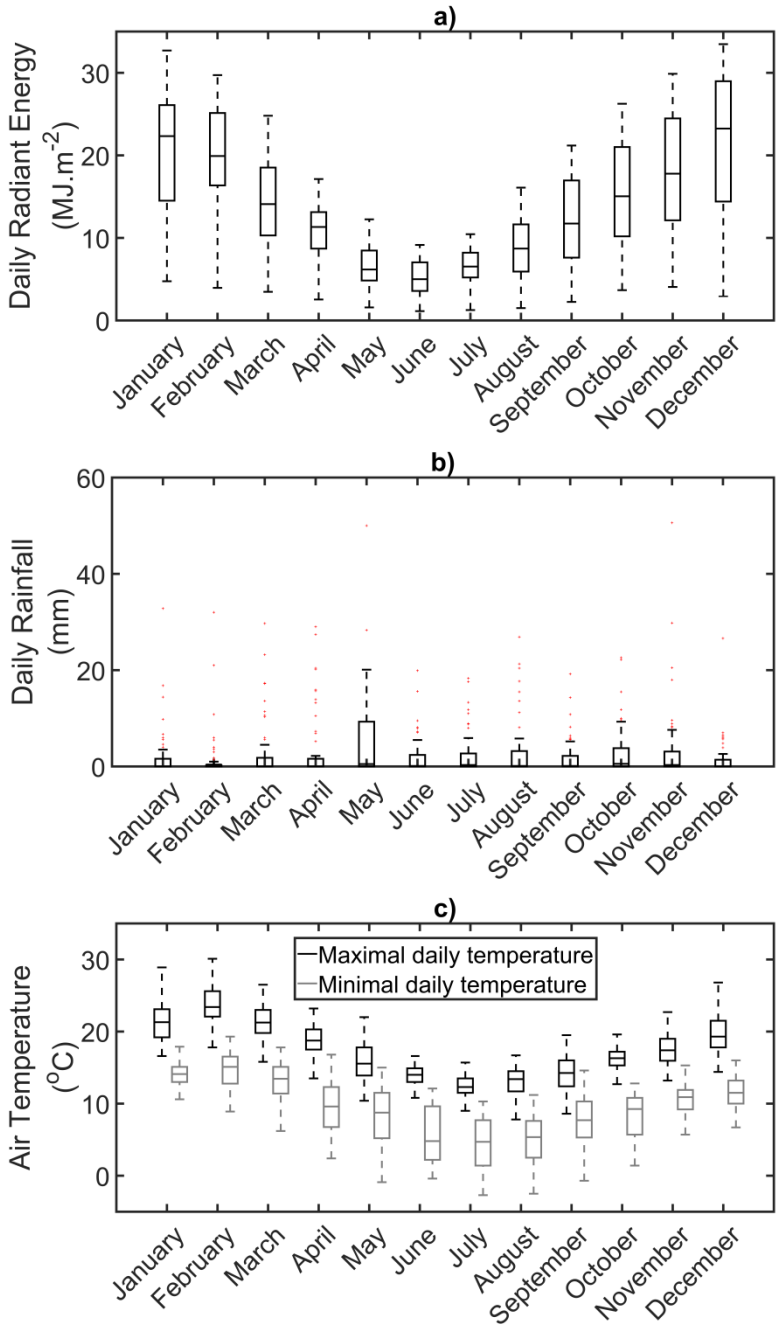

Figure 3 - 1 Meteorological conditions in Palmerston North: daily sunlight incident energy (a), daily precipitation (b, outliers are represented by red dots), and daily maximum and minimum temperature[29] (c).

3.1.2. WASTEWATER CHARACTERISTICS

As described in Chapter 2 section 2.2.1.1., the HRAPs were fed with real domestic wastewater, at the Palmerston North wastewater treatment plant, downstream from a primary

[29] In each figure, the distributions are based on the following number of data points: January N = 62, February N = 57, March N = 62, April N = 60, May N = 62, June N = 55, July N = 62, August N = 62, September N = 60, October N =62, November N = 60, December N = 54 (several days of data were missing for June 2016 and December 2016).

settler. Monitoring of the quality of the wastewater fed to the HRAPs enabled us to determine the statistical distribution of the wastewater main characteristics as described in Table 3 - 1.

By comparing the measured characteristics with values for typical compositions of untreated wastewater as given by Eaton et al. (1998), the wastewater used was concluded to be in line with a typical medium strength wastewater. COD and TOC corresponded to a low strength wastewater, and the TSS concentration was below the value for a low strength wastewater (median value measured 78.06 $mg.L^{-1}$ against 120 $mg.L^{-1}$ reported for a low strength wastewater). This is not surprising as the wastewater was collected downstream of a primary settler. Hence, a significant amount of suspended solids, including those of organic origin, were removed compared to the values given by Eaton et al. (1998).

Exceptionally high concentrations of nitrate and nitrite were measured in the wastewater for two samples, while even high strength domestic wastewater is not expected to hold any.

E. coli cell counts were relatively high (median $3.91 \cdot 10^{6}$ MPN.100 mL^{-1} measured for *E. coli* compared to 10^{5} -10^{8} No.100 mL^{-1} for faecal coliforms in high strength untreated wastewater).

In conclusion, despite some exceptional events affecting its quality, the wastewater used was conform to typical domestic wastewater. This reassures us that the results obtained from the pilot HRAPs are transposable to full scale set-ups, provided the pond's operative conditions also conform to full-scale HRAPs.

Table 3 - 1: Statistical distribution of the characteristics of the wastewater fed to the pilot scale HRAPs[30]

	COD ($mg.L^{-1}$)	sCOD ($mg.L^{-1}$)	N-NH3 ($mg.L^{-1}$)	TSS ($mg.L^{-1}$)	Chloride ($mg.L^{-1}$)	Nitrate ($mg.L^{-1}$)	Nitrite ($mg.L^{-1}$)	Phosphate ($mg.L^{-1}$)	Sulphate ($mg.L^{-1}$)	TOC ($mg.L^{-1}$)	TC ($mg.L^{-1}$)	IC ($mg.L^{-1}$)	TN ($mg.L^{-1}$)	DOC ($mg.L^{-1}$)	DC ($mg.L^{-1}$)	DIC ($mg.L^{-1}$)	DN ($mg.L^{-1}$)	*E. coli* (MPN.100 mL^{-1})
5 percentile	123	48.5	7.07	42.2	4.02	0.00	0.00	2.11	14.6	41.1	60.1	14.3	14.7	18.5	36.6	7.62	6.95	$1.30 \cdot 10^{6}$
25 percentile	185	83.4	17.8	60.0	34.0	0.08	0.00	4.52	23.0	64.8	94.1	22.7	37.0	33.6	57.5	16.2	24.3	$2.52 \cdot 10^{6}$
Median	238	109	23.4	78.1	41.0	0.46	0.38	6.12	28.6	83.2	116	28.8	45.7	46.6	72.5	23.3	32.7	$3.91 \cdot 10^{6}$
75 percentile	318	144	29.7	110	50.9	1.96	0.98	7.81	36.8	104	141	38.4	53.0	60.0	88.0	32.9	41.9	$6.15 \cdot 10^{6}$
95 percentile	507	200	37.4	225	86.0	6.79	2.83	9.66	59.3	138	169	50.8	68.6	170	197	45.2	55.4	$1.10 \cdot 10^{7}$
Max	1157	690	43.8	557	165	154	61.0	168	113	192	223	63.9	118	802	818	67.0	105	$2.60 \cdot 10^{7}$
Min	49.0	13.0	1.50	21.7	0.04	0.00	0.00	0.14	5.48	21.1	17.7	4.87	0.50	12.1	17.7	0.22	0.70	$6.20 \cdot 10^{4}$
Mean	279	122	23.2	98.1	43.7	2.41	1.63	7.83	32.1	86.2	117	30.7	44.7	65.7	90.6	24.9	33.1	$4.74 \cdot 10^{6}$
Std	166	80.9	9.22	71.9	22.1	11.5	7.31	16.7	15.4	30.5	33.7	11.7	17.3	96.1	94.7	11.7	16.0	$3.37 \cdot 10^{6}$
N	87	79	89	206	188	188	184	182	188	189	189	188	183	184	184	184	178	142

[30] The complete monitoring of *E. coli* cell count in the wastewater for the duration of the study is shown in Appendix 8.

3.2. THE GENERAL PERFORMANCES OF HRAPS

This section presents the behaviour of the pilot scale HRAPs, first in terms of operation, then in terms of effluent characteristics, and finally in terms of environmental conditions of the algal broth (i.e. pH, temperature, and DO concentration).

The aim is to provide evidence that the HRAPs were operated in conditions relevant to full scale ponds and that the results of the disinfection performance analysis can therefore be extended to HRAPs at any scale for "normal" operations.

3.2.1. HRAP OPERATIONS

While the depth was fixed at 0.25 m (within the range of typical values for HRAPs, see Chapter 1, Table 1 - 3), the HRT and paddlewheel speed used could be varied.

As explained in Appendix 3, the HRT proved to be challenging to control, while temporary breakdowns affected the paddlewheel speed. Table 3 - 2 displays the statistical distribution of the values reported for both these parameters. Only values corresponding to normal operations of the HRAPs as defined in Chapter 2 section 2.2.1.1. were reported.

The paddlewheel speed was measured sporadically at first and regular measurement was only introduced later in the monitoring routine. The values shown in Table 3 - 2 are therefore only partially indicative of the HRAPs operation during this study.

The HRT was in the range of normal operations for HRAPs over 95% of the time (1 – 14 days, see Table 1 - 3). While the paddlewheel speed[31] has little meaning for a general HRAP set up as the mixing provided will depend on the geometry of the pond (e.g. depth, total volume, shape of the paddlewheel), the study shown in Appendix 9 highlighted the direct relationship in our set-up between the paddlewheel speed and the aeration coefficient of the HRAPs, and the paddlewheel speed and the linear speed of the HRAP broth. Both these coefficients have a direct meaning for the mixing and aeration conditions of HRAPs, and guidelines for linear speed of the algal broth were found to be in accordance with the values thus determined for this study (normal operations being 0.15 – 0.30 $m.s^{-1}$ as stated by Park et al., 2011). Unfortunately, little research was found investigating aeration coefficients for HRAPs. It was therefore not possible to give any context to the values reported.

[31] The paddlewheel speed is shown as it was the only 'mixing parameter' recorded on a regular basis

Table 3 - 2: Satistical distribution of HRAPs design variables

	HRT (d)	Paddlewheel speed (RPM)	Corresponding broth linear speed[1] ($cm.s^{-1}$)
5 percentile	7.47	6.50	14.5
25 percentile	8.67	9.50	21.2
Median	10.3	10.5	23.4
75 percentile	11.2	11.5	25.6
95 percentile	13.2	12.5	27.8
Max	17.0	12.7	28.4
Min	4.33	6.25	13.9
Mean	10.1	9.96	22.2
Std	2.01	1.98	NA
N	139	63	NA

[1] Calculated from the study presented in Appendix 9.

3.2.2. HRAP EFFLUENT CHARACTERISTICS

In this section, the performances of the pilot scale HRAPs used in the present study are compared with performances of HRAPs found in published literature. The aim is to provide evidence that the studied HRAPs had a normal behaviour and were representative of a full scale set-up.

The effluent characteristics measured for the pilot scale HRAPs (with the exception of *E. coli* removal characteristics for which results are extensively presented in section 3.3.), are shown in Table 3 - 3; the effluent quality in terms of performance of the pilot scale HRAPs (i.e. nutrient removal efficiencies and biomass productivity) are shown in Table 3 - 4; and performances of outdoor HRAPs fed with real wastewater, at scales ranging from pilot scale (0.2 m^3) to full-scale (4,375 m^3), as reported in the literature are shown in Table 3 - 5.

As can be seen in Table 3 - 5, HRAPs generally provide average to good removal of carbonaceous contaminants (here COD), similar to the pilot scale HRAPs which provided fair to average removal rates of TOC, COD (25-percentile above 50% and 75-percentile below 85% for all).

Average to high TN and ammonium removal rates were generally reported in the literature, ammonium removal efficiencies (RE) above 85% and up to 99% having often been found. This is also consistent with results from the pilot scale HRAPs which mostly showed very high removal of ammonia-N (25 percentile of 94.7%).

Phosphorous removal (total or orthophosphate) was often reported as poor despite occasional high removal rates, which compares well with the consistently poor RE found in the pilot scale HRAPs (13.9% average, 75-percentile of 53.3%).

The biomass productivity measured by the present study was in the lower range of the values reported in Table 3 - 5 although the values measured covered the whole range of published data.

As a conclusion, the pilot scale HRAPs studied here were found to behave as regular full scale outdoor HRAPs and the conclusions provided in the following with regards to *E. coli* removal are expected to be transferable for full scale HRAPs treating primary wastewater.

Table 3 - 3: Statistical distribution of pilot scale HRAP effluent characteristics

	TSS ($mg.L^{-1}$)	COD ($mg.L^{-1}$)	sCOD ($mg.L^{-1}$)	$N\text{-}NH_4^+$ ($mg.L^{-1}$)	Cl^- ($mg.L^{-1}$)	NO_3^- ($mg.L^{-1}$)	NO_2^- ($mg.L^{-1}$)	PO_4^{3-} ($mg.L^{-1}$)	SO_4^{2-} ($mg.L^{-1}$)	TOC ($mg.L^{-1}$)	DOC ($mg.L^{-1}$)	TN ($mg.L^{-1}$)	DN ($mg.L^{-1}$)
5 percentile	91.4	107	16.3	0.11	29.7	3.70	0.53	1.44	23.7	38.3	11.6	18.6	9.20
25 percentile	153	190	43.0	0.28	36.4	37.8	1.14	2.37	30.6	68.2	15.6	26.6	13.3
Median	248	274	79.0	0.52	42.4	51.5	1.70	3.56	35.3	94.2	19.8	31.5	16.2
75 percentile	324	345	117	1.38	47.9	72.0	3.07	4.62	41.2	119	25.4	36.3	19.6
95 percentile	488	535	186	8.31	61.3	100	13.6	7.72	50.3	188	51.7	47.6	25.4
Max	943	1157	690	10.5	83.9	140	40.1	161	69.1	324	398	69.6	30.1
Min	46.7	67.0	7.00	0.02	23.5	0.49	0.00	1.12	17.1	31.0	10.8	14.4	7.05
Mean	265	298	94.8	1.51	43.2	53.1	3.83	6.17	36.6	97.5	29.6	31.9	16.7
Std	146	175	93.3	2.44	10.1	28.1	6.56	18.8	8.61	48.7	47.7	8.30	4.74
N	137	70	67	56	133	133	132	133	133	133	131	130	115

Table 3 - 4: Statistical distribution of pilot scale HRAPs performances in terms of nutrients removal efficiencies (COD, TOC, N-NH_4^+, TN, PO_4^{3-}) and biomass productivity

	RE COD[1] (%)	RE TOC[2] (%)	RE N-NH_4^+ (%)	RE TN[3] (%)	RE PO_4^{3-} (%)	Productivity (g $TSS.m^{-2}.d^{-1}$)
5 percentile	42.9	54.9	69.4	37.8	-56.3	2.01
25 percentile	61.3	70.4	94.7	55.3	8.9	3.72
Median	74.8	76.1	97.9	64.5	34.6	6.16
75 percentile	81.3	81.7	98.9	72.9	53.3	8.63
95 percentile	93.3	87.8	99.6	81.4	75.8	15.79
Max	96.4	94.2	99.9	85.9	85.7	27.59
Min	11.5	32.8	38.8	29.2	-1594.3	0.99
Mean	70.7	74.4	93.4	63.8	13.9	7.03
Std	17.2	10.8	11.4	13.2	147.5	4.69
N	65	124	56	107	132	136

[1] Calculated using the measurements from the filtrated HRAP broth as the effluent value i.e. $RE = (COD_{WW} - COD_{HRAP\,filtrated})/COD_{WW}$ as performed by Posadas et al. (2015a) and Ruas et al. (2017);

[2] Calculated using the measurements from the filtrated HRAP broth as the effluent value i.e. $RE = (TOC_{WW} - TOC_{HRAP\,filtrated})/TOC_{WW}$ as performed by Posadas et al. (2015a) and Ruas et al. (2017);

[3] Calculated using the measurements from the filtrated HRAP broth as the effluent value i.e. $RE = (TN_{WW} - TN_{HRAP\,filtrated})/TN_{WW}$ as performed by Posadas et al. (2015a) and Ruas et al. (2017).

Table 3 - 5: Wastewater treatment performances achieved during outdoor real wastewater treatment in HRAPs (adapted from Muñoz and Gonzalez-Fernandez, 2017 and Young et al., 2017)

Wastewater	Volume (L)	HRT (d)	COD (Removal Efficiency RE, %)	Nitrogen (RE, %)		Phosphorous (RE, %)		Productivity ($g.m^{-2}.d^{-1}$)	Reference
				TN	N-NH4+				
Primary settled domestic	860	10.3	74.8	64.5	97.9	34.6		6.16	Present study (median values)
Facultative treated domestic	22,500	5	90.37 (BOD_5)	59.65	90				Banat et al. (1990)
Domestic	570	3 – 10		57 – 73					Garcia et al. (2000)
Primary pond treated domestic	38,250	7.5	22 (BOD_5)	86	86	66	59		Craggs et al. (2003)
Primary pond treated domestic	38,430	7.5	54.5 (BOD_5)	58.0	85	10.5	13.7		Craggs et al. (2003)
Swine manure	464	10	76 ± 11	88 ± 6 (TKN)		10		21 – 28	de Godos et al. (2009)
Swine manure	464	10	56 ± 3	98 ± 1		≤ 15			de Godos et al. (2010)
Primary domestic	4,375,000	8 - 9	50 (BOD_5)		65	19		8	Craggs et al. (2012)
Secondary domestic	530	10		60 ± 1				8.3 ± 1.4	Arbib et al. (2013a)
Secondary domestic	533	8		92.1 ± 1.4		95.1 ± 0.8		19.8 ± 0.4	Arbib et al. (2013b)
Sceptic tank treated domestic	61,400 – 124,000	4.5 – 9.1	90.2 - 93.4 (BOD_5)		61.1 – 73.5		6.5 – 21.2		Buchanan (2014)
Facultative treated domestic	61,400 – 124,000	4.5 – 9.1	51 – 72 (BOD_5)		35 - 83		0.02 – 0.1		Buchanan (2014)
Primary treated domestic	4,375,000	5.5 – 9			47 – 79	20 – 49			Sutherland et al. (2014a)
Primary domestic	4,375,000	5.5 – 9			79 ± 13	49 ± 22			Sutherland et al. (2014b)
Domestic	500	4 – 8	66 – 85		99				Matamoros et al. (2015)
Primary domestic	700 – 850	3 – 7	84 ± 7	79 ± 14		57 ± 12		4 ± 0 – 17 ± 1	Posadas et al. (2015a)
Fish farm + primary domestic	180	7 – 20	77 ± 7	83 ± 10 (TKN)		94 ± 6		5	Posadas et al. (2015b)
Septic tank treated domestic	64,000	5	91.8						Young et al. (2016)
Domestic	180	5 ± 0.4	67 ± 11	39 ± 6	96 ± 3	16 ± 4		4.2 ± 1.1	Ruas et al. (2017)

3.2.3. ENVIRONMENTAL CONDITIONS IN PILOT SCALE HRAPS

Because of the changing meteorological conditions and the influence of microbial activity, environmental conditions changed significantly in HRAPs across seasons. Results from 'continuous' data logging of temperature, DO concentration, and pH every 15 minutes (see Chapter 2 section 2.2.1.1.) are presented in Figure 3 - 2.

These results highlight the high variability of such parameters over both seasonal and monthly time scales. DO concentrations frequently reached above 20 $mg.L^{-1}$, and levels above 25 $mg.L^{-1}$ were occasionally observed. pH levels above 10 were commonly encountered (i.e. within the 95 percentile) over 7 months of the year, and pH levels above 11 were recorded in extreme cases. pH levels above 9.4, which were reported as the threshold of pH induced decay in the dark (Parhad and Rao, 1974), were frequently observed except for the period from April to August.

As can be seen, conditions in HRAP A and HRAP B were closely matched. This indicates that environmental conditions in HRAP are primarily dependant on external factors (i.e. meteorological conditions and operational factors) and that therefore results from this Chapter can be expected to show reproducibility. Nevertheless, pH and DO concentration occasionally differed significantly between both ponds (e.g. April): such differences were associated with the large colonisation of HRAP B by small animals which may have grazed on algae and therefore prevented larger variations of pH and DO concentration.

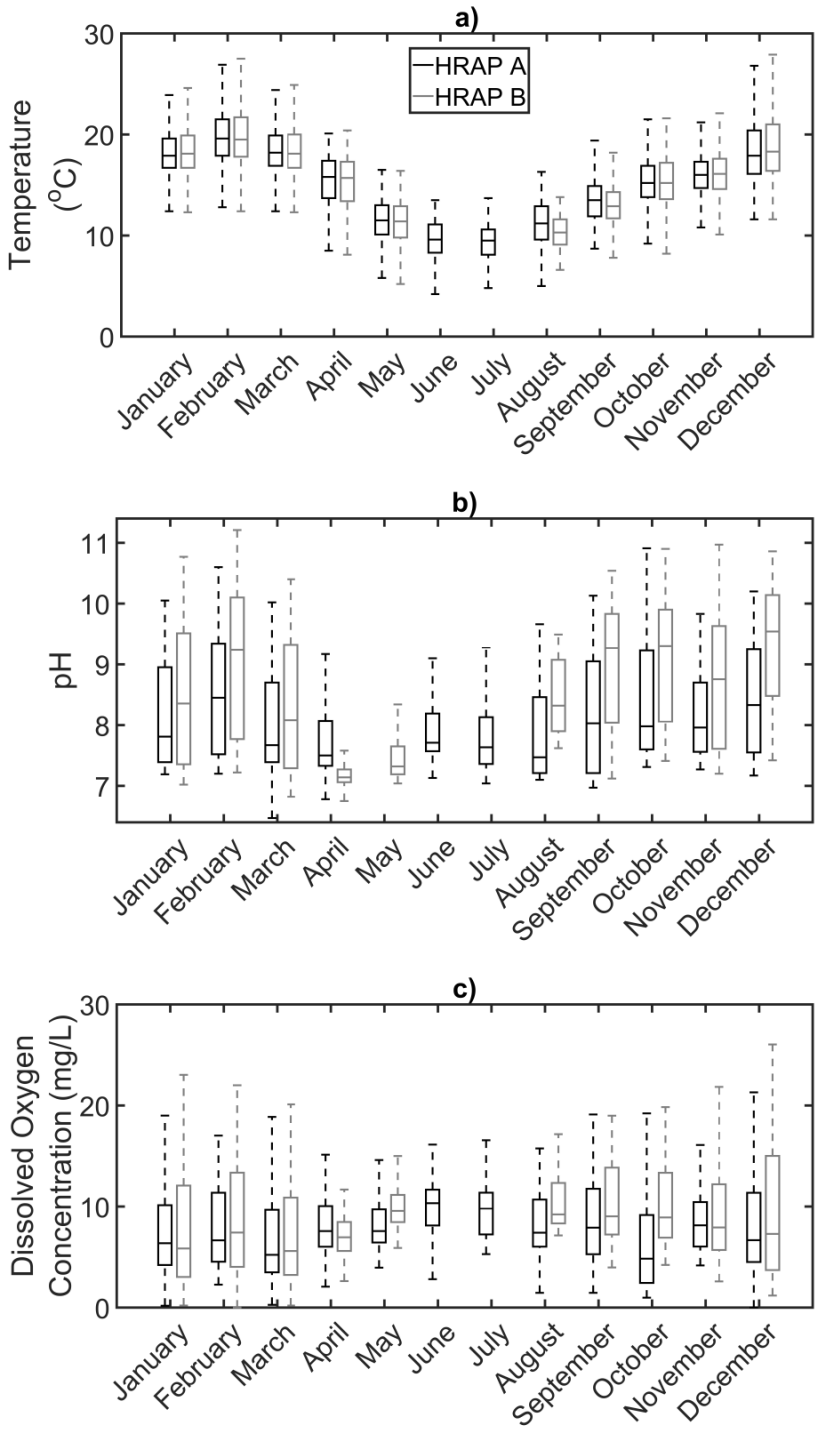

Figure 3 - 2: Results from temperature, pH, and DO concentration monitoring[32]

[32] See next page footnote.

Based on the temperature distributions, three main meteorological conditions can be distinguished, classified as:

- A warm season, from December to March, when minimum temperatures remained well above 10°C while maximum temperature could approach or exceed 25°C,
- A cold season, from May to August, when minimum temperatures were recorded as low as 5°C and maxima temperature would rarely reach 15°C,
- Transition seasons, including the months of April, and September, October, and November.

E. coli removal performances will be analysed in light of these seasons in the section 3.3.2.

3.3. *E. COLI* REMOVAL PERFORMANCE

3.3.1. RESULTS FROM GENERAL MONITORING

The disinfection performances calculated from regular monitoring of pilot scale HRAPs are displayed in Figure 3 - 3 in terms of *E. coli* cell counts (a)), *E. coli* log removal (b)), and *E. coli* decay coefficient (c)).

Results from both pilot scale HRAPs showed consistently high removal of *E. coli* (mean log-removal = 1.77, median = 1.81, N = 128) despite divergences in their general conditions (e.g. operational issues, TSS concentration, and nitrate concentration). The magnitude of *E. coli* removal in the pilot scale HRAPs was generally higher than that of MPs reported in the literature (mean log removal 1.29, median = 0.99 based on the values reported in Table 1 - 4[33])

[32] Number of data points for each set:

Temperature	January	February	March	April	May	June	July	August	September	October	November	December
HRAP A	2396	2208	3488	2783	2817	3029	3598	2871	2595	2240	2470	3027
HRAP B	2305	2190	2278	2785	2815	0	0	867	1018	2108	2499	2397

pH	January	February	March	April	May	June	July	August	September	October	November	December
HRAP A	2305	2213	3494	2788	0	3030	3600	2873	2599	2240	2472	2620
HRAP B	2308	2191	2780	2787	2819	0	0	867	826	2108	2502	2398

DO	January	February	March	April	May	June	July	August	September	October	November	December
HRAP A	2395	2208	3488	2783	2817	3028	3598	2871	2595	2239	2470	3027
HRAP B	2305	2190	2778	2784	2815	0	0	864	1018	2108	2499	2397

[33] Median and mean *E. coli* disinfection performance by MPs were calculated considering each value reported in Table 1 - 4 as an individual value with no other consideration to give any particular weight to a value compared with the others.

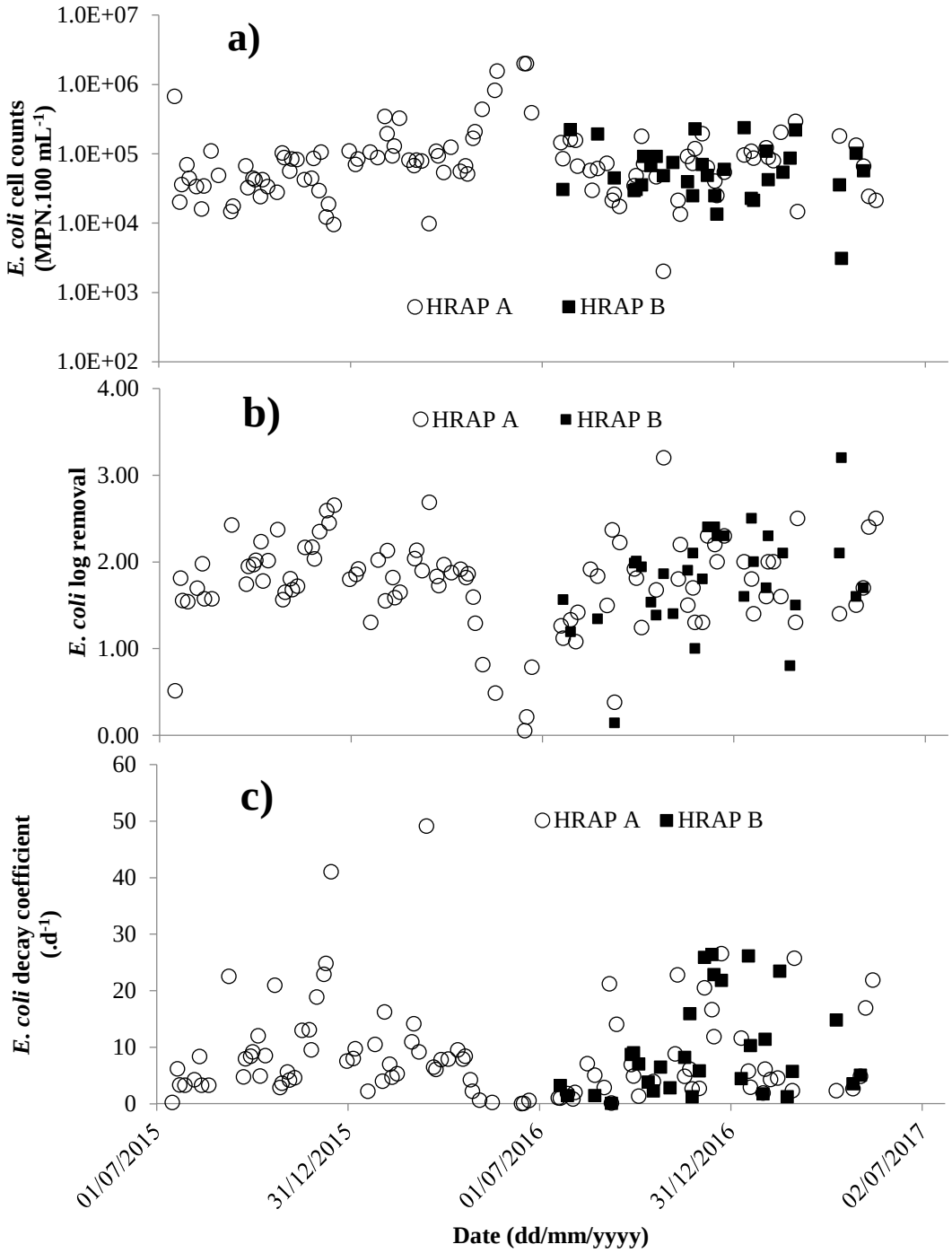

Figure 3 - 3: Pilot scale HRAPs disinfection performances. a) HRAP raw *E. coli* cell counts; b) HRAP performances in terms of *E. coli* log removal; c) HRAP performances in terms of *E. coli* decay coefficient[34].

[34] *E. coli* decay coefficient k was computed assuming no growth of *E. coli* in the algal broth and that HRAPs were at pseudo-steady state and well mixed, resulting in $k = \frac{1}{HRT} \cdot \left(\frac{C_{IN}}{C_{OUT}} - 1\right)$ (d^{-1}), where HRT is the hydraulic retention time (d), C_{IN} is the *E. coli* cell count of the influent (MPN.100 mL^{-1}), and C_{OUT} is the *E. coli* cell count of the effluent (MPN.100 mL^{-1}).

Significant variations in the disinfection performance of the HRAPs were recorded. Nine samples showed log removal below 1.0, and 29 were below 1.5. Three of the samples with log removal below 1.0 could be explained by low *E. coli* cell counts measured in the corresponding influent wastewater sample. All others disinfection performances below 1-log unit were reported between May and July when high rainfalls and poor sunlight radiation lead to very low algal concentrations, low pH, and low temperature.

Peak log removal levels of 3.20 were measured at two different samplings. Interestingly, one of these days was an averagely sunny late October day with no significant variations in pH, DO concentration, or temperature, while the other sample was obtained on a cloudy April day with almost no variation of the same parameters. As no peculiarity was noticed in any of the other parameters monitored, the high *E. coli* log removal in the first sample could not be clearly explained. However, the second was obtained from HRAP B at a time when this pond was visibly colonized by macroscopic invertebrates (possibly *cladocera*, unverified). This suggests that predation may contribute considerably to *E. coli* removal in HRAPs although such a performance was only reported once despite a period of colonization covering a couple of months.

In conclusion, with the exclusion of the worst winter days, HRAPs provided consistently high removal of *E. coli*. Large variations in the disinfection performances were nevertheless found over short time periods, probably reflecting the multiplicity of the factors involved in *E. coli* removal in HRAPs.

The pilot scale HRAP disinfection performance herein reported agrees with the literature on other existing HRAPs (see Table 1 - 5). Ruas et al., (2017) and Young et al. (2016) reported *E. coli* removal performance generally higher than what was observed during our study. However, Ruas et al., (2017) study was carried out under tropical climate and in a greenhouse resulting in significantly higher broth temperature. In the study by Young et al. (2016), results were obtained in arid but temperate climate in winter. Because the set-up used is the same as Buchanan, (2014) and Fallowfield et al. (2018) who reported disinfection performance similar to our set-up, it is unclear what caused the discrepancy with our studies.

3.3.2. SEASONAL VARIATIONS OF *E. COLI* DECAY COEFFICIENT IN HRAP

Since the mechanisms that were identified in the literature as affecting *E. coli* removal in HRAPs were reported to be influenced by mostly seasonal parameters (e.g. sunlight radiation, algal activity, see Chapter 1 section 1.3.3.), *E. coli* decay coefficient measured in the pilot scale HRAPs were expected to show seasonal dependence. However, no obvious

seasonality can be seen in Figure 3 - 3 for *E. coli* raw cell count, log removal, and decay coefficient besides a sharp drop in performance in winter.

In the case of *E. coli* raw cell counts and log removal in the HRAPs, the lack of clear seasonal variability may be caused by consistently higher concentrations of *E. coli* in the wastewater in summer (see Appendix 8). In addition, in order to preserve algae and prevent wash-out at times of high rainfall and low sunlight irradiance, the HRT was set at a 10 days target in winter as opposed to 7 days (and occasionally below) for the rest of the year. Therefore, the "*E. coli* loading" in the HRAPs during summer was significantly higher than during winter.

The loading should however not influence decay coefficients fluctuations. To investigate if any trend could be observed, an extended analysis was performed. Figure 3 - 4 groups the decay coefficient data by month providing the statistical distribution of the *E. coli* decay coefficients for each month, allowing comparison with the environmental parameters provided in Figure 3 - 2. Figure 3 - 5 shows the statistical distribution of the decay coefficient per meteorological period as defined in section 3.2.3.

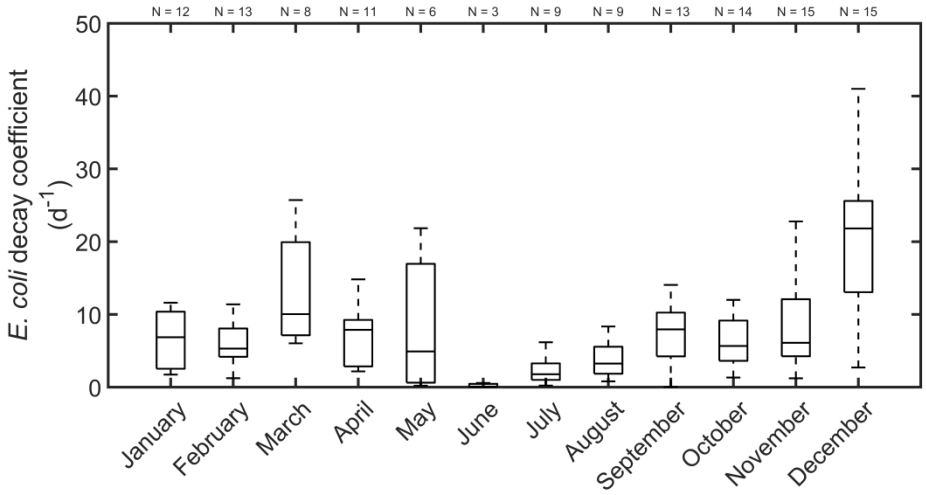

Figure 3 - 4: Distribution of *E. coli* decay coefficient per month.
The distributions are based on the following number of data points: January N = 12, February N = 13, March N = 8, April N = 11, May N = 6, June N = 3, July N = 9, August N =9, September N = 13, October N =14, November N = 15, December N = 15.

Figure 3 - 4 fails to show clear seasonal trends for the decay coefficient. Although poor and average decay coefficients were consistently recorded during the winter and spring months respectively, only average decay coefficients were found in January and February, with

higher decay coefficients found on average in March and more unexpectedly in May[35]. The highest performances were reported in December but the wide spread in the results reflects inconsistency in the HRAP performance. Figure 3 - 5 shows a clearer seasonal dependence of *E. coli* decay coefficient but also shows its inconsistency.

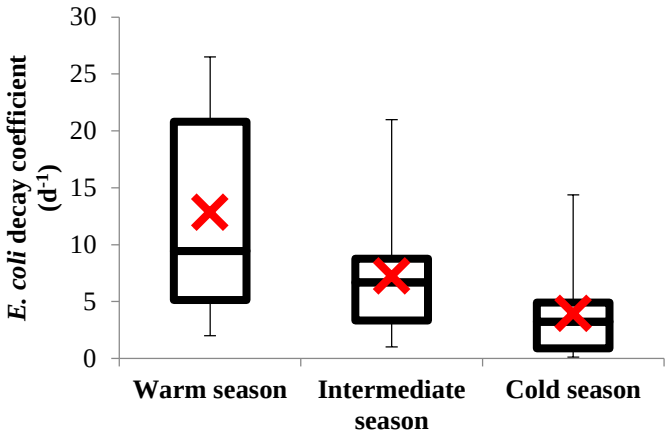

Figure 3 - 5: Statistical distribution of *E. coli* decay coefficient for each season
(N = 48, 36, 27 for warm, intermediate, and cold seasons respectively, box-plots represent the 5, 25, 50, 75, and 95 percentile, red-crosses represent average values).

In conclusion, mechanisms of *E. coli* removal influenced by parameters having seasonal variations (e.g. sunlight radiation, algal activity) are likely to be significant but either inconsistent or shadowed by other 'non-seasonal' mechanisms.

3.3.3. RELATIONSHIP BETWEEN *E. COLI* REMOVAL AND HRAP PARAMETERS

In order to further investigate whether the present study of *E. coli* removal in pilot scale HRAPs could help determine which mechanisms[36] are potentially significant, *E. coli* decay coefficient was tested for correlation with all the parameters monitored during this study by individual linear regression. The complete results of these linear regressions (R^2, N, and p-value[37]) are shown in Table S10 - 1 (Appendix 10).

[35] Higher performances recorded in May could be related to the macroscopic invertebrate invasion but no evidence can be provided.
[36] As listed in Chapter 1 section 1.3.2.
[37] The p-value tests the null hypothesis that the coefficient (slope of regression) is equal to zero based on a t distribution. A small p-value indicates that the coefficient is unlikely to be equal to zero and that an influence on the tested parameter on *E. coli* decay coefficient is likely.

Based on this analysis, we identified all the parameters associated with *E. coli* decay coefficient in the HRAP with $R^2 > 0.1$ and $p < 0.05$ as potentially significantly related to *E. coli* removal[38].

3.3.3.1. Parameters with significant relationships with *E. coli* removal

Significant positive correlations were found between *E. coli* decay coefficient and TSS concentration in the HRAPs ($R^2 = 0.170$, $p = 1.94 \cdot 10^{-6}$), TSS productivity ($R^2 = 0.109$, $p = 1.82 \cdot 10^{-4}$), COD concentration in the wastewater ($R^2 = 0.132$, $p = 0.0035$), chloride concentration in the HRAPs ($R^2 = 0.192$, $p = 5.43 \cdot 10^{-7}$), *E. coli* cell counts in the wastewater ($R^2 = 0.124$, $p = 5.38 \cdot 10^{-5}$), the total sunlight irradiance received within the 24h before the sampling ($R^2 = 0.137$, $p = 2.19 \cdot 10^{-5}$ shown in Figure 3 - 6 as an illustration), and the maxima hourly sunlight intensity recorded within the 24h before the sampling ($R^2 = 0.149$, $p = 8.53 \cdot 10^{-6}$). No significant negative correlations were found.

All the correlations were poor indicating none of these parameters by themselves singularly govern the decay of *E. coli*.

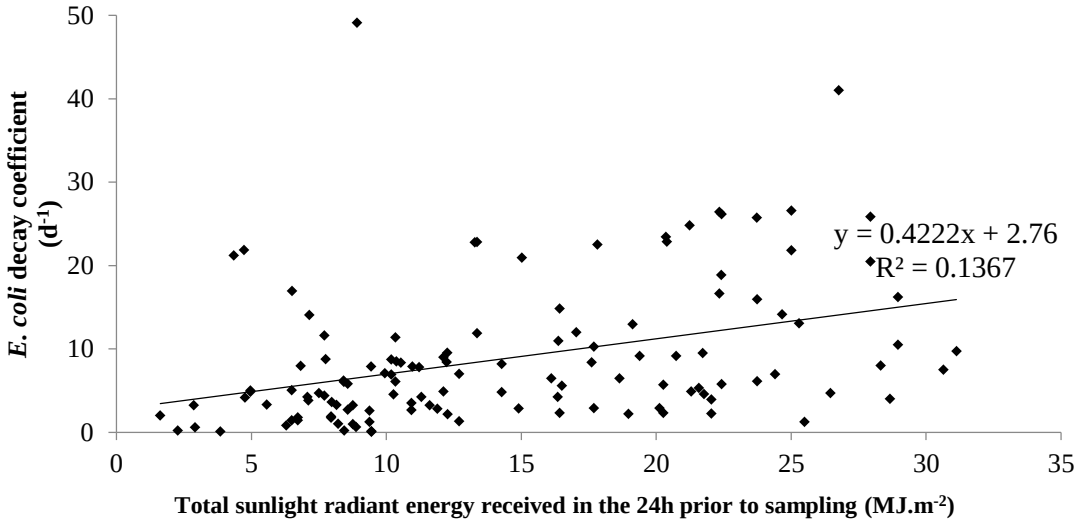

Figure 3 - 6: Example of positive correlation between *E. coli* decay coefficient and a measured parameter (total sunlight radiant energy received in the 24h before sampling in this instance)

The same analysis was performed on *E. coli* log removal instead of decay coefficient, with the same conclusions although no relationship was found with HRAP TSS concentration ($R^2 = 0.056$) and wastewater COD concentration ($R^2 = 0.027$).

[38] Correlations were deemed significant when the p-value associated to the linear correlation was below 0.05 (testing for the absence of effect).

3.3.3.2. Parameters with no apparent relationship with *E. coli* removal

No correlations were observed between *E. coli* decay coefficient and the COD concentration in the HRAP broth (R^2 = 0.0147) including the filtrated phases (R^2 = $5x10^{-6}$), nor with the TSS concentration in the wastewater influent (R^2 = 0.0304). The lack of correlation between *E. coli* removal efficiency and these parameters suggests nutrient availability unlikely affect *E. coli* decay in HRAPs under the conditions studied, despite this factor being mentioned in the literature (Barcina et al., 1997; Decamp and Warren, 1998).

Ammonia concentrations in both the wastewater influent and the HRAP broth (shown in Figure 3 - 7 as an illustration) were also not correlated with *E. coli* decay coefficient (R^2 = 0.0005 and 0.0083 respectively) suggesting that ammonia toxicity did not contribute to the overall disinfection, despite this being mentioned in the literature (Maynard et al., 1999).

Finally, the temperature recorded at 9 a.m., and the maximum temperature, the maximum pH, and the maximum DO concentration recorded within the 24h period before the sampling, were not correlated to *E. coli* decay coefficient, despite the literature suggesting a significant impact of these parameters (Davies-Colley et al., 1999; Marais, 1974).

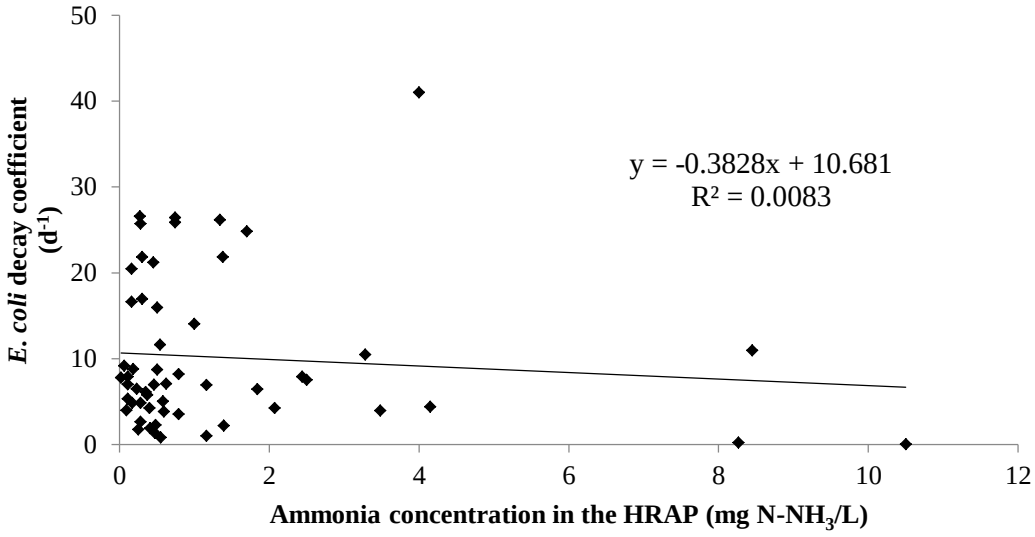

Figure 3 - 7: Example of an absence of correlation between *E. coli* decay coefficient and a measured parameter (ammonium/ammonia concentration in this instance)

3.3.3.3. Conclusion of correlation analysis

This analysis showed that even though some parameters are mathematically correlated with *E. coli* decay coefficient, all correlations remained poor. This is probably related to the high variability of HRAP broth (e.g. variations in optical properties leading to variations of sunlight mediated disinfection), but also to the diverse direct and indirect influence that these

parameters may have with *E. coli* removal. The study of pilot scale HRAPs could therefore provide only limited information on the most significant mechanisms of *E. coli* decay in HRAPs[39]. Consequently, laboratory scale experiments were conducted to isolate and quantitatively evaluate each potential mechanism individually (see Chapter 4).

3.3.4. RESULTS FROM DAILY PROFILES AND AFTERNOON SAMPLING

The literature suggests that *E. coli* removal is maximized by the co-action of higher pH and DO concentration with sunlight intensity (Curtis et al., 1992; Davies-Colley et al., 1999). In addition, the continuous monitoring of pH, DO concentration, and temperature confirmed significant daily variations in the magnitudes of these parameters, as shown in Figure 3 - 8. It was therefore suspected that initial monitoring (regular sampling at 9 A.M.) could miss important information about the system's behaviour. Potential daily variations of *E. coli* removal performance, and associations with daily pH, DO concentration, and temperature fluctuations in the pilot scale HRAP were therefore investigated.

Results from the study of daily profiles for the methodology described in Chapter 2, section 2.1.1. are given in the following section. Results from 4 different days are presented dealing with a range of different conditions in the ponds (30/09 – 01/10/2015: sunny spring day with mild temperature; 12 – 13/10/2015: cloudy spring day; and 03 – 04 and 10 – 11/02/2015: two hot sunny summer days).

3.3.4.1. Variations of environmental parameters over 24h

The logged data of pH, DO concentration, temperature, and sunlight intensity on the days monitored are presented in Figure 3 - 8.

All parameters displayed high daily variations. Days with lower sunlight intensity showed more moderate variations of all the measured parameters. Interestingly, while sunlight intensity reaches its maxima between 12 and 2 P.M; pH, DO concentration, and temperature appeared to peak in the afternoon around 3 p.m. in spring and around 5 p.m. or later on warmer summer days. This is probably because sufficient sunlight is available to maintain high photosynthetic activity until such hours (and warm up the algal broth) while gas loss (O_2 and CO_2) at the air-water interface was too slow to compensate for the surplus of production of these gases.

[39] In view of the high natural variability and high experimental uncertainty due to this type of work, we deemed that Principal Component Analysis would not be conclusive and decided, instead, to focus on environmental work under more controlled conditions.

The maxima in pH and DO concentration on the 03 – 04/02/2016 and 10 – 11/02/2016 are similar to the extreme values reported in the literature, despite a depth (0.25 m) in the average range (cf. Table 1 - 3) making such high variations[40] unexpected. This could be explained by the paddlewheel, which was reported to turn more slowly than targeted on both of these days (not measured). This would lower the gas transfer at the algal broth-air interface[41] and lead to higher pH and DO concentration peaks.

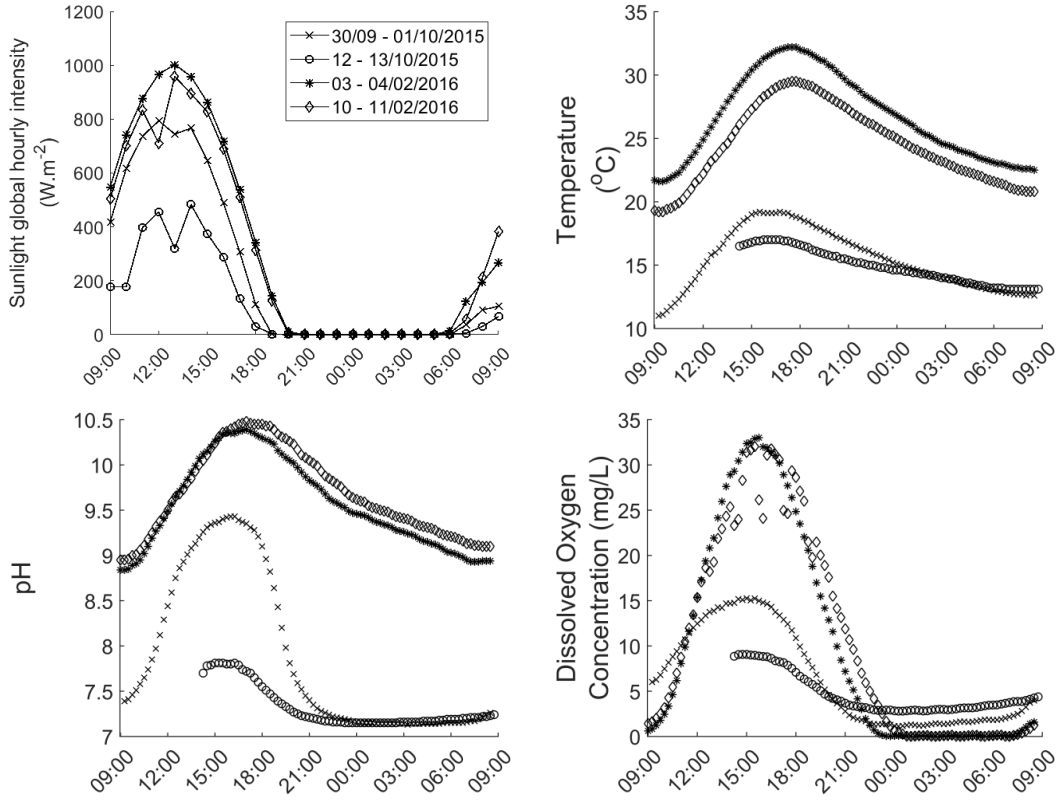

Figure 3 - 8: Daily variations of important disinfection parameters of the HRAPs.
Clockwise from top-left: sunlight intensity, temperature, dissolved oxygen concentration, and pH.

3.3.4.2. Variations of *E. coli* cell counts over 24h

Results from the *E. coli* cell count measurements are shown Figure 3 - 9. Sunlight intensity, pH, DO concentration, and temperature recordings of the corresponding days were shown in Figure 3 - 8.

Figure 3 - 9 a) and b) show results obtained during the transition season. The *E. coli* cell counts in the HRAP were very similar and constant for both days. Interestingly, both days were characterized by radically different environmental conditions: 30/09/2016 was a sunny day with sunlight peak intensity around 800 W/m^2 and showing significant variations of pH

[40] pH peaking above 10.4, DO concentration peaking above 30 mg/L.
[41] As shown in Appendix 9.

(7.13 – 9.43), DO (1.12 – 15.27 mg/L), and temperature (11.0 – 19.2°C) in the HRAP; 12/10/2015 was a dull cloudy day, the peak sunlight intensity not reaching 500 W/m^2 and pond parameters recorded that day experienced little to mild variations (pH: 7.15 – 7.81, DO: 2.79 – 9.07 mg.L^{-1}, temperature: 13.1 – 17.0°C).

Figure 3 - 9 c) and d) display results from two summer days characterized by high peaks of sunlight intensity (> 950 W.m^{-2}). This resulted in peaks of high magnitude for pH (> 10.3), DO (> 32.0 mg.L^{-1}), and temperature (> 27 °C) for both days. *E. coli* cell counts for both days showed a huge variation of 115- and 48-fold within the same day on the 03/02/2016 and 10/02/2016 respectively. The curves also showed a relatively rapid return of *E. coli* cell counts during the night to values similar to the previous morning. This is most likely to be driven by the feeding of *E. coli* cells from the influent while the decay rate in the pond is lower.

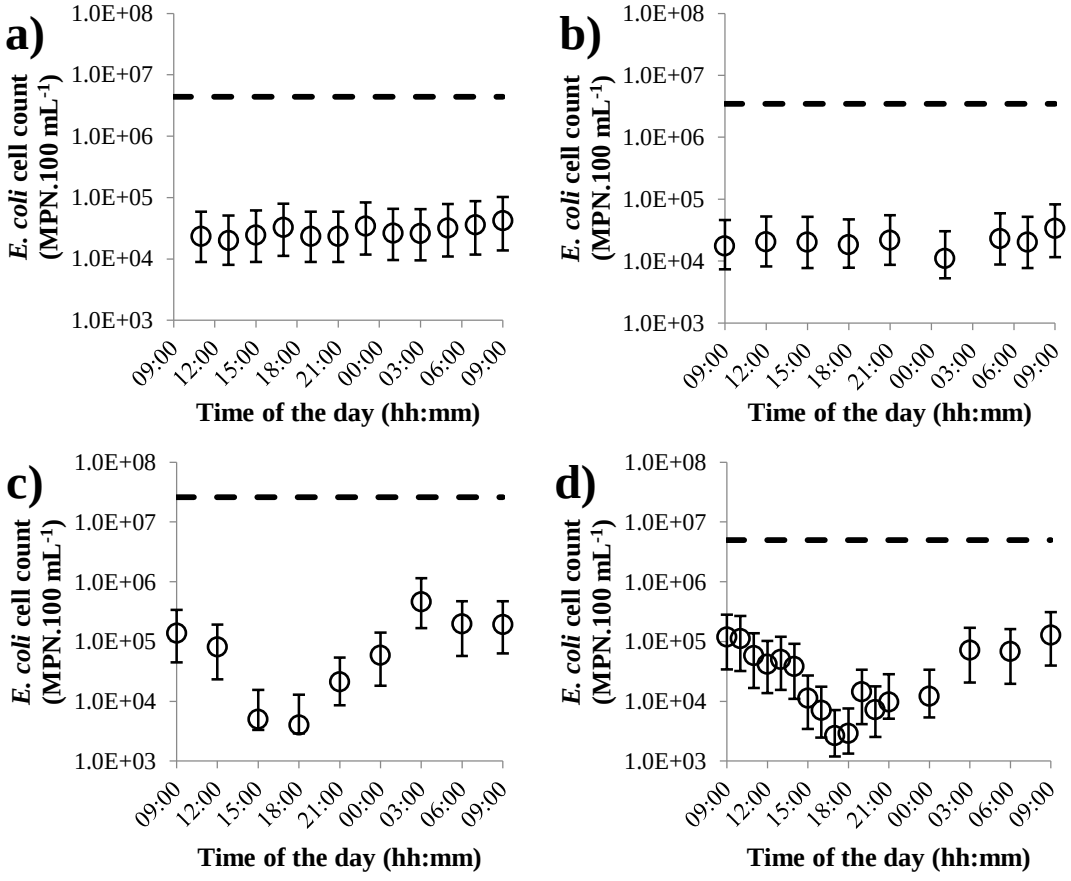

Figure 3 - 9: *E. coli* cell counts daily profiles on the 30/09—01/10/2015 (a), 12—13/10/2015 (b), 03—04/02/2016 (c), and 10—11/02/2016 (d).
The dashed lines represent the *E. coli* content in the influent of the corresponding day

3.3.4.3. Afternoon sampling results

In order to confirm the daily profile results and possibly improve our understanding of the parameters involved in accelerated *E. coli* removal, HRAP samples were systematically

collected in the afternoon using an autosampler (see Chapter 2 section 2.2.1.2.) aiming to catch the lowest *E. coli* cell counts in the HRAP A for each day of monitoring. This study surprisingly did not show lower *E. coli* cell counts in the afternoon compared to those found in the morning ($p = 0.7298$, $N = 47$[42]).

Aiming at relating the measured environmental parameters variations with *E. coli* disinfection performance, the following was found:

- Only two days reported a peak pH above 10. Neither of the two samples presented showed particularly elevated decay of *E. coli* which could be explained by the low maximums for hourly sunlight intensity and total sunlight energy reported for these days (506 and 711 $W.m^{-2}$, and 12.7 and 15.38 $MJ.m^{-2}$ respectively).
- Nine of the days sampled presented maximum hourly sunlight intensity above 800 $W.m^{-2}$, two of which were above 1,000 $W.m^{-2}$. Interestingly, the latter two samples showed relatively low *E. coli* cell counts (below the median concentration, and less than half of the average concentration) but their concentrations were comparable with the samples collected at 9 A.M. the following day indicating the high sunlight intensity did not improve the *E. coli* decay any further. The peaks of pH and DO concentrations measured on those days were 9.81 and 9.88, and 14.85 and 15.77 mg $O_2.L^{-1}$ respectively, thus showing significant peaks but significantly lower than that recorded on the daily profiles of the 03 – 04 and 10 – 11 of February 2016.
- None of the days sampled experienced a DO concentration above 20 $mg.L^{-1}$.

3.3.4.4. Discussion

The lack of significant variation in *E. coli* decay reported on 30/09 – 01/10/2015, despite a high peak sunlight intensity on that day (over 800 $W.m^{-2}$) suggests that sunlight mediated mechanisms were not significant that day. Instead, the relatively constant *E. coli* cell counts indicate that most of the decay was probably mediated by dark mechanisms having little daily fluctuation.

On days presenting high *E. coli* cell count fluctuations (3rd and 10th of February), *E. coli* cell count minima were reached late in the (5 to 6 P.M., as can be seen in Figure 3 - 9). This is significantly later than sunlight intensity peaks reported on these days (1 to 2 P.M.) which provides further evidence that direct sunlight damage has little influence on the overall *E. coli* decay in HRAPs. On these same days, pH, DO concentration, and temperature peaked at 5 – 6 P.M., and none of these parameters experienced variations as important on 30/09/2015

[42] One sample t-test comparing the difference between the *E. coli* cell counts measured in the afternoon and in the morning, testing the null hypothesis that the mean is equal to zero (positive mean being the alternative hypothesis.

and 12/10/2015[43] therefore indicating that one or several of these parameters were possibly involved in the sudden elevation of *E. coli* decay, whether through indirect photo-oxidation (e.g. implication of DO concentration or/and pH) or the direct impact of one of the parameters (e.g. pH).

Nevertheless, the potential action of another dark mechanism on both days in the month of February (whether or not affected by pH, DO concentration, or temperature) cannot be ruled out by this study.

E. coli cell counts were surprisingly not significantly higher in the morning samples than in the afternoon samples, despite measurements also being performed in summer. However, the study was conducted between March 2016 and June 2017, thus including the summer 2016 – 2017 which was reported as "particularly dour for the southwest of the North Island[44]" (NIWA National Climate Center, 2017). The combination of a limited number of samplings, operational issues, and a poor summer conditions, likely explained that no sampling coincided with days combining high sunlight intensity, high temperature, and high algal activity (that would result in high pH and DO concentration levels), these being the conditions expected to lead to extreme decay coefficient based on daily profile observations (see section 3.3.4.2.). Hence the extreme decay coefficients evidenced in February during daily profiles experiments are not contradicted by the afternoon sampling study. Instead, results suggest that only specific conditions of pH and DO concentration are associated to elevated decay and that these conditions were not consistently reached in the pilot scale HRAPs. The afternoon sampling campaign also provided further evidence that sunlight intensity had little direct impact on *E. coli* disinfection.

3.3.4.5. Conclusion

Sunlight with moderate levels of pH, DO concentration, or temperature was concluded to have little effect on disinfection, possibly due to the scattering of light counterbalancing the impact of direct sunlight disinfection in HRAPs at full scale.

Although the implication of pH, DO concentration, and temperature in high *E. coli* removal performances is likely, results from daily profiles and afternoon samplings did not allow confirmation of which parameters (and therefore which mechanisms) are prevailing.

[43] When *E. coli* cell counts in the HRAP remained fairly constant
[44] Of New Zealand, i.e. the location of the pilot scale HRAPs used in the present study

This conclusion further motivated the study conducted at laboratory scale, during which suspected mechanisms were isolated in order to be quantitatively evaluated individually (see Chapter 4).

Limitations of daily profile experiments and afternoon sampling campaign

The results presented in the daily profile study have to be treated with caution:

- *E. coli* content in the wastewater influent was only measured at 9 a.m., i.e. at the end of the sampling. It is therefore possible that the concentration of *E. coli* in the influent varied significantly between different HRAP broth sampling times. Nevertheless, a 'daily profile' performed once on the wastewater (see Appendix 11) did not evidence any significant variation in *E. coli* cell count throughout the day.
- Similarly, the flow rate may have experienced unknown variations. While the flow rate was controlled at the start and end of each profile and showed no significant shifts for each profile presented, fluctuations throughout the day cannot be excluded.

The storage of samples in the fridge also raises the question of how much decay happened between sampling and measurement. However, the fact that two days with no apparent enhanced decay were recorded confirms that the samples were not affected by storage at least at non-extreme pH, temperature, and DO concentration.

3.4. CONCLUSION

This study provides a comprehensive data set over two years, for outdoor HRAPs treating real domestic wastewater. It shows that HRAPs provide consistent and efficient wastewater disinfection, potentially at a higher level than maturation ponds, thus providing a reliable alternative to this technology. Being conducted in outdoor conditions using real wastewater, this study indicates that such results should be directly transposable to a full scale set up[45]. The fact that poor *E. coli* performances were only found in winter at times of extreme weather conditions (e.g. low temperature combined with high rainfall) suggests that good control of algal density and protection of the pond during extreme weather events (e.g. protection against rain) may prevent major reductions in disinfection performances.

[45] At the time this study was started, no such result was reported in the literature; at the time this study was written, other research teams also proved the suitability of HRAP to provide efficient wastewater disinfection (Young et al., 2016).

Only poor or no correlation between *E. coli* decay coefficient and any single HRAP parameter could be found. No mechanism of decay could therefore be highlighted from the study of HRAPs, probably due to the high variability within the system. Nonetheless, the complete lack of correlation between *E. coli* decay coefficient and some parameters were good indicators of the likely irrelevance of some mechanisms of disinfection in HRAPs as suspected in the literature. Hence:

- NH_3 was unlikely to be toxic to *E. coli* at levels found in HRAPs
- Starvation and competition for nutrients were found to be unlikely to influence *E. coli* removal under HRAP conditions

In addition, grazers invaded the HRAP B from April to June 2017. While the presence of grazers was accompanied by low algal density (which was reflected by a lack of variations of pH and DO concentration in HRAP B despite similar TSS in both ponds), *E. coli* cell counts in both HRAPs remained similar. The most likely explanation for this is the control of the *E. coli* population by direct or indirect[46] predation. Predation is therefore likely to be significant in HRAPs, but its prediction and control is seemingly unachievable.

Since it is impossible to determine from pilot scale HRAP monitoring results whether one mechanism or a combination of mechanisms in particular should be accounted responsible for most, if not all, of *E. coli* decay in HRAPs, this will be the object of laboratory and bench scale investigations, presented in Chapter 4 and Chapter 5 respectively.

Wastewater discharge compliance: a competitive strength for HRAPs

Taking Palmerston North wastewater treatment plant as an example, compliance is reached when the daily mean of *E. coli* cell counts in samples collected downstream of the wastewater treatment plant in the Manawatu river do not exceed 300 CFU.100mL^{-1}, with no more than 10% of the samples collected that day exceeding 1,200 CFU.100mL^{-1}. Samples are only collected when the Manawatu river flow is below 37 $m^3.s^{-1}$. Palmerston North wastewater treatment plant is a 100 000 person equivalent (pe) facility, and assuming 1 pe translates to 200 $L.d^{-1}$ (giving a wastewater effluent flowrate of 0.23 $m^3.s^{-1}$), a 100-fold dilution factor of the plant effluent in the river can conservatively be estimated (although the Manawatu flow rate[47] may be lower than 37 m^3/s). Therefore, up to $3 \cdot 10^4$ CFU/100 mL in the wastewater treatment plant effluent would be deemed acceptable for discharge. This objective, materialised by the dashed line in Figure 3 - 10, is reached using the HRAP

[46] i.e. adsorption by algae and subsequent grazing of algae

[47] Data from the 05/01/2016 to the 05/01/2017 on the Manawatu river flow in Palmerston North gave the following distribution: 5 percentile: 16.0 $m^3.s^{-1}$ and 25 percentile: 52.4 $m^3.s^{-1}$ for a minimal flow recorded at 14.5 $m^3.s^{-1}$. 37.0 $m^3.s^{-1}$ corresponds to the 17 percentile over this period (N = 365).

technology in many instances despite this study set-up functioning with no intention of process optimization for disinfection.

Because the best and most consistent *E. coli* removal rates were achieved in warmer conditions, there is an opportunity to use HRAPs for wastewater treatment places needing good effluent quality in summer. This need is common whether because the effluent is diluted in a river with little concern in winter due to high flow (e.g. Palmerston North), or because the discharge is performed in recreational waters with no health concern in winter accompanied by lower pathogen loads in the wastewater (e.g. coastal resort).

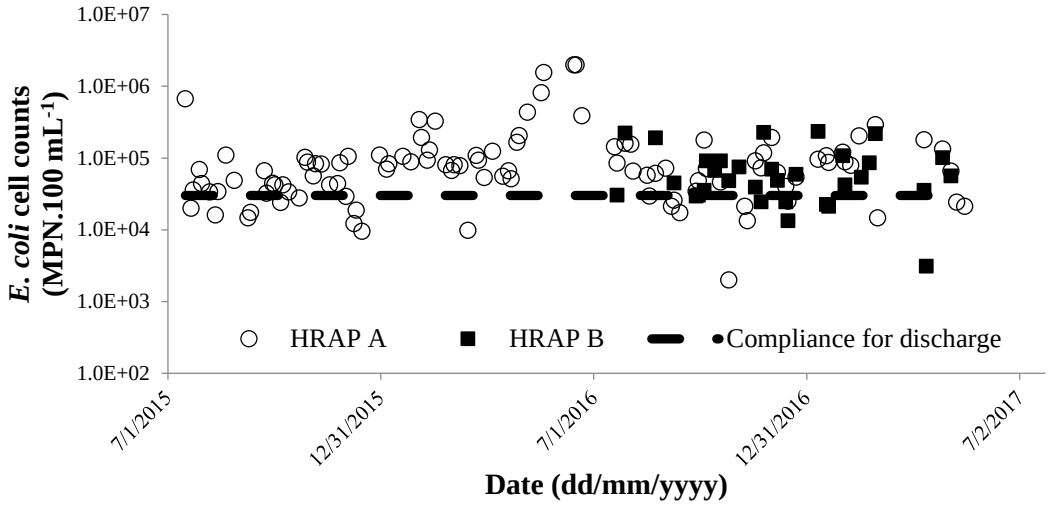

Figure 3 - 10: *E. coli* cell counts measured in pilot scale HRAPs effluent; Comparison with compliance for the release of the effluent in the Manawatu river at Palmerston North wastewater treatment plant

Chapter 4: Identifying mechanisms that cause significant *E. coli* decay at laboratory scale

This Chapter presents results from laboratory studies aiming at quantifying the relative impact of individual disinfection mechanisms on *E. coli*. Results from experiments conducted in darkness are first discussed, followed by experiments conducted under natural illumination[48].

4.1. DARK MECHANISMS

The set of conditions investigated in this section and the mechanisms targeted are presented in Table 4 - 1[49]. The set of conditions were chosen in order to isolate one single mechanism of *E. coli* decay in each reactor as much as possible.

Table 4 - 1: Experimental conditions and mechanisms investigated under dark conditions

Experimental matrix	pH	Temperature	Chemical addition	Mechanism targeted
Distilled water	Not controlled	5 – 35 °C	None	Natural decay[1]
Distilled water	Not controlled	25 – 40°C	None	Heat inactivation
Phosphate buffered distilled water	7 – 8	5 – 35°C	None	pH mediated toxicity
Carbonate buffered distilled water	9 – 11	5 – 35°C	None	pH mediated toxicity
Distilled water	Not controlled	5 – 35 °C	NH_4Cl	Ammonia toxicity
Phosphate buffered distilled water	8	5 – 35°C	NH_4Cl	Ammonia toxicity
Carbonate buffered distilled water	10	5 – 35°C	NH_4Cl	Ammonia toxicity
Filtered wastewater	Not controlled	Not controlled (ambient temperature 21±2˚C)	None	Wastewater constituents toxicity
Filtered HRAP	Not controlled	Not controlled (ambient temperature 21±2˚C)	None	Algal metaboli es oxicity

[1] This test was used as control in the assessment of other experiments.

[48] All the results presented were obtained using the strain of *E. coli* #1 (wild type) unless stated otherwise.

[49] Specific experiments were also performed to assess the impact of attachment onto suspended solids on *E. coli* cell counts in HRAP broth and wastewater (see Appendix 17). As explained in Chapter 2, the impact of predation was not assessed.

4.1.1. NATURAL DECAY

Figure 4 - 1 displays an example of the variations of *E. coli* cell count in a dark control with no specific harmful conditions. As can be seen, cell count remains relatively constant despite temporal variation which is probably due to experimental error (see Appendix 12 for error analysis). The associated decay coefficient was calculated from the linear regression of the cell counts (log-transformed) over time (the rate is shown in Figure 4 - 1). A histogram displaying the distribution of all measured decay coefficients calculated from dark controls performed using RO water or neutral pH buffer (6.5 < pH < 8.5) is shown in Figure 4 - 2. As can be seen, the distribution of the decay coefficients can be considered as normal and spread around zero (average of 0.27 ± 3.2 d^{-1}, N =49)[51]: a t-test (at the 95% confidence level) did not reject the hypothesis that the measurements were normally distributed centred at zero (p = 0.531). While the temperature could vary from 5 – 35°C between the different dark decay coefficients measured, the analysis presented in Appendix 13 shows broth temperature and natural decay coefficient are independent in the absence of identified harmful conditions.

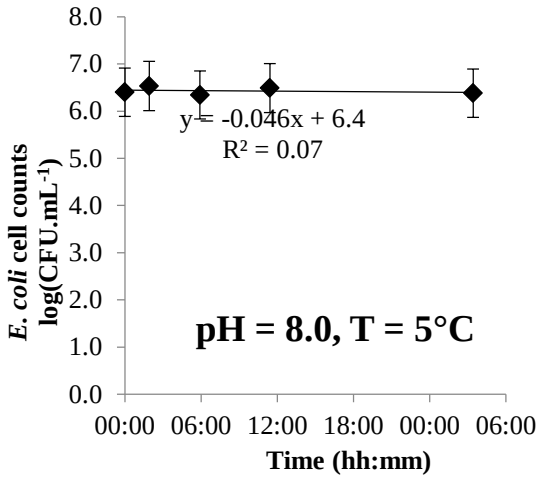

Figure 4 - 1: Evolution of *E. coli* cell count in the dark in the absence of harmful conditions. First order decay coefficient calculated[50] was 0.11 d^{-1}.

As the analysis described in Appendix 12 showed, the log-transformed *E. coli* cell count measured using poor plate method is associated with an error of 8% at the 95% confidence level. To put this into perspective, assuming a constant *E. coli* cell count[52] of $40 \cdot 10^6$ $CFU.mL^{-1}$ over 2h (i.e. no decay, as seen here), a worst-case scenario on measurement uncertainty would cause the measured decay coefficient to vary between ± 41 d^{-1} (± 3.5 d^{-1} in the case of a 24h experiment). In this study, all decay coefficient values higher than 2.3 d^{-1}

[50] The first order decay coefficient is calculated from the regression of *E. coli* cell counts transformed using the natural logarithm. The cell counts displayed in Figure 4 - 1 are transformed using the decimal logarithm since that is common practice. The coefficient displayed in Figure 4 - 1 (slope of the regression) must therefore be multiplied by ln(10) to find the true first order decay coefficient (in d^{-1}).

[51] One outlier (value -15.2 d^{-1}) was identified using the Grubbs test at the 5% significance level and was excluded from the analysis.

[52] Representative of initial counts during this study, see Appendix 14.

or lower than -2.3 d^{-1} were computed over short-term experiments (< 24h), suggesting the large variation seen in dark controls (ranging between -7.4 and 9.2 d^{-1}) was related to experimental uncertainty.

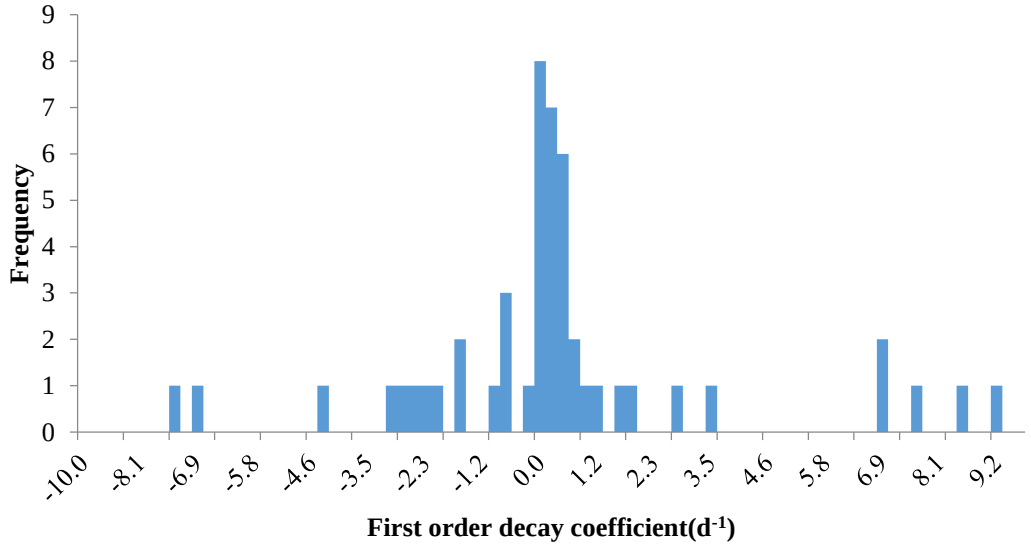

Figure 4 - 2: Distribution of the first order decay coefficients measured in dark controls of experiments

The normal distribution centred on zero indicates that *E. coli* decay in darkness and in the absence of any known harmful conditions is probably insignificant[53]. This confirms findings from Lisle et al. (1998) who reported that *E. coli* O157:H7 was unaffected after incubation for up to 14 days in M9 minimal medium, and Cook and Bolster (2007) who reported a high *E. coli* survival in natural water (decay coefficient of 0.04 d^{-1} over 400 days of incubation. Our study therefore concluded that natural decay was insignificant in darkness.

This result contradicts findings from the study of pilot scale HRAPs where significant *E. coli* decay was not influenced by the variation of parameters such as pH or sunlight intensity, suggesting significant background decay coefficients[54] that could not be related to any identified mechanism (see Chapter 3). As discussed in Chapter 2 section 2.1., laboratory experiments have limited relevance to algal broth conditions and such discrepancies could be expected. Investigations at bench scale in HRAP broth (see Chapter 5) were designed to confirm and identify the origin of such differences between pilot and laboratory scale.

[53] Due to the absence of nutrients in the experimental broth, the incidence of negative decay coefficients are certainly explained by experimental errors.
[54] Evaluated at 10.4 d^{-1} at 20°C

4.1.2. HEAT INACTIVATION

Early tests conducted with *E. coli* ATCC® 10536™ showed no significant decay at temperatures up to 40°C (data not shown) and the wild type strain was not significantly impacted by temperatures up to 35˚C (see controls at neutral pH during pH toxicity tests at various temperature, section 4.1.3.3.). This is not surprising because *E. coli* optimally grows at 37.5°C, the temperature of the human gut, and tolerates temperature up to 48°C (Madigan and Martinko, 2006). As temperatures above 35°C have not been reported in HRAPs (Table 1 - 3), heat inactivation was rejected as a potential mechanism of *E. coli* removal in HRAPs.

4.1.3. TOXICITY

4.1.3.1. Algal toxicity

No significant decay was recorded in flasks supplied with filtered 'algal solutions'[55]. Based on this data, algae-based toxicity is unlikely a significant disinfection mechanism in HRAP (see Chapter 5 for further discussion as bench-sale assays potentially challenged this conclusion). This conclusion must be considered with caution due to the geographical and temporal diversity of algal species found in HRAPs (Cho et al., 2017) and thus of their metabolites.

4.1.3.2. Wastewater toxicity

No significant decay was recorded in flasks supplied with filtered or centrifuged wastewater although colonies from plates inoculated with *E. coli* and incubated for 8 days in wastewater filtrate were abnormally small, suggesting a lack of fitness. Wastewater toxicity was therefore excluded as significant disinfection mechanism in this study. As far as we know, wastewater toxicity has never been reported in the literature but it is unclear whether or not this mechanism has been specifically tested.

[55] This result is despite the fact that, in order to produce a potential 'worse-case' scenario, the filtrate was obtained either from a HRAP sample pre-cultivated (in incubator, see Chapter 2 for culture conditions details) to enhance algal activity or a HRAP sample collected after a sunny day (05/03/2017 at 5 P.M from HRAP A; the total received sunlight energy at 5 P.M. that day was 20.17 $MJ.m^{-2}$, the maximal hourly sunlight intensity being 830.6 $W.m^{-2}$.

4.1.3.3. pH toxicity[56]

Published evidence that pH toxicity could cause significant *E. coli* decay in HRAPs is limited; despite this, a first test at laboratory scale showed significant decay at pH 10 and ambient temperature (first order decay coefficient of 3.3 d^{-1} over 3 days of incubation). Because pH values above 10 were frequently recorded in the pilot scale HRAPs (see Chapter 3, section 3.2.3.), pH toxicity appears to be a potentially significant mechanism of decay in these systems. In addition, because high pH values were associated with high pond temperatures, *E. coli* decay was quantified under combinations of pH and temperatures relevant to HRAPs conditions. An example of the kinetics of *E. coli* death under harmful conditions of pH and temperature is shown in Figure 4 - 3.

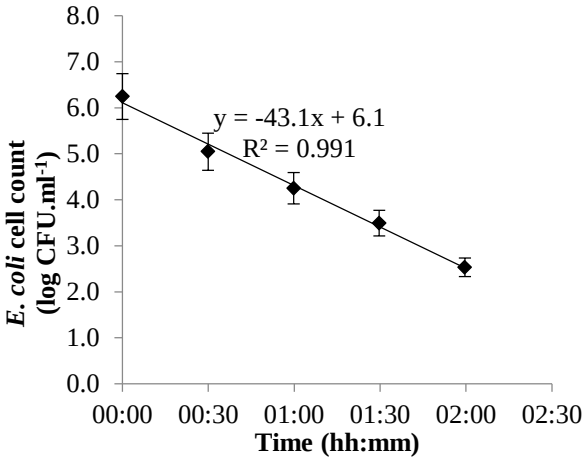

Figure 4 - 3: Changes in *E. coli* cell counts at pH 10 and 35°C[57]

At a given pH, *E. coli* decay coefficient increased exponentially with temperature (as illustrated in Figure 4 - 4 at pH 10), and for a given temperature, *E. coli* decay coefficient increased exponentially with pH (or linearly with the concentration of OH^- ions), as illustrated in Figure 4 - 5 for 30°C. The influence of pH and temperature on *E. coli* decay coefficient could thus be described by Equation 4 - 1:

$$k(T, pH) = a(T) \cdot 10^{pH - 14} \qquad (4 - 1)$$

where k is *E. coli* first order decay coefficient (d^{-1}) at the broth temperature T (°C) and broth pH (both controlled at the end of each experiment), and $a(T)$ is a temperature dependent fitting parameter.

[56] pH toxicity involves the disruption of enzymatic activity and energy production via the proton pump (Krulwhich et al., 2011).

[57] *NB*: while the linear correlation indicates a slope of 43.1 d^{-1}, this value is obtained from the log-transformed *E. coli* cell counts using the decimal logarithm and is thus not the first order decay coefficient. The first order decay coefficient would be obtained using the natural logarithm, being in that case 99.2 d^{-1} (ratio ln(10))

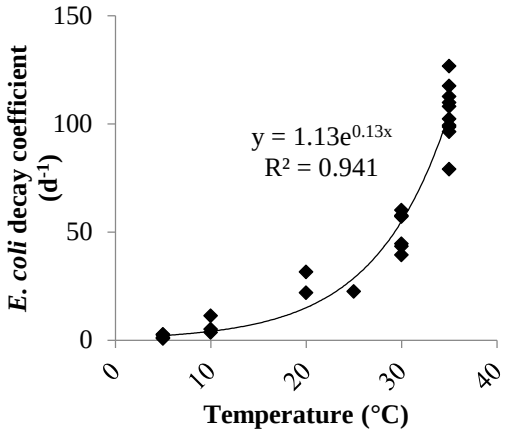

Figure 4 - 4: Influence of temperature on *E. coli* decay coefficient at pH 10

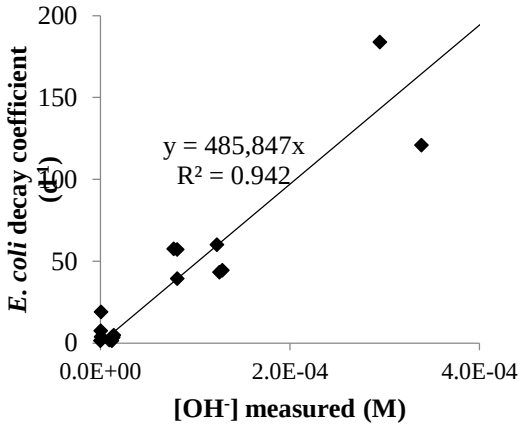

Figure 4 - 5: Influence of pH on *E. coli* decay coefficient at 30°C

The values of $a(T)$ at each temperature tested, listed in Table 4 - 2, were obtained from the linear regressions of the decay coefficients against [OH^-] (calculated as 10^{pH-14} where pH is the pH measured in the flask at the end of the experiment), as shown in Figure 4 - 5.

Table 4 - 2: Results from the linear regression between [OH^-] and *E. coli* decay coefficient for a given temperature

T (°C)	5	10	20	25	30	35
$a(T)$ (L.mol^{-1}.d^{-1})	16,489	41,303	187,347	183,355	485,847	1,189,785
R^2	0.703	0.955	0.899	0.963	0.942	0.965
N	10	7	8	7	19	19

The values of $a(T)$ were then plotted against temperature and a linear relationship was found between $\ln(a)$ and temperature as depicted in Figure 4 - 6. The influence of temperature on the decay coefficient at a given pH can therefore be described by the following Marais-type equation (Marais, 1974):

$$a(T) = k_{20} \cdot \theta^{T-20} \quad (4 - 2)$$

where θ = 1.14 is the temperature-compensation coefficient and k_{20} = 1.38 · 10^5 d^{-1} is the value of *E. coli* decay coefficient at 20˚C and pH 14. Both parameter values were calculated from the results of this study based on the linear regression of $\ln(a)$ against temperature.

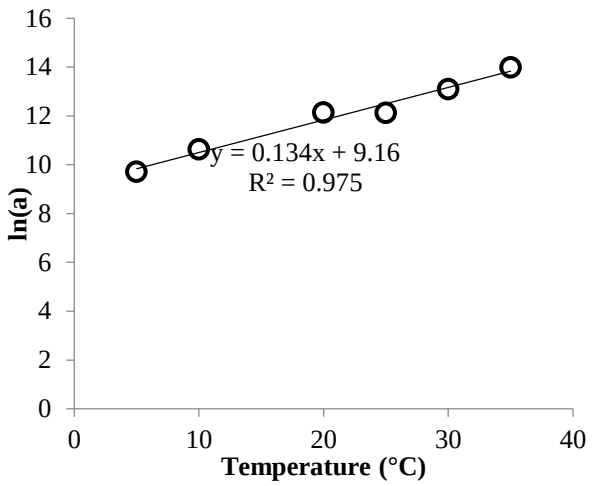

Figure 4 - 6: Impact of broth temperature on ln(a).

E. coli decay coefficient in the dark can therefore be estimated using Equation 4 - 3. The full data set of measured versus predicted decay coefficients using Equation 4 - 3 is shown in Figure 4 - 7.

$$k(pH,T) = k_{20} \cdot \theta^{T-20} \cdot 10^{pH-14} \quad (4 - 3)$$

Because of the very fast decays occurring at pH above 10.5, only two values of decay coefficient could be calculated under these conditions at 35°C and caution should be exercised when using Equation 4 - 3 to calculate *E. coli* decay at elevated pH (no data obtained for pH above 10.2 is shown in Figure 4 - 7). Regardless, the values of θ and k_{20} calculated here can be considered accurate for pH 7 to 10, and temperatures 5 to 35 °C (R^2 = 0.930, N = 103).

Based on Equation 4 - 3, pH-induced decay coefficient of *E. coli* was computed for pH and temperature ranging from 7 to 11 and 0 to 35°C respectively, as shown in Figure 4 - 8. It was predicted that *E. coli* decay would become significant[58] at pH above 10.8 within the entire range of temperature tested (i.e. > 5°C), above pH 9.9 for temperatures at 20°C, and from pH 9.0 at 35 °C. pH-induced decay was predicted to become high[59] at pH 9.5 and temperatures > 34°C, pH 10 and T > 25°C, or pH 11 and T > 7°C.

[58] Results from pilot scale HRAPs suggested a constant natural decay coefficient of about 10.4 d^{-1} at 20°C (this result is demonstrated in Chapter 5 section 5.2.1.). Hence, decay coefficients above 10.4 d^{-1} have been considered significant in this analysis.

[59] Decay ceofficients are deemed high above 26 d^{-1} (95 percentile of the *E. coli* decay coefficient measured during pilot scale monitoring)

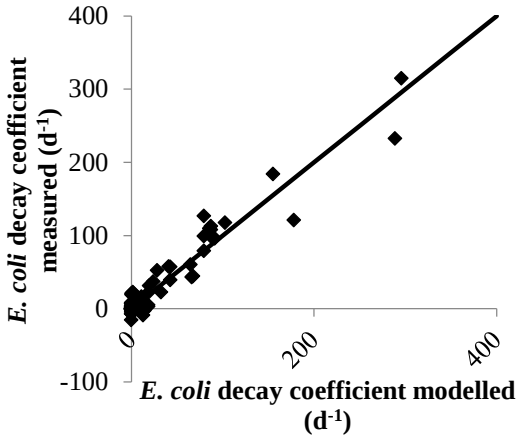

Figure 4 - 7: Comparison of measured and modelled *E. coli* decay coefficient for all tested pH (between 7 and 10.2) and temperatures (between 5 and 35°C)

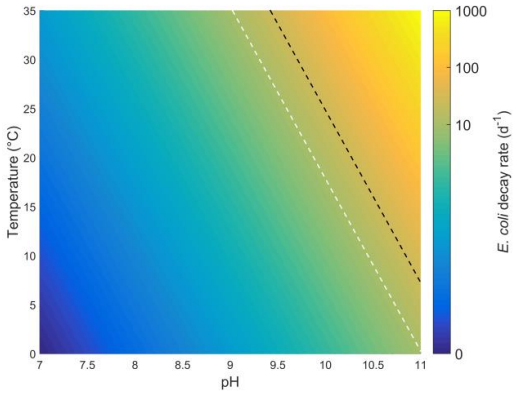

Figure 4 - 8: Variations of modelled *E. coli* decay coefficient according to pH and temperature.
The white and black lines define the ranges of pH and temperature from which *E.coli* decay coefficient is deemed significant and high respectively.

The findings of this study on pH toxicity were applied to the distribution of the pH and temperature conditions in the pilot scale HRAPs as shown in Figure 4 - 9[60]. It was found that the pH and temperature conditions in the algal broth theoretically trigger a decay coefficient of *E. coli* of significant magnitude (i.e. > 10.4 d^{-1}) and high magnitude (i.e. > 26 d^{-1}) for 4.91 and 4.94 % of the total time respectively (see Figure 4 - 10). This shows that pH toxicity has the potential to contribute significantly to *E. coli* disinfection measured in HRAPs. Such potential of HRAP will be further discussed in Chapter 7.

Because the decay repartition shown in Figure 4 - 10 is characteristic of the design of the pilot scale HRAP used in this study and because both HRAPs design and operation (e.g. working depth, feeding regime) can probably be optimized, the contribution of pH to the overall decay of *E. coli* in HRAPs could be significantly improved by identifying ways of favouring high pH in HRAPs.

[60] The density of pH and temperature was calculated as the total data points measured within each boundary of the pH -temperature plan (mesh of 0.25 for pH and 1°C for temperature) divided by the total amount of available data (N = 48,416). The data were obtained from almost-continuous measurement of both parameters for over a year in both pilot scale HRAPs.

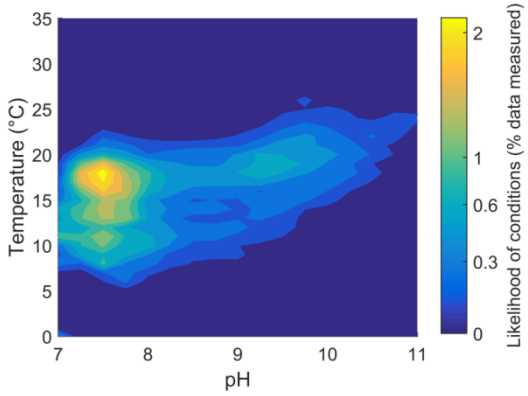

Figure 4 - 9: Distribution of the temperature and pH conditions recorded during pilot scale HRAPs monitoring (N = 48,416, see Chapter 3).
The definition is 1°C for temperature and 0.25 for pH

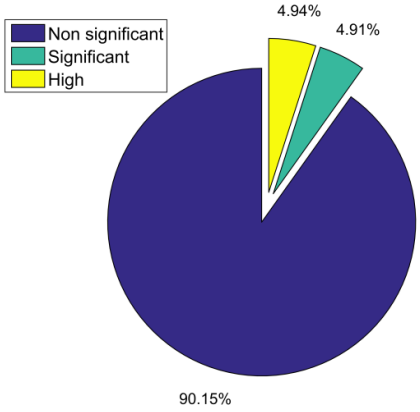

Figure 4 - 10: Time repartition between non-significant, significant, and high pH toxicity for *E. coli* in pilot scale HRAPs (N = 48,416)

As discussed in Chapter 1, pH toxicity has never been considered as a key mechanism of *E. coli* decay in algal ponds (the impact of pH has mostly been investigated in relation to indirect photo-oxidation). Possibly, as research on disinfection in algal technology has been generally restricted to maturation ponds which are characterized by lower pH (see Table 1 - 3), pH has not yet been identified as a crucial parameter for disinfection by itself in algal ponds. Hence, only Parhad and Rao (1974) have to date investigated the effect of pH on *E. coli* cells in algal systems. Their study identified a pH effect in the dark, irrespective of the alkaline buffer used or the origin of the pH increase (i.e. algal activity or alkaline buffer addition), and reported significant decay above pH 9.4. Outside the specific context of algal ponds, Mendonca et al. (1994) investigated the effect of pH of 9 – 12 on *E. coli* and also confirmed the exponential increase of decay with pH, reporting rates as high as 2,304 d^{-1} at pH 11 and 37°C (cf. 1,280 d^{-1} according to our model in these conditions).

Although the equation developed in this work echoes the first order decay coefficient of coliforms in waste stabilization ponds as modelled by Marais (1974) with respect to temperature[61] (an equation which has been frequently used or adapted in the literature, Auer and Niehaus, 1993; Mancini, 1978; Mayo, 1995; Ouali et al., 2015; Xu et al., 2002), the combined impact of pH and temperature on *E. coli* decay has never been specifically modelled before to the best of our knowledge.

[61] $k(T) = k_{20}.\theta^{T-20}$.

4.1.3.4. Ammonia toxicity

The impact of NH_3 concentration on *E. coli* decay coefficient is illustrated in Figure 4 - 11. The values of the decay coefficients shown were normalized at 20˚C (based on Equation 4 - 3) to allow comparison between results obtained at different temperatures. No significant decay was recorded at pH < 10 regardless of the amount of NH_4Cl added to the experimental broth.

As expected based on the results discussed earlier, significant decay was recorded at pH 10. The impact of temperature at pH 10 for different additions of NH_4Cl salt is shown in Figure 4 - 12. As can be seen, *E. coli* decay at pH 10 was not significantly enhanced by the addition of ammonium salt, regardless of the temperature, even at a high concentration representative of wastewater influent[62]. Although *E. coli* removal appears to increase with the amount of NH_4Cl added (Figure 4 - 12), this correlation was not significant at the 95% confidence interval. Consequently, and considering the low NH_4^+/NH_3 concentration typically found in HRAPs, NH_3 toxicity is not expected to cause significant *E. coli* decay in HRAPs used to treat primary settled wastewater, further confirming findings from the pilot scale HRAPs (see Chapter 3 section 3.3.3.2.). This is an important conclusion considering that NH_3 has been proposed as a potential disinfectant in algal ponds (Maynard et al., 1999) but evidence of this impact had hitherto been lacking.

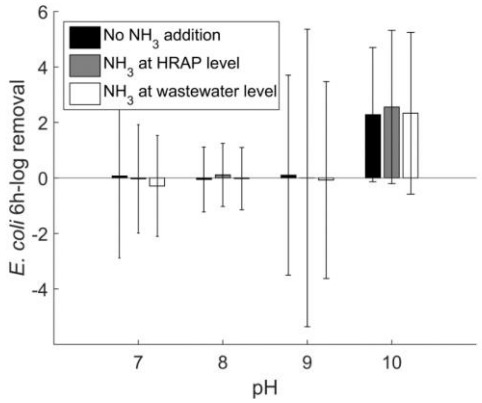

Figure 4 - 11: Effect of NH_3 salt addition on *E. coli* removal performances[63,64] corrected for temperature at different pH

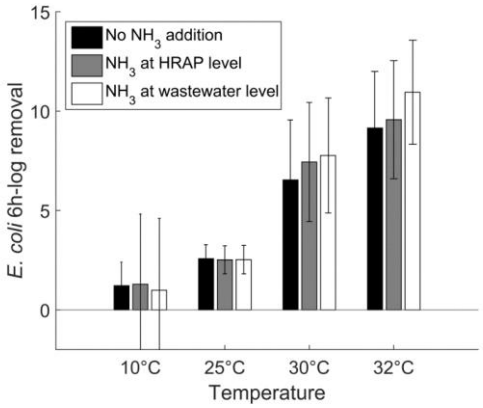

Figure 4 - 12: Effect of NH_3 salt addition on *E. coli* decay at pH 10 for different temperatures

[62] Typical wastewater influent concentration is around 20 mg $N\text{-}NH_3.L^{-1}$, whereas the concentration in the HRAP broth is typically 1 mg $N\text{-}NH_3.L^{-1}$

[63] *E. coli* removal performances were compared in terms of log-removal, normalized for a 6h experiment, as different experiment times were used at the different temperatures (e.g.8h at 5°C vs 2h at 32°C)

[64] The error bars were calculated based on the differences between the counting errors (8%, plate count method) of initial and final counts.

4.2. LIGHT INDUCED MECHANISMS

As presented in Chapter 1 section 1.3.3.2., sunlight radiation can cause direct disinfection through UV-B radiation, and indirect photo-oxidation involving the excitation of photo-sensitizers of endogenous and exogenous origin, supporting the production of ROS. Both indirect photo-oxidation mechanisms were reported to be wavelength dependent and may be enhanced/inhibited by environmental conditions (e.g. pH and DO). Since sunlight is considered to be a critical parameter for *E. coli* removal in algal ponds (Davies-Colley et al., 1999), the light-induced mechanisms for *E coli* disinfection were investigated at laboratory scale. A set of conditions were chosen in order to isolate or exacerbate one single mechanism of *E. coli* decay in each reactor as much as possible. The conditions tested are summarized up in Table 4 - 3.

Table 4 - 3: Experimental conditions and light-induced mechanisms targeted[1]
All experiments were conducted in open beakers incubated under natural illumination: light intensity, temperature and dissolved oxygen concentration therefore varied during and between experiments

Experimental broth	pH	Optical filter	Mechanism of decay targeted
Distilled water	Not controlled	None	Direct UV-B damage and endogenous photo-oxidation[2]
Carbonate buffer	9 – 11	None	Direct UV-B damage and endogenous photo-oxidation at high pH[2]
Phosphate buffer	7 – 8	None	Direct UV-B damage and endogenous photo-oxidation at neutral pH[2]
Distilled water	Not controlled	High pass (UV-B cut off)	Endogenous photo-oxidation caused by UV-A and VIS radiations
Carbonate buffer	10	High pass (UV-B cut off)	Endogenous photo-oxidation at high pH caused by UV-A and VIS radiations[2]
HRAP and wastewater filtrates	Not controlled	None	Direct UV-B damage, endogenous photo-oxidation, and exogenous photo-oxidation[3]
Buffered HRAP filtrate	7, 10	None	Direct UV-B damage, endogenous photo-oxidation, and exogenous photo-oxidation at neutral and high pH
HRAP filtrate	Not controlled	High pass (UV-B cut off)	Endogenous and exogenous photo-oxidation caused by UV-A and VIS radiations

[1] Each light experiment was associated with a dark control not listed in Table 4 - 3; [2] These broths were assumed free of photosensitizers. Carbonate radicals were however reported to be able to form in certain conditions e.g. presence of halogens (Nelson et al., 2018) and results for carbonate buffered reactors should be considered with care; [3] The specific impact of exogenous photo-oxidation was evaluated by comparing tests conducted in the presence of photosensitizers (e.g. filtrates) with tests conducted in broths assumed free of photosensitizers.

Due to the absence of an appropriate experimental set up, the impact of dissolved oxygen (DO) concentration under sunlight irradiation was not investigated at laboratory scale

despite being reported as significant in the literature (Curtis et al., 1992; Davies-Colley et al., 1999; Ouali et al., 2015). To compensate the lack of study at laboratory scale, emphasis was put on the study of DO concentration impact on *E. coli* decay during bench scale experiments (see Chapter 5). The relative importance of each of the three recognized mechanisms (direct DNA damage, endogenous photo-oxidation, and exogenous photo-oxidation) is discussed below.

4.2.1. DATA ANALYSIS

As evidenced by the linear correlation shown in Figure 4 - 13, *E. coli* decay under sunlight exposure could be described by first order kinetics when sunlight intensity was relatively constant. Sunlight radiation however fluctuated during experiments. The duration of exposure to sunlight with changes in sunlight intensity also caused changes in temperature which means *E. coli* removal cannot be described by first order kinetics with a constant coefficient over the entire experiment. First-order kinetics decay coefficients (i.e. $\ln\left(\frac{C_{t-\Delta t}}{C_t}\right)/\Delta t$, d^{-1}) were therefore calculated based on two consecutive data points rather than linear regressions performed over several data points (as was done for dark assays). Temperature was only controlled at the end of each experiment meaning the exact temperature *E. coli* cells were incubated at between two samplings was not known. This added significant uncertainty to the analysis due to the likely impact of temperature on *E. coli* decay (through sunlight mediated or dark mechanisms). This uncertainty was considered with care when comparing counting results from different experiments, or from the same experiment at different sampling times. An especial effort to account for the broth temperature was made when analysing decay at high pH (see section 4.1.3.3.)

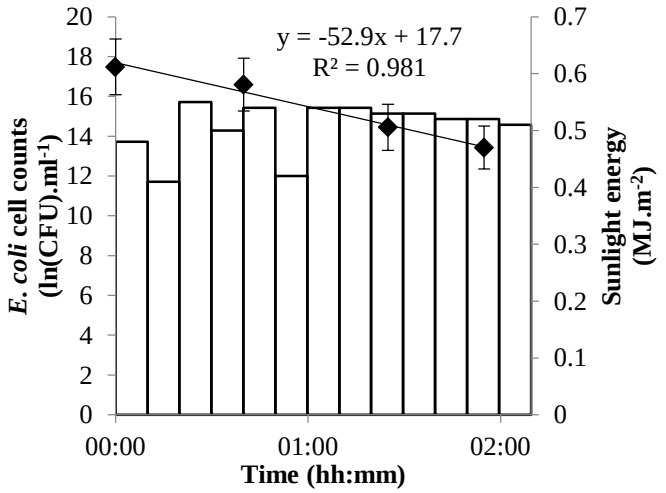

Figure 4 - 13: Change in *E. coli* cell counts in an open beaker filled with RO water and exposed to direct sunlight radiation

To assess the influence of light intensity on disinfection, *E. coli* decay coefficients (d^{-1}) were analysed against the average sunlight intensity ($W.m^{-2}$) between sampling times, and *E. coli*

log removals (dimensionless) were analysed against the total sunlight energy ($MJ.m^{-2}$) received between sampling times.

4.2.2. DIRECT PHOTO-DAMAGE (UV-B DAMAGE AND ENDOGENOUS PHOTO-OXIDATION)

4.2.2.1. Full sunlight spectrum

Figure 4 - 14 displays results from open beakers filled with pure or buffered[65] RO water at neutral pH and exposed to direct sunlight. Only direct DNA damage and endogenous photo-oxidation are expected in these reactors due to the absence of exogenous photosensitizers (Maraccini et al., 2016c). A linear relationship between the log removal and light dose ($MJ.m^{-2}$) was determined (see Figure 4 - 14) as expected based on well-established UV disinfection technology design (U.S. Environmental Protection Agency, 1986). The uncertainty associated with the plate count measurement was probably important and could explain the outlier shown as a dark symbol in Figure 4 - 14. A Grubbs test performed on the residuals from the linear regression confirmed this data point (5.12 $MJ.m^{-2}$; 3.86) as a statistical outlier ($p < 0.001$[66]). A linear regression was thus performed without including this data point (shown in Figure 4 - 14), and confirmed the linear relationship between sunlight dose ($MJ.m^{-2}$) and *E. coli* log removal ($R^2 = 0.845$, N = 12) with a proportionality coefficient of 0.341 $m^2.MJ^{-1}$. In terms of decay coefficients, this translates to a linear relationship between *E. coli* decay coefficient (d^{-1}) and sunlight intensity ($W.m^{-2}$), with a proportionality constant of 0.0678 $m^2.W^{-1}.d^{-1}$.

[65] Chemicals introduced in buffered solutions were believed to not act as exogenous photosensitizers since solutions tested with moderate pH (below 9) were not found to trigger any enhanced decay compared with pure RO water.

[66] The hypothesis of normal distribution of the residuals was not rejected by Shapiro-Wilk test ($p = 0.791$).

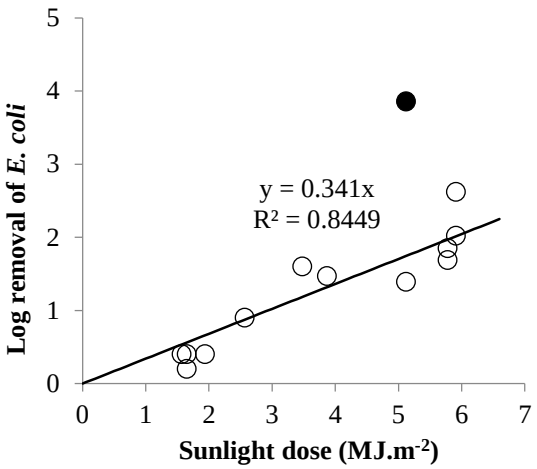

Figure 4 - 14: Effect of sunlight dose on *E. coli* decay at neutral pH (outlier shown as closed circle).

The results obtained are difficult to compare with the literature because few studies have been conducted with comparable set-ups and providing the inputs needed to calculate the sunlight dose and the log decay (see Table 1 - 11). Maraccini et al. (2016b) for example reported *E. coli* log removals of 0.69 and 0.73 (strains K12 and O157:H7, respectively) at a sunlight dose of 5.04 $MJ.m^{-2}$, which is lower than all the disinfection rates reported here for sunlight doses above 3.4 $MJ.m^{-2}$ (e.g. 1.39 at 5.12 $MJ.m^{-2}$). Maraccini et al. (2016b) however used an optical filter removing UV-B radiation, therefore suggesting the higher *E. coli* decay recorded during our study was mostly caused by direct UV-B damage. Muela et al. (2002) reported a log removal of 1.48 at 3.5 $MJ.m^{-2}$, which better agrees with the present study, but these authors used PAR wavelength[67] in saline solution meaning direct UV-B damage was not taking place. The different geometries of the set-up used (e.g. E-flasks vs open beakers) could explain the differences in the results reported. In addition, Maraccini et al. (2016b) and Muela et al. (2002) both used 'laboratory' *E. coli* strains while in this work, laboratory strain ATCC 10536 was evidenced to be less resistant to sunlight radiations than the wild type (see Appendix 15). Despite these differences, the results reported are within the same order of magnitude and confirmed the sensitivity of *E. coli* cells to direct sunlight exposure. Upscaling these results to a full HRAP broth is however challenging due to the differences in reactor geometries (e.g. depth of 25 cm versus 5 cm) and optical properties (opaque broth versus pure water). Due to competitive absorption of light by other components in wastewater, the overall effect of UV-B damage and endogenous photo-oxidation is therefore expected to be much lower in full-scale HRAPs than reported in this section. The impact of

[67] Artificial light source

sunlight disinfection in comprehensive algal broth was further investigated during bench experiments (see Chapter 5).

4.2.2.2. Direct damage by UV-A and visible light radiations

Two tests were performed to compare *E. coli* decay at neutral pH and in the absence of photosensitizers in open beakers and in beakers covered by a light filter as described in Chapter 2 section 2.2.2. Theoretically, *E. coli* decay in a covered beaker is only caused by endogenous photo-oxidation due to UV-A because only UV-B is known to trigger direct DNA damage (Curtis et al., 1992; Davies-Colley et al., 1999; Kadir and Nelson, 2014; Silverman and Nelson, 2016). Based on the importance of UV-B damage during *E. coli* exposure to sunlight described in the literature (Curtis et al., 1992; Silverman and Nelson, 2016), lower decay coefficients were expected in beakers covered with optical filters than open beakers (especially in the absence of exogenous photosensitizer).

A first test was conducted in the absence of photosensitizers at neutral pH: similar decay coefficients were recorded with or without UV-B[68]. This indicates a marginal impact of UV-B. This experiment was repeated but this time, the removal of UV-B caused a 50% reduction in decay coefficient[69]. This agrees with the findings from Silverman and Nelson (2016) who reported decay coefficients of 75.1 d^{-1} under full simulated sunlight against 41.0 d^{-1} using the same light but filtering out wavelengths below 320 nm. This experiment was not repeated due to experimental difficulties and instead the impact of sunlight on *E. coli* decay was further investigated during bench scale assays described in Chapter 5. The results presented here nevertheless suggest that in the absence of exogenous photosensitizers, endogenous photo-oxidation due to the action of UV-A and VIS contributes to most of photo-damage of *E. coli*. The respective contributions of DNA damage and endogenous photo-oxidation were not distinguished in the experiments conducted at bench and pilot scale in this study. These mechanisms will therefore be always referred to together as "direct photo-damage" in the following sections.

4.2.3. SUNLIGHT EXPOSURE AT HIGH PH

As demonstrated earlier, pH toxicity significantly impacted *E. coli* decay above temperature-dependent thresholds. Since various authors have reported that sunlight mediated *E. coli*

[68] Decay coefficient of 37.4 (CI_{95} = [9.2 – 65.6]) and 33.2 d^{-1} (CI_{95} = [4.4 – 60.7]) were reported in uncovered and covered beakers respectively. The differences generated over 2 hours are not significant in light of experimental error.

[69] Decay coefficient of 11.7 (CI_{95} = [-11.1 – 34.5]) and 5.1 d^{-1} (CI_{95} = [-17.5 – 27.7]) were reported in uncovered and covered beakers respectively. The differences generated over 2 hours are not significant in light of experimental error.

decay was enhanced at high pH (Ansa et al., 2008; Benchokroun et al., 2003; Curtis et al., 1992; Davies-Colley et al., 1999), tests were performed under sunlight at pH 10.

The impacts of sunlight intensity ($W.m^{-2}$) and dose ($MJ.m^{-2}$) on *E. coli* decay coefficients (d^{-1}) and log removal (-) are shown in Figure 4 - 15, respectively at both neutral pH (full dots) and high pH (empty dots). At pH 10 and high sunlight intensities, some decay coefficients and log removal could not be calculated since no viable *E. coli* cells were found in the second sampling. As expected, *E. coli* decay under sunlight was significantly enhanced at high pH: The average ratio between *E. coli* log removals measured at high pH and *E. coli* log removals measured at neutral pH (under similar temperatures and light doses) was 3.7 (minimum 0.94, maximal value 9.1, N = 5)[70]. The high variability is probably caused by measurement uncertainty as well as the mechanism's sensitivity to pH and temperature (as evidenced by the impact of temperature on pH toxicity in darkness, see section 4.1.3.3.)

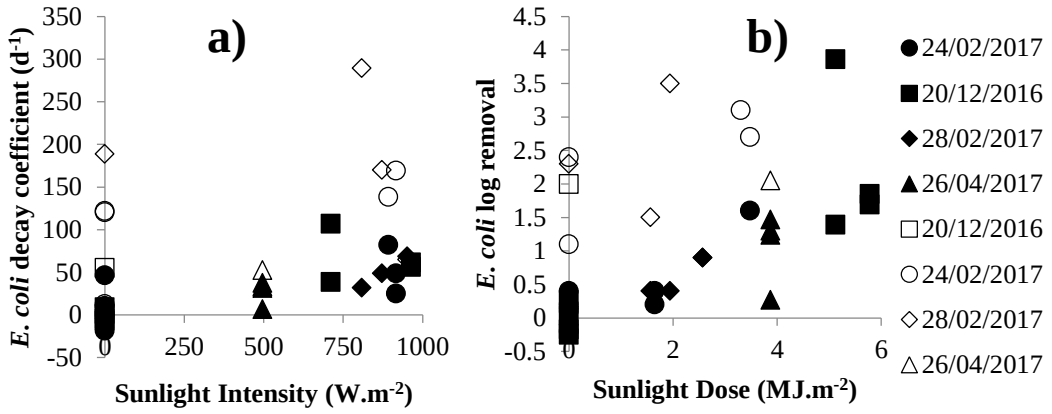

Figure 4 - 15: Influence of sunlight intensity on *E. coli* decay coefficients (a) and sunlight dose on *E. coli* log removal (b)[71].
Empty dots represents data from beakers filled with RO buffered at pH = 10 while full dots represent data from beakers filled with RO buffered at neutral pH.The shape of dots referred to the date of the experiment as shown in the legend.

While *E. coli* decay under sunlight was significantly faster at high pH than neutral pH, it is unclear if high pH enhanced the rate of sunlight-mediated disinfection mechanisms or if pH toxicity had an additive effect to the sunlight-mediated disinfection mechanisms. To investigate this, the values of the decay coefficients obtained at high pH under sunlight were compared to the values of the decay obtained at high pH in each control conducted in darkness. Because temporal changes in light intensity caused temporal changes in broth

[70] This value was probably underestimated due to missing data at pH = 10 and high sunlight radiations/intensities.
[71] As explained above, all values were calculated between 2 successive samplings.

temperature (both under sunlight and in darkness as all beakers were incubated outdoors), this comparison could only be performed based on data recorded at the same - sampling times. Unfortunately, significant temperature differences were still observed between open beakers and dark reactors[72]. The experimental decay coefficients in open beakers were therefore compared to the theoretical pH-induced decay coefficients [73] estimated from the pH and temperature measured in the open beakers at the end of the experiment[74] (Figure 4 - 16). Only three decay coefficients could be calculated to enable a direct comparison of experimental coefficients measured under sunlight exposure and in darkness. As can be seen, the *E. coli* decay coefficients recorded with sunlight exposure and high pH were on average 73 % higher[75] than the decay coefficients recorded in darkness at high pH. However, the experimental 'light coefficients' were on average 180 % higher than the theoretical 'pH-induced decay coefficients computed at the experimental pH and temperature values recorded in the light assays (N = 5)[76,77].

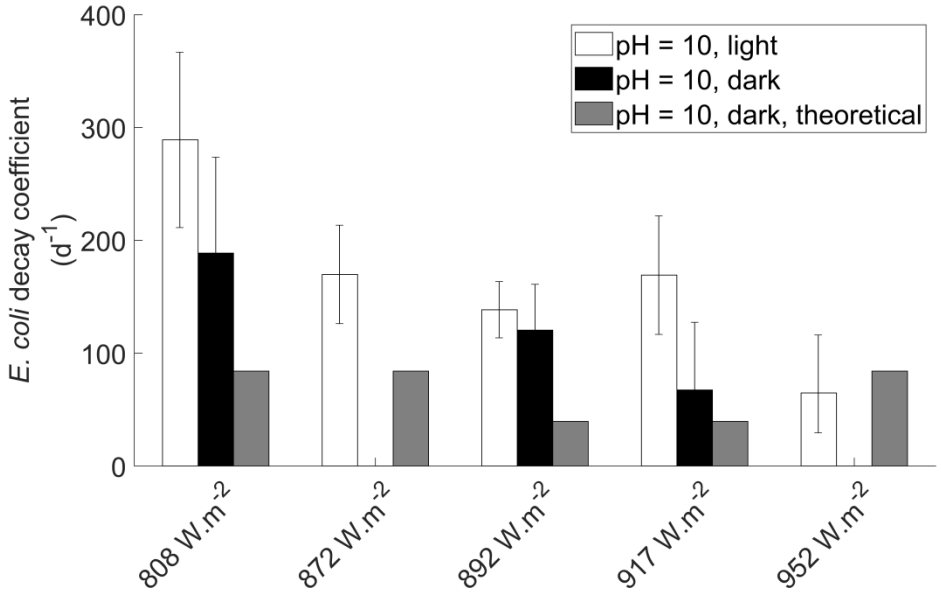

Figure 4 - 16: Comparison of *E. coli* decay coefficients at elevated pH when submitted to sunlight radiations and in darkness

[72] Evaporation prevention in closed beaker probably caused temperature to increase significantly
[73] i.e. according to Equation 4 - 3 developed in section 4.1.3.3.
[74] This measured value is not an ideal value since temperature was found to be highly dynamic during the experiment, and is not expected to be well depicted by the end-of-experiment temperature. It is however, the most accurate value available.
[75] 53,15, and 151 % in order of increasing sunlight intensity
[76] 243, 102, 250, 327, and -0.23 % in order of increasing sunlight intensity
[77] The decay coefficient measured at 952 $W.m^{-2}$ is probably also underestimated due to experimental error as the *E. coli* cell counts measured at the start of the exposition period was unexpectedly low. The data point was nevertheless kept since it could not be classified as a statistical outlier.

In order to further determine whether pH caused an additive toxic effect or a synergetic effect[78], the difference between the 'light coefficient' recorded at pH 10 and the theoretical 'pH-induced' coefficient calculated at the corresponding pH and temperature was compared to 'light decay' recorded at neutral pH (thus only caused by direct photo-damage). Relative improvements of 544 %, 76 %, 177 %, 415 %, and a mitigation of 128 %[79] were recorded in order of increasing sunlight intensity. Despite the large variation in the magnitude of the impact, the results suggested a positive interaction between sunlight and pH rather than solely an addition of toxicity effects. Unfortunately, measurement uncertainty (arising from the counting method and variability in the environmental conditions) did not allow for a more precise assessment.

The literature is lacking to assess the accuracy of the decay coefficients measured under sunlight exposure at high pH: Benchokroun et al. (2003) reported a decay coefficient of 49.7 d^{-1} at 372.2 $W.m^{-2}$ and pH 9.59 (T = 29°C) in sterilized wastewater, i.e. in the presence of photosensitizers, while Curtis et al. (1992) reported a decay coefficient > 66.3 d^{-1} at pH 9.4 (temperature unknown) under natural sunlight. These values are lower than the coefficients recorded in this study (decay coefficients all above 120 d^{-1}), which may be explained by the lower pH and temperature used in these past studies compared with the present study (pH = 10, T > 30°C).

4.2.4. IMPACT OF PHOTOSENSITIZERS

The use of wastewater filtrates as experimental broths was expected to expose *E. coli* cells to exogenous photosensitizers due to the presence of dissolved organic matter (Curtis et al., 1992; Davies-Colley et al., 1999; Kohn and Nelson, 2007; Mostafa et al., 2016; Oladeinde et al., 2018; Silverman et al., 2013). Under sunlight, higher decay coefficients are therefore expected in broths containing photosensitizers than in flasks filled with distilled water.

4.2.4.1. Exogenous photo-oxidation under full sunlight irradiation

Decay coefficients achieved in the presence (filtrates) or absence (pure water) of exogenous photosensitizers at neutral pH (all other conditions being similar) are displayed in Figure 4 -

[78] Assuming sunlight-induced direct damage is not sensitive to temperature

[79] Relative improvements were computed as $(\tilde{k}_{light}^{10} - k_{light}^{7})/k_{light}^{7}$ where $\tilde{k}_{light}^{10}$ is the difference between the decay coefficient measured at pH 10 in sunlight and the theoretical decay coefficient at pH 10 in darkness at the reported temperature, and k_{light}^{7} is the decay coefficient measured under the same sunlight conditions at neutral pH.

17. The measurement errors associated with these experiments[80] were very high due to the combination of low decay coefficient with short periods between samplings (error bars are therefore not shown). As can be seen, the presence of exogenous photosensitizers does not appear to increase decay coefficients and this was confirmed using a t-test at the 5% significance level[81] (N = 11, p = 0.560).

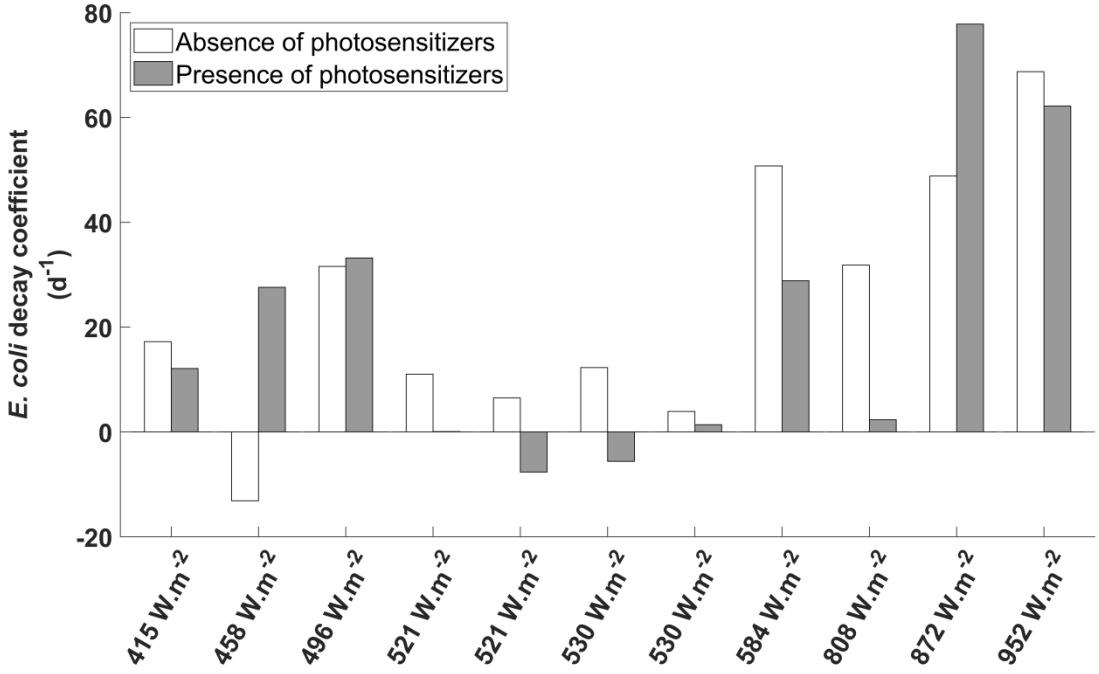

Figure 4 - 17: Decay coefficient of *E. coli* measured in the presence and absence of photosensitizers in the liquid broth under natural sunlight

As high pH damages bacterial cells by increasing their permeability to exogenous ROS (Davies-Colley et al., 1999), the introduction of photosensitizers at elevated pH was expected to further enhance the rate of *E. coli* decay under sunlight. Results from tests performed in HRAP filtrates buffered at pH 10 are shown in Figure 4 - 18. Again, the introduction of exogenous photosensitizers was not associated with a clear increase in decay coefficients. Due to the small sample size (N = 3), no statistical test was performed.

[80] Assuming an 8% error on the log-transformed *E. coli* cells counts

[81] The mean of the differences between the decay coefficients measured with and without photosensitizers was hypothesized to equal zero with the alternative hypothesis being that the difference is superior to zero: the t-test accepted the null hypothesis, thus rejecting the hypothesis of improved decay in the presence of photosensitizers.

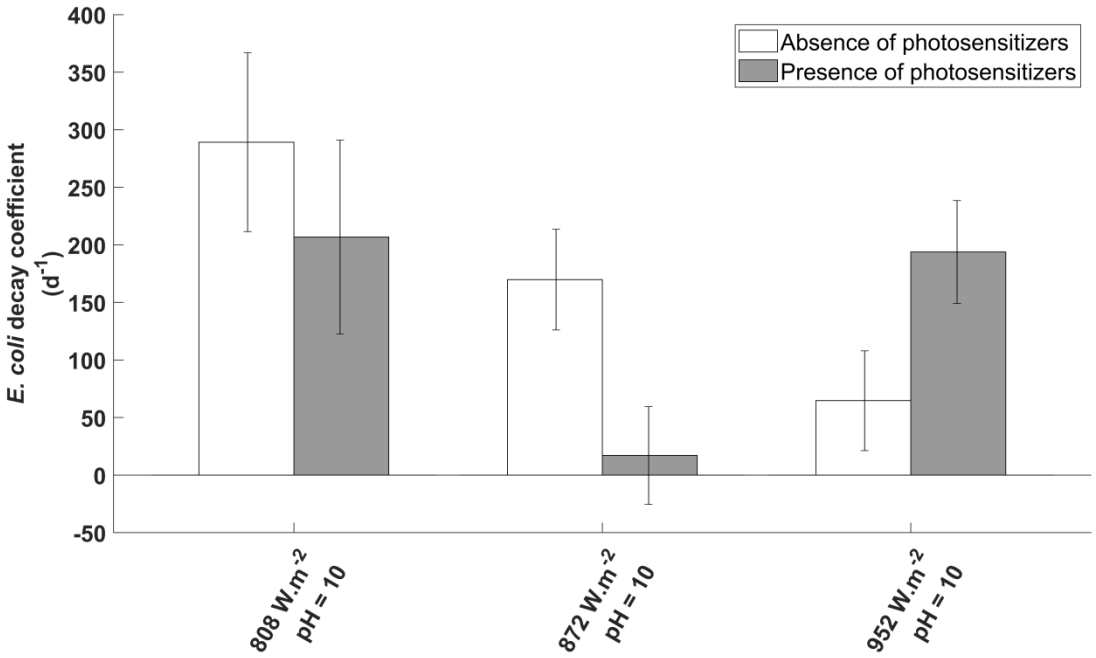

Figure 4 - 18: Decay coefficient of *E. coli* measured in the presence and absence of photosensitizers in the liquid broth under natural sunlight at pH 10

Overall, these tests suggest *E. coli* decay under full sunlight irradiation is not significantly improved by the presence of photosensitizers, meaning exogenous photo-oxidation is likely not quantitatively significant in HRAPs. It is possible that instead of (or despite) leading to the creation of ROS species, the chemicals in the HRAPs filtrate were absorbing sunlight thus causing the attenuation of sunlight-mediated damage to *E. coli* cells. This finding agrees with the conclusion of Maraccini et al. (2016) who found gram-negative bacteria to be little affected by exogenous photo-oxidation in general, natural organic photo-sensitizer being unable to enhance bacterial decay.

4.2.4.2. Exogenous photo-oxidation from UV-A and visible light

Because exogenous photo-oxidation is suspected to be activated by longer wave radiation, a test was performed at neutral pH to isolate the impact of UV-A and visible radiations (VIS) on exogenous photo-oxidation using HRAP filtrates to introduce photosensitizers (Table 4 - 4). In the following, the term ‘direct photo-damage’ is used to describe the combined effect of DNA damage by UV-B and endogenous photo-damage by UV-B, UV-A (and possibly VIS).

As can be seen from the results displayed in Table 4 - 4, no improvement in decay was recorded under UV-B deprived sunlight in HRAP filtrate (in expected presence of exogenous photosensitizers) compared with RO water (in absence of exogenous

photosensitizers). It is concluded that UV-A and VIS radiations trigger little damage from exogenous photo-oxidation at neutral pH for *E. coli.*

Table 4 - 4: Tests performed to investigate the mechanisms of *E. coli* disinfection using long wave radiations (λ > 320 nm) at neutral pH

Substrate	Presence of optical filter	Potential disinfection mechanism(s)	Log removal
RO water	Yes	Endogenous photo-oxidation by UV-A and VIS	1.30 [0.17 – 2.43]
HRAP filtrate	Yes	Endo and exogenous photo-oxidation by UV-A and VIS	1.24 [0.095 – 2.38]

4.3. CONCLUSIONS

***E. coli* removal in darkness**:

Natural decay (e.g. starvation), heat inactivation, wastewater toxicity, algal toxicity, and NH_3 toxicity did not cause significant *E. coli* decay in darkness and under the other experimental conditions tested in this study. In contrast, pH toxicity was significant above threshold values decreasing with temperature (e.g. pH > 9.9 at T 20˚C or pH 9.0 at T 35˚C). Interestingly, this mechanism of removal has not been well investigated in previous studies of disinfection in algal ponds, possibly because high pH values are only expected during periods of high light intensity[82] when sunlight-mediated mechanisms have been the principal mechanisms under investigation. This study is therefore the first that quantifies the impacts of pH and temperature on *E. coli* decay under a range of conditions relevant to HRAPs. Critically however, the results generated in this Chapter were obtained in conditions poorly relevant to full scale HRAPs (see Table 2 - 1) and validation is required (see Chapter 5).

Photo-damage:

As expected from the literature, direct photo-damage (i.e. the addition of direct DNA damage and endogenous photo-oxidation) significantly impacted *E. coli* survival in clear broth, (*E. coli* log-removal was linearly correlated to the sunlight dose received). As an example, under sunlight radiation of 1,000 $W.m^{-2}$, direct photo-damage could sustain 4.9 log removal of *E. coli* cells in just 4h. Endogenous photo-oxidation from direct natural sunlight was found to cause most of the direct photo-damage, mostly supported by UV-A and VIS wavelengths although this result remained unclear.

[82] Due to intense algal activity at high light intensities

Oppositely, exogenous photo-oxidation did not affect *E. coli* decay, even in filtrates from HRAP broth and wastewater at neutral pH (two relatively 'clear' broths). As stated by Maraccini et al. (2016b), dissolved materials in natural waters can either enhance or mitigate bacterial photo-damage via exogenous photo-oxidation or light absorption respectively. In this work, dissolved materials present in HRAP filtrates appeared more prone to block sunlight radiation than support exogenous photo-oxidation, meaning exogenous photo-oxidation is unlikely to be significant in HRAPs.

As in the case of pH toxicity, the findings discussed above were obtained in conditions poorly representative of full scale HRAPs and neglected the impact of essential parameters such as DO concentration. While exogenous photo-oxidation will likely remain negligible in full scale HRAP, validation of results obtained for direct photo-damage was needed (see Chapter 5).

Chapter 5: *E. coli* disinfection at bench scale; modelling and validation

During laboratory scale experiments, the decay of *E. coli* was evaluated under various conditions of illumination (darkness, sunlight, filtrated sunlight), pH (7 – 10), temperature (5 – 40°C), broth (RO water, wastewater and High Rate Algal Pond, HRAP, filtrates), and ammonium concentration. The study concluded that pH toxicity was the only significant mechanism[83] of disinfection in darkness, and endogenous photo-oxidation was probably the main mechanism under illumination at neutral pH. At elevated pH under sunlight, significant *E. coli* decay coefficients were measured, supported by both pH toxicity and sunlight mediated damage. It was however unclear whether effects of these two mechanisms were additive or synergistic. The impact of exogenous photo-oxidation was inconsistent and unlikely to be significant in the tested conditions.

As these results were achieved in relatively 'clear' media (RO water and filtrates), which promoted photo-oxidation mechanisms, and at 'normal' dissolved oxygen (DO) concentrations, findings must be confirmed under conditions relevant for HRAP full algal broth (e.g. high TSS, high variations of environmental parameters, see Table 1 - 3), and the models developed at laboratory scale must be parameterized for such conditions. Batch bench scale experiments were therefore conducted in 3 – 4 L reactors filled with freshly sampled HRAP microcosms in order to simulate relevant conditions of light-supply, and increases in DO concentration and pH observed in full-scale HRAPs during daytime[84].

Four experiments were carried out and each experiment included three tests conducted in the following order (see Chapter 2 section 2.2.3. for details): a HRAP microcosm was withdrawn from pilot scale HRAP, introduced into 2 reactors (Reactors A and B) and incubated under different conditions (e.g. high vs low DO, high vs neutral pH) depending on the specific experimental purpose. Following adjustment of experimental conditions, the two reactors were exposed to sunlight and monitored for *E. coli* cell count for up to 2 hours. Following this first test, cultured wild-type *E. coli* were added to obtain a final cell count of

[83] Above a temperature-dependant threshold (e.g. 21°C at pH 9.4, 10°C at pH 10)

[84] As discussed in Chapter 2, the area-volume ratio of laboratory experiments is irrelevant to simulate light-supply and was too high to enable significant O_2 super-saturation; the bench scale reactors filled with HRAP samples were instead designed to simulate relevant vertical light attenuation in HRAP broth under relevant mass transfer conditions.

approx. 10^6 MPN.100 mL^{-1} and the reactors were again exposed to sunlight and monitored for up to 2 hours. Finally, *E. coli* were added again to give approximately the same final cell density and the reactors were incubated in darkness for the third test[85].

In this Chapter, the results from these bench scale experiments are analysed and compared to the results from laboratory scale experiments (see Chapter 4) in order to verify conclusions and parameterize in full algal broth the decay models previously established (see Chapter 4).

The newly parameterized model was then tested against data from the pilot scale HRAP's presented in Chapter 3. This validation has two purposes:

1 Demonstrating that the most quantitatively significant mechanisms have been identified and that their impact was accurately quantified (present Chapter).
2 Providing a tool for improving the design and operation of HRAPs with respect to wastewater disinfection (Chapters 6 and 7).

5.1. BENCH SCALE EXPERIMENTS RESULTS

5.1.1. GENERAL MONITORING AND DATA ANALYSIS PROCEDURES

A typical set of results obtained from the monitoring of a bench scale reactor is shown in Figure 5 - 1 (broth pH, DO concentration, and temperature) and 5 – 2 (incident sunlight intensity and *E. coli* cell count) to illustrate the analytic procedure used[86]. The experiment shown compares *E. coli* cell count variations in two reactors filled with HRAP broth, illuminated by natural sunlight, kept at near-neutral pH, and under either 'normal' mass transfer conditions or continuous N_2 bubbling to lower DO concentration. As can be seen, photosynthesis caused pH and DO to increase in the first reactor (0.1 M HCl was added three times to keep the pH close to neutral) whereas N_2 bubbling was associated with a more stable pH (0.1 M HCl was added only once)[87] and DO concentrations below 2 $mg.L^{-1}$. Due to the variability of sunlight intensity illustrated in Figure 5 - 2 (see data at 13:20, 13:30, and 13:40), disinfection performance was assessed using *E. coli* log-removal (or decay

[85] The rationale of this protocol was detailed in section 2.2.3.
[86] The full dataset for all bench scale experiments is available in Appendix 16.
[87] This experiment was the second of three experiments carried out with the same HRAP broth in the reactor. In the first experiment, pH rose quicker in the reactor bubbled with N_2 than in the reactor with no bubbling (mixing provided by a vertical propeller), suggesting CO_2 was removed more rapidly in the reactor bubbled with N_2 (possibly through degassing or increased assimilation due to better mixing conditions). In the second experiment, less inorganic carbon would therefore be available in the N_2-bubbled reactor (as re-carbonation was not allowed between experiment due to continuous N_2 bubbling and sunlight exposure) and photosynthetic activity could have become inhibited, resulting in a more stable pH.

coefficients) calculated from consecutive measurements[88]. The same protocol was used in dark assays.

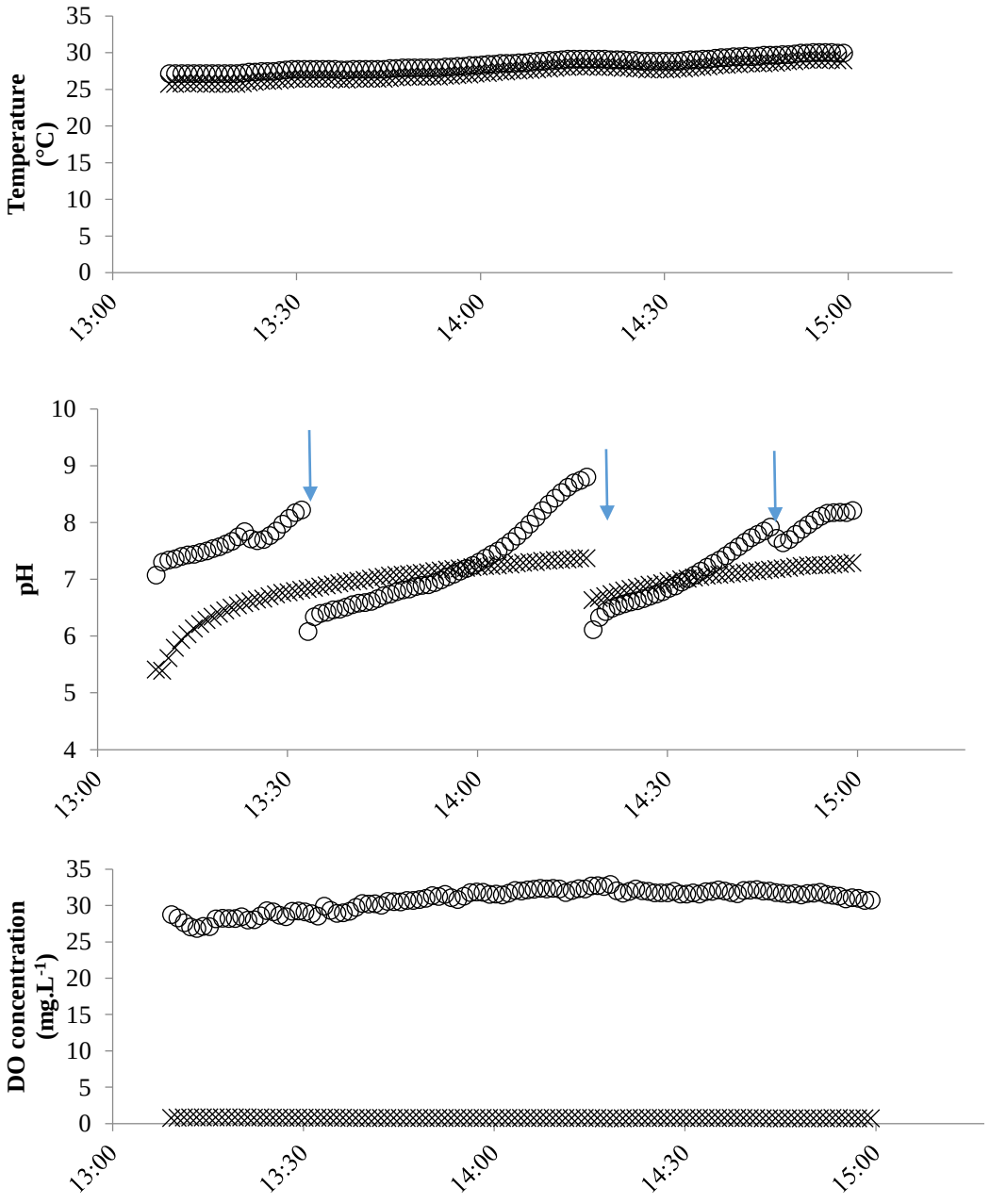

Figure 5 - 1: Changes in temperature, pH, and DO concentration in bench scale reactors filled with HRAP broth and exposed to sunlight.
Open circles (o) show data from reactor operated under 'normal' conditions and crosses (×) show data from reactor bubbled with N_2 gas to maintain a low DO concentration. The vertical arrows indicates time at which 0.1 M HCl was added to the reactors in order to maintain near neutral conditions of pH.

[88] Rather than calculating the first order decay coefficient via linear regression over the entire dataset.

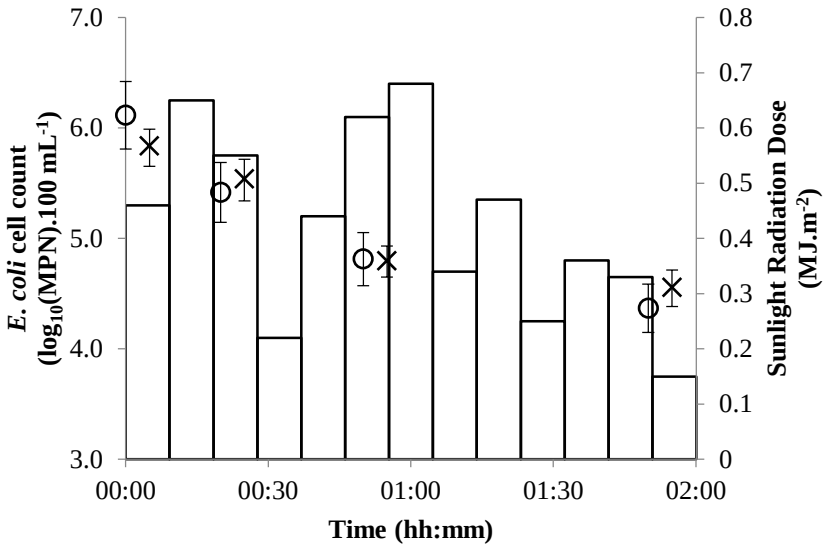

Figure 5 - 2: Changes in *E. coli* cell counts in bench scale reactors filled with HRAP broth and submitted to sunlight.
Open circles (○) show data from reactor operated under 'normal' conditions and crosses (×) show data from reactor bubbled with N_2 gas to maintain a low DO concentration. The histogram repsresents the sunlight radiation dose received during 10 min periods. Error bars show the 95% confidence interval associated with the MPN function used in Quanti-Tray.

5.1.2. *E. COLI* DISINFECTION IN DARKNESS

In darkness, *E. coli* decay coefficient ranged from 13.5 d^{-1} (pH 7.3, 22.6 mg DO L^{-1}, 34.3 °C) to 166.0 d^{-1} (pH 10.7, 20.0 mg DO L^{-1}, 31.0 °C) depending on experimental conditions[89], as shown in Figure 5 - 3.

In agreement with findings from laboratory experiments (Chapter 4), the highest decay coefficients reported (> 100 d^{-1}) were achieved at pH above 10. In three occurrences (all at pH higher than 10.6), no viable *E. coli* cells were found in the second sample collected[90] (and all samples collected thereafter). A simple linear regression analysis with individual parameters confirmed pH was the only experimental parameter significantly impacting *E. coli* decay at the 5% significance level (R^2 = 0.525, p-value[91] = 0.0419). The impact of DO concentration on decay was not statistically significant ($R^2 = 9.82 \cdot 10^{-4}$, p-value = 0.9413).

[89] As pH, DO, and temperature fluctuated during the experiments, the data shown for these parameters represent averages between 2 consecutive samples.
[90] Based on the initial count and the time between the first and second sampling, the decay coefficient during one of these events was superior to 192.6 d^{-1} (pH 10.9, 33.6°C, 23.2 mg DO.L^{-1}).
[91] N = 8, p-values testing against null effect in linear regression.

High decay coefficients (32 – 75 d^{-1}) were achieved at neutral pH in bench reactors and these 'high decays' were unlikely to be explained by high DO concentrations[92]. This high *E. coli* mortality may be related to a high natural death rate at high temperature (> 28°C), as reported in the literature (Blaustein et al., 2013; World Health Organization, 2011). Because these high 'background' dark decay coefficients were measured in HRAP microcosms exposed to sunlight 4 hours before being placed in darkness, another hypothesis for these unexpectedly elevated decay coefficients is the production of algal antibiotics during prior light exposure[93], a mechanism proposed by Bahlaoui et al. (1997) to explain seasonal variations in faecal coliform removal in HRAPs. Such a toxicity effect was, however, never recorded during laboratory experiments conducted using filtrates from HRAP microcosms pre-exposed to sunlight (see Chapter 4).

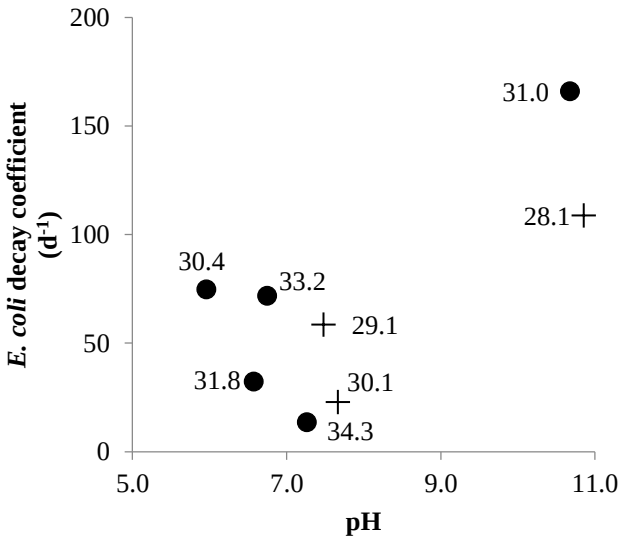

Figure 5 - 3: Decay coefficients calculated during batch assays conducted in darkness according to the pH measured in the broth .
Closed circle (●) represents data recorded when DO concentration was higher than 16 $mg.L^{-1}$ and crosses (×) when DO concentration was lower than 0.5 $mg.L^{-1}$. The numbers beside each data point give the broth temperature (°C).

In the following, the term "uncharacterized dark" decay will be used to describe the background *E. coli* decay occurring in darkness at neutral pH due to unknown mechanisms.

5.1.3. *E. COLI* DISINFECTION UNDER SUNLIGHT

5.1.3.1. Environmental conditions tested

In order to determine if an experimental parameter (e.g. pH) has an impact on *E. coli* disinfection, it is important to demonstrate there is no data bias and that parameters can be assumed to be independent.

[92] A two samples t-test accepted the hypothesis that the decay coefficients measured at high (> 16 $mg.L^{-1}$, N = 5) and low (< 2 $mg.L^{-1}$, N = 3) DO concentrations were not statistically different (p = 0.8418).
[93] The initial DO concentrations in the reactors tested in darkness without bubbling of N_2 were always above 25 $mg.L^{-1}$, confirming intense photosynthesis had taken place in the reactors before the microcosms were placed in darkness.

Simple regression analyses were carried out between each parameter (pH, DO concentration, temperature, and sunlight intensity[94]). The R^2 and associated p-values are shown in Table 5 - 1. Only DO concentration and temperature were significantly correlated (R^2 = 0.308, p = $6.17 \cdot 10^{-6}$). The impact of temperature should therefore be considered when analysing the effect of DO concentration on *E. coli* decay in the bench experiments, and statistical analysis should either consider DO concentration or temperature to avoid overfitting. No other apparent correlations were found, meaning that the effect of one parameter on the decay of *E. coli* death would be unlikely to be related to the impact of another parameter.

Table 5 - 1: Results from simple linear regression between each environmental parameter of interest (N = 58)[1].

R^2 / p-value	Sunlight intensity	pH	DO concentration	Temperature
Sunlight Intensity		0.0609	0.108	0.0487
pH	0.0573		0.00427	0.00169
DO concentration	0.0102	0.62		0.308
Temperature	0.0961	0.759	$6.17 \cdot 10^{-6}$	

[1]The values displayed above the diagonal are the R^2 coefficients between two parameters, the values under the diagonal are the associated p-value, testing for the hypothesis of null effect at the 5% significance level.

To further identify potential data bias (e.g. high pH and high DO are more frequent at high light intensity), the distributions of pH, DO concentration, and temperature were plotted against sunlight intensity data quartiles, as shown in Figure 5 - 4. As can be seen, the data collected should enable the study of the impacts of pH and DO concentration under sunlight because data at both high levels (i.e. pH > 9.4 and DO concentration > 8 $mg.L^{-1}$) and low levels (i.e. pH < 8 and DO concentration < 2 $mg.L^{-1}$) are available in all sunlight intensity quartiles. In particular the impact of pH and DO can be studied independently from the impacts of photo-oxidation.

Because temperature could not be controlled, significant variations occurred and the algal broth reached up to 38.2 °C (two samples were also withdrawn under significantly colder temperatures). The impact of temperature as a cofactor (i.e. by affecting the rate of disinfection mechanisms rather than causing death itself) was therefore carefully considered when analysing data.

[94] All calculated as the average of the values recorded (1 minute data logging) between two consecutive samples.

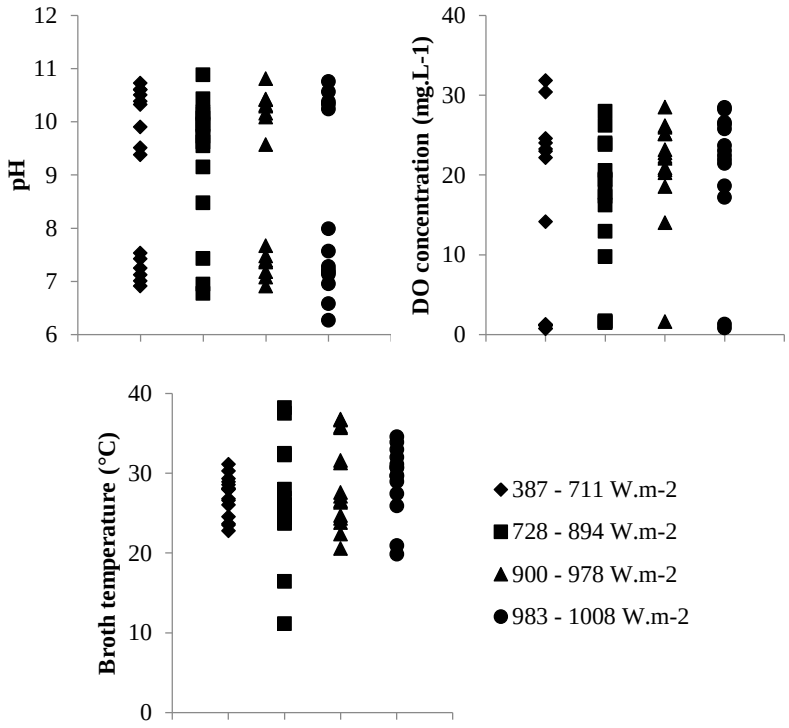

Figure 5 - 4: Distributions of pH, DO concentration, and temperature in bench scale reactors within sunlight intensity quartiles

5.1.3.2. Impact of environmental parameters on *E. coli* removal

All *E. coli* decay coefficients recorded under sunlight are shown in Figure 5 - 4. Although the two highest decay coefficients calculated were achieved at some of the highest sunlight intensities recorded (> 950 $W.m^{-2}$), high decay coefficients were also observed at lower sunlight intensities and non-significant decay coefficients were measured at high sunlight intensity. As a result, *E. coli* decay coefficient was not statistically correlated to sunlight intensity ($R^2 = 0.043$, $p = 0.144$[95], $N = 51$).

To confirm this finding while mitigating data uncertainty[96], decay coefficients were clustered in sunlight intensity quartiles as shown in Figure 5 - 5. A one-way ANOVA performed on the decay coefficients thus clustered confirmed the decay coefficients measured under different sunlight intensities did not differ at the 5% significance level ($p = 0.102$), indicating the impact of sunlight energy on the rate of *E. coli* decay in HRAP microcosms is unlikely to be significant. This finding agrees with results from the HRAP pilot monitoring (daily profile) which showed the highest decay was achieved in late afternoon when sunlight was relatively low (Chapter 3).

[95] Testing against a null effect of sunlight

[96] Due to the accumulation of experimental variability and uncertainty (not measured), and the mathematical uncertainty of the MPN function associated with Quanti-Tray measurements.

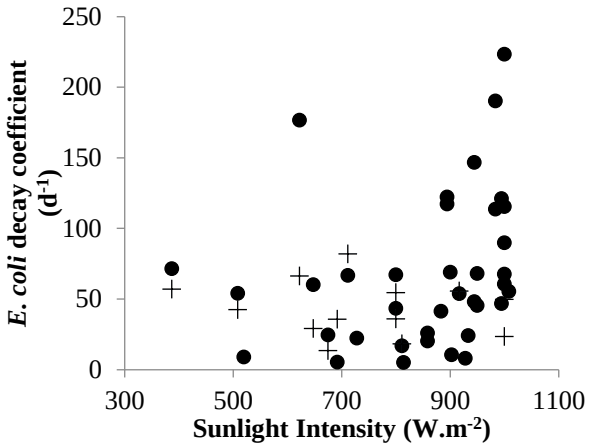

Figure 5 - 4: Impact of average sunlight intensity on *E. coli* decay coefficient during bench scale experiments.
Closed circle (●) represents data recorded when DO concentration was higher than 8 mg.L^{-1} and crosses (+) data recorded when DO concentration was lower than 1.7 mg.L^{-1}

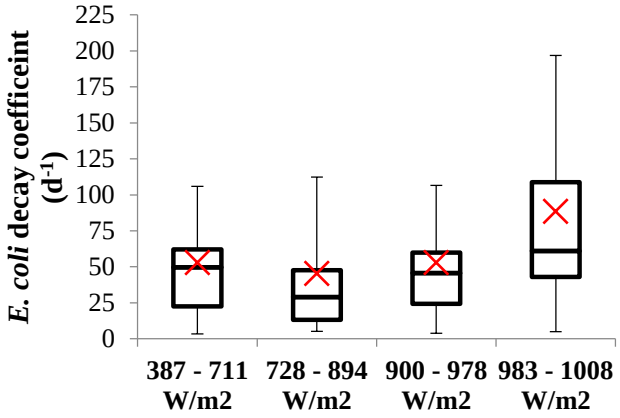

Figure 5 - 5: *E. coli* decay ceofficient distribution for each quartile of the average sunlight intensity received between consecutive samplings
(N = 15, 13, 10, and 13 respectively)

Given that the decay coefficients reported under sunlight were often high but not correlated to sunlight intensity, further analysis was conducted to establish potential correlations between pH, DO concentration, and decay coefficient in these tests. For this purpose, decay coefficients were clustered within light intensity quartiles based on DO concentration (low < 2 mg/L, and high, > 8 mg/L), and pH (considered low below 9.4 and high above this threshold based on laboratory findings). To identify the potential impact of temperature, experimental decay coefficients were also corrected for temperature (based on the Equation 4 - 3, and shown in Figure 5 - 6b). As can be seen in Figure 5 - 6, high decay coefficients values were not systematically associated with high/low pH and DO values, even when

compensated for temperature. In addition, while the highest decay coefficients calculated were obtained under conditions of high pH and high DO concentrations, this was probably related to the impact of temperature on pH toxicity as shown by the temperature-corrected data. Surprisingly, "low decay coefficients" (< 50 d^{-1})[97] were frequently associated with high pH (> 9.5). A 3-way ANOVA[98] confirmed the lack of correlation between sunlight intensity, DO, and pH and either non-temperature-corrected (p = 0.1069, 0.1058, and 0.2641, respectively) or temperature corrected decay coefficients (p = 0.6289, 0.6787, and 0.3826, respectively). The number of decay coefficients measured at both neutral pH and low DO concentrations was too small for a more in-depth numerical analysis. Results from such samples are however discussed in next section.

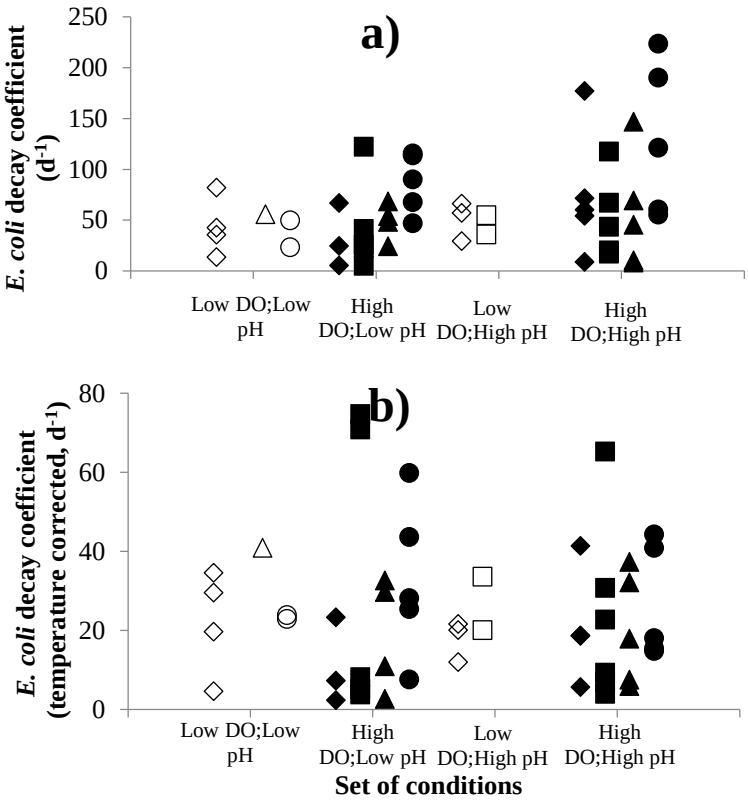

Figure 5 - 6: *E. coli* decay coefficient measured per set of conditions (DO concentration and pH), and per quartile of sunlight intensity recorded (Q1 = ♦; Q2 = ■; Q3 = ▲; Q4 = ●)

[97] While 50 d^{-1} would be considered a high decay coefficient in the context of the pilot scale HRAP monitoring, this value is relatively low compared with the highest values reported in bench scale study. A coefficient of 50 d^{-1} also corresponds to the value predicted at pH 10 and 30°C in darkness according to Equation 4 - 3 and is thus the expected minimum in most of the instances of this study.

[98] Data were categorized by sunlight quartile, neutral (< 9.5) and high (> 9.5) pH, low (< 2 $mg.L^{-1}$) and high (> 8 $mg.L^{-1}$) DO concentration.

5.1.3.3. Comparative results between tests performed on a same day

As the chemical and biological characteristics of HRAPs can vary greatly over time, algal broth temporal variability could explain the lack of trends observed when analysing the entire data set as done above. In this section, each experiment is analysed individually based on the final disinfection efficiencies (calculated as $log_{10}\left(\frac{C_0}{C_{end}}\right)$) experimentally achieved, the total sunlight dose received ($MJ.m^{-2}$), and the averaged pH, DO concentration, and temperature recorded (Table 5 - 2). As a reminder, each set of experiments included 3 tests conducted on the same day in the following order:

1. A HRAP microcosm was exposed to sunlight for up to 2 hours under different conditions of pH and DO concentration (Reactor A and B in Table 5 - 2).
2. Cultured wild-type *E. coli* (see Chapter 2 section 2.2.2.1.) was added to both reactors to reach a final cell count of approx. $10^6 \cdot 100$ mL^{-1} and the reactors were again exposed to sunlight for up to 2 hours.
3. *E. coli* was added again and the reactors were incubated in darkness.

Impact of sunlight exposure: Only sunlight mediated decay and uncharacterized dark decay were expected to influence *E. coli* survival under anoxic and neutral pH conditions on 14/11/2017 (Reactor B). The similar decay coefficients reported under sunlight and in darkness confirmed that sunlight mediated decay mechanisms had little significance in the full algal broth.

Impact of DO concentration: DO concentration had no significant impact on *E. coli* decay at neutral pH on 14/11/2017 and no apparent impact during the first test performed on 02/11/2017, but DO concentration was associated with improved decay both under sunlight (test 2) and in darkness (test 3). We postulate that the differences between the tests conducted on 02/11/2017 were caused by the combination of higher pH and higher temperature experienced during tests 2 and 3 under high DO concentrations[99] since pH toxicity impact on *E. coli* was demonstrated to be highly sensitive to temperature (Chapter 4). We therefore conclude that DO concentration has no significant impact on *E. coli* removal in HRAP. This could be expected since we had dismissed the impact of sunlight on *E. coli* decay in bench experiments earlier: as DO concentration is not known to influence *E.*

[99] Reactor A (high DO) had a lower volume (approx. 3 L) than Reactor B (low DO, approx. 4 L) resulting in consistently higher temperatures in Reactor A after long exposure to sunlight radiation.

coli survival in the absence of sunlight radiation (Benchokroun et al., 2003; Curtis et al., 1992), it should have little impact in a light-limited system.

Impact of pH: On 16/11/2017, *E. coli* removal under sunlight was significantly faster at pH 10.4 - 10.8 than neutral pH, and *E. coli* removal in darkness was significantly faster at pH 10.9 than neutral pH. These results confirmed laboratory scale findings that pH toxicity is a significant contributor to *E. coli* decay, albeit at a lesser magnitude than previously recorded (see Chapter 4 section 4.1.3.3.).

Impact of uncharacterized dark decay: At neutral pH, the decay coefficients were similar in darkness and under sunlight on 14/11/2017, but higher in darkness on 16/11/2017[100], suggesting uncharacterized dark decay was the main removal mechanisms in these tests. On 23/11/2017, *E. coli* cells introduced into the HRAP broth were inactivated within minutes in darkness at neutral pH (and high DO concentration[17]). As these very high decay coefficients were recorded in the absence of any of the harmful conditions identified during laboratory scale experiments, these results provide evidence that dark decay is the main contributor to *E. coli* decay in full algal broth.

[100] The experiment carried out on 14/11/2017 was performed at low DO concentration while the experiment carried out on 16/11/2017 was performed at high DO concentration. Based on the results previously discussed which showed DO had little influence on *E. coli* removal, this is not expected to be relevant to this discussion.

Table 5 - 2: Results from bench experiments by experiment

Experimental set		Temperature (°C)		DO (mg.L^{-1})		pH		Light dose (MJ.m^{-2})	Time (h:m)	*E. coli* log removal[1]	
		Reactor		Reactor		Reactor				Reactor	
Date	Phase	A	B	A	B	A	B			A	B
02/11/2017	Light 1	25.5	25.4	17.1	1.5	9.7	9.7	4.95	1:50	1.48 [1.15 - 1.80]	1.24 [0.95 - 1.57]
	Light 2	30.0	27.7	23.1	1.3	10.5	10.6	3.06	1:30	2.77 [2.40 - 3.18]	1.34 [1.19 - 1.47]
	Dark	31.0	28.2	19.8	0.36	10.7	10.9	0	1:05	3.01 [2.24 - 2.98]	1.97 [1.29 - 2.03]
14/11/2017	Light 1	24.3	22.9	22.0	1.2	7.3	7.5	5.64	1:55	1.09 [0.77 - 1.40]	1.32 [0.95 - 1.70]
	Light 2	28.6	27.3	30.8	0.8	7.4	6.9	4.91	1:50	1.75 [1.37 - 2.12]	1.28 [0.94 - 1.60]
	Dark	31.1	29.6	24.4	0.5	6.3	7.6	0	1:40	1.61 [1.26 - 2.01]	1.23 [0.85 - 1.60]
16/11/2017	Light 1	27.7	26.9	23.6	15.2	10.4	7.3	6.95	2:00	2.47 [2.07 - 2.88]	1.61 [1.26 - 1.97]
	Light 2	32.0	31.7	28.2	23.3	10.8	6.9	5.97	1:50	2.83 [2.44 - 3.24]	1.59 [1.18 - 2.06]
	Dark	34.0	33.8	20.3	23.7	10.9	7	0	0:45	> 2.61[2]	1.22 [0.85 - 1.65]
23/11/2017	Light 1	31.3	30.3	23.9	21.4	10.2	7.2	7.15	2:00	3.66 [2.94 - 4.63]	1.24 [0.93 - 1.55]
	Light 2	36.6	36.8	24.9	25.8	10.4	7.1	2.84	0:50	> 4.05[2]	0.59 [0.19 - 1.00]
	Dark	39.6	38.3	17.9	25.2	10.4	6.3	0	0:00[3]	>>[3]	>>[3]

[1] The values in bracket show the 95% confidence interval calculated from the Quanti-Tray MPN table uncertainty;
[2] No live *E. coli* cells were detected in the second sample withdrawn at the dilution tested. A minimal log removal was calculated based on the first cell count measured and the analytical detection limit of Quanti-Tray countings;
[3] No *E. coli* were detected in the first sample (i.e. within 10 minutes following the cells suspension in the algal broth) so no removal efficiency could be measured (> 4 log removal within minutes).

5.1.4. DISCUSSION

Bench scale assays conducted using HRAP microcosms confirmed the impact of high pH toxicity on *E. coli* disinfection efficiency both in darkness and with exposure to sunlight (section 5.1.3.3.), albeit at a lower magnitude than predicted from laboratory scale measurements, in agreement with results from laboratory assays conducted in RO water or filtrates. This lower impact of sunlight direct damage and pH toxicity was not associated to the compensation of *E. coli* decay by cell growth in nutrient rich algal broth since *E. coli* growth is not expected in HRAP broth (as discussed in section 2.2.2.4.).

Photo-damage was not likely to have been significant during bench scale assays (as demonstrated by the lack of impact of sunlight intensity on decay coefficients in sections 5.1.3.2. and 5.1.3.3.), in contrast to laboratory scale experiments where photo-damage caused *E. coli* death. This discrepancy may be explained by light attenuation in the HRAP microcosms. Because DO is suspected to influence the production of free radicals during

sunlight irradiation (Castro-Alférez et al., 2016; Davies-Colley et al., 1999; Imlay, 2013), light attenuation preventing photo-oxidation is also likely to explain the lack of impact of DO concentration on decay coefficients in HRAP microcosms[101].

High 'uncharacterized dark' decay coefficients were reported in darkness at neutral pH during bench assays and were possibly caused by unidentified mechanisms (e.g. formation of antibiotics by algae). Uncharacterized dark decay is henceforth defined as the macro-scale manifestation of a number of unknown dark mechanisms leading to a 'background' decay in both darkness and light (light supply may however indirectly affect some of these mechanisms, e.g. via temperature increase). While not expected to be significant at the start of this study, this "mechanism" potentially contributed to the bulk of *E. coli* removal in HRAP broth.

Discrepancies between laboratory scale and bench scale results are diverse and have a high significance for our understanding of *E. coli* decay in HRAP broth. The origins of these differences are further discussed in Appendix 17, in which the experimental conditions used in both phases are listed and compared. The aim is to highlight potentially overlooked differences that may explain the inconsistencies between the decay coefficients measured at laboratory and at bench scale. In particular, the conditions to which *E. coli* cells were exposed before being introduced in the reactors may have influenced their fitness and therefore their decay response to the conditions experienced during both experimental steps (the potential impact of cell fitness on the patterns of *E. coli* decay observed was for instance discussed by Blaustein et al, 2013). However, as explained in Appendix 17, the inoculum used during bench scale experiments were obtained from the same strain and cultivation method as during laboratory scale experiments, minimizing the discrepancy in that regard during both experimental phases.

[101] DO fuels photo-oxidation by providing a source for ROS formation, but the effect is likely to be marginal considering attenuation of sunlight in HRAPs.

5.2. *E. COLI* DECAY IN HRAPS: MODEL PARAMETERIZATION

5.2.1. *E. COLI* DECAY PREDICTION AT BENCH SCALE

Based on bench scale experiments, only uncharacterized dark decay, pH-toxicity, and, to a lesser extent, direct photo-damage[102] have the potential to significantly impact *E. coli* survival in HRAPs. In order to better characterize the respective contribution of these mechanisms during bench assays, and possibly evidence the existence of unidentified disinfection mechanisms, the disinfection efficiency in bench HRAP microcosms was predicted based on laboratory data and compared to bench scale experimental data. For this purpose, *E. coli* decay was modelled using first-order kinetics, assuming the HRAP microcosms were well mixed[103] (i.e. *E. coli* cell density, pH, and temperature are uniform), and that *E. coli* decay mechanisms are taking place independently. Synergistic or antagonistic effects between mechanisms were assumed to be negligible. Changes in *E. coli* cell count in the HRAP broth C can be described as:

$$\frac{dC}{dt} = \left(k_{nat} + k_{pH} + k_{sun}\right) \cdot C \qquad (5 - 1)$$

where k_{nat}, k_{pH} and k_{sun} are the specific first order kinetics coefficients associated with uncharacterized dark decay, pH toxicity, and photo-damage respectively.

The value of k_{pH} was calculated as (see Chapter 4 section 4.1.3.3.):

$$k_{pH}(pH,T) = k_{pH}^{20} \cdot {\theta_{pH}}^{T-20} \cdot 10^{pH-14} \qquad (4 - 3)$$

where pH and T represent broth pH and temperature (°C), θ_{pH} is the correction factor for temperature (determined to be equal to 1.14), and k_{pH}^{20} corresponds to the decay coefficient at 20°C and pH 14 ($1.4 \cdot 10^5$ d^{-1}).

The value of k_{sun} was predicted using the linear relationship developed in section 4.2.2.1. adjusted for light attenuation as commonly performed in the literature (Béchet et al., 2015; Bello et al., 2017; Craggs et al., 2004; Dahl et al., 2017) leading to the Equation 5 - 2 (see Appendix 18 for calculation details):

[102] Including direct DNA damage and endogenous photo-oxidation.
[103] This assumption is justified and discussed in Appendix 2

$$k_{sun}(t) = \frac{\alpha . Hs(t)}{\sigma . d} * (1 - e^{-\sigma . d}) \quad (5 - 2)$$

where Hs is the incident sunlight intensity at the water surface ($W.m^{-2}$), d is the water column depth (m), σ the light extinction coefficient of the algal broth (m^{-1}), and α is the proportionality factor between sunlight intensity and decay coefficient (0.0678 $m^2.W^{-1}.d^{-1}$, determined in section 4.2.2.1.). In this study, the water column depth was 0.25 m and the broth optical density was estimated to be 64 m^{-1} based on algae samples from the pilot scale HRAPs[104].

Because uncharacterized dark decay was not significant at laboratory scale, no models were developed for this mechanism. However, bench scale experiments evidenced high dark decay for *E. coli* in HRAPs broth, probably greatly influenced by broth temperature. We thus attempted to model the uncharacterized dark decay according to the Marais equation (Marais, 1974) as is often performed in the literature (Canale et al., 1993; Mayo, 1995; Ouali et al., 2015):

$$k_{nat}(t) = k_{nat}^{20} \cdot {\theta_T}^{T-20} \quad (5 - 3)$$

In Equation 5 - 3, T is the pond temperature, k_{nat}^{20} is the constant natural decay coefficient at 20°C, and θ_T is the temperature correction coefficient.

Equation 5 - 3 was calibrated using data from pilot scale HRAP daily profiles evidencing limited variations in pH as well as stable *E. coli* cell count over 24 h[105]: we therefore hypothesized that under these specific conditions *E. coli* decay was dominated by a temperature-dependent dark decay (see Figure 3 - 8 for the sunlight and pH data, and Figure 3 - 9 for *E. coli* cell count data). Because *E. coli* cell count was relatively stable throughout each day, we assumed the pond was at pseudo-steady state and the value of the natural decay coefficient k_{nat} was estimated using a steady state balance, meaning it could be calculated as $k_{nat} = \frac{1}{HRT} \cdot \left(\frac{C_{IN}}{C} - 1\right)$ for each value of *E. coli* cell count available during these days (see section 3.3.1.).

[104] Average of light extinction coefficients measured at 683 nm (N = 35, std = 22.9 m^{-1}). As a comparison, Maiga et al. (2017) measured light extinction coefficients ranging from 11 to 16 m^{-1} for PAR and UV-B respectively in facultative ponds.

[105] i.e. 12 – 13/10/2015, 29 – 30/10/2015, and 16 – 17/03/2016 (see Chapter 3 section 3.3.), for which maximum pH was resp. 7.81, 9.38, and 8.78, all below 9.4 identified as the threshold of noticeable pH toxicity (see Chapter 4) section 4.1.3.3.

As can be seen in Figure 5 - 7 comparing predicted and measured rates of *E. coli* uncharacterized dark decay, the values θ_T = 1.14 and k_{nat}^{20} = 10.4 d^{-1} provided the best fit between predicted and measured *E. coli* decay coefficients for the three days tested (R^2 = 0.15, N = 32). Significant uncertainty was associated with k_{nat}^{20} value due to variability of the data set: the impact of the uncertainty on k_{nat}^{20} on the model is represented in Figure 5 - 7 by displaying predictions at k_{nat}^{20} values of 4 and 20 d^{-1}, which allowed covering the full range of the measured decay coefficients. The performance of Equation 5 - 3 at predicting *E. coli* decay in HRAP broth was further analysed in this section based on bench scale experimental results.

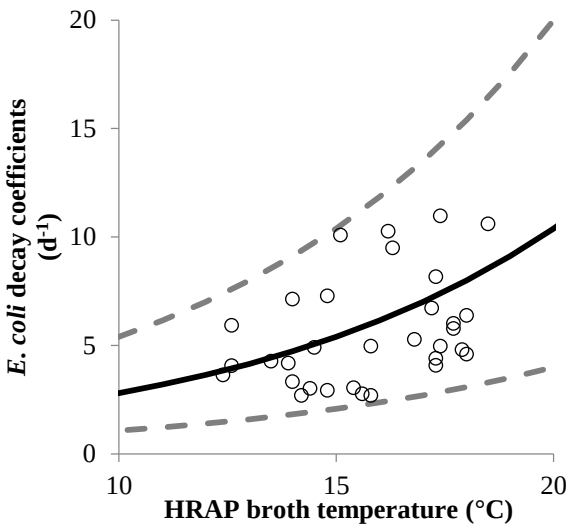

Figure 5 - 7: Comparison of modelled (black line) vs. measured (o) rates of *E. coli* uncharacterized dark decay in pilot scale HRAP as a function of broth temperature.
Dashed lines show predictions at k_{nat}^{20} values of 4 and 20 d^{-1} (framing all measured decay coefficients).

The first order decay coefficient in the bench reactors was then calculated using the experimental values of broth pH and temperature recorded every minute (see Chapter 2 section 2.2.3.4.) and sunlight intensities (10 minute intervals) obtained from the NIWA data base (location Palmerston North, agent number 21963). The decay coefficient was thus calculated for every minute of the experiments, assuming the sunlight intensity was constant over 10 minute periods. *E. coli* cell counts were successively calculated from the first measured count from Equation 5 - 1 using Euler method with a 1 minute time step.

5.2.2. BENCH SCALE PREDICTION AND MODEL PARAMETERIZATION

As can be seen in Figure 5 - 8 comparing predicted versus measured *E. coli* cell counts in bench reactors, the model poorly predicted *E. coli* cell counts at low cell densities (< 10^4 CFU.100 ml^{-1}) and significantly underestimated *E. coli* cell counts at high cell densities (> 10^4 CFU.100 ml^{-1}, Figure 5 - 8b), meaning the model tended to overestimate *E. coli* decay coefficient. An outlier (-16.43 log.100mL^{-1}; 3.13 log.100mL^{-1}), measured at pH 10.9, 28.0

mg DO.L^{-1}, 32.5 °C, and under 858.3 W.m^{-2} of sunlight radiation was removed from Figure 5 - 8.

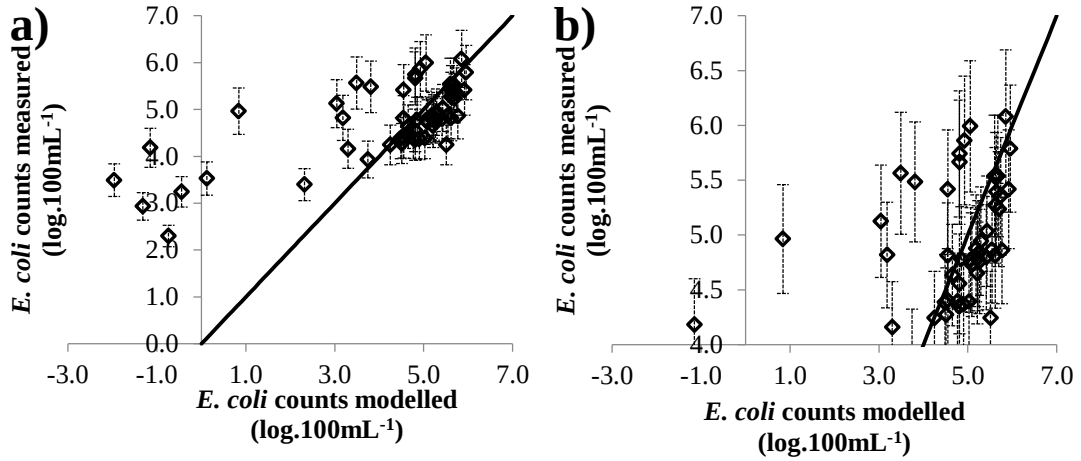

Figure 5 - 8: Measured[106] vs modelled log transformed *E. coli* cell counts. a) All data; b) Data for cell counts measured above 10^4 CFU.100 mL^{-1}.
The dark line shows the equality of both values.

In order to determine potential causes of prediction inaccuracies, a multilinear regression was performed on the prediction residuals against the average sunlight intensity received between consecutive samples, the sunlight dose received since the last sample, the sunlight history[107], and the averaged values of pH, DO concentration, and temperature between consecutive samples. The results of this analysis are shown in Table 5 - 3.

Table 5 - 3: Results from the multilinear regression of the difference between measured and modelled log-transformed *E. coli* cell counts with parameters (N = 55, R^2 = 0.52, p-value[1] = $2.17 \cdot 10^{-6}$)

Parameter	Estimate	Standard error	t-Stat	p-value[2]
Intercept	-10.7	3.45	-3.10	$3.26 \cdot 10^{-3}$
Sunlight intensity (W.m^{-2})	$4.69 \cdot 10^{-4}$	$1.73 \cdot 10^{-3}$	0.271	0.788
Sunlight dose received between consecutive samplings (MJ.m^{-2})	0.628	0.575	1.09	0.281
Sunlight dose cumulated since the start of experiment (MJ.m^{-2})	0. 10	0.170	3.00	$4.24 \cdot 10^{-3}$
pH	1.09	0.189	5.77	$5.58 \cdot 10^{-7}$
DO concentration (mg.L^{-1})	0.0230	0.0384	0.599	0.552
Temperature (°C)	-0.0991	0.150	-0.660	0.512

[1] Testing for a constant modelling
[2] Testing for a null effect

[106] An average 7.9 % error on the log transformed cell count was associated with the MPN function of the Quanti-Tray measurements. Because this error is generated by the MPN function characteristics, it is expected to be lower at high cell counts than at low counts. Adding the experimental error and variability, 10% uncertainty was assumed on the measured *E. coli* cell counts through Quanti-Tray method for simplicity.
[107] The sunlight history is the total energy received since the start of an experiment.

This analysis revealed that pH significantly affected the variation of the prediction residual (p-value << 0.05). The positive value of the associated 'estimate' (1.09, standard error of 0.189) indicates pH was involved in the under-estimation of *E. coli* cell counts (i.e. decay coefficient over-estimation). This can be seen in Figure 5 - 9, as residuals (measured minus modelled *E. coli* cell counts) were spread between -1.3 and +1.7 log units at pH under 9.4 but regularly above 2 (N = 8) at pH above 9.4. Because microbial communities are well known to form biofilms that protect them against various adverse factors (Katharios-Lanwermeyer et al., 2014) including moderate pH (Babauta et al., 2012; De Boer et al., 1993; Charles et al., 2017; Hunter and Beveridge, 2005)[108], the presence of solids and other microbial species in the HRAP microcosms used at bench scale probably protected *E. coli* from pH toxicity. As the impact of temperature on pH toxicity is unlikely to be affected by the broth composition, only the value k_{pH}^{20} used in Equation 4 - 3 should be adjusted for field conditions. Taking advantage of the stable pH (10.8 – 10.9) experienced in darkness at low DO concentration[109], results from the test 3 performed on 02/11/2017 (Reactor B) were used to calibrate k_{pH}^{20}. While an average value of 293 d^{-1} was expected from Equation 4 - 3 from pH alone, k_{pH} was experimentally estimated to be 100 d^{-1} and the value of k_{pH}^{20} was likewise reduced from $1.2 \cdot 10^5$ d^{-1} to $3.1 \cdot 10^4$ d^{-1} to predict *E. coli* cell counts accurately. Equation 4 - 3 was corrected accordingly and *E. coli* cell counts in bench scale reactors were modelled again following the same protocol.

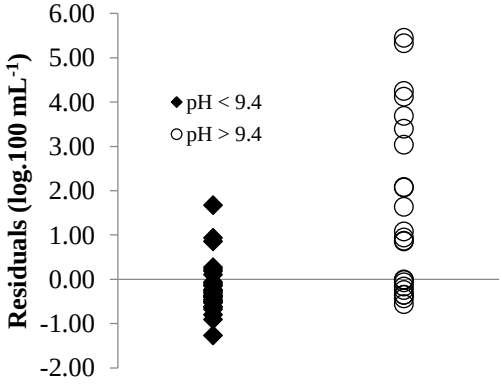

Figure 5 - 9: *E. coli* cell count modelling residuals (measured minus modelled) according to low (< 9.5) and high (> 9.5) pH[110]

[108] Charles et al. (2017) found *Alishewanella* and *Dietza spp.* could survive pH 12.0 due to the formation of flocs.

[109] This reactor did not experience an unexpectedly high mortality, suggesting die-off was mainly caused by pH toxicity.

[110] One extreme residual (19.6) obtained for pH 10.9 is not shown in Figure 5 - 8. A Grubbs test identified this data point as an outlier of the whole data set ($p < 0.001$, test carried despite test for normality being rejected). This data point can however not be dismissed from the analysis as its discrepancy is possibly related to experimental variability, rather than experimental error.

Figure 5 - 10 displays experimental versus modelled data after k_{pH}^{20} was parameterized. As can be seen, the model no longer seems to overestimate *E. coli* decay (underestimate cell density)[111]. A new multilinear regression was performed on the prediction residuals (measured minus modelled) to identify parameters potentially linked to systematic decay underestimation or overestimation, as this could evidence mechanisms of *E. coli* decay currently unaccounted for.

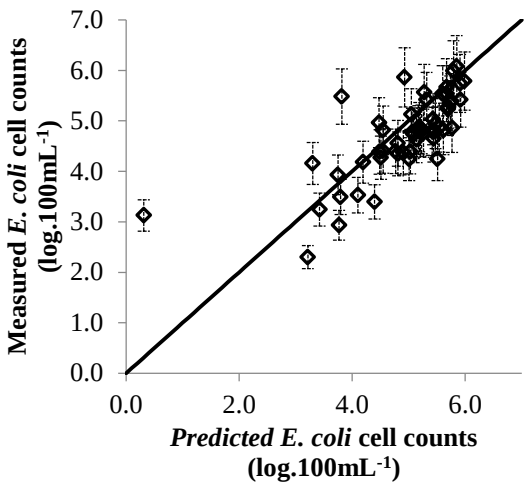

Figure 5 - 10: Measured[106] vs predicted log transformed *E. coli* cell counts.
The dark line shows the equality of values.

Table 5 - 4: Results from the multilinear regression of the difference between measured and modelled log-transformed *E. coli* cell counts with in situ parameters (N = 55, R^2 = 0.305, p-value[1] = 0.00593)

	Estimate	Standard error	t-Stat	p-value[2]
Intercept	-2.55	0.896	-2.85	$6.41 \cdot 10^{-3}$
Sunlight intensity ($W.m^{-2}$)	$2.01 \cdot 10^{-4}$	$4.49 \cdot 10^{-4}$	0.447	0.657
Sunlight dose received between consecutive samplings ($MJ.m^{-2}$)	0.0869	0.149	0.583	0.563
Sunlight dose cumulated since the start of experiment ($MJ.m^{-2}$)	0.0740	0.0440	1 68	0.0992
pH	0.0520	0.0490	1.06	0.294
DO concentration ($mg.L^{-1}$)	-0.0127	$9.96 \cdot 10^{-3}$	-1.28	0.208
Temperature (°C)	0.0463	0.0389	1.19	0.240

[1] Testing for a constant modelling
[2] Testing for a null effect

As evidenced by the data displayed in Table 5 - 4, no parameter significantly affected the variations of the residuals (all p-values > 0.05). This suggests that i) experimental variability was too high to identify a parameter associated with residual variations and/or ii) the existence of an unknown mechanism not correlated to the tested parameters. Importantly, sunlight dose was no longer significantly related to the residuals deviation (as this was the case before revision of k_{pH}^{20}), suggesting the relationship initially found was possibly due to the natural correlation of sunlight dose with pH caused by algae photosynthesis.

[111] The outlier identified earlier has shifted to the coordinates (0.31; 3.13) and is now shown in Figure 5 - 10.

5.2.3. VALIDATION OF *E. COLI* REMOVAL MODELLING IN HRAPS AT PILOT SCALE:

5.2.3.1. Methodology

As demonstrated in previous section, *E. coli* removal was modelled assuming that the first order decay coefficient in the HRAP (k_{HRAP}, d^{-1}) could be calculated as:

$$k_{HRAP} = 10.4 \cdot 1.14^{T-20} + 31{,}000 \cdot 1.14^{T-20} \cdot 10^{pH-14} + \frac{0.0678.Hs}{\sigma.d} \cdot (1 - e^{-\sigma.d}) \quad (5 - 4)$$

where T is the HRAP broth temperature (°C), pH is the HRAP pH, Hs is incident sunlight intensity ($W.m^{-2}$), σ is the light attenuation coefficient of the HRAP broth (m^{-1}), and d is the HRAP working depth (m). This model was validated against data obtained from the study of daily profiles in pilot scale HRAPs (experimental results described in Chapter 3 section 3.3.4.).

Assuming the HRAP is well mixed (this assumption is discussed in Appendix 2), and accounting for the pond inlet and outlet contribution to *E. coli* removal, *E. coli* cell counts in the HRAP can be calculated according to Equation 5 - 5.

$$\frac{dC}{dt} = \frac{Q_{IN}}{V} \cdot (C_{IN} - C(t)) - k_{HRAP}(t) \cdot C(t) \quad (5 - 5)$$

where $C(t)$ and $k_{HRAP}(t)$ are the *E. coli* cell count in the HRAP (MPN.100 mL^{-1}) and the first order decay coefficient (d^{-1}) for a given instant t respectively, Q is the influent and effluent flowrate (assumed equal, $m^3.d^{-1}$), C_{IN} is *E. coli* cell count in the influent (MPN.100 mL^{-1}), and V (m^3) is the HRAP volume.

E. coli cell counts were calculated using Euler method with a 15 minutes time interval over 24 hours for each 'daily profiles' experimental dataset. For each time interval, k_{HRAP} was calculated from Equation 5 - 4 using experimental values of temperature and pH (measured in 15 minutes interval[112]) and sunlight intensity data provided by the NIWA public database (agent number 21963[113]).

5.2.3.2. Results

The overall performance of the modelling is shown in Figure 5 - 11 (measured cell counts versus predicted cell counts). Individual simulations are shown in Figure 5 - 12.

[112] As described in Chapter 2 section 2.2.1.1., pH, temperature, and DO concentration were logged for every 15 minutes during the 24h periods of each daily profile using a Multimeter Thermo Scientific™ Orion Star™ A326.

[113] Only hourly sunlight areal energy was available from NIWA database. Sunlight mean intensities over an hour were calculated and linearly interpolated to obtain sunlight intensities for each 15 minute intervals.

As can be seen from the data displayed in Figure 5 - 11, the model predicts *E. coli* cell counts within a single order of magnitude without clear under- or overestimating trends (average absolute error of 0.22 log-unit, $R^2 = 0.378$). The two extreme mortality events that were recorded on 03 – 04/02/2015 (Figure 5 - 12d) and 10 – 11/02/2005 (Figure 5 - 12e) were not predicted. Our hypothesis is that the combination of high sunlight energies (18.1 and 21.6 $MJ.m^{-2}$ from 9 A.M. to 5 P.M. respectively) and high temperatures (maxima of 32.2 and 29.5°C respectively), caused the production of biocidal compounds by microalgae on these days. Days presenting similar sunlight intensities but milder temperature did not show such variations in *E. coli* cell counts e.g. on 30/09 – 01/10/2015 (18.1 $MJ.m^{-2}$ cumulated sunlight radiations between 9 A.M. and 5 P.M., maximal temperature of 19.2°C).

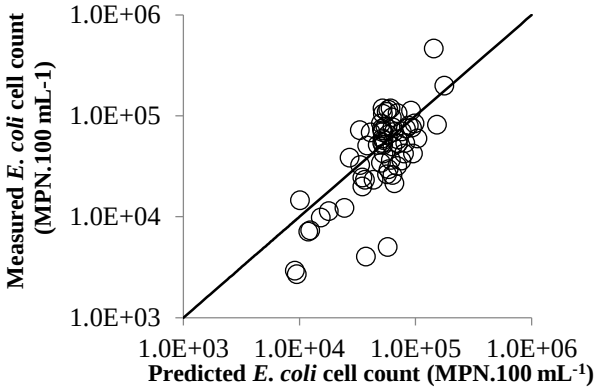

Figure 5 - 11: Measured versus predicted *E. coli* cell counts based on the pilot scale HRAP daily profile datasets

We conclude that Equation 5 - 4 describes variations of *E. coli* cell count in HRAP within less than one order of magnitude although high mortality events cannot be predicted.

.

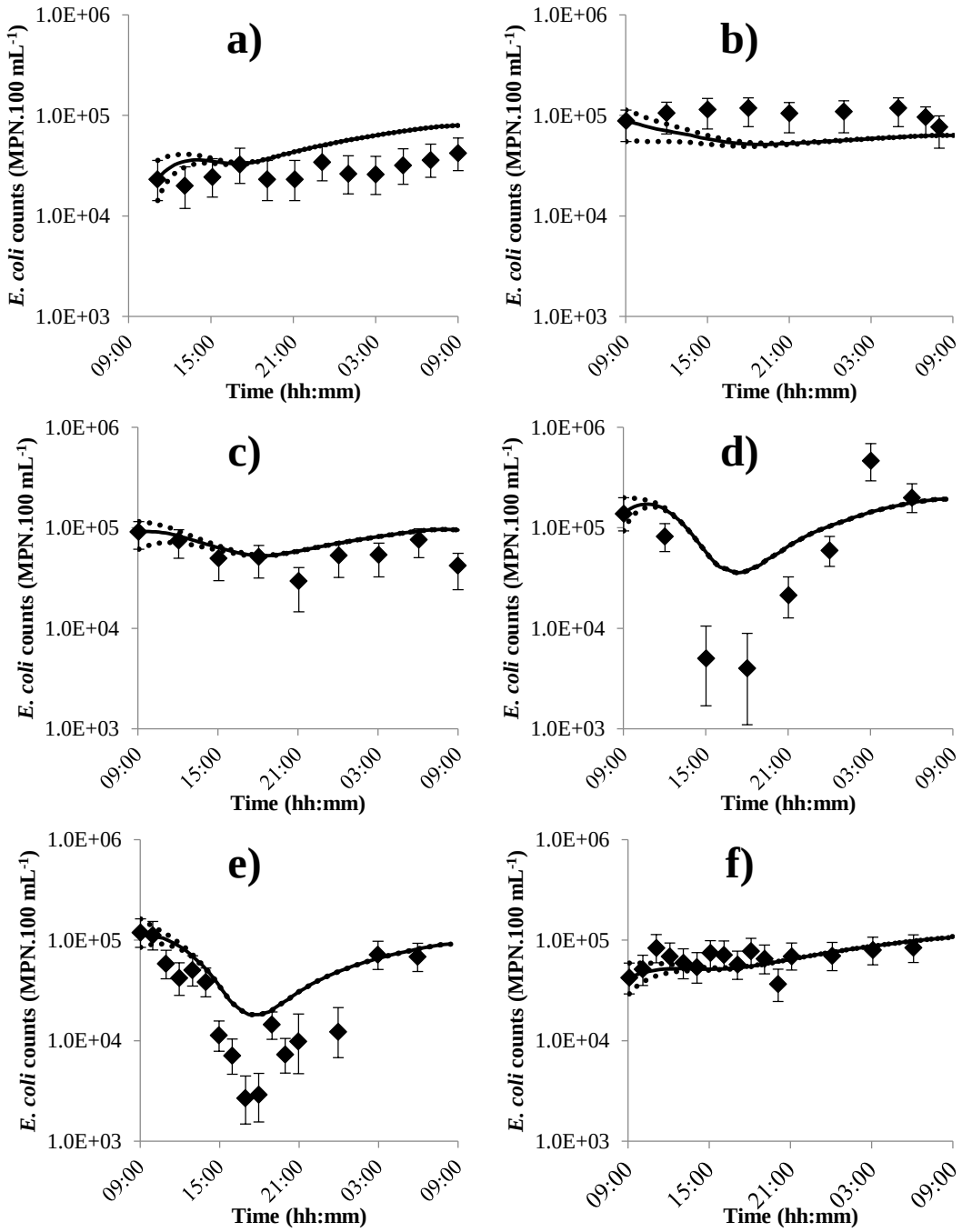

Figure 5 - 12: Measured (♦) versus predicted (continuous line) *E. coli* cell counts during pilot scale HRAPs operation on 30/09 – 01/10/2015 (a), 29 – 30/10/2015 (b), 16 – 17/11/2015 (c), 03 – 04/02/2016 (d), 10 – 11/02/2016 (e), and 16 – 17/03/2016 (f). Uncertainty bars show the uncertainty associated with the MPN function.

5.2.3.3. Sensitivity analysis

A sensitivity analysis was conducted to identify parameters and model inputs causing significant change in model prediction errors and subsequently identify areas for potential model improvement. The sensitivity to the following parameters and inputs was assessed:

1. The values of the parameters used in Equation 5 - 4 (e.g. temperature coefficient factors) which were derived experimentally from a limited dataset and therefore hold significant uncertainty;
2. The values of pH, temperature, and sunlight intensity used in the model calculations[114] which are affected by measurement uncertainty;
3. *E. coli* cell counts in the wastewater feed (C_{IN}) and the HRAP HRT which were assumed to be constant and equal to the value measured at the end of the 24h monitoring period during simulations. The true values are different as cell counts probably fluctuated over time (see Appendix 11 for further discussion);
4. The influent flowrate which may have been fluctuating between measurement, although the pond HRT was checked prior to and following each 24h sampling period, showing no significant difference;
5. The first experimental value of the *E. coli* cell count in the HRAP, chosen as the starting value of the counts in the simulations, which measurement uncertainty may impact model predictions.

Method

The sensitivity to *E. coli* starting cell count was tested by comparing model predictions obtained when changing it for the upper and lower bounds of the 95% confidence intervals[115].

Other sources of sensitivity were investigated by independently adjusting the values of parameters and inputs within their range of uncertainty (see Table 5 - 5), and computing the average absolute relative error of the model predictions for *E. coli* cell counts[116] during HRAP daily profiles over the full dataset.

[114] According to ThermoFisher Scientific, pH was measured with an accuracy of ± 0.002 pH (but with a resolution of ± 0.01 pH), and temperature with an accuracy of ± 0.1 °C. Higher levels of uncertainty were tested thus simulating other scenarios than measurement error e.g. sensor calibration error. No data on the sunlight radiation measurement uncertainty was found.

[115] Interval associated with the MPN function, not taking into account experimental error due to e.g. sampling, sample storage, and sample dilutions.

[116] Calculated as $\frac{1}{N} \cdot \sum_1^N \left(\frac{|[E_{coli}]_{measured} - [E_{coli}]_{modelled}|}{[E_{coli}]_{measured}} \right) \cdot 100$ as performed by Béchet et al. (2010)

The same sensitivity analysis was performed on two reduced datasets: first by only including the two summer days (03 – 04/02/2016 and 10 – 11/02/2016), and second by excluding these two summer days. This analysis was done to identify factors that may explain the model 'weakness' at predicting high mortality summer events (see Figure 5 - 12 d and e) and verify the performance of the predictions for 'regular' days.

Table 5 - 5: Parameters tested during sensitivity analysis

Variable/Parameter	Source of uncertainty	Value	Range of uncertainty
***E. coli* cell count at the start of the simulation**	Measurement uncertainty of first *E. coli* cell count, used as starting value in the simulations	Variable	±7.9 %[1]
Decay coefficient at 20°C and pH 14, k_{pH}^{20}	Parameterization	31,000 d^{-1}	± 25 %[2]
θ_{pH}	Parameterization	1.14	± 0.02[3]
θ_T	Parameterization	1.14	± 0.02[4]
Proportionality factor between sunlight intensity and decay coefficient	Parameterization	0.0678 $m^2.W^{-1}.d^{-1}$	± 0.023[5]
Light absorbance of the algal broth, σ	Parameterization	64 m^{-1}	23 – 115[6]
Dark decay coefficient at 20°C, k_{nat}^{20}	Parameterization	10.4 d^{-1}	4 – 20[7]
HRAP depth	Measurement	25 cm	± 1
Sunlight Intensity	Measurement	Variable	± 10 %[8]
pH	Measurement	Variable	± 0.01
Temperature	Measurement	Variable	± 0.1 °C
HRAP HRT	Daily fluctuation	Variable	± 10 %[8]
***E. coli* cell count in wastewater**	Daily fluctuation	Variable	± 10 %[8]

[1] Average uncertainty at the 95 % confidence level associated with the MPN function used for quanti-tray countings;
[2] 25% corresponds to $1.96 \cdot \sigma$ of the distribution of the *E. coli* decay coefficients measured at pH 10 and 35°C (see Chapter 4 section 4.1.3.3.) being 95% confidence interval for normally distributed data (N = 10, data confirmed to follow a normal distribution by a Kolmogorov-Smirnov test, p = 0.949);
[3] Calculated by Monte-Carlo analysis assuming 25% uncertainty on the decay coefficient at given temperature and pH (uncertainty estimated based on observations at pH 10 and 35°C, the largest dataset available, N = 10);
[4] Same confidence interval used as for θ_{pH};
[5] Calculated as $s_{\hat{\beta}} \cdot t_{N-2}^{*}$ based on the linear regression performed (N = 12, see Chapter 4 section 4.2.2.1) where $s_{\hat{\beta}}$ is the standard error of the estimator of the regression slope and t_{N-2}^{*} is 97.5th percentile of Student law at 10 degrees of freedom (resulting in a 95% confidence level due to being a two-tailed test, Montgomery and Runger, 2003);
[6] Based on the min and max observed in pilot scale HRAP samples;
[7] Values found to strictly encompass all measurements (see Chapter 5 section 5.2.1.);
[8] Proposed

Results

As can be seen in Figure 5 - 12, the uncertainty of the initial *E. coli* cell count had little impact on the global performance of the model: the grey dashed lines figuring these calculations converge quickly with the base simulation (continuous line).

Full data set: As can be seen from Figure 5 - 13 on the left, the average error of the model predictions was mainly sensitive to uncertainty in the uncharacterized dark decay coefficient at 20°C (k_{nat}^{20}), followed by uncertainty in temperature measurements and to a lesser extent by uncertainty in pH measurements (all other parameters tested had comparatively little impact). These observations are consistent with previous evidence that uncharacterized dark decay and pH toxicity are the main contributors to *E. coli* decay (section 5.1.), and that both mechanisms are temperature-dependent. This conclusion is also supported by the lack of sensitivity to parameters and inputs influencing light disinfection mechanisms. The pH and temperature probes used were calibrated prior to each experiment, so these measurements are unlikely to generate significant prediction error in our simulations. Interestingly, increasing the value of k_{nat}^{20} by 25% reduced the average error from 83.0% to 57.3%. As the parameter k_{nat}^{20} accounts for all dark mechanisms not specifically identified, this sensitivity suggests a large part of the average error is caused by unknown factors. Increasing the values of θ_T and θ_{pH} (temperature coefficient for *E. coli* natural and pH-dependent decay, respectively) to 1.16 also reduced average error.

Summer days dataset: On the two summer days selected when *E. coli* decay was especially high, the average absolute error of the prediction was mainly sensitive to uncertainty in the value of k_{nat}^{20}, temperature measurement, and pH measurement: this is similar to what was observed when testing the full dataset, which again agrees with the mechanistic findings from this study. Interestingly, the very low sensitivity to light-dependant parameters and inputs confirmed that light-based mechanisms were unlikely to have caused the 'unexplained' high decay coefficients reported around 5 P.M. Reducing k_{nat}^{20} by 25% reduced the average error from 141.6 % to 84.0 %, which, while significant, is insufficient to fully explain the lack of model accuracy. As in the case of the full data set, increasing the values of θ_T and θ_{pH} to 1.16 reduced error.

Dataset excluding summer days: Unlike what was observed in the two prior sensitivity analyses, reducing k_{nat}^{20} had little impact on the average error of the dataset excluding summer days. Likewise, increasing the values of θ_T and θ_{pH} to 1.16 negatively impacted the average error on the dataset excluding summer days.

Conclusion: Because the coefficient of determination (R^2) of the model prediction was reduced (from 0.378 down to 0.080) when increasing k_{nat}^{20} from 10.4 to 20 d^{-1}, we concluded

that increasing k_{nat}^{20} reduces the errors of the 'full' and 'summer' datasets by reducing the values of the 'extreme' summer residuals. However, this still globally decreased model accuracy (as illustrated in Figure 5 - 14). The value of k_{nat}^{20} was therefore left unchanged. For similar reasons, the values of θ_T and θ_{pH} were also left unchanged.

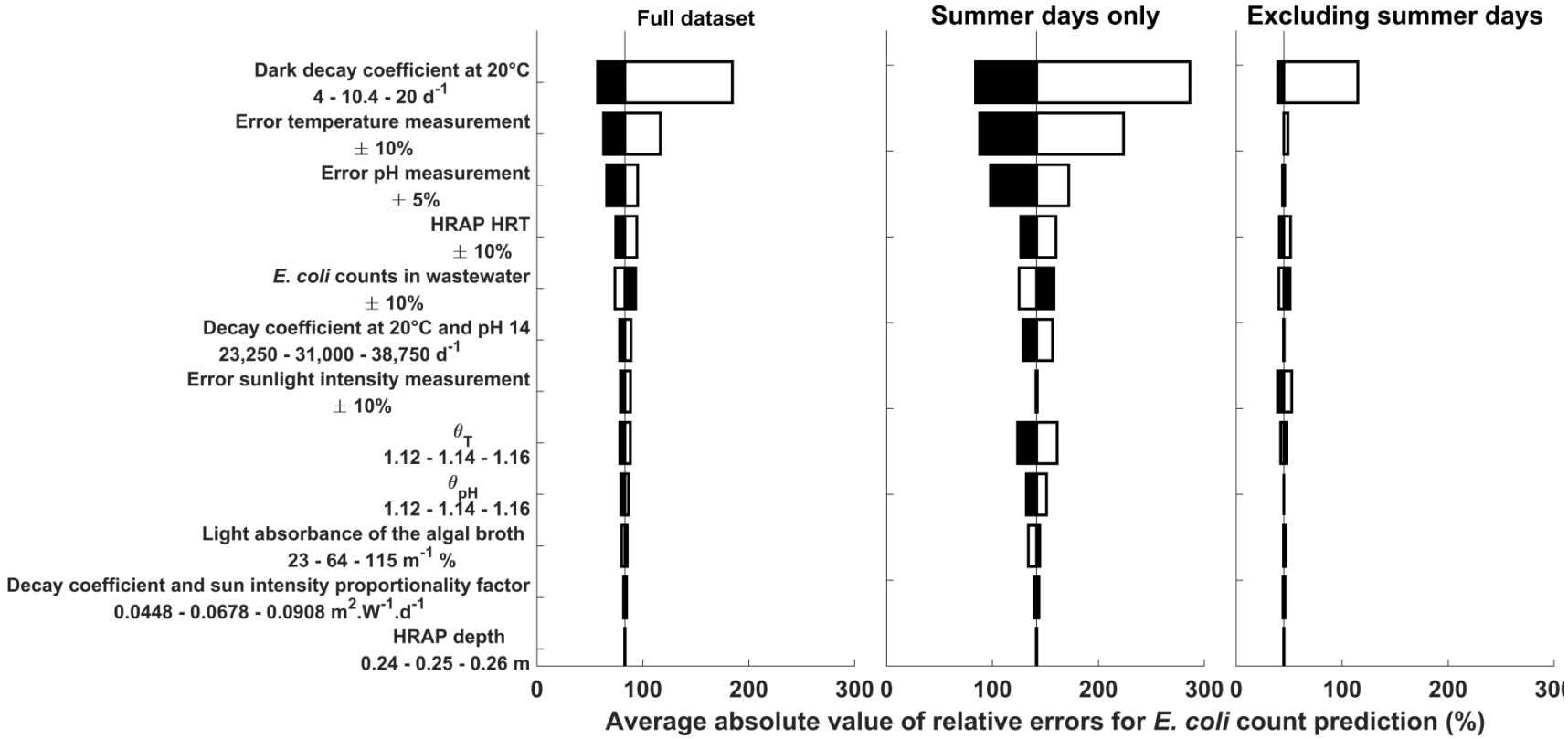

Figure 5 - 13: Impact of uncertainty in model inputs on average absolute error of *E. coli* cell count prediction during HRAPs daily profiles. Results are shown for the full data set, the data set limited to summer days, and the data set excluding summer days. Black bars show the impact of the upper value of the parameter tested while white bars show the impact of the lower value.

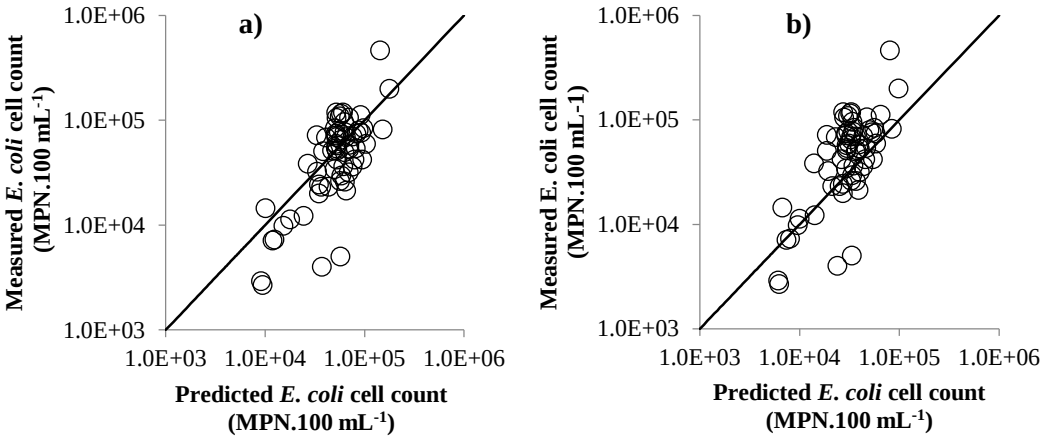

Figure 5 - 14: Comparison of model performance for a) k_{nat}^{20} = 10.4 d^{-1} and b) k_{nat}^{20} = 20 d^{-1}

Conclusion

Overall, the sensitivity analysis showed:

- Results were consistent with previous findings in that *E. coli* decay was mainly caused by uncharacterized dark decay and pH-toxicity in HRAPs, and that both mechanisms are temperature dependent.
- Results were consistent with the hypothesis that an additional disinfection mechanism is occurring under specific 'extreme' conditions of pH and temperature, because peak error could not be explained by uncertainty of the current model parameters and inputs.
- Accurate measurements of pH and temperature are important to minimize errors in model prediction;
- Uncertainty/variability in k_{nat}^{20} is likely to be generating important uncertainty/error in the model predictions.

5.2.3.4. The contribution of different disinfection mechanisms in HRAPs

Using our model, we can infer the respective contributions of the different "known mechanisms" (direct photo-damage, pH toxicity, and uncharacterized dark decay) on the overall *E. coli* removal.

As shown in Figure 5 - 15, uncharacterized dark decay dominated *E. coli* removal across all seasons but neither pH toxicity nor photo-damage can be neglected as they can become quantitatively significant depending on the environmental conditions experienced.

Photo-damage could account for as much as 50% of the overall decay just before midday on a sunny day under moderate temperature (e.g. 30/09 – 01/10/2015). These conditions are mostly expected in winter when algal density is low (low light attenuation) and sunlight intensity can still be significant[117].

pH toxicity accounted for half of the explained decay in February (summer) and was only negligible on 16 – 17/03/2016.

[117] Maximal sunlight intensities of 500 $W.m^{-2}$ are commonly recorded in June in Palmerston North

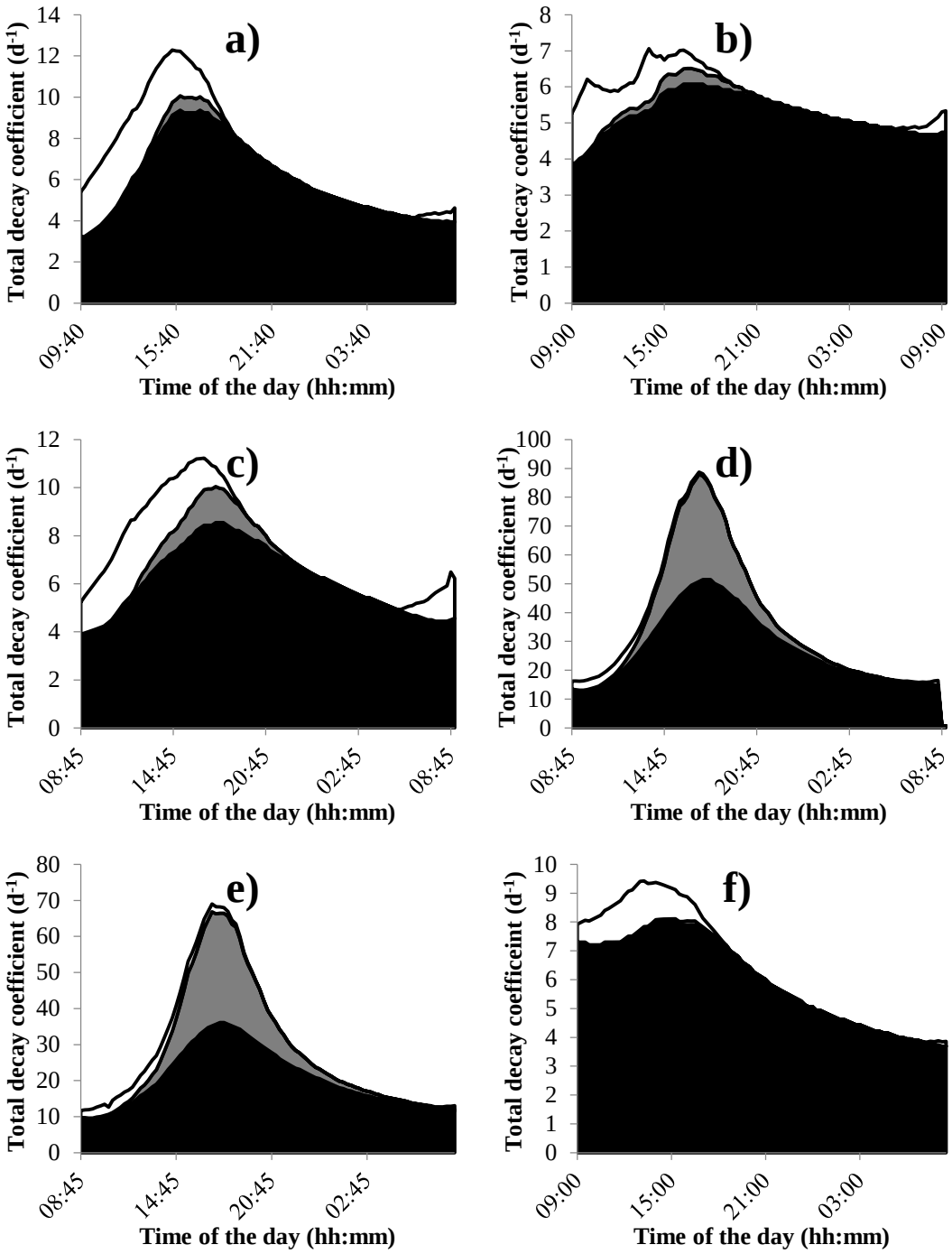

Figure 5 - 15: Contribution of decay mechanisms to the overall decay coefficient of *E. coli* according to the model developed by this study.
Results are shown for the 30/09 – 01/10/2015 (a), 29 – 30/10/2015 (b), 16 – 17/11/2015 (c), 03 – 04/02/2016 (d), 10 – 11/02/2016 (e), and 16 – 17/03/2016 (f). The black area represents the contribution of uncharacterized dark decay, the grey area the contribution of pH toxicity, and the white area the contribution of direct photo-damage. The total decay coefficient corresponds to the top envelop curve.

5.2.3.5. Comparison with existing models for *E. coli* decay in algal ponds

Existing models of *E. coli* (or coliform) decay in algal ponds were compared for their ability to predict *E. coli* cell counts across the daily profiles recorded during pilot HRAP operation.

Craggs et al. (2004) modelled *E. coli* removal in HRAPs using a first order decay coefficient given by the following equation:

$$k(t) = k_d + k_s \cdot G(t) \quad (5 - 6)$$

Where k_d is the dark disinfection rate (d^{-1}), k_s is the "light only" disinfection rate coefficient ($m^2.MJ^{-1}$), and $G(t)$ is the total solar irradiance ($MJ.m^{-2}.s^{-1}$). k_d was modelled as a constant equal to 0.48 d^{-1}, and k_s was experimentally calculated as a constant equal to 0.083 $m^2.MJ^{-1}$ (i.e. $7.2 \cdot 10^{-3}$ $m^2.W^{-1}.d^{-1}$ in units directly comparable with the coefficient α as developed in this study). The authors took into account sunlight radiation attenuation in the algal broth by computing the total solar irradiance $G(t)$ as the mean irradiance in the water column $\bar{G}(t)$:

$$\bar{G}(t) = \frac{G}{K \cdot z} \cdot (1 - e^{-K \cdot z}) \quad (5 - 7)$$

Where K is the spectral irradiance attenuation coefficient in the UV range and z is the pond depth. In the present study, Craggs et al. (2004) model was implemented with the same value of spectral irradiance attenuation as used for our modelling (64 m^{-1}, see 5.2.1). Because this coefficient was determined based on visible radiations for which light attenuation is significantly lower than for UV radiations (Maiga et al., 2017), *E. coli* decay could have been expected to be overestimated when running the simulation. Nevertheless, as can be seen in Figure 5 - 16, *E. coli* decay was significantly underestimated when using Craggs' model. Although being the only model specifically developed for HRAPs found in the literature, Craggs et al. (2004) work was based on batch experiments in algal broth characterized by mild variations of pH (always below 9.3), i.e. in conditions differing with our pilot scale HRAP, which potentially explains the inconsistencies between our respective findings.

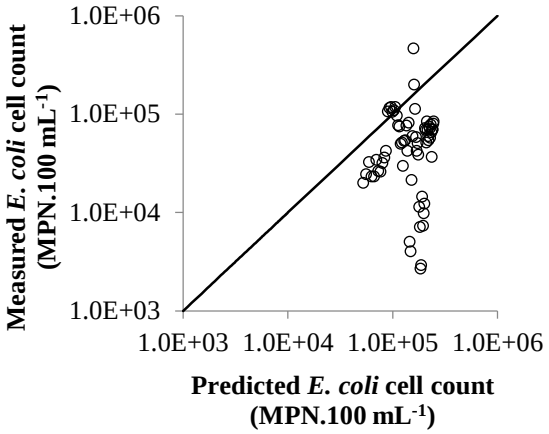

Figure 5 - 16: Measured versus predicted *E. coli* cell counts using Craggs et al. (2004) model

Several models developed for waste stabilization ponds were also tested:

- The Marais (1974) equation, summarized to a single Arrhenius-like term of temperature, largely underestimated decay (Figure 5 - 17a).
- The model developed by Ouali et al. (2015), which accounts for pH, temperature, sunlight intensity and DO concentration, largely overestimated *E. coli* decay (decay coefficients over 1,000 d^{-1}, data not shown). This is probably because this model was developed based on data obtained in the laboratory, thus in conditions poorly representative of field conditions (e.g. surface to volume ratio, magnitude of light irradiance, light source).
- The model developed by Nguyen et al. (2015) was tested by implementing the monthly endogenous, exogenous, and natural decay coefficients reported by these authors in our dataset (Table S6 in the authors' publication[118]). This model also resulted in poor predictions of *E. coli* decay ($R^2 = 1.12 \cdot 10^{-2}$, Figure 5 - 17b).

It is interesting to note that while none of the other models tested could accurately predict our experimental dataset, their predictions were close to the experimental average[119]. This shows that these models may still be useful for yearly average predictions but not for fine tuning optimization of HRAPs.

[118] Because this study was performed in the Northern hemisphere, the rates used in the present simulation were the rates measured for the month in 'seasonal phase opposition' from our daily profile (e.g. August instead of February).

[119] The predicted *E. coli* cell counts averaged over the full data set were $5.88 \cdot 10^5$ MPN.100 mL^{-1} (present study), $6.49 \cdot 10^5$ MPN.100 mL^{-1} (Nguyen et al., 2015), $1.22 \cdot 10^6$ MPN.100 mL^{-1} (Marais 1974), and $1.54 \cdot 10^6$ MPN.100 mL^{-1} (Craggs et al. 2004) therefore all within 1 order of magnitude of the experimental value ($6.14 \cdot 10^5$ MPN.100 mL^{-1}).

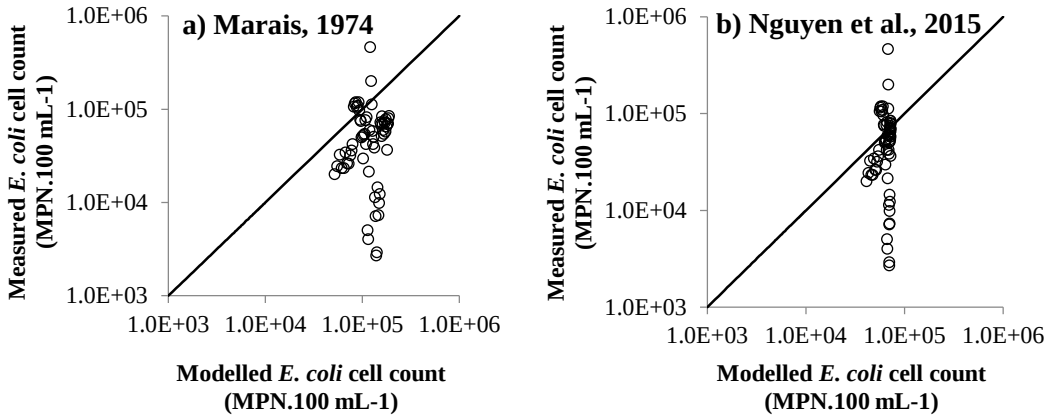

Figure 5 - 17: Measured versus predicted *E. coli* cell counts using Marais (1974) (a) and Nguyen et al. (2015) (b) models.

To conclude, only the model developed in this thesis appears to generate 'reasonable' predictions of *E. coli* cell counts in pilot scale HRAPs and predict the diurnal variations of these counts[120]. While it is still unclear which model would best predict HRAP disinfection performance at full-scale, the facts that full-scale HRAPs experienced considerable changes in pH and temperature (Buchanan, 2014; Craggs et al., 2012) and that sunlight-mediated disinfection appears to be of limited significance suggest that our model should also best predict *E. coli* decay in full-scale ponds.

5.3. CONCLUSIONS

Although experimental variability and uncertainty during bench scale experiments impaired data analysis, significant evidence confirmed sunlight intensity has little direct impact on *E. coli* removal in HRAP due to high light attenuation in opaque algae-laden broths. Poor light penetration is also likely to explain why DO concentration did not affect *E. coli* survival (free radicals are formed from the reaction of O_2 with photons) and its contribution to *E. coli* decay was concluded to be negligible in HRAPs. The significant impact of pH was confirmed, albeit to a lesser extent than observed during laboratory studies probably due to *E. coli* shielding by flocs. Bench scale assays evidenced a high uncharacterized dark decay under the conditions tested influenced by temperature.

[120] Marais equation did predict diurnal variations in *E. coli* cell counts but the magnitude of these variations was not accurate

Overall, these results agree with observations from the pilot scale HRAP monitoring which evidenced high dark decay and low light impact. The high impact of pH had also been suspected after observing high mortality in late afternoon during summer at pilot scale. Although the bench scale study confirmed this hypothesis, pH toxicity could not explain the magnitude of the late afternoon mortality by itself, suggesting that unidentified mechanism(s) and/or synergies probably contributed to significant *E. coli* removal under specific conditions (e.g. synergies of water temperature > 30°C, sunny days, high pH).

Our findings are critical because most past research on pathogen removal in algal ponds has focused on sunlight-mediated mechanisms and our study shows that more emphasis should be given to dark mechanisms. Precise assessment of pH toxicity, dark temperature-dependent decay, or further investigations on other mechanisms such as algal toxicity that could not be identified during this study may provide valuable tools for the prediction of HRAP performance for disinfection.

Based on the results from this study, we re-evaluated the *E. coli* disinfection model developed at lab scale. After accounting for the high uncharacterized dark decay, light attenuation, and pH toxicity, we were able to predict *E. coli* cell count variations over 24h periods in pilot scale HRAPs with an average absolute error of 0.22 log-units (N = 64). However, the model underestimated the highest decay coefficients recorded in February in mid- and late-afternoon. Unexplainably high decay coefficients were also found in the dark during bench assays, suggesting the possible release of algae biocides following an episode of high exposure to sunlight accompanied to elevated temperature (> 35°C). Because the model was developed assuming the three different decay mechanisms previously identified to be significant have an additive effect on the overall *E. coli* decay in HRAP, the model may miss some interferences between different mechanisms. In particular, some un-modelled synergistic effect between mechanisms could also explain that the highest *E. coli* decay coefficients could not be predicted. The model herein developed was nevertheless more accurate than existing models described in the literature for coliform decay in algal ponds and will be used for the theoretical optimization of HRAP disinfection performance (Chapter 7) based on the predictions of environmental conditions in HRAPs (Chapter 6).

We acknowledge that the parameters in the model of k_{nat} (Equation 5 - 3) were initially calibrated using data from HRAP daily profiles and that this data was also used for model

validation. Because an independent calibration was also performed using bench scale experiments results prior to final validation, we consider the present model of *E. coli* decay in HRAPs suitable for investigating disinfection optimization in HRAPs treating wastewater. Nevertheless, an independent study and validation of this model is still needed[121].

[121] This work could not be performed as uncharacterized dark die-off was found significant only during the last experimental phase of the present study.

Chapter 6: Modelling of temperature and pH in HRAPs

Experimental studies described in Chapters 4 and 5 revealed that uncharacterized dark decay and pH toxicity above 9.4 contributed significantly to *E. coli* removal in High Rate Algal Ponds (HRAPs). The impact of both mechanisms increasing exponentially with temperature, we hypothesized that increasing the co-occurrence of elevated pH and temperature could improve disinfection in HRAPs. In order to assist design, a model was developed to predict temperature and pH in HRAPs as a function of HRAP design, operation, and meteorological data. The general concept is presented in Figure 6 - 1.

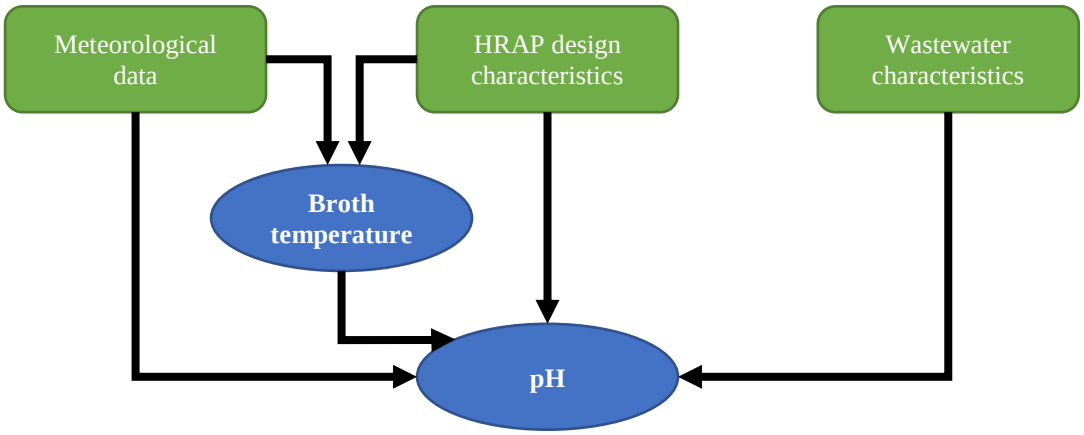

Figure 6 - 1: Simplified model conceptual structure

The following Chapter describes the construction and validation of models predicting broth temperature and pH in HRAPs (dissolved oxygen concentration was modelled as additional output). The model was coded and solved with Matlab® R2015a[122] (Mathworks, Massachusetts, USA).

[122] The code is available via https://github.com/pchambonn/Pathogenicity-removal-in-algae-based-wastewater-treatment-systems---Understanding-the-mechanisms-inv

6.1. HRAP BROTH TEMPERATURE MODELLING

6.1.1. MODEL DEVELOPMENT

Broth temperature (T_p, K) was predicted based on the model (and assumptions) described by Béchet et al. (2011) and validated for HRAPs by the same authors. The main assumptions and equations of this model are summarized in Box 6 - 1.

The parameters and variables used in the model are listed in Table 6 - 1 (physical parameters), Table 6 - 2 (HRAP design parameters), and Table 6 - 3 (meteorological variables). The base values displayed were used in all simulations unless stated otherwise.

Table 6 - 1: Physical parameters used for temperature modelling

Parameter	Base value	Range/error	Unit	Symbol
Density of water	998	-[1]	$kg.m^{-3}$	ρ_w
Water specific heat capacity	4180	-[1]	$J.kg^{-1}.K^{-1}$	Cp_w
Water emissivity	0.97	0.95 – 0.99[2]	-	ε_w
Stephan Boltzmann constant	$5.67 \cdot 10^{-8}$	-[1]	$W.m^{-2}.K^{-1}$	$\sigma_{Stephan}$
Air emissivity	0.8	0.75 – 0.95[3]	-	ε_a
Water latent heat	$2.45 \cdot 10^{6}$	-[1]	$J.kg^{-1}$	L_w
Air kinematic viscosity	$1.5 \cdot 10^{-5}$	± 10%[4]	$m^2.s^{-1}$	ν_a
Ideal gas constant	8.314	-[1]	$J.K^{-1}.mol^{-1}$	R
Water molecular weight	0.018	-[1]	$kg.mol^{-1}$	M_w
Air thermal conductivity	$2.6 \cdot 10^{-2}$	± 10%[4]	$W.m^{-1}.K^{-1}$	λ_a
Air thermal diffusivity	$2.2 \cdot 10^{-5}$	± 10%[4]	$m^2.s^{-1}$	α_a
Soil specific heat capacity	1250	± 10%[4]	$J.kg^{-1}.K^{-1}$	Cp_s
Soil density	1900	± 10%[4]	$kg.m^{-3}$	ρ_s
Soil reference temperature	13.6	± 10%[4]	°C	$T_{s,ref}$
Soil thermal con uctivity	1.7	0.2 – 4[2]	$W.m^{-1}.K^{-1}$	k_s
Photosynthetic efficiency	0.02	0.01 – 0.05[3]	-	PE

[1] Physical parameters associated with low variability and which effect was therefore not assessed;
[2] Davies et al. (1971);
[3] Béchet et al. (2011);
[4] Parameters associated with poorly known uncertainty/variability. The influence of the variations of these parameters on the model predictions was assessed based on the ranges listed in the present table, and were not investigated further due to the low sensitivity of the model predictions to these parameters (see results).

Table 6 - 2: Design and operational parameters used for temperature modelling

Parameter	Base value	Range/error	Unit	Symbol
Pond length	1	-	m	lx
Pond surface	3.42[1]	± 10%[2]	m^2	S
Pond depth	0.25[1]	± 10%[2]	m	d
HRT	7.9[3]	± 25%[4]	d	HRT
Operation mode	Continuous		-	-

[1] Real value of the pilot scale HRAP which data was used for validation in this study;
[2] Range used for the assessment of parameter sensitivity, not representative of the pilot set-up;
[3] Median value observed in the pilot scale HRAP from 22/07/2016 to 29/07/2017;
[4] Observed standard deviation of the HRT measured on the pilot scale algal ponds used in this thesis.

Table 6 - 3: Meteorological inputs variables used for temperature modelling

Variable	Unit	Symbol used
Solar radiation	$W.m^{-2}$	Hs
Rain water flow	$m^3.m^{-2}.s^{-1}$	q_r
Dry bulb temperature	K	T_a
Dew point temperature	K	-
Relative humidity	%	-
Surface wind speed	$m.s^{-1}$	-

Hourly meteorological data were obtained from the New Zealand National Institute of Water and Atmospheric Research (NIWA) database (Palmerston North location, agent number 21963). Since rapid changes in pH and temperature (within minutes) were evidenced during pilot scale HRAP monitoring (see Chapter 3), the meteorological data were linearly interpolated to generate profile over intervals under 1 minute (see section 6.2.2. for further discussion). To initiate the simulations, the experimental broth temperature at time 0 was used as initial predicted value.

Box 6 - 1: Summary of the model developed by Béchet et al. (2011) for HRAP broth temperature prediction

Main assumptions

- The HRAP is assumed well mixed
- Algal broth physical properties were assumed to be that of water under standard conditions
- Solar radiation (obtained from NIWA data base as global solar radiation) was assumed to only consist in direct solar radiation.
- Air and solar radiative fluxes were assumed fully absorbed by the algal broth.

Summary of the equations included in the model

$$\rho_w \cdot S \cdot d \cdot Cp_w \cdot \frac{dT_p}{dt} = Q_{ra,p} + Q_{ra,s} + Q_{ra,a} + Q_{ev} + Q_{conv} + Q_{cond} + Q_f + Q_r \quad (6 - 1)$$

In Equation 6 – 1, $Q_{ra,p}$ is the radiation from the HRAP surface, $Q_{ra,s}$ is the total solar radiation received by the HRAP, $Q_{ra,a}$ is the radiation flux from the air to the HRAP, Q_{ev} is the evaporative flux, Q_{conv} is the convective flux at the pond surface, Q_{cond} is the conductive flux with the ground at the HRAP bottom, Q_f is the heat flux due to inlet and outlet flow, and Q_r is the heat flux due to rain (all expressed in W).

The equations used to compute these thermal fluxes can be found below:

$$Q_{ra,p} = -\varepsilon_w \cdot \sigma_{Stephan} \cdot {T_p}^4 \cdot S \quad (6 - 2)$$

$$Q_{ra,s} = (1 - PE) \cdot Hs \cdot S \quad (6 - 3)$$

$$Q_{ra,a} = \varepsilon_w \cdot \varepsilon_a \cdot \sigma_{Stephan} \cdot {T_a}^4 \cdot S \quad (6 - 4)$$

$$Q_{ev} = -m_e \cdot L_w \cdot S \quad (6 - 5)$$

$$Q_{conv} = h_{conv} \cdot (T_a - T_p) \cdot S \quad (6 - 6)$$

$$Q_{cond} = k_s \cdot S \cdot \frac{dT_s}{dz}(z = 0) \quad (6 - 7)$$

$$Q_f = \rho_w \cdot Cp_w \cdot q_i \cdot (T_i - T_p) \quad (6 - 8)$$

$$Q_r = \rho_w \cdot Cp_w \cdot q_r \cdot (T_a - T_i) \cdot \mathrm{S} \quad (6 - 9)$$

In Equation 6 – 5, m_e is the rate of water evaporation (kg.s^{-1}.m^{-2}). Details for its calculation can be found in Béchet et al. (2011).

In Equation 6 – 6, h_{conv} is the convection coefficient (W.m^{-2}.K^{-1}). Details for its calculation can be found in Béchet et al. (2011).

In Equation 6 – 7, T_s is the soil temperature (K), and z is the soil depth (m). T_s was calculated by solving Equation 6 – 10, assuming $\frac{\partial^2 T_s}{\partial z^2}(z, t = 0) = 0$, $T_s(z = 0, t) = T_p(t)$, and $T_s(z = l_{s,ref}, t) = T_{s,ref}$ where $l_{s,ref}$ is the depth from which soil temperature is assumed constant. Details for $l_{s,ref}$ calculation can be found in Béchet et al. (2011).

$$\frac{\partial^2 Ts}{\partial z^2}(z, t) = \frac{Cp_s \cdot \rho_s}{k_s} \cdot \frac{\partial Ts}{\partial t}(z, t) \quad (6 - 10)$$

In Equation 6 – 8, q_i is the inlet flowrate (m^3.s^{-1}) and T_i is the inlet temperature (K).

6.1.2. MODEL ACCURACY AND VALIDATION

Model predictions

Examples of model predictions compared with measured data over selected periods of time[123] are shown in Figure 6 - 2. As can be seen, the model could accurately describe the daily temperature increase and decrease, although discrepancies are visible. The model for example often predicted a faster night time cooling than observed resulting in predicted temperature generally lower than measured (see also model validation). During the winter (e.g. July 2017), predicted temperatures variations sometimes diverged significantly from the measured data, as already observed by Béchet et al. (2011); the likely explanation is the lower contribution of sunlight intensity to thermal transfer during winter than summer[124]: because solar heat flux exclusively depends on sunlight intensity and thus holds little uncertainty in comparison with other heat fluxes (e.g. evaporative heat flux, air convective flux), the lower contribution of solar heat flux during winter results in higher significance of less accurate fluxes, and therefore in higher model error in winter.

In agreement with our study, Béchet et al. (2011) had concluded the model inaccuracy were mostly related to the assumption of constant air emissivity (this is further discussed in the sensitivity analysis) and the impact of paddlewheel mixing on temperature due to shading and its contribution to evaporation (both of these contributions were neglected). Béchet et al. (2011) based their model validation on data from a HRAP of 31.8 m^2 free surface, and operated at 0.3 m depth, to be compared with the HRAP of the present study (3.42 m^2 free surface, operated at 0.25 m depth), meaning the paddlewheel relative size to the HRAP was higher in the present study. Model prediction errors were however similar in both studies[125], and a general positive skew of model residuals[126] was found during our study, even though neglecting paddlewheel impact is expected to contribute to a model negative skew (both shading and evaporation negatively impact HRAP temperature): this again indicates air emissivity uncertainty contributed the most to model error, as further discussed in model sensitivity analysis.

[123] The rationale for the choice of the period of time presented is given in section 6.2.2.
[124] Solar heat fluxes contributed to less than 10% of daily temperature gain in winter, against up to 50% during summer.
[125] Average absolute error for maximum and minimum temperature (model outputs used by Béchet et al.) of 1.3°C and 1.2°C, against 1.35°C of average absolute error over the full data set in our study (see model validation).
[126] Calculated as measured minus predicted temperature, see Figure 6 - 3.

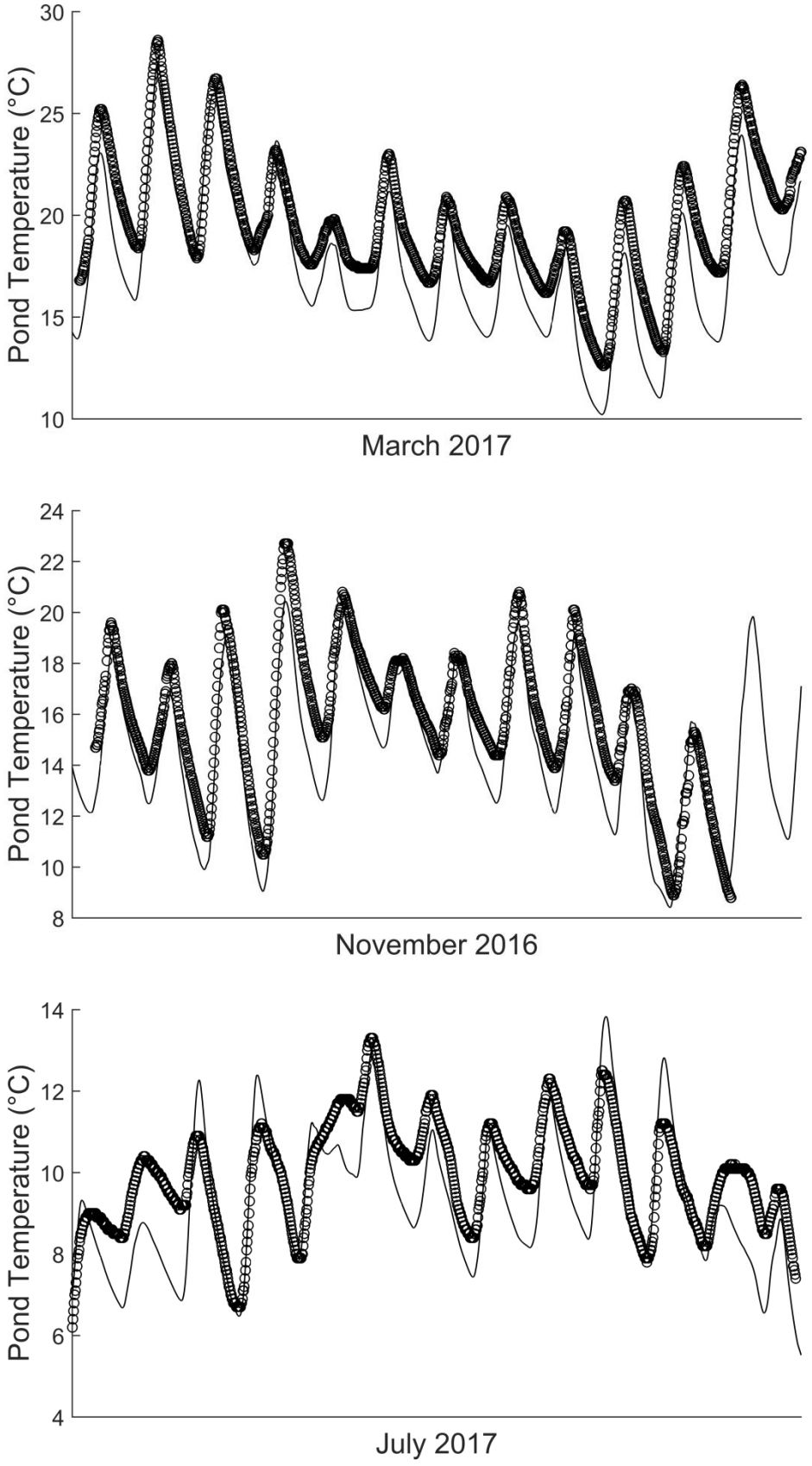

Figure 6 - 2: Comparison of modelled (-) with measured (o) temperature over three different periods (March 2017, November 2016, and July 2017)

Model validation

Broth temperature was simulated from 22/07/2016 to 29/07/2017[127] for validation. This period was selected because consistent experimental data was available for temperature and pH. The distribution of residuals (measured minus predicted) for the model of HRAP broth temperature is shown in Figure 6 - 3. As can be seen, the residuals distribution was not exactly centred on zero (positive skew). The model therefore had a tendency to underestimate temperature. This was further investigated as explained below. The goodness of fit was evaluated using simple linear regression with no intercept[128] between modelled (x) and measured (y) temperature (Figure 6 - 3, left). The model showed satisfactory performance[129] (β = 1.0034; R^2 = 0.9225; root squared mean error = 1.23°C; standard error of β = 2.66 10^{-5}; N = 25,906). Based on this data, the temperature was predicted with an uncertainty of ± 2.41°C[130] over the period assessed; the average observed prediction error[131] was 1.35°C.

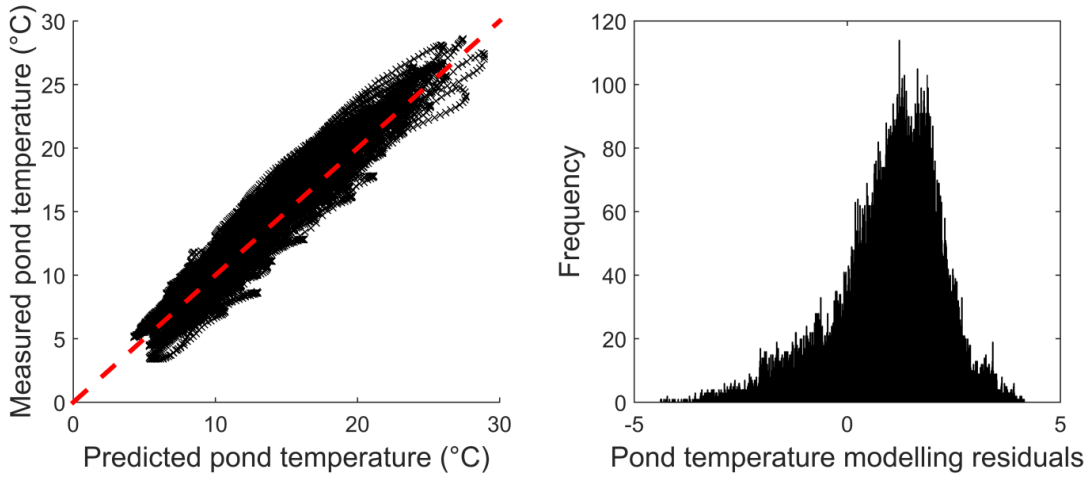

Figure 6 - 3: HRAP temperature (measured versus predicted) and associated distribution of model residuals (measured minus predicted)

[127] Some weather data were missing between 12 and 16/12/2016 and 27 and 31/12/2016. Both periods were excluded from the analysis.
[128] The test consists in evaluating β assuming the relationship between modelled temperature (x) and measured temperature (y) is $y = \beta.x$
[129] The perfect modelling would show a β coefficient equal to 1, and both standard error for the β coefficient and root mean squared error (RMSE) as low as possible.
[130] The 95% confidence interval is assumed to be 1.96 times the RMSE (true for a normal distribution)
[131] Calculated as the average of the absolute values of the residuals.

Model sensitivity analysis

The sensitivity of the model fitness to variability in input parameters was assessed based on the variability/uncertainty ranges listed in Table 6 - 1 and Table 6 - 2. The results of the sensitivity analysis are shown in Figure 6 - 4[132].

As can be seen, the model fitness was mostly sensitive to air emissivity, as previously determined by Béchet et al., (2011). Increasing this parameter resulted in a β coefficient closer to 1 (thus reducing the apparent 'underestimation' noted above), but also increased the root mean squared error indicating a more significant error in the model predictions. Air emissivity has been reported to increase with dew point temperature (Berdahl and Martin, 1984) and, therefore, air relative humidity. Because underestimation of temperature by the model is mostly observed during night time (see comparison between measured and predicted temperature for different time periods in Figure 6 - 2), when relative humidity is higher, we hypothesized that the value of air emissivity used in the simulations (constant value) was generally less accurate at night[133] than during the day. The high sensitivity of the modelled temperature to air emissivity suggests that divergences between the real and the simulated value of air emissivity explain most of the model inaccuracy. Because assessing air emissivity precisely was beyond the scope of this study, it was kept constant at 0.8 during simulations. No other variations in parameters significantly influenced the model fitness.

Interestingly, variations in soil thermal conductivity and HRAP depth lowered both the model RMSE and the coefficient β indicating a slightly improved accuracy of the model predictions. These improvements were however minor and may only be due to compensating the model positive skew (see Figure 6 - 3, right) due to other sources of inaccuracies (e.g. air emissivity). No changes were therefore made to these parameters in the rest of the simulations.

[132] Parameters which impact is not visible in Figure 6 - 4 had lesser influence than any other parameter shown.

[133] Air emissivity appear under-estimated at night (see Figure 6 - 2), when air relative humidity is higher, resulting in lower heat influx from the air, see Equation 6 – 4).

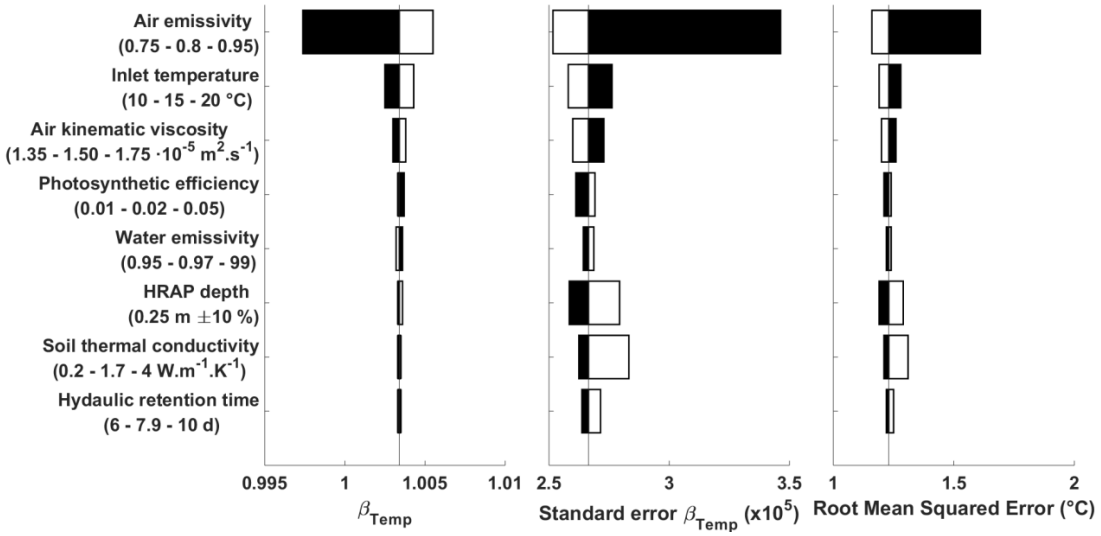

Figure 6 - 4: Sensitivity of the temperature prediction to input parameters' variability. Black and white bars show the output values predicted using the upper and lower values, respectively, of the parameter tested

6.1.3. CONCLUSION

HRAP broth temperature could be predicted over a full year with an uncertainty of ± 2.41°C[134]. Because the model could explain temperature variations over a diurnal cycle (therefore the effect of varying solar loads) and could provide realistic range of temperature variations (as illustrated by the low average absolute error observed of 1.35°C), the model was considered fit for the purpose of providing realistic representation of HRAP broth temperature in order to discuss disinfection performances.

The sensitivity analysis indicated that better knowledge on air emissivity and its variations with weather parameters would significantly improve the prediction of HRAP broth temperature. In addition scale effect (in particular due to the inflated impact of the paddlewheel) probably limited the model accuracy.

6.2. MODELLING PH VARIATIONS IN HRAPS

6.2.1. MODEL DESCRIPTION

The general schematic representation shown in Figure 6 - 5 summarizes the main parameters needed in order to model pH variations in HRAPs. The justification for the use of the

[134] Error at the 95% confidence level computed as 1.96·*RMSE*.

variables appearing in Figure 6 - 5 and the calculations for the determination of these variables are described in the following.

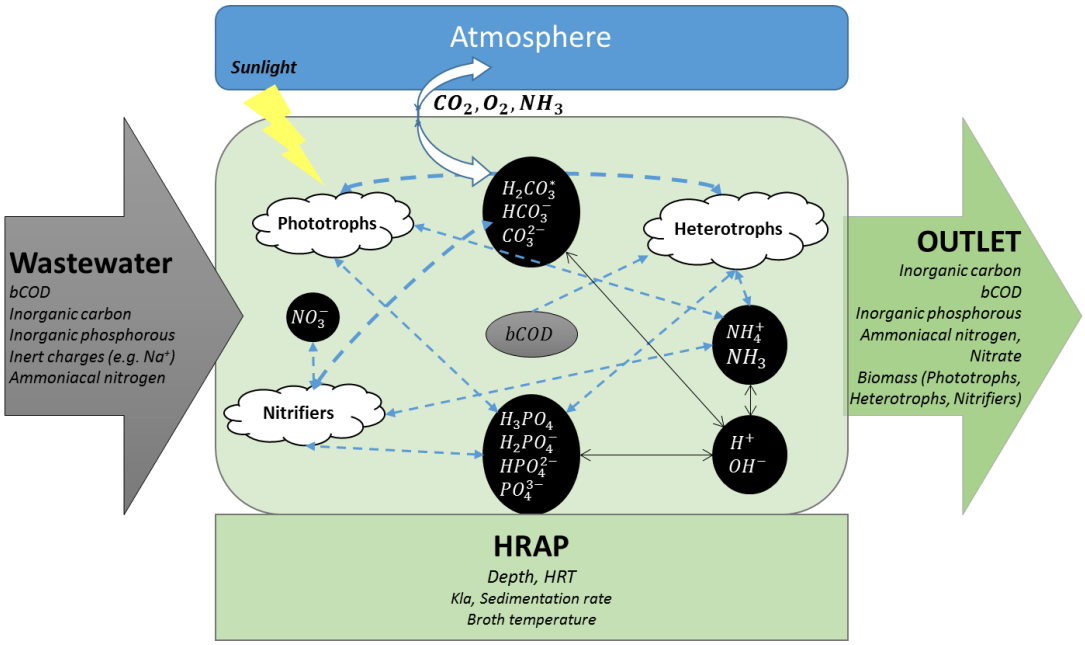

Figure 6 - 5: Conceptual modelling for pH calculations

6.2.1.1. General approach

In surface water lacking a strong external buffer (e.g. wastewater), the pH at equilibrium with the Earth atmosphere is normally dictated by the carbonic buffer system involving the dissolution of CO_2, its hydration into carbonic acid (H_2CO_3), and the successive conversion of carbonic acid into bicarbonate (HCO_3^-) and carbonate (CO_3^{2-}). During wastewater treatment, various biological reactions can influence pH via the release (e.g. nitrification) or consumption of protons and other chemical species (especially CO_2). In HRAP, imbalances between the rates of inorganic carbon (IC) algal consumption and atmospheric CO_2 diffusion cause large increases in pH during the daytime. With this focus, the model developed in this study combines the dynamic prediction of temporal changes in IC concentration, based on the rates and stoichiometry of the biological reactions involved, with the solution of acid-base reactions and electroneutrality (considered as instantaneous in comparison to biological reactions and gas diffusion). Because the concentration of dissolved oxygen (DO, kg $O_2 \cdot m^{-3}$) can affect microbial activity, changes in DO concentration were also modelled. Likewise, changes in total Inorganic Phosphorus (IP, kg $P \cdot m^{-3}$) and ammoniacal nitrogen (IN, kg $N.m^{-3}$) were predicted (the potential impact of P precipitation at pH above 10 was neglected). This process involved 3 main steps:

1. The stoichiometry of the biological reactions were determined to compute the yields for uptake or release of key chemicals directly (e.g. CO_2) or indirectly (e.g. O_2) involved in pH variation.
2. The rates of the reactions contributing to the consumption or introduction of these chemicals were calculated and, using the stoichiometric yields earlier determined, used to predict changes in key species concentrations.
3. The concentration of H^+ (i.e. pH) was determined from the equilibrium equations.

6.2.1.2. Stoichiometry and yields

The main biological reactions contributing to pH variations are listed in Table 6 - 4, together with their relevant yields (see Appendix 20 for details). In addition to heterotrophic and phototrophic microbial activities, the activity of ammonium oxidizing bacteria (henceforth called nitrifiers for simplicity) was considered because significant nitrifying activity was recorded in the pilot ponds[135] and because nitrifiers can affect pH (Metcalf and Eddy Inc., 2003). No other microbial activities were taken into account. The uptake and release of inorganic phosphorous were calculated assuming all biomass contained 1% of P per dry biomass mass[136] unit (Schuler and Jenkins, 2003).

[135] A median concentration of 51.48 $mg.L^{-1}$ (N = 133) of nitrate was reported in the HRAP despite low concentration in the wastewater influent (median concentration 0.38 $mg.L^{-1}$, N = 188).
[136] Biomass modelled was modelled in terms of volatile suspended solids (VSS)

Table 6 - 4: Stoichiometry and associated yields of uptake/production of inorganic nutrients for each biological mechanism accounted for in pH variations model

Mechanism	Equation/Yield	Symbol	Value
Photosynthesis	$416 \cdot CO_2 + 29 \cdot NH_4^+ + 331 \cdot H_2O \rightarrow C_{416}H_{749}O_{228}N_{29} + 467.5 \cdot O_2 + 29 \cdot H^+$		
	O_2 production	Y_O^a, g $O_{2produced}$·g $VSS_{produced}^{-1}$	1.53
	CO_2 uptake	Y_C^a, g $C_{uptaken}$·g $VSS_{produced}^{-1}$	0.510
	NH_4^+ uptake	Y_N^a, g $N_{uptaken}$·g $VSS_{produced}^{-1}$	0.0415
Algae decay	$C_{416}H_{749}O_{228}N_{29} + 467.5 \cdot O_2 + 29 \cdot H^+ \rightarrow 416 \cdot CO_2 + 29 \cdot NH_4^+ + 331 \cdot H_2O$		
	O_2 uptake	$Y_O^{a,d}$, g $O_{2uptaken}$·g $VSS_{decayed}^{-1}$	1.53
	CO_2 production	$Y_C^{a,d}$, g $C_{produced}$·g $VSS_{decayed}^{-1}$	0.510
	NH_4^+ production	$Y_N^{a,d}$, g $N_{produced}$·g $VSS_{decayed}^{-1}$	0.0415
Heterotrophic growth	$0.706 \cdot C_{10}H_{19}NO_3 + 3.83 \cdot O_2 + 0.294 \cdot NH_4^+ \rightarrow C_5H_7NO_2 + 0.294 \cdot H^+ + 2.06 \cdot CO_2 + 3.65 \cdot H_2O$		
	O_2 uptake	Y_O^h, g $O_{2uptaken}$·g $VSS_{produced}^{-1}$	1.08
	CO_2 production	Y_C^h, g $C_{produced}$·g $VSS_{produced}^{-1}$	0.219
	NH_4^+ uptake	Y_N^h, g $N_{uptaken}$·g $VSS_{produced}^{-1}$	0.0364
Heterotrophic decay	$C_5H_7NO_2 + 5\,O_2 + H^+ \rightarrow NH_4^+ + 2\,H_2O + 5\,CO_2$		
	O_2 uptake	$Y_O^{h,d}$, g $O_{2uptaken}$·g $VSS_{decayed}^{-1}$	1.42
	CO_2 production	$Y_C^{h,d}$, g $C_{produced}$·g $VSS_{decayed}^{-1}$	0.531
	NH_4^+ production	$Y_N^{h,d}$, g $N_{produced}$·g $VSS_{decayed}^{-1}$	0.124
Nitrification	$1.86O_2 + 0.098CO_2 + NH_4^+ \rightarrow 0.0196C_5H_7NO_2 + 0.98NO_3^- + 0.094\,H_2O + 1.98H^+$		
	O_2 uptake	Y_O^n, g $O_{2uptaken}$·g $VSS_{produced}^{-1}$	26.9
	CO_2 uptake	Y_C^n, g $C_{uptaken}$·g $VSS_{produced}^{-1}$	0.531
	NH_4^+ uptake	Y_N^n, g $N_{uptaken}$·g $VSS_{produced}^{-1}$	6.32
	NO_3^-	Y_Σ^n, mol NO_3^- produced·g $VSS_{produced}^{-1}$	0.442[1]

[1] Because NO_3^- concentration is only needed for the electroneutrality balance (Equation 6 - 12), the production yield is given in mol.g VSS^{-1}.

Kinetic equations:

The equations describing the rates of the mechanisms considered are summarized in Table 6 - 5, (see Appendix 20 for details on biological rates). The meanings of the symbols used with their input values are listed in Table 6 - 6.

Table 6 - 5: Kinetics equations associated with the mechanisms implicated in pH variations calculations

Mechanism	Units	Volumetric rate
Atmospheric CO_2 diffusion	g C.m^{-3}.s^{-1}	$Kla_{CO_2} \cdot (CO_2^{S,*} - CO_2^S)$
Atmospheric O_2 diffusion	g O_2.m^{-3}.s^{-1}	$Kla_{O_2} \cdot (O_2^{S,*} - O_2^S)$
Atmospheric NH_3 diffusion	g N-NH_3.m^{-3}.s^{-1}	$Kla_{NH_3} \cdot (NH_3^{S,*} - NH_3^S)$
Photosynthesis	kg VSS.m^{-3}.s^{-1}	$r_g^a = \frac{IC}{K_C + IC} \cdot \frac{PE \cdot 0.47 \cdot Hs \cdot S}{HV \cdot V}$
Algae decay	kg VSS.m^{-3}.s^{-1}	$r_d^a = -\frac{DO}{K_{DO}^a + DO} \cdot k^a \cdot X^a$
Heterotrophic growth	kg VSS.m^{-3}.s^{-1}	$r_g^h = \frac{DO}{K_{DO}^h + DO} \cdot X^h \cdot \left(\frac{\mu(T_p) \cdot bCOD}{K_S(T_p) + bCOD}\right)$
Heterotrophic decay	kg VSS.m^{-3}.s^{-1}	$r_d^h = -\frac{DO}{K_{DO}^h + DO} \cdot X^h \cdot k^h(T_p)$
Nitrifiers growth	kg VSS.m^{-3}.s^{-1}	$r^n = Y^n \cdot [NO_3^-] \cdot \frac{q_{out}}{V}$

As can be seen in the photosynthesis equation listed in Table 6 - 5, the photosynthetic growth rate was moderated for the concentration of inorganic carbon concentration (IC, kg C·m^{-3}) as commonly done in the literature (Bai et al., 2015; Costache et al., 2013; Lee and Zhang, 2016; Malek et al., 2016). While model found in the literature generally assumed carbon limitation originates from limitation of the dissolved CO_2 concentration or the addition of dissolved CO_2 and HCO_3^- concentrations, we assumed that algae were able to uptake any form of dissolved organic carbon[137] and IC concentration was calculated as:

$$IC = [HCO_3^-] + [CO_3^{2-}] + [H_2CO_3^*] \quad (6 - 11)$$

Microbial growth was also assumed to never be limited by nitrogen or phosphorus availabilities. Although these assumptions were not specifically verified, HRAPs generally operate in carbon limited state (Craggs et al., 2012). Besides i) many algae can uptake nitrate as N source (Delgadillo-Mirquez et al., 2016) which was abundant in the pilot scale HRAP of the present study[138], and ii) phosphate concentration in the HRAPs was never below 0.37 mg $P - PO_4^{3-}$.L^{-1} in this study (5th percentile of 0.46 mg $P - PO_4^{3-}$.L^{-1}), thus remaining above the threshold phosphorous limitation for algae (ca. 0.1 mg $P - PO_4^{3-}$.L^{-1} according to Young and King, 1980).

[137] Since pH variations follow a bell shaped increase up to pH 11 (see Chapter 3), it is unlikely that algae activity is limited by the absence of CO_2 and HCO_3^-: if algae were not able to process all forms of inorganic carbon, the curve of pH increase during daytime would be expected to experience a brutal slope reduction when a non-assimilated species starts predominating in the algal broth due to pH shifts.

[138] A median concentration of 51.48 mg /L (N = 133) of nitrate was reported in the HRAP

Table 6 - 6: Kinetic parameters for biological reactions

Parameter	Symbol	Base value	References
Photosynthetic efficiency	PE	2.0 %	Guieysse et al. (2013)
Algae heat value	HV	24.7 MJ.kg VSS^{-1}	Béchet et al. (2013)
Algae affinity for IC	K_C^a	0.00432 g $C.m^{-3}$	Novak and Brune (1985)
Algae affinity for DO during decay	K_{DO}^a	0.02 $mg.L^{-1}$	Solimeno et al. (2015)
Algal broth optical density	σ	64 $m^2 \cdot kg^{-1}$	Average value measured in this study
Algae decay rate at 20°C in light[1]	k_{20}^a	$1.39 \cdot 10^{-6}$ s^{-1}	Metcalf and Eddy Inc. (2003) for heterotrophic decay
Algae decay rate at 20°C in darkness[1]	k_{20}^a	$1.67 \cdot 10^{-6}$ s^{-1}	Ratio of 1.2 with respiration in light conditions (Béchet et al., 2015)
Heterotroph affinity for DO	K_{DO}^h	0.2 $mg.L^{-1}$	Solimeno et al. (2017)
Heterotroph maximal specific growth at 20°C[1]	μ_{20}^h	$6.94 \cdot 10^{-5}$ s^{-1}	Metcalf and Eddy Inc. (2003)
Heterotroph affinity for bCOD at 20°C[1]	$K_{S_{20}}^h$	20 mg $bCOD.L^{-1}$	Metcalf and Eddy Inc. (2003)
Heterotroph yield at 20°C[1]	Y_{20}^h	0.40 g VSS·g $bCOD^{-1}$	Metcalf and Eddy Inc. (2003)
Heterotroph decay rate at 20°C[1]	$k_{d_{20}}^h$	$1.39 \cdot 10^{-6}$ s^{-1}	Metcalf and Eddy Inc. (2003)
Debris production fraction (algae and bacteria)	f_{si}	0.15	Metcalf and Eddy Inc. (2003)
Nitrification biomass yield	Y^n	0.0365 g VSS.g NO_3^- $produced^{-1}$	Stoichiometry (see Table 6 - 4)
Nitrate concentration in the effluent	$[NO_3^-]$	51.5 mg $NO_3^-.L^{-1}$	Median value from HRAP monitoring
Temperature correction factors			
Algae decay rate	θ_{k_d}	1.04	Metcalf and Eddy Inc. (2003) for heterotrophic decay
Specific heterotroph growth rate	θ_μ	1.07	Metcalf and Eddy Inc. (2003)
Heterotroph decay rate	θ_{k_d}	1.04	Metcalf and Eddy Inc. (2003)
Heterotroph bCOD affinity constant	θ_{K_S}	1	Metcalf and Eddy Inc. (2003)

[1] Correction for temperature was applied to such parameters (P) based on temperature correction factors θ (factors at the end of the present Table) following the calculation $P(T_p) = P_{20} \cdot \theta^{T_p - 20}$ where P_{20} is the value of P at 20°C and T_p is the broth temperature (°C) (see Appendix 20).

The concentrations of $O_2^{S,*}$ and $CO_2^{S,*}$ were calculated based on formula described by Metcalf and Eddy Inc. (2003). Because ammonia atmospheric concentration can be considered as insignificant, the saturation concentration $NH_3^{S,*}$ was set to zero (Solimeno et al., 2015). Kla_{O_2} was determined experimentally, and Kla_{CO_2} and Kla_{NH_3} were computed based on the

experimental value of Kla_{O_2} and the relative magnitude of the gas diffusivities (see Appendix 9).

6.2.1.3. Chemical equilibria

Assuming hydration and acid-base reactions are much faster than biological and mass transfer reactions, the concentration of H^+ can be determined by solving the equilibria listed in Table 6 - 7 for each set of environmental conditions.

Table 6 - 7: Equilibrium reactions and associated constants used in the computation of H^+ concentration

Reaction	Constant	Value (20°C)
$\boldsymbol{H_2CO_3^* \leftrightarrow HCO_3^- + H^+}$	$pK_{C1}(T_p)$[1,2]	6.36
$\boldsymbol{HCO_3^- \leftrightarrow CO_3^{2-} + H^+}$	$pK_{C2}(T_p)$[1]	10.38
$\boldsymbol{H_3PO_4 \leftrightarrow H_2PO_4^- + H^+}$	pK_{P1}	2.12
$\boldsymbol{H_2PO_4^- \leftrightarrow HPO_4^{2-} + H^+}$	pK_{P2}	7.21
$\boldsymbol{HPO_4^{2-} \leftrightarrow PO_4^{3-} + H^+}$	pK_{P3}	12.66
$\boldsymbol{NH_4^+ \leftrightarrow NH_3 + H^+}$	pK_N	9.25
$\boldsymbol{H_2O \leftrightarrow OH^- + H^+}$	$pK_w(T_p)$	7

[1] The variation of the equilibrium constants pK_{c1}, pK_{c2}, and pK_w according to HRAP broth temperature T_p were accounted for based on Metcalf and Eddy Inc. (2003).

[2] For simplicity, and as conventionally done in the literature (Christensen and Li, 2014), the concentrations of dissolved carbon dioxide (CO_2^s) and carbonic acid ($H_2CO_3^*$) were summed and expressed as $H_2CO_3^*$, and the $H_2CO_3^*/HCO_3^-$ equilibrium was associated with a pKa value of 6.36.

The formation/consumption of organic acids was neglected. The equation of electroneutrality (6 - 12) was determined by assuming that the difference between the positive and negative charges of all neutral ions (e.g. Cl^-, Na^+, Ca^{2+}), designated as $\sum$ in the following, was constant and equal to $2.4 \cdot 10^{-3}$ M based on PNCC monitoring data[139]:

$$\sum + [H^+] + [NH_4^+] = [OH^-] + [HCO_3^-] + 2 \cdot [CO_3^{2-}] + [H_2PO_4^-] + 2 \cdot [HPO_4^{2-}] + 3 \cdot [PO_4^{3-}] \quad (6 - 12)$$

As the pH in the HRAP fluctuated between 6.8 and 11.2, the concentrations of H_3PO_4 (and therefore, the $H_3PO_4/H_2PO_4^-$ equilibrium) can be neglected in the computation of the pH.

Inorganic carbon, inorganic phosphorous and ammoniacal N concentration evolution

Changes in the concentrations in algae, heterotrophs, nitrifiers, bCOD, total inorganic phosphorous (IP, kg $P \cdot m^{-3}$), ammoniacal nitrogen (IN, kg $N \cdot m^{-3}$)[140], and total inorganic

[139] PNCC wastewater treatment plant operators provided us with wastewater analysis reports compiled over 15 years in Palmerston North. The value of $\sum$ was determined from the median values of the concentrations of inert ions (mainly Cl^-, Na^+, K^+, SO_4^{2-}) and the total hardness of the wastewater. The authors gratefully acknowledge the team at PNCC wastewater treatment for their kind help.

carbon (IC, kg C·m^{-3}) in the HRAP broth were computed through mass balance. For this purpose, the concentration of dissolved species was assumed homogeneous but the concentration of suspended solids (biomass, debris, and organic materials) was assumed to be affected by settling at the pond outlet. A sedimentation factor[141] (< 1) was therefore used in the biomass mass balance applied to all particulate matter (see Appendix 20 for microbial mass balances development).

IC was calculated as:

$$V \cdot \frac{dIC}{dt} = IC_{in} \cdot q_{in} + Kl_{a_{CO_2}} \cdot (CO_2^{s,*} - CO_2^{s}) \cdot V + (1 - f_d) \cdot Y_C^{a,d} \cdot r_d^a - Y_C^a \cdot r_g^a - IC(t) \cdot q_{OUT} + Y_C^h \cdot r_g^h + (1 - f_d) \cdot Y_C^{h,d} \cdot r_d^h - Y_C^n \cdot r^n \quad (6 - 13)$$

IP ($= [H_2PO_4^-] + [HPO_4^{2-}] + [PO_4^{3-}]$) was calculated as:

$$V \cdot \frac{dIP}{dt} = 0.01 \cdot \left((1 - f_d) \cdot r_d^a - r_g^a\right) + 0.01 \cdot \left((1 - f_d) \cdot r_d^h - r_g^h - r^n\right) + IP_{IN} \cdot q_{IN} - IP(t) \cdot q_{OUT} \quad (6 - 14)$$

IN ($= [NH_4^+] + [NH_3]$) was calculated as:

$$V \cdot \frac{dIN}{dt} = IN_{in} \cdot q_{in} + Kla_{NH_3} \cdot (NH_3^{s,*} - NH_3^{s}) \cdot V + (1 - f_d) \cdot Y_N^{a,d} \cdot r_d^a - Y_N^a \cdot r_g^a - IN(t) \cdot q_{OUT} - Y_N^h \cdot r_g^h + (1 - f_d) \cdot Y_N^{h,d} \cdot r_d^h - Y_N^n \cdot r^n \quad (6 - 15)$$

Where IC_{in} is the total inorganic carbon in the inlet (kg C.m^{-3}), IP_{IN} is the total inorganic phosphorous in the inlet (kg P.m^{-3}), and IN_{in} is the total ammoniacal N in the inlet (kg N.m^{-3}).

Final calculation of pH

pH calculation was based on the assumption that the chemical equilibria listed in Table 6 - 4 are reached instantly while mass transfer mechanisms (e.g. the flux of carbon dioxide from the atmosphere) have limiting kinetics. The shift in the concentrations of chemical species computed by solving the equilibria for a new set of experimental conditions at a time t was

[140] The notation *IN* was used although other inorganic species of nitrogen than NH_4^+ and NH_3 exist in the algal broth.

[141] The sedimentation is used as the ratio of suspended solids concentration effectively reaching the outlet, by the concentration at the bottom of the pond and was evaluated experimentally (cf. Appendix 21).

assumed to not trigger any further transfer of any chemical species (e.g. no further absorption of carbon dioxide from the atmosphere) until the next time step in the calculations. From equilibrium and electroneutrality equations, each chemical species can be substituted as a function of H^+ concentration. Then, a seven order polynomial of $[H^+]$ can be developed from the system, the roots of which are potential solutions for $[H^+]$ concentration[142]. The coefficients of the polynomial are shown in Appendix 22. This polynomial was solved using Matlab. A large number of simulations showed this polynomial has only one positive solution, which was selected to calculate $[H^+]$ concentration. The remaining unknowns (the 8 other dissolved species) were then computed based on the pH and the equilibrium constants.

DO concentration

The mass balance over DO in the HRAP accounting for the consumption and production by microorganisms, and the transfer of O_2 at the air-water interface is described by Equations 6 - 16.

$$V \cdot \frac{dO_2}{dt} = Kla_{O_2} \cdot (O_2^{s,*} - O_2^s) \cdot V + Y_O^a \cdot r_g^a - (1 - f_d) \cdot Y_O^{a,d} \cdot r_d^a - q_{OUT} \cdot O_2(t) - Y_O^h \cdot r_g^h - (1 - f_d) \cdot Y_O^{h,d} \cdot r_d^h - Y_O^n \cdot r^n \quad (6 - 16)$$

[142] i.e. $\frac{1}{[H^+]}$ is a solution of $a_0 + a_1.X + a_2.X^2 + a_3.X^3 + a_4.X^4 + a_5.X^5 + a_6.X^6 + a_7.X^7 = 0$

Box 6 - 2: Summary of the model developed for pH predictions

Main assumptions

- Acid-base reactions were assumed to be instantaneous
- The formation/consumption of organic acids was neglected
- Precipitation reactions were neglected
- H_3PO_4 concentration in the algal broth was neglected
- Photosynthesis, heterotrophic growth and nitrification were the only bio-reactions considered to have a significant impact on pH.
- The decay of nitrifiers was neglected
- Biomass growth was assumed to uptake 1 g of P per 100 g of dry biomass formed
- Biomass decay was assumed to release 1 g of P per 100 g of dry biomass decayed
- Growth and decay of microbes were modelled according to the reactions shown in Table 6 - 4
- Microbial growth was not limited by inorganic nitrogen and phosphorus availability
- A sedimentation factor was applied to all particulate matter (< 1, ratio between suspended solids concentration effectively reaching the outlet and the true concentration in the HRAP)

Model equations

The broth electroneutrality was calculated as:

$$\sum + [H^+] + [NH_4^+] = [OH^-] + [HCO_3^-] + 2 \cdot [CO_3^{2-}] + [H_2PO_4^-] + 2 \cdot [HPO_4^{2-}] + 3 \cdot [PO_4^{3-}]$$

where $\sum$ is the difference between the positive and negative charges of all neutral ions.

The rate of reaction was associated with each biological activity considered significant, were calculated as (kg VSS.m^{-3}.s^{-1}):

Photosynthesis	kg VSS.m^{-3}.s^{-1}	$r_g^a = \frac{IC}{K_C + IC} \cdot \frac{PE \cdot 0.47 \cdot Hs \cdot S}{HV \cdot V}$
Algae decay	kg VSS.m^{-3}.s^{-1}	$r_d^a = -\frac{DO}{K_{DO}^a + DO} \cdot k^a \cdot X^a$
Heterotrophic growth	kg VSS.m^{-3}.s^{-1}	$r_g^h = \frac{DO}{K_{DO}^h + DO} \cdot X^h \cdot \left(\frac{\mu(T_p) \cdot bCOD}{K_S(T_p) + bCOD}\right)$
Heterotrophic decay	kg VSS.m^{-3}.s^{-1}	$r_d^h = -\frac{DO}{K_{DO}^h + DO} \cdot X^h \cdot k^h(T_p)$
Nitrification	kg VSS.m^{-3}.s^{-1}	$r^n = Y^n \cdot [NO_3^-] \cdot \frac{q_{out}}{V}$

The gas transfer at the air-water interface for CO_2, O_2, and NH_3 were calculated as

Atmospheric CO_2 diffusion	g C.m^{-3}.s^{-1}	$Kla_{CO_2} \cdot (CO_2^{s,*} - CO_2^s)$
Atmospheric O_2 diffusion	g O_2.m^{-3}.s^{-1}	$Kla_{O_2} \cdot (O_2^{s,*} - O_2^s)$
Atmospheric NH_3 diffusion	g N-NH_3.m^{-3}.s^{-1}	$Kla_{NH_3} \cdot (NH_3^{s,*} - NH_3^s)$

The evolution of concentration in inorganic carbon, inorganic phosphorous, and ammoniacal nitrogen were calculated as:

$$V \cdot \frac{dIC}{dt} = IC_{in} \cdot q_{in} + Kl_{a_{CO_2}} \cdot (CO_2^{s,*} - CO_2^s) \cdot V + (1 - f_d) \cdot Y_C^{a,d} \cdot r_d^a - Y_C^a \cdot r_g^a - IC(t) \cdot q_{OUT} + Y_C^h \cdot r_g^h + (1 - f_d) \cdot Y_C^{h,d} \cdot r_d^h - Y_C^n \cdot r^n$$

$$V \cdot \frac{dIP}{dt} = 0.01 \cdot \left((1 - f_d) \cdot r_d^a - r_g^a\right) + 0.01 \cdot \left((1 - f_d) \cdot r_d^h - r_g^h - r^n\right) + IP_{IN} \cdot q_{IN} - IP(t) \cdot q_{OUT}$$

$$V \cdot \frac{dIN}{dt} = IN_{in} \cdot q_{in} + Kla_{NH_3} \cdot (NH_3^{S,*} - NH_3^S) \cdot V + (1 - f_d) \cdot Y_N^{a,d} \cdot r_d^a - Y_N^a \cdot r_g^a - IN(t) \cdot q_{OUT} - Y_N^h \cdot r_g^h + (1 - f_d) \cdot Y_N^{h,d} \cdot r_d^h - Y_N^n \cdot r^n$$

pH was determined by solving a seven degree polynomial developed from the chemical equilibrium equations, the quantities IC, IP, and IN, and electroneutrality equation (see Appendix 22).

6.2.2. MODEL VALIDATION

Broth pH was simulated from 22/07/2016 to the 29/07/2017[143]. This period was selected because consistent experimental pH and DO concentration were available.

Materials and methods

Meteorological data over the selected period were obtained from NIWA database as for the validation of HRAP broth temperature modelling (see section 6.1.2.). Design parameters are listed in Table 6 - 8 and the wastewater characteristics in Table 6 - 9. The HRAP broth temperature was obtained using the modelling presented in Section 6.1. of the present Chapter. Finally, the values used for the variables initialisation during simulations are shown in Appendix 23.

Table 6 - 8: Design parameters used for the modelling of HRAP broth pH and DO concentration

Parameter	Base value	Symbol used
HRAP depth[1]	0.25 m	d
HRAP surface[1]	3.42 m^2	S
O_2 mass transfer coefficient at the air/water interface[2]	1.0x10^{-4} s^{-1}	Kla_{O_2}
CO_2 mass transfer coefficient at the air/water interface[2]	9.1·10^{-5} s^{-1}	Kla_{CO_2}
NH_3 mass transfer coefficient at the air/water interface[2]	8.6·10^{-5} s^{-1}	Kla_{NH_3}
Sedimentation rate[3]	0.8	ρ_{sedim}

[1] Value from pilot scale set up;
[2] Rate determined experimentally (cf. Appendix 9);
[3] Rate determined experimentally (cf. Appendix 21)

[143] Some weather data were missing between 12 and 16/12/2016 and 27 and 31/12/2016. Both periods were excluded from the analysis.

Table 6 - 9: Wastewater characteristics used for the modelling of HRAP broth pH and DO concentration

Parameter	Base value	Symbol used
Temperature	15 °C	T_{IN}
COD concentration[1]	300 mg.L^{-1}	COD_{IN}
Coliform concentration[1]	4.7*10^{10} MPN.m^{-3}	$C_{coli_{IN}}$
Inorganic carbon concentration[2]	50 mg C.L^{-1}	TC_{IN}
Inorganic phosphorous concentration[3]	2.0 mg P.L^{-1}	TP_{IN}
Heterotrophic bacteria concentration[4]	0 mg.L^{-1}	$X_{bacteria_{IN}}$
Inert charge balance[5]	2.4 mmol.L^{-1}	Σ_{IN}

[1] Based on the mean of the values measured in the wastewater influent (cf. Chapter 3, section 3.1.2) ;
[2] Value determined based on alkalinity data compiled over 15 years in Palmerston North provided by PNCC wastewater treatment plant operators, assuming the alkalinity is exclusively formed of bicarbonate ;
[3] Value determined based on phosphorous concentration data compiled over 15 years in Palmerston North provided by PNCC wastewater treatment plant operators;
[4] Assumption;
[5] Based on wastewater data provided by Palmerston North wastewater treatment plant analysis (see footnote [139] for further details).

During simulation for validation, the HRAP broth temperature was computed at a time step of 1/100th of an hour in order to get simulated values at a time step below 1 minute. DO and IC concentrations were often found to artificially decrease below zero at this time step. In these cases, the calculation was taken one step back from "n" and a new time step (by dividing initial time step by a 'refinement factor') was used between step n-1 and n. The inputs for pH calculation were linearly interpolated over the new calculation points introduced and the calculation was restarted from the step n-1. The refinement factor generally used in the presented simulations was 3. In some instances the step of calculation was divided several times, which caused long computation times. A limit was therefore introduced so that the step of time in the calculation could not decrease below 1s. If this time step was reached, the negative data were set to 0.001 (mg O_2.L^{-1} or mg C.L^{-1}), and the calculations were resumed at the step n. Sensitivity analysis showed that increasing the initial time step to 1/4th of an hour, varying the refinement factor from 2 to 100, and the time step limit between 0.01 and 900 seconds did not produce significantly different results (e.g. below 1.1% and 0.5% relative impact on average daily maximal temperature and average daily maximal pH[144].

The values of all input parameters listed in previous paragraphs were kept constant throughout the simulation[145]. Thus, the HRT, wastewater characteristics (e.g. COD), and

[144] Both outputs were used as indicator of model performance in section 6.3.
[145] Regardless of the time-span of the simulation.

nitrate productivity were assumed constant despite knowing these parameters underwent significant variations (see Table 3 - 1).

Changes in pond volume (and dilution effect) due to evaporation and rainfall were accounted for, meaning the water column depth could possibly be different to the depth set as design input[146]. The pond depth however could not increase above the value set as design input, and the outlet flow rate was calculated as the addition of inlet and rain flow rates minus evaporation 'flow' rate.

Model predictions

Examples of model predictions compared with measured data over selected periods of time both for pH and DO concentration are shown in Figure 6 - 6, Figure 6 - 7, and Figure 6 - 8. As can be seen, periods were identified when both pH and DO concentration were accurately predicted (Figure 6 - 6), when both predicted pH and DO concentration were systematically overestimated (Figure 6 - 7), and when both predicted pH and DO concentration were systematically underestimated (Figure 6 - 8). Interestingly, no other patterns were observed over significant periods of time (e.g. systematic overestimation of pH but underestimation of DO concentration). Because the trends were consistently observed over significant periods of time (instead of randomly alternating), we hypothesise that the errors associated are more probably due to 'real' variability in model inputs (during each period), rather than conceptual error in the model or 'random' uncertainty in model input. This is further discussed following the model validation and sensitivity analysis.

[146] Practically, the inlet and rain flows were always found to compensate evaporation losses so pond depth remained constant.

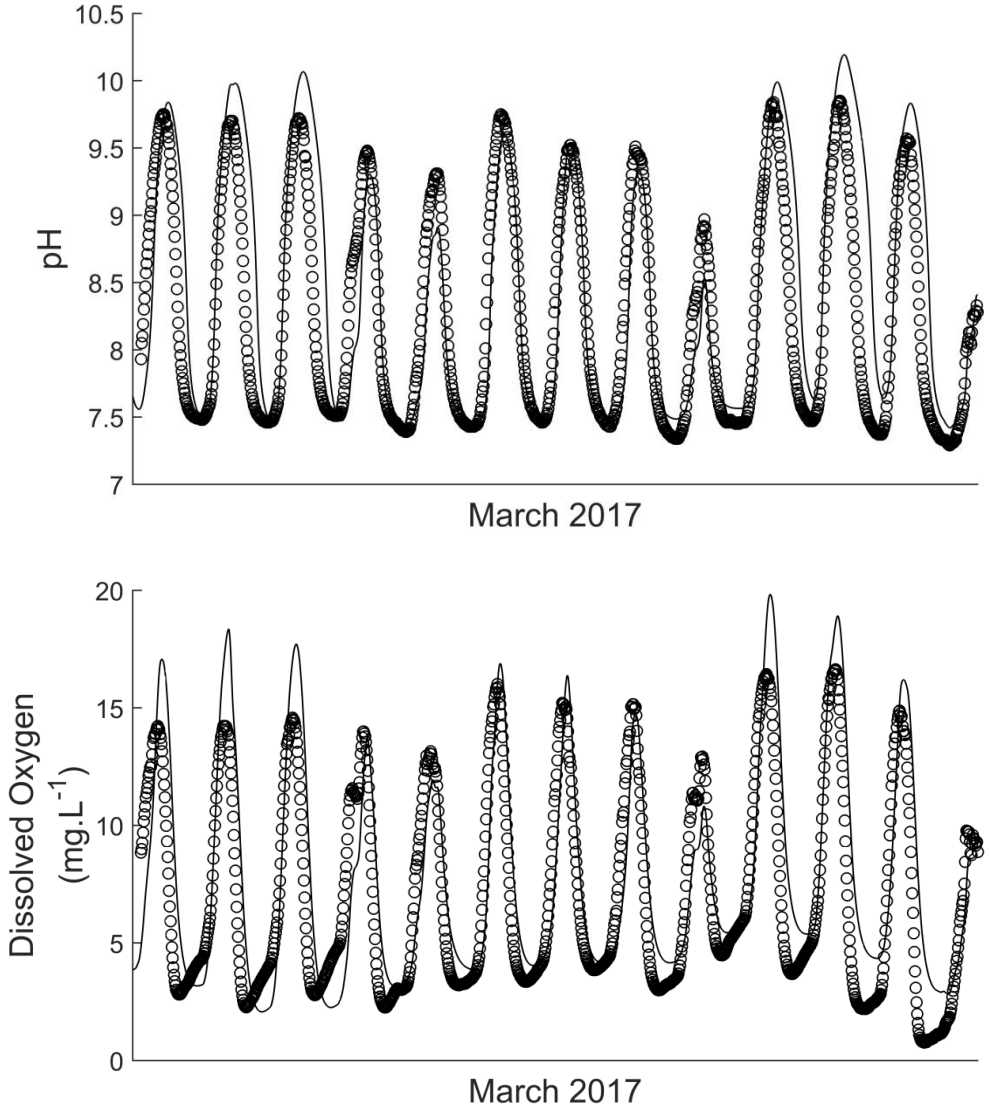

Figure 6 - 6 Comparison between modelled (-) and measured (o) pH (top) and DO concentration (bottom). Period during which the model accurately estimated variables in comparison with observations in the HRAP (March 2017)

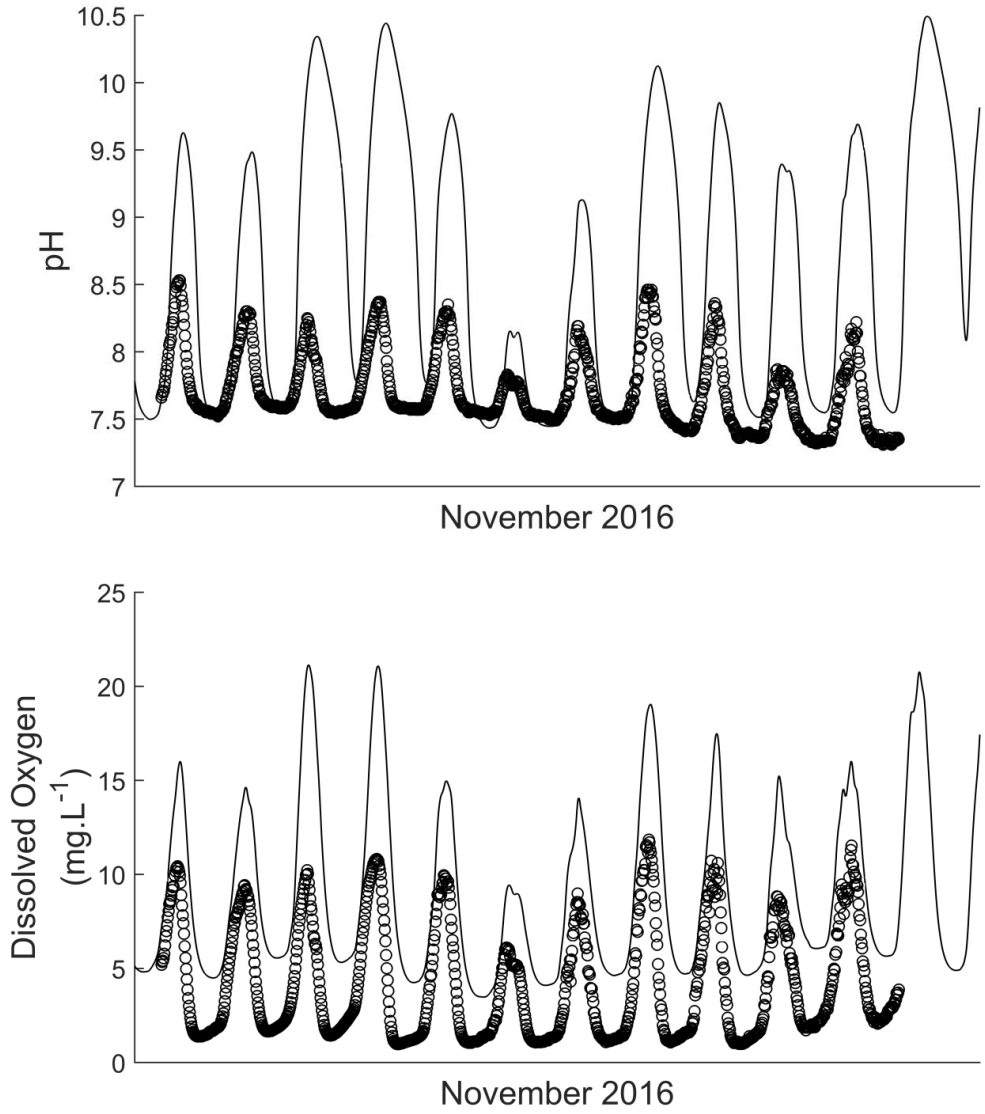

Figure 6 - 7: Comparison between modelled (-) and measured (o) pH (top) and DO concentration (bottom). Period during which the model over-estimated variables in comparison with observations in the HRAP (November 2016)

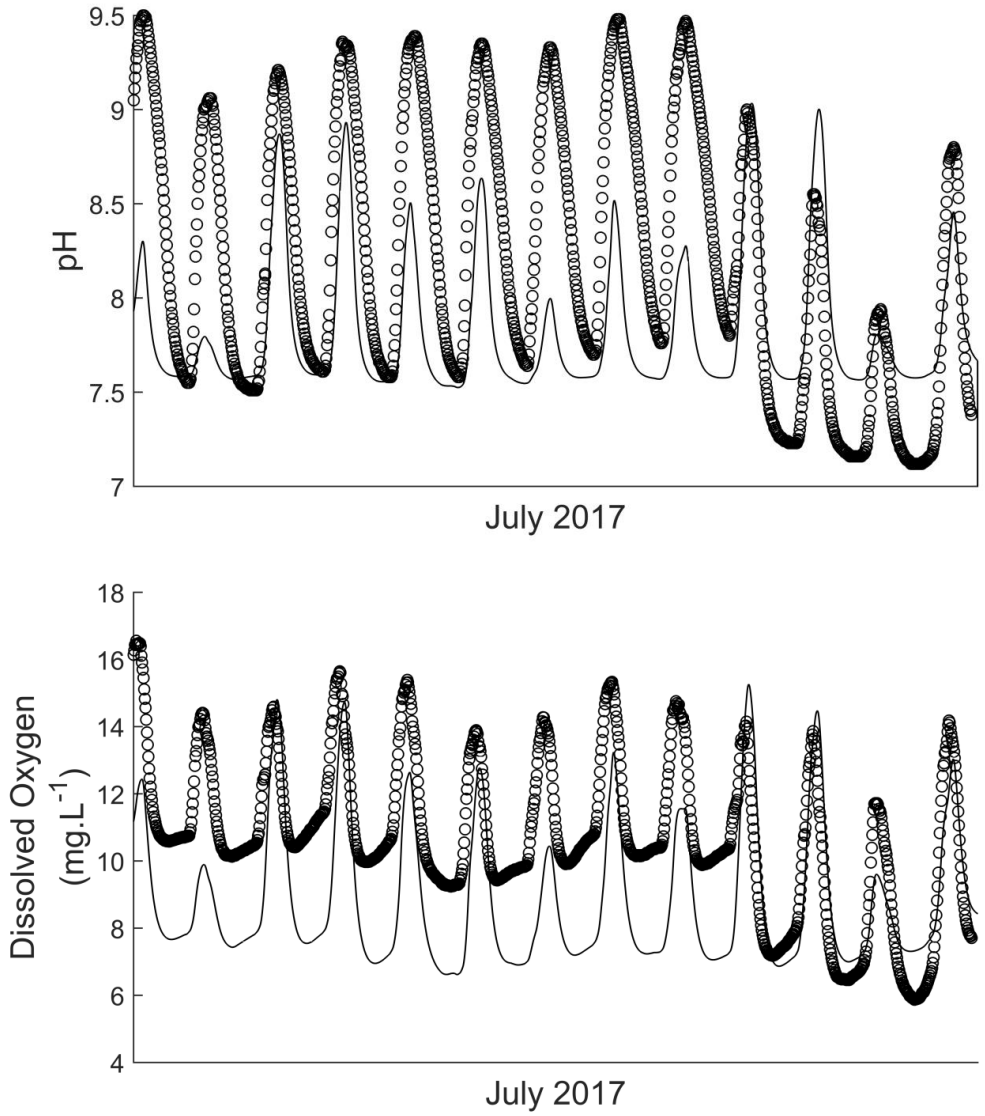

Figure 6 - 8: Comparison between modelled (-) and measured (o) pH (top) and DO concentration (bottom). Period during which the model under-estimated variables in comparison with observations in the HRAP (July 2017)

Model validation

The distribution of residuals (measured minus predicted) for the model of HRAP broth pH and DO concentration is shown in Figure 6 - 9. Only results for pH are analysed below although results for DO concentration model goodness of fit are also shown. As can be seen in Figure 6 - 9, the pH model residuals distribution was centred on zero (average of the residuals of -0.117). However, the distribution was not normal indicating non-random errors were likely impacting the model goodness of fit.

The goodness of fit for pH predictions was further evaluated using simple linear regression with no intercept[147] between modelled (x) and measured (y) data (Figure 6 - 9, left). Results show average modelling performance[148] (β = 0.97756; R^2 = 0.590; root squared mean error = 0.708; standard error of β = $5.54 \cdot 10^{-4}$; N = 23,817)[149]. Based on this data, HRAP broth pH was accurately predicted on average (β close to one) but with an uncertainty of ±1.39[150] (pH unit) over the period assessed. The average observed prediction error[151] was 0.501 (pH unit).

[147] The test consists in evaluating β assuming the relationship between modelled temperature (x) and measured temperature (y) is $y = \beta . x$

[148] A perfect model would yield a β coefficient equal to 1, with both the standard error for the β coefficient and the root mean squared error (RMSE) being as low as possible.

[149] The DO model goodness of fit parameters value are β = 0.93784; R^2 = 0.6354; root squared mean error = 2.64; standard error of β = $1.80\ 10^{-3}$.

[150] Calculated as 1.96 times the RMSE (95% confidence interval assuming normal distribution of the data)

[151] Calculated as the average of the absolute values of the residuals.

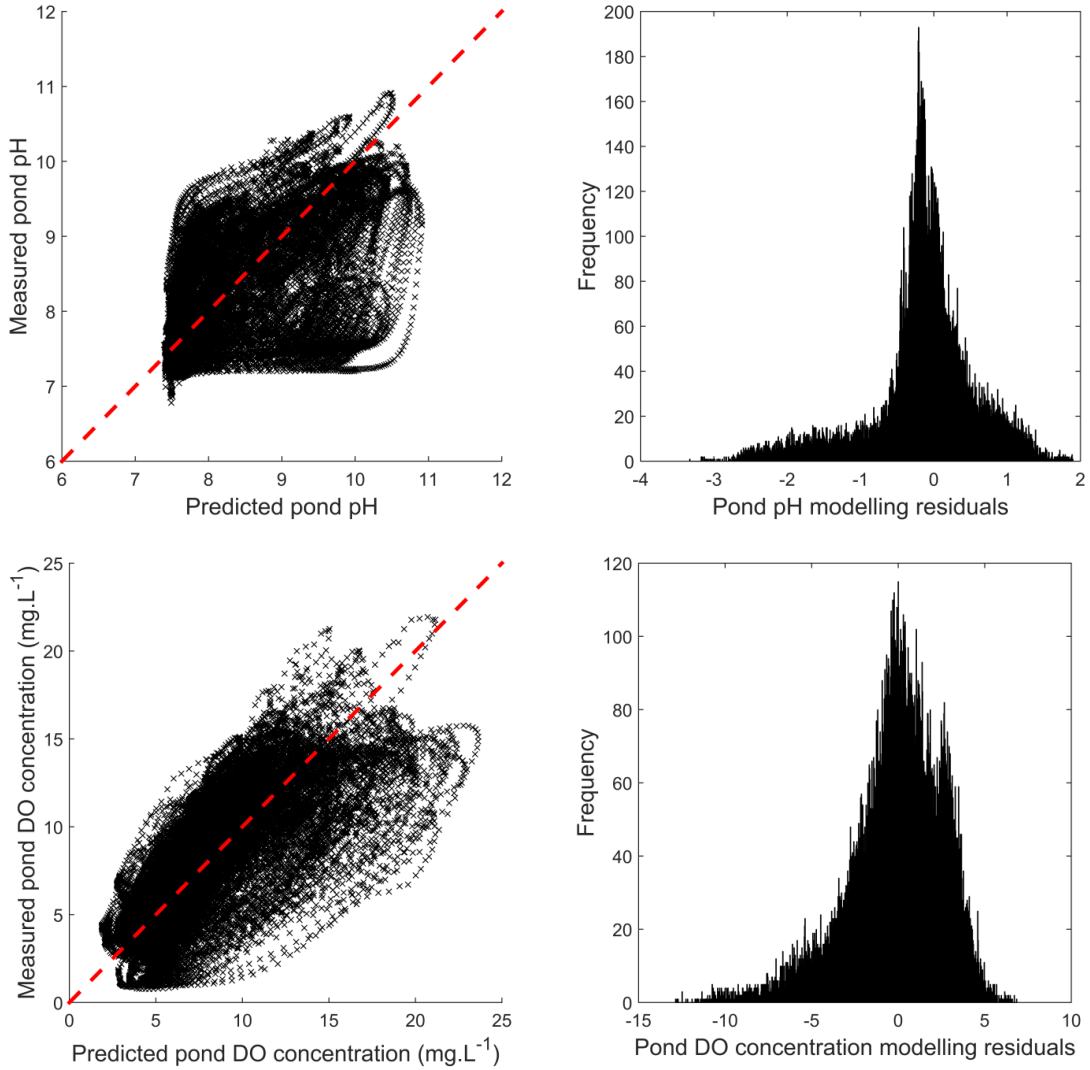

Figure 6 - 9: HRAP pH (top) and DO concentration (bottom) measured versus predicted and associated distribution of modelling residuals (measured minus predicted)

Model sensitivity analysis

The sensitivity of the model fitness to variability in input parameters was assessed based on the variability/uncertainty range defined in Appendix 24. The results of the sensitivity analysis are shown in Figure 6 - 10[152]. As can be seen, algae photosynthetic efficiency (PE) and wastewater COD concentration had a large effect on the model goodness of fit for pH. All other parameters tested had a limited impact compared with PE and wastewater COD concentration, meaning the variability of PE and wastewater COD concentration (both assumed constant) likely explain most of model uncertainty. While relatively less important, the variability of many of the other parameters assumed to be constant (e.g. IC

[152] Parameters not represented in Figure 6 - 10 had a lower effect on pH model goodness of fit than any of the parameters shown.

concentration, charge balance, HRT) could also have a large compounded effect on the prediction accuracy.

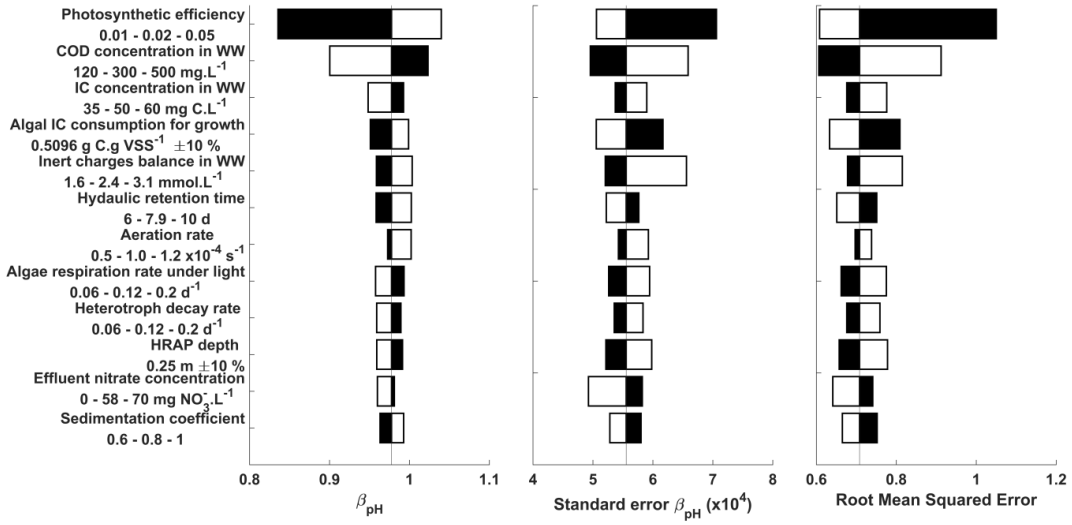

Figure 6 - 10: Sensitivity of the pH modelling toward calculation parameters.
Black and white bars show the output values predicted using the upper and lower values, respectively, of the parameter tested

The sensitivity analysis indicated that inputting a lower value of PE and a higher value of COD concentration could improve the goodness of fit ($\beta = 1$ and lower prediction errors). However, the model R^2 was only 0.2218 when PE was set to 0.01. Algae fitness (and thus PE) may vary significantly over time (depending on change of dominating specie, bloom of grazers), possibly explaining the alternating periods of systematic over- or under- estimation of both pH and DO concentration. Examples of the impact of implementing different PE on modelled variations pH and DO concentration are shown in Figure 6 - 11 (initial overestimation of pH and DO concentration, corrected using PE = 0.01) and Figure 6 - 12 (initial underestimation of pH and DO concentration, corrected using PE = 0.025). The fit was visibly improved by the change of PE in both cases (in particular for pH) although significant discrepancies between measured and simulated values remain, indicating other model hypotheses hinder the goodness of fit. While the model accuracy could be improved by fine-tuning the PE value between 0.01 and 0.02, the value of 0.02 was kept for all simulations due to the lack of information on what a correct value of PE should be.

In the case of COD concentration, inputting a higher value significantly reduced the fit quality of the DO concentration model[153]. Because the value used in the base case (300 mg

[153] $\beta_{DO} = 1.14$, $SE_{\beta_{DO}} = 0.00255$, $RSME = 3.03$, R^2 = 0.6654 (see footnote [149] for comparison with base case)

$O_2.L^{-1}$)[154] was expected to best represent COD concentration for a year-long simulation, this value was also kept for all simulations.

Interestingly, the impact of temperature predictions on the model goodness of fit was not found to influence pH model goodness of fit significantly[155,156].

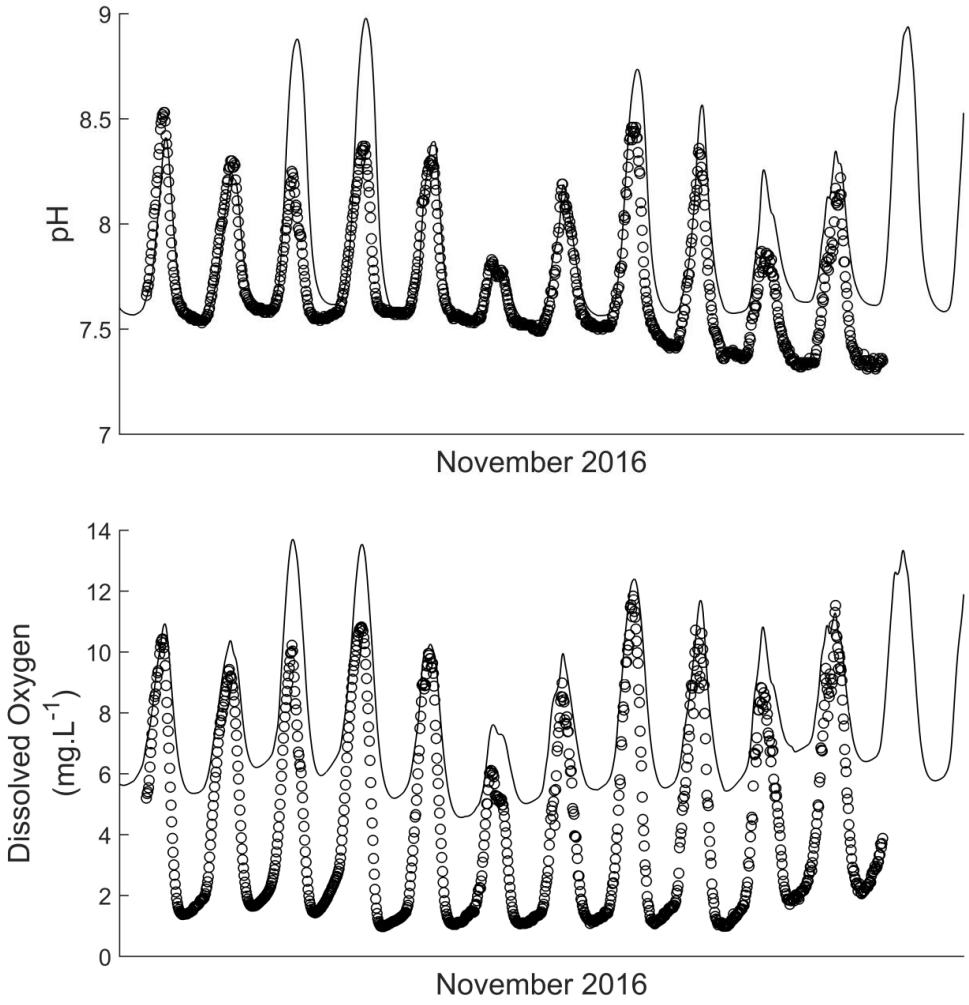

Figure 6 - 11: Comparison between modelled and measured pH (top) and DO concentration (bottom). Period during which the model over-estimated the variables in comparison with observations in the HRAP (November 2016), but simulated with PE = 0.01

[154] Observed average value during pilot scale HRAP study.

[155] This was tested by adding or withdrawing 2.41°C (temperature predictions 95% confidence interval, see section 6.1.) to the HRAP broth temperature at each time step of the calculation.

[156] $\beta_{pH} = 0.973$, $SE_{\beta_{pH}} = 5.64 \cdot 10^{-4}$, $RSME = 0.724$, R^2 = 0.588 when temperature was underestimated, $\beta_{pH} = 0.982$, $SE_{\beta_{pH}} = 5.45 \cdot 10^{-4}$, $RSME = 0.693$, R^2 = 0.591 when temperature was overestimated.

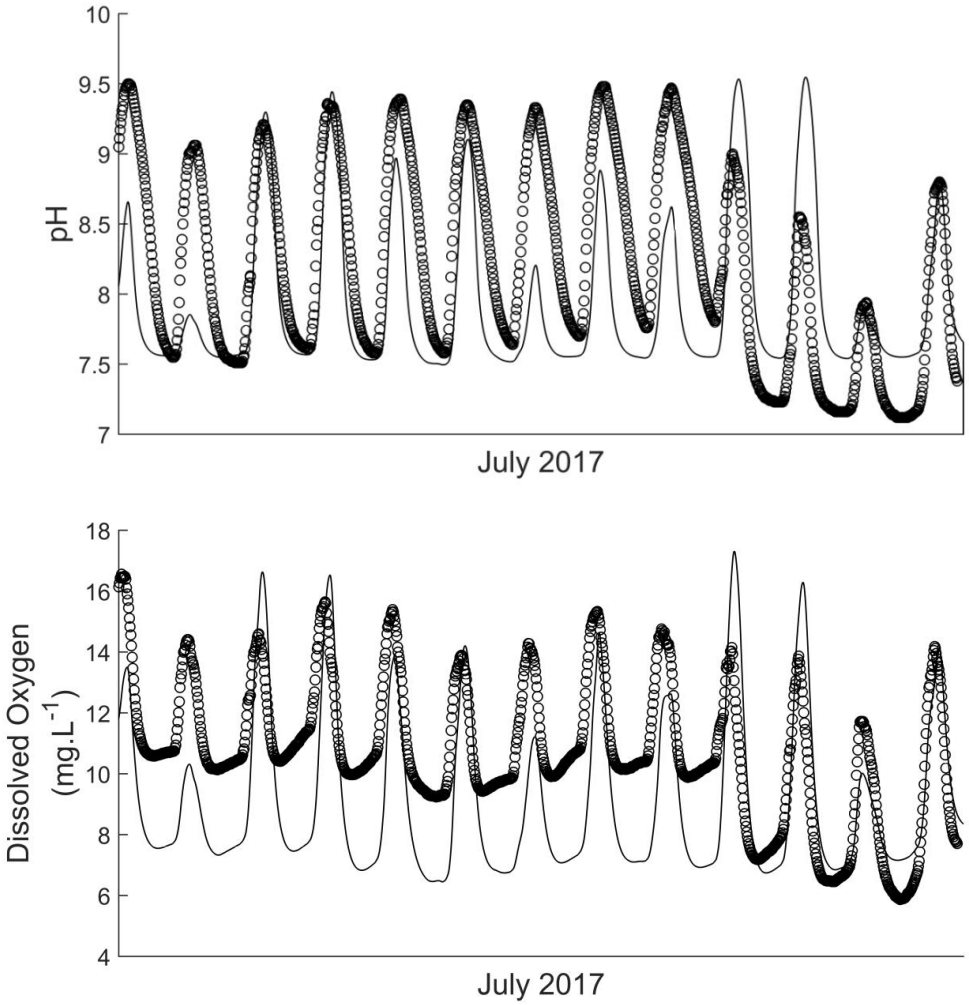

Figure 6 - 12: Comparison between modelled and measured pH (top) and DO concentration (bottom). Period during which the model under-estimated variables in comparison with observations in the HRAP (July 2017), but simulated with PE = 0.025

Despite significant model errors, the fact that pH and DO concentration could be accurately predicted over periods of several days evidenced that the model could yield accurate estimations over a period of time entailing significant variations in environmental conditions. This shows that the model provided a good representation of mechanisms influencing pH and temperature and, therefore, that the model is a suitable tool to test how process operation and design affect pH and temperature (although the magnitude of the influence may remain uncertain). The high occurrence of periods when pH and DO are both systematically overestimated (as evidenced by the large negative residuals in Figure 6 - 9) suggests that the conditions inputted in the simulation are representative to an 'ideal' pond that is not affected by negative events (e.g. grazers invasion).

6.2.3. CONCLUSION

While the model overall performance was disappointing (R^2 = 0.590, average observed prediction error[157] = 0.501 pH unit), the results showed that pH and DO could be accurately predicted during several days (see Figure 6 - 6) and that therefore, the model provides a good description of the mechanisms influencing these parameters. In light of this observation, the model was concluded to provide accurate description of HRAP pH variations provided the HRAP biomass is in "ideal conditions" (e.g. algae PE equal to 0.02, absence of grazers).

Because our aim is to determine if 'controllable' parameters (i.e. operations, design, and location) can be manipulated to improve disinfection performances in HRAPs which was demonstrated to be primarily influenced by temperature fluctuations and the occurrence of high pH (see Chapter 5), the model was concluded validated for the specific purpose of evaluating how variations in design, operations, wastewater quality, and weather conditions impact HRAP pH and temperature.

The sensitivity analysis suggested that more accurate predictions could be obtained by dynamically predicting the algae PE and integrating the variations of dynamic parameters in the model inputs (critically COD concentration of the wastewater). These refinements were however outside the scope of this research.

6.3. ASSESSING THE INFLUENCE OF HRAPS PARAMETERS ON WASTEWATER DISINFECTION USING SENSITIVITY ANALYSIS

The model presented above was developed to optimize *E. coli* removal by increasing temperature and pH (see Chapter 5). The influence of input parameters on the model predictions was investigated by assessing the model sensitivity to inputs with focus on high temperatures and high pH based on the following four criteria:

i. the average of the daily maximum predicted temperatures,
ii. the cumulated time during which temperature was predicted to be over 20°C,
iii. the average of the daily maximum predicted pH, and

[157] Calculated as the average of the absolute values of the residuals.

iv. the cumulated time during which pH was predicted to be over 10.

This new sensitivity analysis was performed by varying model parameters individually according to the range described in Appendix 24. The results of the analysis are displayed in Figure 6 - 13 and Figure 6 - 14 for temperature and pH respectively[158].

As can be seen in Figure 6 - 13, the occurrence of high temperatures was highly sensitive to the air emissivity. Sensitivity to air emissivity was likely increased by the combination of the high influence of air emissivity variations on HRAP temperature predictions (see section 6.1.2.), and the large range of values for air emissivity tested due to our poor knowledge of this parameter[159]. Variations of global solar intensity, air dry bulb temperature, and air dew point temperature also significantly influenced the model predictions. All other parameters had a restricted effect on the predicted incidence of high temperature (e.g. variations within the tested range would induce variations of the averaged daily maximal temperature below 0.5°C).

The sensitivity analysis shows that, besides the location of the HRAP (determining the weather conditions), very little control can be achieved on HRAP broth temperature: HRAP depth was the only controllable parameter enabling to improve the occurrence of high temperatures. The optimization of HRAP disinfection performance is further discussed in Chapter 7.

[158] Only parameters with significant impact are shown.
[159] Precisely estimating air emissivity was beyond the scope of this study

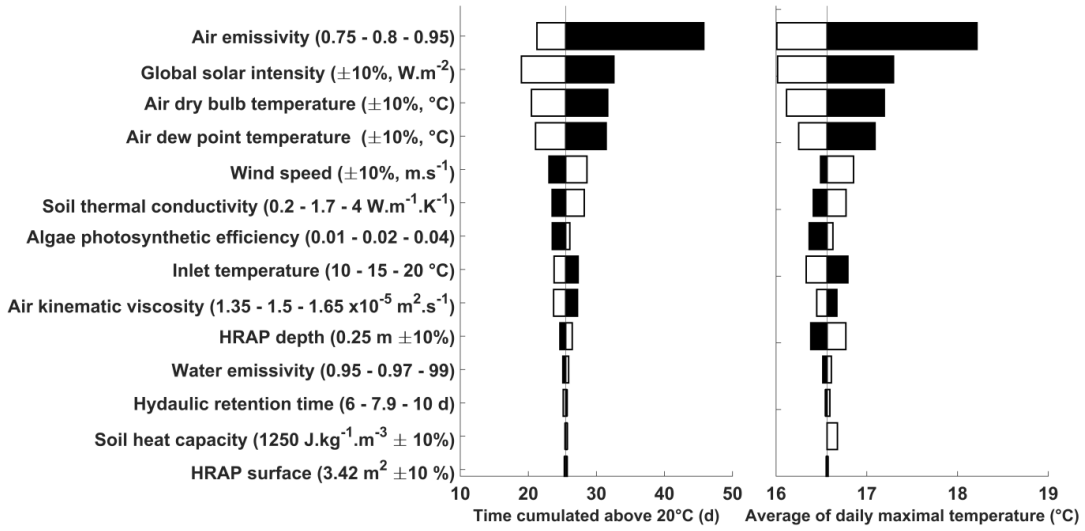

Figure 6 - 13: Sensitivity of the model outputs (time cumulated over 20°C and average of daily max temperature) to model parameters.
Black and white bars show the output values predicted using the upper and lower values, respectively, of the parameter tested

The occurrence of high pH was significantly influenced by many parameters. Most importantly, changes in algae PE can either increase or cancel the incidence of harmful pH levels. Unfortunately, it is difficult to control biological properties[160] during wastewater treatment so the influence of these parameters is not discussed in this thesis. Wastewater quality (via COD concentration, IC concentration, ammoniacal-N concentration, and inert charge balance) had a significant influence on pH levels in the HRAP, but because wastewater characteristics are site specific and not controllable as for biomass properties, this will not be further discussed in this thesis. Nevertheless, the present sensitivity analysis indicates that knowledge on wastewater characteristics informs on the feasibility of disinfection using HRAPs. Among the 'controllable parameters, HRAP design (via pond depth, HRT, and aeration rate) had the most significant effect on the incidence of elevated pH. Interestingly, weather only had a significant (yet limited) impact via the global solar intensity, suggesting location should not have a critical influence on pH mediated decay of *E. coli*. How to optimize HRAP disinfection performance based on these results is more precisely discussed in Chapter 7.

[160] Including algae PE, but also algae decay rate, microbial inorganic nutrients consumption yields, etc.

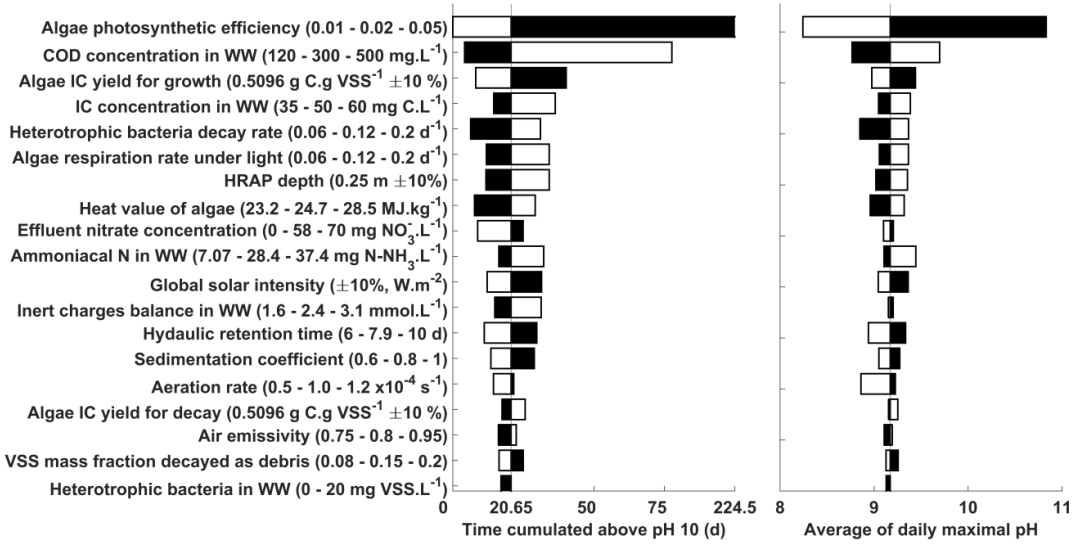

Figure 6 - 14: Sensitivity of the pH model outputs (time cumulated over pH 10 and average of daily max pH) to model parameters.
Black and white bars show the output values predicted using the upper and lower values, respectively, of the parameter tested. NB: the axis for 'Time cumulated above 20°C' is non-linear and skips from 75 d to 224.5 d

6.4. CONCLUSION

HRAP broth temperature and pH were predicted over a full year with an average absolute observed error of 1.35°C and 0.501 pH unit respectively.

Despite limitations of the model goodness of fit, simulations showed that variations in temperature, pH, and DO were accurately predicted over periods of several days (see Figure 6 - 6), indicating the model accurately describes the mechanisms influencing pH and temperature. Therefore, the model developed was concluded to be fit for evaluating how variations in design, operations, wastewater quality, and weather conditions affect HRAP pH and temperature.

Strategies to improve the model fitness were identified but testing these improvements was beyond the scope of this study:

1- Dynamically predicting air emissivity will likely improve temperature prediction significantly.
2- Predicting and/or improving the inputs of critical variable parameters (e.g. COD concentration in the wastewater, nitrate concentration in the HRAP) should improve pH prediction.

3- Dynamically predicting algae photosynthetic efficiency should improve pH prediction.

In order to formally validate the model, the simulation should be compared to experimental data obtained during period of 'healthy' algae growth (e.g. no algae grazing).

Prior analysis in section 6.3. showed that i) HRAP location (i.e. weather conditions) may largely influence temperature levels but would have only limited effect on pH; ii) wastewater quality may increase or limit the possibility of using HRAPs for wastewater disinfection; iii) disinfection performance using HRAPs may be further improved through design.

In Chapter 7, we will explore quantitatively how variations in HRAP design, operation strategies, and climate may increase *E. coli* removal in HRAPs using the environmental model developed in this Chapter and the disinfection model developed in Chapter 5.

Chapter 7: Optimization of HRAPs for wastewater disinfection

In Chapter 6, a model was developed to predict pH and temperature in a HRAP broth based on HRAP design, wastewater quality, and meteorological conditions. Since it was shown in Chapter 5 that pH, temperature, and sunlight distribution in the algal broth allowed predictions of *E. coli* disinfection in HRAPs, it was possible to combine the chemical-physical model (pH, temperature, sunlight) with the biological disinfection model in order to evaluate the theoretical wastewater disinfection performances of HRAPs operated under various conditions. In this Chapter, simulations were performed to evaluate the impacts of HRAP design (7.1.), cultivation mode[161] (7.2.), and climatic conditions (7.3.) on wastewater disinfection in HRAPs.

HRAP disinfection performance was evaluated in terms of average *E. coli* decay coefficient (d^{-1})[162] and the total log-removal of *E. coli* cells over the full duration of the simulation (expressed as $\log\left(\frac{N_{IN}}{N_{OUT}}\right)$, where N_{IN} is the total number of *E. coli* cells entering the HRAP and N_{OUT} is the total number of *E. coli* cells exiting the HRAP). When required, results were also analysed in terms of number of days of compliance i.e. the number of days for which the daily average *E. coli* cell count in the effluent was below discharge guidelines for microbial quality in Palmerston North[163].

Simulations were performed over a year of meteorological data for Palmerston North, New Zealand (01/08/2016 – 01/08/2017) as described in Chapter 6. The model was coded and

[161] E.g. continuous versus semi-continuous discharge, mixing regimes

[162] The instant decay coefficient k_d was calculated for each step of time of the simulation according to Equation 5 - 4 using predicted pH, predicted temperature, and experimental sunlight data used as inputs. Since all time-steps were not equal, the average decay coefficient $\overline{k_d}$ is calculated as $\overline{k_d} = \frac{1}{T} \cdot \int_0^T k_d \cdot dt$ where T = 1 year and dt is the duration of each step of time of the simulation.

[163] As detailed in Chapter 3 section 3.4., the microbial quality of the treated wastewater in Palmerston North is regarded as compliant when *E. coli* cell count is below $3 \cdot 10^4$ cells.100 mL^{-1}.

solved with Matlab® R2015a[164] (Mathworks, Massachusetts, USA). In the simulations, unless otherwise stated, the HRAP was operated in continuous mode and designed such that the water level cannot rise above the design depth level. If pond depth was predicted to decrease below 80 % of the design depth (due to water evaporation), a volume of wastewater compensating the depth deficit was added to the pond[165]. Specific adjustments to the calculations during simulations when testing for different HRAP cultivation modes and meteorological conditions are described in the relevant sections. Nitrifying bacteria activity was neglected in all simulations since this mechanism was not accurately (dynamically) modelled[166].

Simulations were performed to assess the impact of variations in design, HRAP operations and configuration, and climate, against a base case scenario (pilot scale HRAP operated in the conditions presented in Chapter 6 and located in Palmerston North). In our base case scenario, the average decay coefficient was 6.13 d^{-1}, the total log removal was 1.57, and the number of days of compliance was 0. Simulations predicted that in our base case, *E. coli* removal was primarily supported by uncharacterized dark decay (average decay coefficient 5.22 d^{-1}, 86.5 % of total *E. coli* decay), and marginally improved by sunlight and pH mediated disinfection mechanisms (average decay coefficient of 0.620 and 0.288 d^{-1} respectively, contribution to total *E. coli* decay of 11.1 % and 2.3 % respectively).

Limitations of results from simulations

The model was developed and validated under the assumption that the HRAP broth is well-mixed. While justified for our pilot scale study, this assumption is unlikely to be valid at larger scale as discussed in Appendix 2. Hence, results presented in this Chapter should be considered with caution. Because the equations used to predict the environmental conditions and disinfection mechanisms are based on values determined under "local" conditions (e.g. pH, nutrient availability), coupling a CFD model of HRAP (e.g. Hadiyanto et al., 2013) with the models herein developed may provide disinfection predictions better applicable at larger scale. Such study was outside the scope of our work.

Nitrifying activity tends to acidify the algal broth, and therefore neglecting it may lead to overestimation of pH dependent disinfection. In the base case scenario, this assumption

[164] The code is available via https://github.com/pchambonn/Pathogenicity-removal-in-algae-based-wastewater-treatment-systems---Understanding-the-mechanisms-inv

[165] This situation was only seen in simulations combining high HRTs with non-continuous operations.

[166] The activity of nitrifying bacteria was modelled assuming a constant nitrate production as measured in the pilot scale HRAPs (see Chapter 6): this assumption is only relevant to the conditions experienced in the pilot scale HRAP.

increased the contribution of pH dependent decay to total *E. coli* decay by 42%. Because in base case scenario pH dependent decay only account for 2.3% of the total *E. coli* decay, the impact of this assumption was negligible (increase of total *E. coli* decay by 0.8% when neglecting nitrifying activity). However, in scenarios where pH dependent decay contribution is relatively high, results should be considered with care, in particular if conditions are known to favour nitrifying activity (e.g. high HRT).

7.1. INFLUENCE OF HRAP DESIGN

The design parameters predicted in Chapter 6 to impact disinfection performance in HRAP were the pond Hydraulic Retention Time (HRT), the pond depth, and the pond oxygen transfer coefficient (Kl_{aO_2}). The base-case values and ranges tested in the simulations are shown in Table 7 - 1. Results from all simulations are shown in Figure 7 - 1.

Table 7 - 1: Design parameters investigated

Parameter	Base value[1]	Range tested[2]
HRT	7.9 days	1 – 14 days
Depth	0.25 m	0.1 – 0.5 m
$\boldsymbol{Kl_{aO_2}}$	$1.0 \cdot 10^{-4}$ s^{-1}	$0.5 – 1.2 \cdot 10^{-4}$ s^{-1}

[1] Base values were chosen based on the simulations for model validation (see Chapter 6).
[2] HRT and depth were tested over the range used for regular HRAP design (see Table 3 - 1); Kl_{aO_2} was tested on the range of values measured in pilot-scale HRAP (see Appendix 9).

Within the ranges tested, low aeration coefficient was associated with decreased disinfection performance. These effects are however marginal and the impact of the aeration coefficient on HRAP disinfection performance (within the range measured on our set up at pilot scale) can be concluded as being negligible.

Increasing HRT and decreasing depths were both associated with improved disinfection: increasing HRT from 8 to 14 d caused the *E. coli* average decay coefficient to increase from 6.13 d^{-1} (base value) to 6.38 d^{-1}, and the total log removal to increase from 1.57 (base value) to 1.82. The contribution of uncharacterized dark decay to overall *E. coli* decay remained almost constant in both simulations, while pH toxicity contribution increased from 2.3 % to 4.3 % (see Figure 7 - 2): therefore, it was concluded that increasing HRT improved HRAP disinfection performance by increasing exposure time to 'generally harmful' conditions, and, marginally, by favouring carbon starvation which increased the pH[167] and its associated disinfection.

[167] The average pH increased from 8.37 at 7.9 d HRT to 8.64 at 14 d HRT.

Decreasing depth from 0.25 m to 0.10 m caused the *E. coli* average decay coefficient and total log removal to increase to 24.83 d^{-1} and 1.70, respectively[168]. Low depths have been proposed for improved disinfection in algal ponds with the rationale of increasing solar disinfection efficiency[169] (Ansa et al., 2012b; Davies-Colley, 2005; Maïga et al., 2009b). However, these simulations predicted that lowering depth mainly causes the broth pH to increase (the average broth pH was 9.84 at 0.10 m depth against 8.37 at 0.25m depth), thus significantly increasing pH induced decay: the contribution of pH toxicity to the overall *E. coli* decay was predicted to increase from 2.3 % to 32.9 %, while the contribution of sunlight mediated disinfection mechanisms would "only" increase from 11.1 % to 15.7 % (see Figure 7 - 3).

The ideal design for wastewater disinfection in HRAPs would therefore be to combine low depth with high HRT. Such design incurs a higher land requirement and higher capital costs (associated with HRAP construction) since increasing HRT and decreasing depth both require increasing pond area when all other process parameters are kept constant.

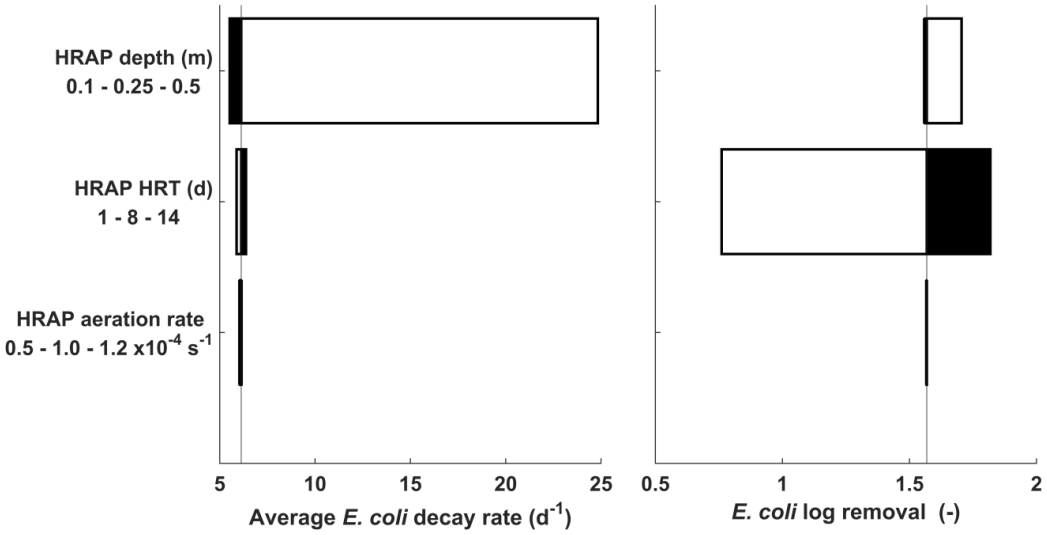

Figure 7 - 1: Predicted changes in average *E. coli* decay coefficient and total *E. coli* log removal under various designs.
The black and white bars represent the values associated with the upper and lower values, respectively, of each parameter tested.

[168] At 0.10 m depth, the model predicted that the HRAP operates in a nitrogen limited state due to intense algal activity. This simulation therefore did not comply with the hypothesis under which the model was developed and the results should be considered with caution.
[169] Lower depth results in higher average light intensity in the water column

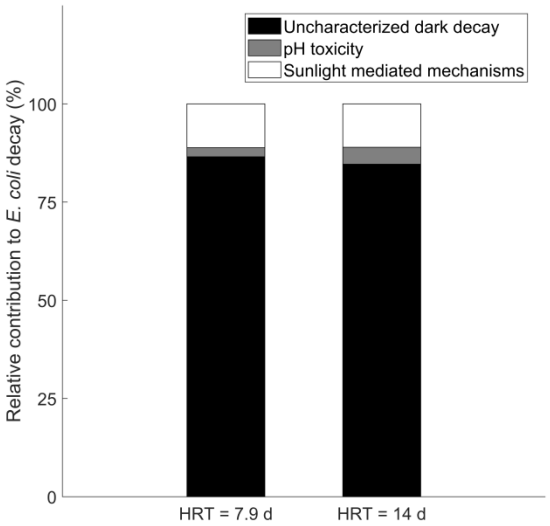

Figure 7 - 2: Relative contribution of simulated disinfection mechanisms to overall *E. coli* decay in base case scenario and at 14 d HRT

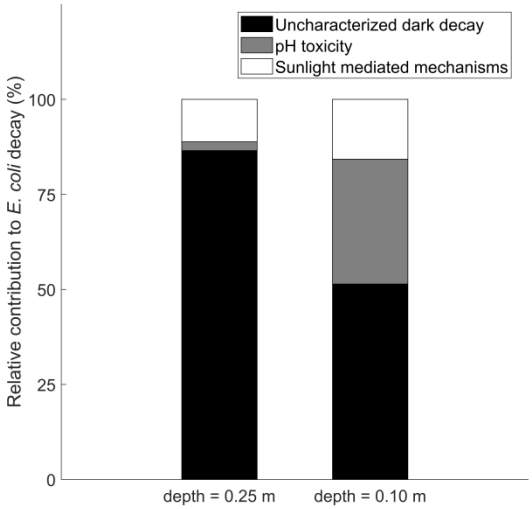

Figure 7 - 3: Relative contribution of simulated disinfection mechanisms to overall *E. coli* decay in base case scenario and at 0.10 m depth

7.2. INFLUENCE OF HRAP OPERATION

7.2.1. NON-CONTINUOUS OPERATING REGIMES

Simulations performed in Chapter 5 showed that the disinfection performance of HRAPs is mainly driven by temperature and, in some situations (e.g. low depth), elevated pH. While heating the algal broth of HRAP would be prohibitively expensive (Béchet et al., 2016), the monitoring of pilot scale HRAP (Chapter 3) suggested high pH peaks can be increased by operation practices[170]. Simulations however showed that low gas transfer coefficient lowers algal density over the long run due to inorganic carbon starvation, which in turn reduces pH variations. To avoid the decrease in algae activity over time, simulations were performed to predict the effect of only decreasing the paddlewheel speed at strategic times, in order to increase the magnitude of daily pH peaks by reducing CO_2 transfer at peak algae activity, while allowing inorganic carbon concentration to recover at other times to maintain good overall algae productivity.

In addition, because pH and temperature consistently peak in the late afternoon, a semi-continuous cultivation regime under which the algal broth is only discharged after these peaks was believed to potentially improve disinfection performance. The following operation regimes were therefore simulated:

[170] A low paddlewheel speed was hypothesized to have caused a low gas transfer at the air-water interface resulting in high pH peaks observed during sunny days

1. The paddlewheel speed is lowered from 10 RPM to 5 RPM in the morning (from 5 A.M. to 12 P.M.), afternoon (from 12 P.M. to 7 P.M.), and late afternoon (from 5 P.M. to 10 P.M.),
2. The paddlewheel speed is lowered from 10 RPM to 5 RPM when sunlight intensity is above a certain threshold (250, 500, 750, or 1,000 $W.m^{-2}$),
3. The HRAP is operated in a semi-continuous mode, meaning the influent is constant but the effluent is only discharged at a set hour each day.

In the first 2 simulations, the outlet flowrate was calculated such that the water depth stayed at or below 0.25 m[171]. In the last scenario, the outlet flowrate was assumed zero outside the time when the pond is partially emptied, while the inlet flow rate is kept constant and based on the design HRT.

Only marginal improvements were predicted when testing the first two scenarios. The best results were obtained when lowering the paddlewheel speed from 12 P.M. to 7 P.M. or when sunlight intensity was above 600 $W.m^{-2}$ (increase in total *E. coli* log removal by 0.011 % and 0.014 % respectively).

Under semi-continuous operation, increased *E. coli* log removal was predicted when discharging the HRAP broth in the afternoon to the late evening (1 P.M. to 11 P.M.), as shown in Figure 7 - 4. The best results were obtained when collecting the HRAP broth at 6 P.M. the overall log removal peaking at 1.70 (8.22 % improvement). Changes in average decay coefficient over the simulations were minor in this scenario (1.80 % decrease when collecting HRAP broth at 6 P.M.) because the value of first order *E. coli* decay coefficient did not actually increase under semi-continuous operation (i.e. there is no significant change in temperature and pH in the broth in comparison to continuous operation[172]). However the pathogens were

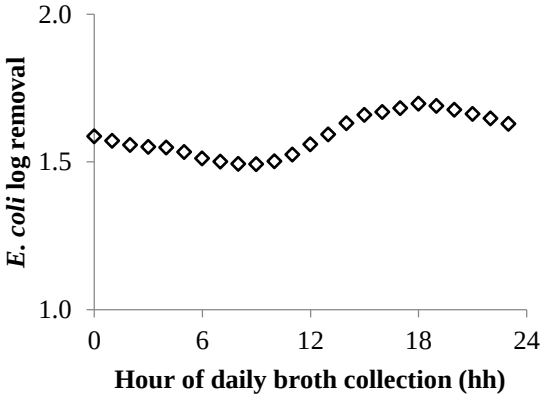

Figure 7 - 4: Variations in total *E. coli* log removal according to the time of broth collection under semi-continuous operation

[171] The simulations account for depth variations due to evaporation and rainfall and associated dilution factor of suspended solids in the broth).

[172] Confirmed by two-sample t-test comparing the distribution of pH and temperature between the base case scenario and the scenario of semi-continuous operations with HRAP broth collection daily at 6 P.M. ($p = 1.44 \cdot 10^{-90}$ for pH; $p = 2.40 \cdot 10^{-4}$ for temperature).

exposed to the most harmful conditions (e.g. high pH and temperature) for a longer period of time under semi-continuous operation, which explained the enhanced performance. Changing the time of effluent removal depending on the season would likely further improve *E. coli* removal efficiency since pH and temperature peak at different hours across the year (see Figure 3 - 8). This hypothesis was not tested in these simulations.

Implementing semi continuous operations should come at no additional cost other than the need for active operations or the implementation of some form of automation; the cost-benefits of this solution is therefore likely to be positive.

7.2.2. HRAPS IN SERIES

As demonstrated by Marais (1974) during the study of faecal bacteria decay in maturation ponds, the use of ponds in series may significantly increase *E. coli* removal. The disinfection performance of equally sized HRAPs in series (n = 1 to 3) was therefore tested at total HRTs of 2, 4, and 7.9[173] d.

The impact of this design on broth temperature and pH in each pond of the series when operated at 7.9 d total HRT and 0.25 m depth is shown in Figure 7 - 5 (n = 1), Figure 7 - 6 (n = 2), and Figure 7 - 7 (n = 3). As can be seen, HRAP broth temperature is similar in each pond of one series, regardless of the number of ponds in the series. However, the pH critically increases downstream in each new HRAP added in the series: thus, broth pHs above 11 were frequently predicted during summer in the last pond of a three-HRAP series.

[173] Base case HRT

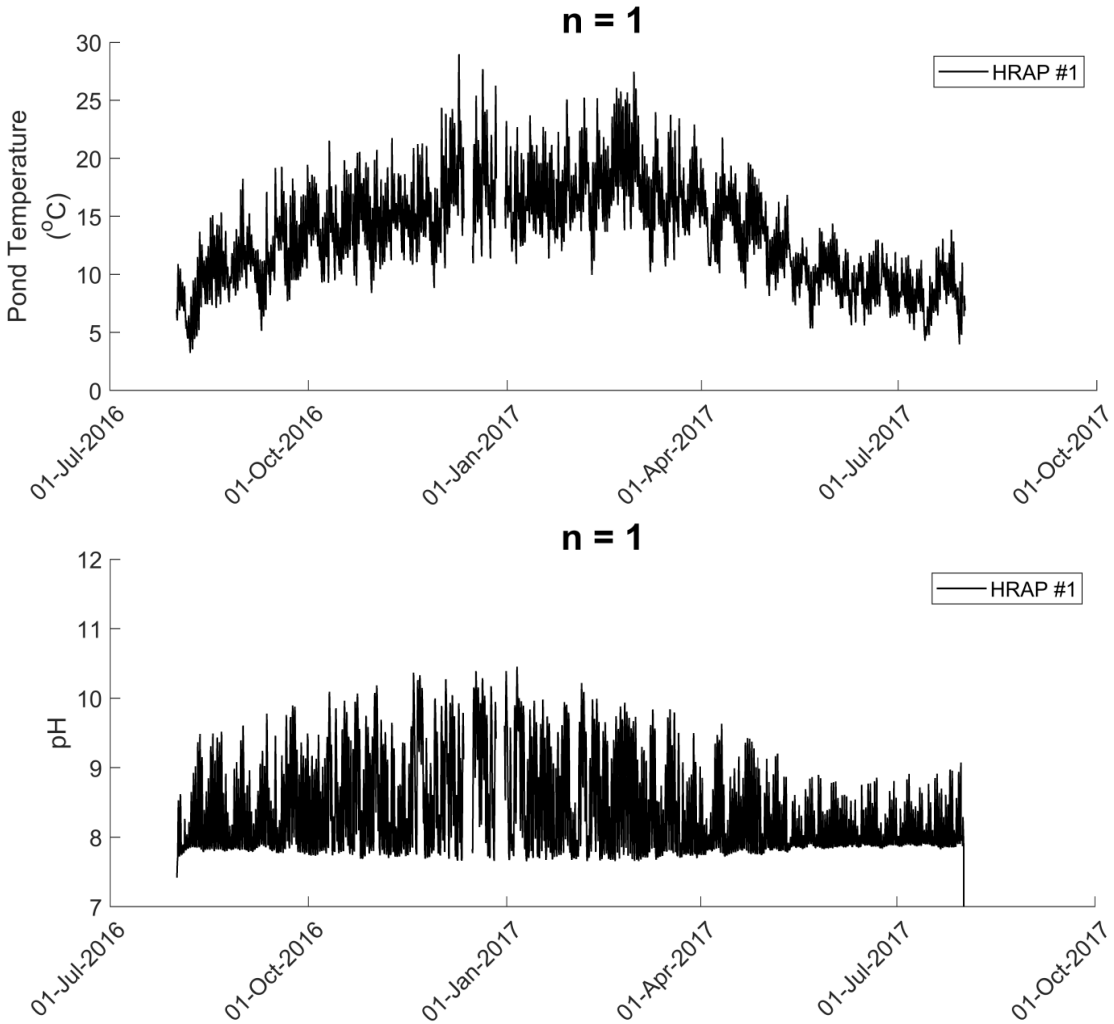

Figure 7 - 5: Predicted variations of the broth temperature and pH of one single HRAP operated at 7.9 HRT and 0.25 m depth

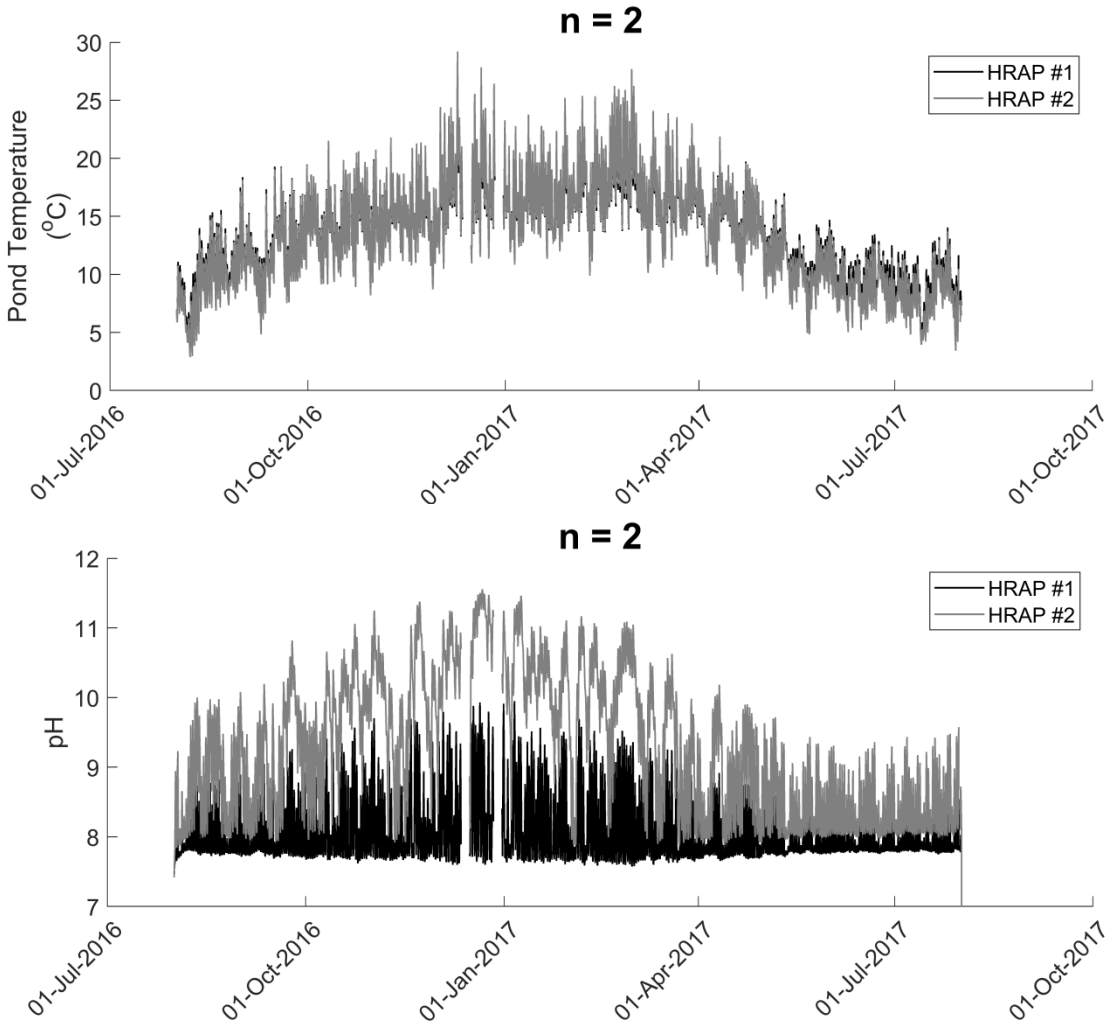

Figure 7 - 6: Predicted variations of the broth temperature and pH of a two-HRAP series operated at 7.9 d total HRT and 0.25 m depth

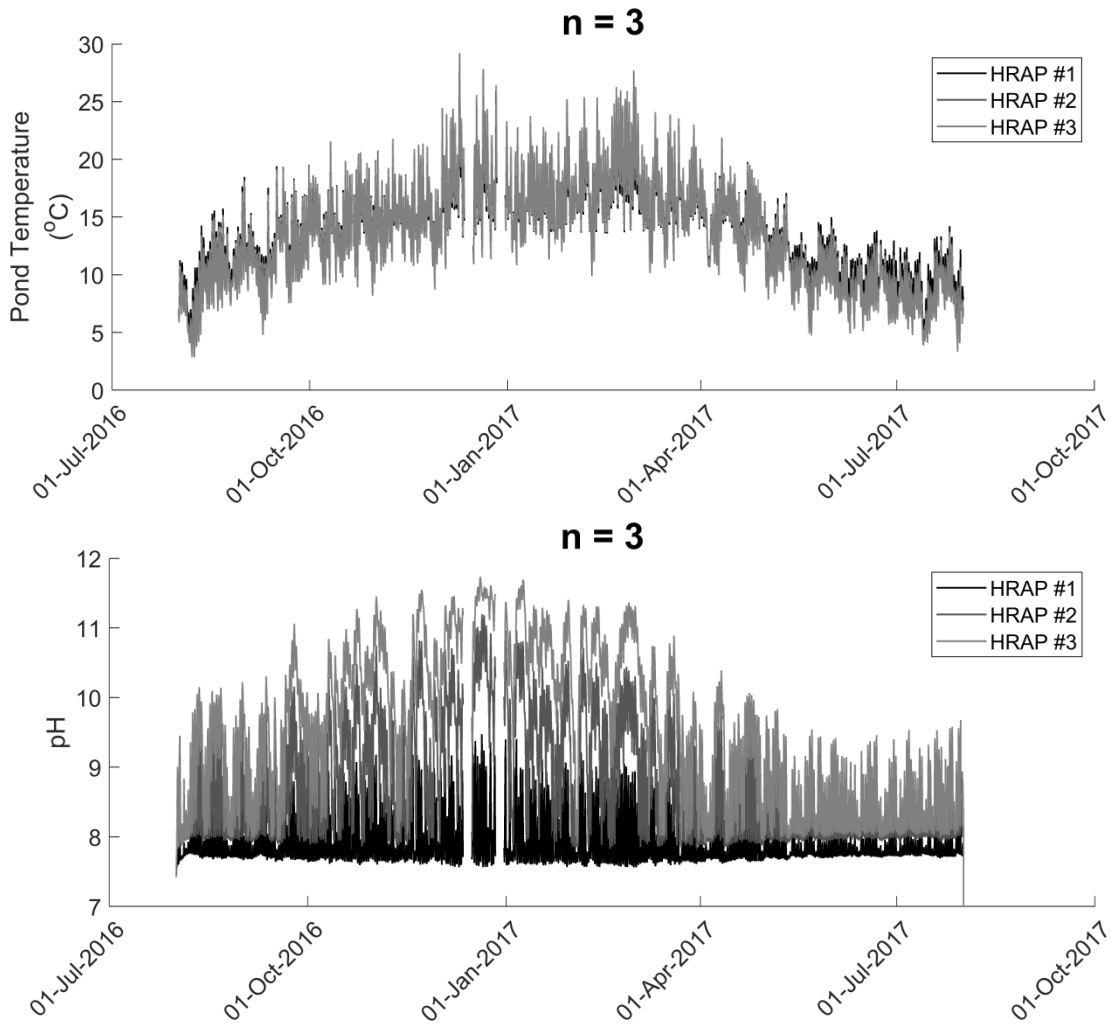

Figure 7 - 7: Predicted variations of the broth temperature and pH of a three-HRAP series operated at 7.9 d total HRT and 0.25 m depth

The resulting disinfection performances and number of days of compliance of the global systems are shown in Figure 7 - 8 and Table 7 - 2, respectively. As can be seen, HRAP disinfection performance was significantly improved by the use of ponds in series for the same total HRT (e.g. total log-removal of 3.09 for 3 ponds in series against 1.57 for one single pond at 7.9 d total HRT). Alternatively, disinfection performance can be conserved at a significantly lower total HRT when using ponds in series (e.g. total log removal of 1.70 for 3 ponds operated at 2 days of total HRT). As can be seen in Table 7 - 2, a configuration of 3 HRAPs in series at the base case HRT is predicted to deliver compliant treated wastewater year-round[174].

Significantly increased pH in downstream HRAPs as shown in Figure 7 - 5, Figure 7 - 6, and Figure 7 - 7 suggest most of the improvement of disinfection is due to an increase of pH toxicity magnitude. However, our simulations suggest that only the contribution of natural decay to overall *E. coli* decay increased in HRAP series (see Figure 7 - 9). The increase of *E. coli* decay in HRAP series is thus above all related to the suitability of this design to first order mechanisms in well mixed reactors.

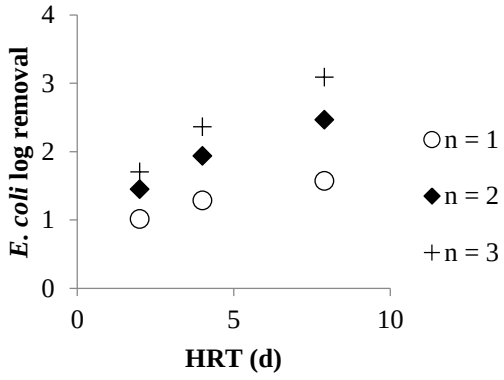

Figure 7 - 8: *E. coli* total log-removal in HRAP in series at varying total HRT (n = number of ponds in series).

Table 7 - 2: Number of days of compliance when using HRAP in series at different total HRT (n = number of ponds in series).

HRT (d)	7.9	4	2
n = 1	0	0	0
n = 2	298	152	1
n = 3	363	274	83

[174] The only 2 days of non-compliance are in winter, when compliance is unlikely necessary due to high receiving river flow (see discussion in section 7.4.).

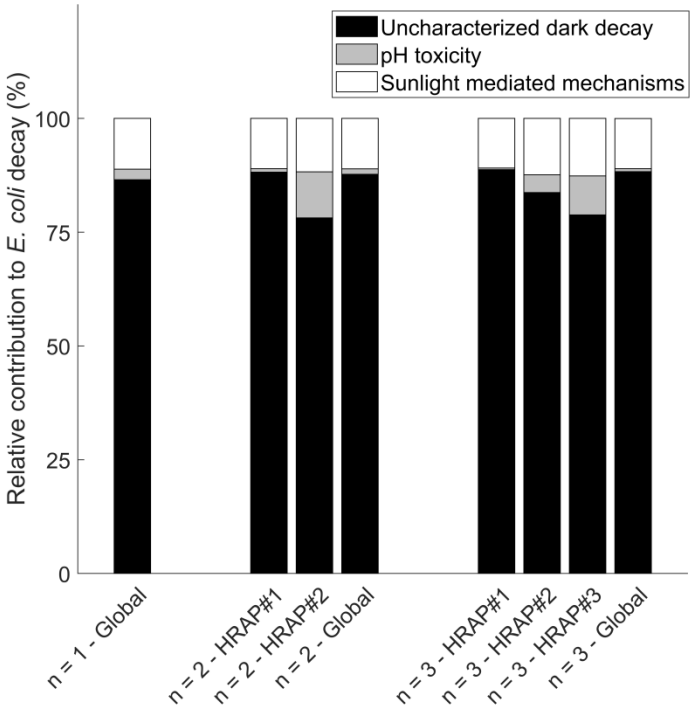

Figure 7 - 9: Predicted relative contribution of single decay mechanisms to overall *E. coli* decay in one single HRAP, a two-HRAP series, and a three HRAP series, all operated at 7.9 d total HRT and 0.25 m depth.
The relative contributions are displayed for each pond of the series and for the global system

Practically, using HRAPs in series should improve *E. coli* removal performance. Consequently, this also means treatment capacity (e.g. surface loading) can be increased without jeopardizing disinfection performance when several HRAPs are operated in series. Hence, using the base case performance as reference (i.e. yearly *E. coli* log removal of 1.57), similar performance can be obtained using significantly lower surface or treating significantly higher volumes for the same land footprint. This is illustrated in Figure 7 - 10, which shows treatment capacity as the volume of water disinfected (achieving 1.57 *E. coli* log removal) per day per square meter of HRAP.

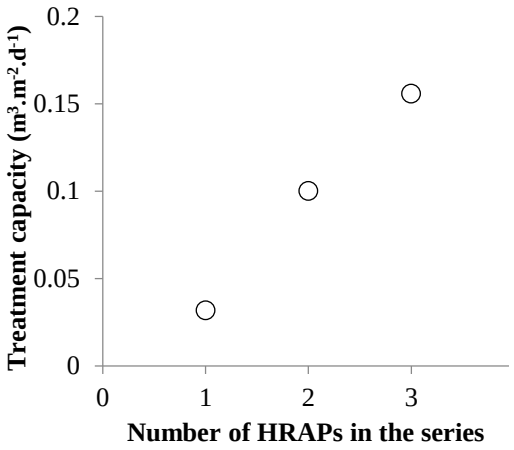

Figure 7 - 10: Treatment capacity for HRAP series (n = 1, 2, 3) corresponding to an average yearly *E. coli* log-removal of 1.57 (base case scenario performance)

While the results presented above highlight the potential of using several HRAPs in series, it is important to remember the simulations are based on assumption that algal activity is not limited by the availability of N[175] or P (i.e. algae activity is only limited by C, which drives pH increase). These simulations predicted that at 7.9 d total HRT, the second pond of a 2-HRAP series and the last two ponds of a 3-HRAP series will be both P- and N-limited during summer; and at 4 d HRT, the last pond of a 3-HRAP and 2-HRAP series will be occasionally P-limited during summer[176]. No other limitations were predicted in all other simulations. Uncertainty on N and P limitation mainly affects algae activity and with it, pH prediction (i.e. pH may not increase as much as predicted if N and/or P availability is limited). However, this would have little impact on natural decay, which is mainly affected by HRT and temperature: this provides confidence the model prediction of disinfection performance is not greatly impacted by nutrient availability.

All simulations were performed based on assumption of well-mixed broth. This assumption, which validity is discussed in Appendix 2, is critical to explain the mathematically predicted improvement of first order processes in a succession of well-mixed ponds. Because it is unclear if large ponds are indeed well-mixed, investigations on *E. coli* removal in HRAPs series at larger scale are critically needed. In that regard, Jupsin et al. (2003) suggested that HRAPs behave as plug-flow reactors with high recirculation rates and Shilton and Sweeney (2005) stated that plug-flow operation is the most effective to first-order kinetics

[175] N availability in terms of NH_3/NH_4^+ supply

[176] P-limitation was predicted only five and four days for the 3-HRAPs and 2 HRAPs series simulations, respectively. NH_4^+ was never predicted below 0.1 mg N- NH_4^+

mechanisms (for being an extreme case of infinite well-mixed reactors in series). Consequently, the disinfection performance of HRAPs may actually increase with scale[177].

7.3. INFLUENCE OF CLIMATE

Meteorological data from New Zealand locations representative of different climates were used to investigate how HRAP design must be adapted to cope with different climatic conditions. The locations were selected based on NIWA identification of different climate zones of New Zealand[178]. Meteorological data and climate characteristics were obtained from New Zealand's National Climate database[179] (Table 7 - 3). Simulations were conducted for each location using the base case scenario i.e. a single pond at the base case value for HRT and depth under continuous operation.

Table 7 - 3: Climate type, location, and main characteristics assesssed in simulations

Climate	Location	NIWA agent Number	Total sunlight energy ($GJ.m^{-2}$)	Total rainfall (mm)	Average dry bulb temperature (°C)
Sub-tropical	Whangarei	40980	5.54	1,330	15.2
Oceanic (high sunshine)	Napier	15876	5.08	837	13.0
Oceanic (low sunshine)	Palmerston North	21963	4.62	1,110	12.7
Semi-arid	Alexandra	39654	4.86	354	9.66
Alpine	Mount Cook	18125	4.85	3,430	7.97

As can be seen in Table 7 - 4 and Figure 7 - 11, *E. coli* decay was predicted to steadily decrease when changing from hot to cold climate. Highest disinfection performances were thus predicted under sub-tropical climate, most likely due to the year-round favourable conditions leading to mild broth temperature in the HRAP.

While higher average broth temperatures were predicted under the high sunshine oceanic climate than the low sunshine oceanic climate, *E. coli* removal performance was predicted to be similar under both climates. Similar conditions in winter were predicted to cause similar collapses in disinfection performances[180], thus evening out the higher disinfection performance predicted over summer under high sunshine oceanic climate[181]. Under semi-arid climate, the very dry and mostly sunny conditions (semi-arid climate) were associated

[177] Provided the prevention of non-ideal flow (e.g. short circuiting, dead zones)
[178] https://www.niwa.co.nz/education-and-training/schools/resources/climate/overview
[179] https://cliflo.niwa.co.nz/; weather stations identified by their agent number.
[180] Predicted average natural decay coefficient of 3.01 d^{-1} over the winter under both climates; average of the data computed for 08/2016 and 06-07/2017.
[181] Average decay coefficients during summer of 11.05 d^{-1} under high sunshine oceanic climate against 9.94 d^{-1} under low sunshine oceanic climate

with poorer disinfection performances than the more northern locations due to the significantly colder weather. Simulations expectedly predicted the poorest disinfection performances under alpine climate, again mostly due to the low temperatures experienced.

Table 7 - 4: HRAP disinfection related performances and broth characteristics computed for each location tested in simulations

Climate	Broth temperature	Broth pH	Average *E. coli* decay coefficient (d^{-1})	*E. coli* log removal (-)
Sub-tropical	17.13	8.41	9.72	1.75
Oceanic (high sunshine)	13.93	8.40	6.85	1.58
Oceanic (low sunshine)	13.47	8.37	6.13	1.57
Semi-arid	11.80	8.39	5.77	1.44
Alpine	9.80	8.59	4.70	1.36

Results show that warmer climates are best suited to the implementation of HRAPs for disinfection. However, disinfection performance even under alpine climate remains comparable or higher to the general performances of maturation ponds (see discussion in section 3.3.1). Still, *E. coli* removal efficiencies were not sufficient to provide compliant effluents in terms of microbial quality[182] at any of the location tested, combining the best design and operations for wastewater disinfection as previously identified may improve *E. coli* disinfection performances. This is described in next section.

[182] As defined in Chapter 3 section 3.4.

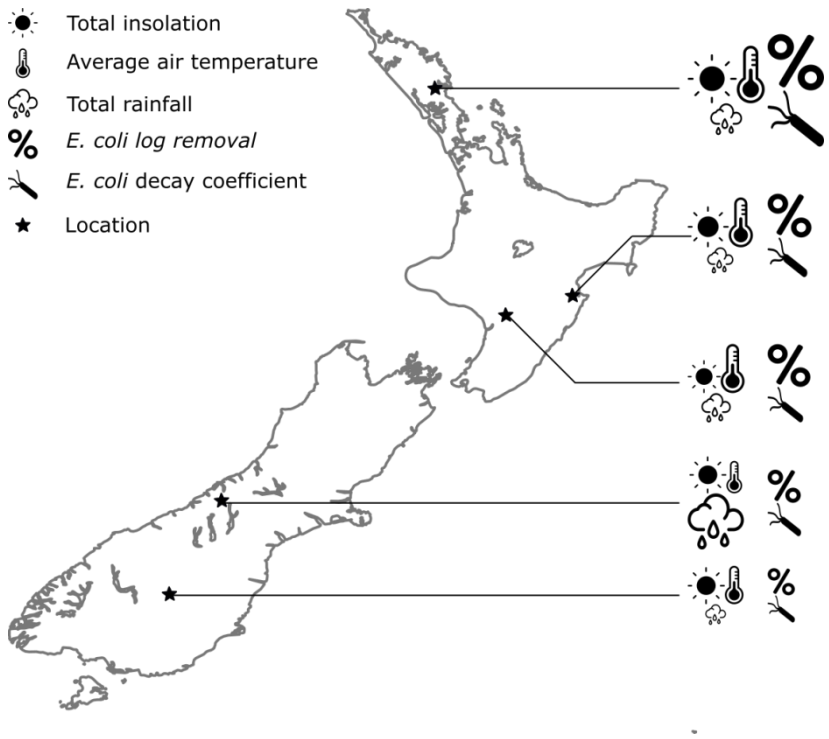

Figure 7 - 11: Simulated HRAP disinfection performances at different locations: the size of the symbols is proportional to the associated value (HRAPs are operated at 7d HRT and 0.25 m depth)

Critically, the results presented here are derived from simulations using a model validated under oceanic (low sunshine) climate. Experimental validation is therefore needed.

7.4. OPTIMIZATION OF WASTEWATER DISINFECTION IN HRAP

We showed in the previous sections that warmer climates were associated with significantly better disinfection performances than colder climates and that lower depth, longer HRT, semi-continuous operations and, above all, the use of HRAP in series should allow significant improvement of HRAP disinfection performances.

The following investigation was therefore aimed at designing HRAP meeting a 'real-life' bacterial quality guidelines for wastewater discharge in the environment. For this purpose, a target *E. coli* cell count of $3.0 \cdot 10^4$ MPN.100 mL^{-1} was used based on Palmerston North wastewater treatment plant discharge into the Manawatu river (see discussion in section 3.4.).

Results from simulations conducted for series (n = 1, 2, or 3) of HRAPs located in Palmerston North and operated at 3, 5, or 7.9 d total HRT under either continuous or semi continuous operation[183] are summarized in Figure 7 - 12.

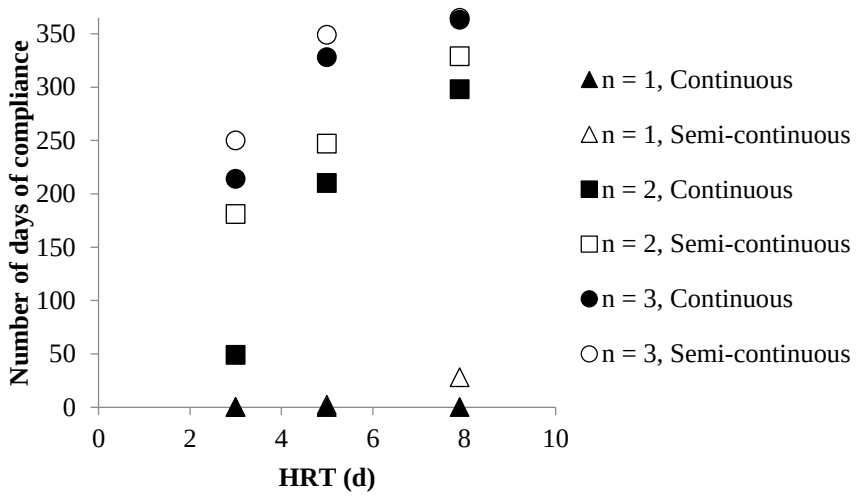

Figure 7 - 12: Number of days of complying effluent for HRAPs in series at varying total HRT and operation modes (n = number of ponds in series).

As discussed in Chapter 3 section 3.4. (footnote [47]), the Manawatu river flow rate in Palmerston North is below 37 $m^3.s^{-1}$ (the limit below which compliance for microbial quality of the effluent should be met in Palmerston North) during 62 days per year. Assuming a safety factor of 2, the objective of designing a HRAP meeting compliance for 125 days during a year was set. We predicted that 3 HRAPs in series operated at 3 days total HRT[184] (Figure 7 - 13) or 2 HRAP in series operated at 4 days total HRT (Figure 7 - 14) satisfy this criteria under continuous operation.

[183] By withdrawing a set volume of algal broth from the last HRAP of the series; the volume withdrawn is calculated to respect the design HRTs and is treated as the final effluent

[184] The minimal HRT for one pond should not be below 1d (see Chapter 1, Table 1 - 3).

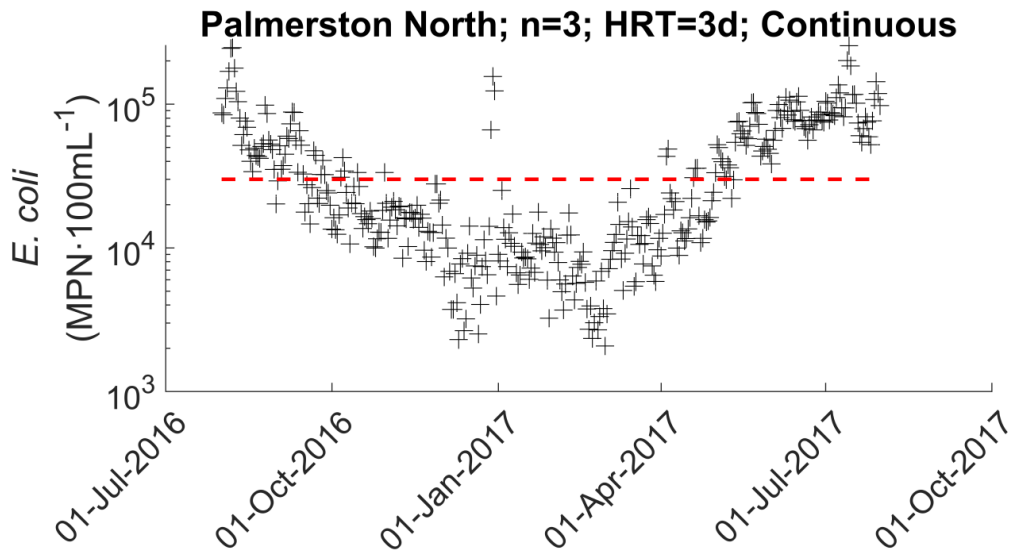

Figure 7 - 13: Predicted daily average *E. coli* cell count in the effluent of a 3-HRAP series operated at 3d HRT and 0.25m depth. The red-dash-line shows the compliance limit for bacterial quality guidelines in Palmerston North.

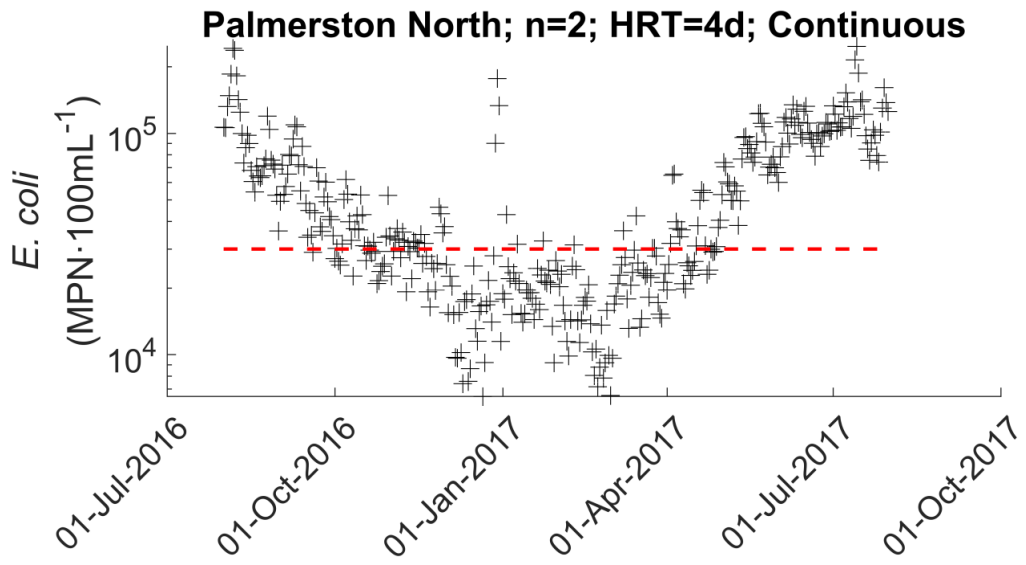

Figure 7 - 14: Predicted daily average *E. coli* cell count in the effluent of a 2-HRAP series operated at 4d HRT and 0.25m depth. The red-dash-line shows the compliance limit for bacterial quality guidelines in Palmerston North.

Simulations conducted under climatic conditions experienced in Palmerston North suggest that HRAP can provide compliant wastewater disinfection. Under cold climates, disinfection performance can be maintained by adding HRAPs in series, increasing the total HRT, lowering the pond depth, and using non-continuous operations: hence a 3-HRAP series operated under alpine climate at 7.9 d HRT was predicted to supply effluent with *E. coli* cell counts below $3.0.10^4$ MPN.mL^{-1} for 297 days of the 1 year simulation.

This study therefore indicates that HRAP is a realistic alternative for wastewater disinfection, providing year round acceptable effluent bacterial quality with best performances reached when it is the most needed (i.e. during summer). While this solution is somewhat land intensive, the area required to comply with guidelines can be reduced drastically by the use of HRAPs in series, and further reduced by semi-continuous operation.

Conclusion

The High Rate Algal Pond (HRAP) technology was developed in the 1960s to enable algae production and recovery during wastewater treatment. In the following decades, numerous studies confirmed the good performance of HRAPs for wastewater secondary treatment. While research on HRAPs has intensified in recent years due to the growing interest in algal biomass production for biofuel feedstock, the potential for wastewater disinfection in HRAPs has remained poorly studied. This is surprising because pathogens can be exposed to similar environmental conditions in HRAPs and maturation ponds, the latter being a well-established algae-based technology of wastewater disinfection. We therefore hypothesized that HRAPs provide efficient wastewater disinfection and that knowledge of the mechanisms involved may help to improve process design and operation. Under this hypothesis, this study aimed at identifying and quantifying the mechanisms of pathogen decay in algal broth and their relationships to algal broth characteristics.

Research strategy

Based on the literature, sunlight mediated mechanisms were suspected to drive pathogen decay in HRAPs, although it was not clear if these mechanisms were mostly driven by direct UV-B damage or by indirect photo-oxidation mechanisms (caused by endogenous or exogenous photosensitizers). Little research had quantitatively investigated pathogen decay in the dark despite various mechanisms being cited as being potentially significant: these mechanisms include natural decay (defined as any observed decay in the absence of known harmful conditions), starvation, predation, chemical toxicity (e.g. pH, NH_3), toxicity from algal metabolites, settling, and heat inactivation.

Experimental data was needed to determine the significance of the pathogen decay mechanisms listed above under conditions relevant to HRAP operation. This was addressed using the following 4-steps strategy:

1. Two pilot-scale HRAPs (approx. 1 m^3) were commissioned and monitored in order to i) evaluate HRAP long-term disinfection performance, and ii) identify *in situ* quantitatively significant disinfection mechanisms.
2. Laboratory scale (< 1 L) experiments were performed under specific conditions enabling the ‘isolation’ of a particular disinfection mechanism and, if needed, systematic quantification of the associated disinfection rate under specific environmental conditions (e.g. temperature, light intensity).

3. Bench scale experiments (1 – 5L) were performed in real HRAP broth to validate laboratory scale findings under conditions more representative of HRAP, but still allowing some level of control to isolate certain mechanisms and reduce environmental variability.
4. A model predicting pathogen decay in HRAPs was developed from laboratory- and bench-scale findings, and coupled with an environmental model predicting HRAP broth conditions. The models were validated against pilot-scale data and the combined model was used to explore how process design and operation can be manipulated to improve wastewater disinfection performance using HRAP.

Due to practical limitations, our experimental study was limited to the investigation of *Escherichia coli* (*E. coli*) removal. This microorganism is widely used as a pathogen decay indicator during full-scale wastewater treatment. A wild type *E. coli* strain was isolated from the local wastewater plant for laboratory and bench scale experiments.

Main experimental results

Pilot scale: The two-year-long monitoring of the outdoor pilot scale HRAPs fed real primary settled wastewater confirmed satisfactory disinfection in HRAPs (mean *E. coli* log-removal of 1.77 ± 0.538, N = 128). The best and most consistent *E. coli* removal rates were achieved during warmer conditions, which is intrinsically beneficial as a higher disinfection performance is generally required during the warmer months of the year due to low flows and higher recreational use of the receiving water. Probably due to the high variability of environmental and operational conditions experienced, no mechanism significantly driving *E. coli* decay could be identified during pilot-scale study. Nonetheless, NH_3 toxicity, and starvation/competition for nutrients were concluded to be unlikely mechanisms for *E. coli* decay in HRAPs treating domestic wastewater. An invasion of grazers in one of the HRAP evidenced that predation may occasionally contribute to overall *E. coli* removal, but this mechanism could not be investigated due to practical challenges[185].

Laboratory scale: In the dark, *E. coli* cell count was not impacted by natural decay (including starvation), heat inactivation, wastewater toxicity, algal toxicity, and NH_3 toxicity. On the contrary, *E. coli* cell count decreased significantly when incubated at high pH, and the toxicity associated with high pH increased exponentially with temperature. In

[185] Since predation would likely only have a sporadic impact on HRAP wastewater disinfection performance, its investigation was also not considered critical

distilled water exposed to natural sunlight, *E. coli* decay coefficient increased linearly with increasing sunlight intensity. Direct photo-damage (the sum of direct DNA damage and endogenous photo-oxidation) caused significant *E. coli* death under the conditions tested. The harmful effect of natural sunlight was significantly mitigated when *E. coli* cells were suspended in filtrates from HRAP broth. This finding suggested that dissolved materials present in HRAP filtrates are more prone to block sunlight radiation than support exogenous photo-oxidation. It was therefore concluded that exogenous photo-oxidation is unlikely to be significant in HRAPs.

Bench scale: In bench-scale assays conducted in HRAP broth, sunlight intensity had little direct impact on *E. coli* removal likely due to high light attenuation in the opaque medium. Likewise, DO concentration did not affect *E. coli* survival. The significant influence of pH on *E. coli* decay evidenced during laboratory experiments was confirmed, albeit to a lesser magnitude probably due to *E. coli* shielding by biomass flocs. Bench scale assays finally evidenced a high temperature-dependent 'uncharacterized' decay in the dark. This uncharacterized dark decay was responsible for most of *E. coli* disinfection in HRAP broth. No underlying mechanism could be formally identified, although toxicity from algal metabolites was suspected to significantly contribute to the decay observed.

Mathematical modelling and predictions

A model predicting *E. coli* decay in HRAP broth was developed based on the mechanisms identified during laboratory and bench scale experiments. *E. coli* cell count variations over 24h in the pilot scale HRAPs could be predicted within one order of magnitude of the measured counts for 6 days distributed across 3 seasons (average absolute error of 0.22 log-unit, N = 64). Diurnal variations of *E. coli* cell counts were also successfully predicted, although the highest decay coefficients recorded in summer in late-afternoon were significantly underestimated. Model based reproduction of pilot scale HRAPs daily profiles confirmed *E. coli* decay is predominantly driven by uncharacterized dark mechanisms. High pH-toxicity may at times account for 50% of the overall *E. coli* decay (e.g. in the late afternoon on the warmest summer days). The decay coefficient associated with sunlight mediated mechanisms may at best account for 20% of the overall *E. coli* decay during cold season mornings (the impact of sunlight mediated mechanisms was predicted to be negligible during summer).

An additional mathematical model was developed to predict the environmental conditions occurring in HRAPs (i.e. pH, temperature, sunlight distribution, and DO concentration) based on HRAP design and weather conditions. Temperature and pH predictions were validated against pilot-scale HRAP data. The HRAP broth temperature and pH could thus be predicted over a full year (07/2016 – 07/2017) with an average absolute error of 1.35°C (N = 25,906) and 0.501 pH-units (N = 23,817), respectively. Because daily variations in pH (and DO concentration) were accurately predicted over periods of several days to weeks, the model was concluded to accurately describe the mechanisms influencing pH and temperature. This model was subsequently combined with the disinfection model to investigate how HRAP design, operations, wastewater quality, and climate impact HRAP disinfection performance.

The use of several HRAPs in series was predicted to considerably improve *E. coli* removal: a 3-HRAP series was thus predicted to provide effluent compliant for microbial quality year round in Palmerston North (0.25 m depth and 7.9 d total HRT). Decreasing water depth, increasing HRT, or operating HRAP semi-continuously (by discharging the effluent once a day at 6 P.M.) were predicted to further increase disinfection performance. Combining HRAP-series with the best design and operation strategies was predicted to deliver complying effluent quality under any New Zealand climate.

Novelty and significance

The monitoring of pilot-scale HRAPs confirmed that HRAP technology achieves significant wastewater disinfection. Such long term monitoring of HRAP disinfection performance in real conditions had never been published when this study was started, although recent long term studies of wastewater disinfection in full-scale HRAP now concurs with these results (Fallowfield et al., 2018; Young et al., 2016).

The potential significance of pH toxicity in the dark appears to have been overlooked since Parhad & Rao (1974) first evidenced this mechanism. This thesis therefore provides the first quantitative relationship between wild-type *E. coli* decay coefficient and pH (in the 7 – 10 range, with limited confidence at 10 – 11) at different temperature (5 – 35 °C). This result is particularly significant since pH toxicity was identified as one of the main mechanisms for *E. coli* decay under conditions frequently experienced in the pilot scale HRAPs monitored.

Sunlight mediated disinfection has limited significance in HRAPs due to high light attenuation in the HRAP broth. This finding is of critical significance since most of the research on wastewater disinfection during algae-based treatment has hitherto focused on sunlight-mediated mechanisms, widely recognised as the main drivers of disinfection in maturation ponds. Instead, most of *E. coli* removal in HRAP broth was caused by "uncharacterized dark decay", defined as an ensemble of unidentified dark mechanisms. This has never been proposed before.

The model of *E. coli* decay coefficient developed during this study could better predict *E. coli* cell count in HRAPs than any existing models of coliforms decay in algae ponds. This model was used to generate new optimization strategies. In particular, the use of HRAPs in series was predicted to provide very efficient removal under a broad range of climatic condition, especially when combined with semi-continuous operation.

Limitations of the study and recommended actions

The universality of *E. coli* (gram-negative bacteria) as microbial indicator has been challenged (World Health Organization, 2011). For example, gram-negative bacteria have been reported to be more susceptible to mechanical and chemical stress (in particular alkaline stress) than gram-positive bacteria due to differences in cell wall structure (Wada et al., 2012). Future studies should therefore investigate indicators with different biology (e.g. gram-positive or spore-forming model indicator organisms, helminths).

Bench scale experiments were performed in spring (November 2017). The results from these experiments may therefore be of limited relevance to other climatic conditions. Bench scale assays, and therefore disinfection model calibration, should ideally be repeated at different times of the year and/or under different climate/locations.

The environmental model was developed under the assumption that the HRAP broth is well-mixed and the model was validated against data from a well-mixed pilot system. The 'well-mixed assumption' is unlikely to remain valid at full-scale and the conclusions reached must

be considered with caution: full-scale disinfection efficiency could be either lower (hydraulic short circuits) or higher (plug-flow like regime) than predicted in Chapter 7.

Finally the disinfection model developed in this study failed to explain the highest *E. coli* decay recorded at bench and pilot scale. Because these 'extreme' decay events were unlikely to be caused by pH toxicity or sunlight mediated disinfection, the conclusions from model analysis remain valid. However, investigations (and independent validation) are still needed to understand the underlying mechanisms of dark decay and improve predictions of *E. coli* decay in algal broth.

Future prospects

As discussed in previous sub-section, the results found during our study focusing on *E. coli* are unlikely to all be valid for other pathogen decay indicators. Although there exists some data on other indicator decay in HRAP in the literature (see Table 1 - 5), the study of decay mechanisms during wastewater treatment in HRAPs for other indicators is still needed to fully understand and quantify the potential of HRAP for disinfection.

While our study provides further evidence that HRAPs can be designed for domestic wastewater disinfection, more data is still needed to establish such knowledge. In particular, existing research has been carried out on set-ups under Mediterranean climate, temperate arid climate, tropical climate, and temperate oceanic climate (our study). Data on the disinfection performance of HRAPs under many sets of conditions is therefore still lacking.

Most notably, this study showed that the majority of *E. coli* removal in HRAPs was caused by uncharacterized dark mechanisms and/or synergies. Because dark mechanisms are traditionally poorly investigated compared with sunlight mediated mechanisms, an in-depth investigation of these dark mechanisms is urgently needed. This would improve the understanding of *E. coli* decay in HRAPs, and possibly provide explanations for certain high *E. coli* mortality events observed in pilot scale HRAPs and in bench scale reactors. This knowledge could then help significantly enhance *E. coli* removal in HRAP by implementing strategies favouring their occurrence.

Experimentally validating the findings from the optimization investigations carried out in Chapter 7 would be of great value to improve the design and operations of HRAPs. The strategies identified to improve the environmental model should be investigated. In particular:

1- Can a dynamic prediction of radiative heat losses (e.g. as function of cloud cover, relative humidity) improve temperature prediction?
2- Can the prediction and/or more accurate inputs of key parameters (e.g. COD concentration in the wastewater, nitrate concentration in the HRAP) improve pH prediction?
3- Can the dynamic prediction of algae photosynthetic efficiency improve pH prediction?
4- Can the model be directly applied under any climate?

Understanding the mechanisms involved in *Escherichia coli* decay during wastewater treatment in high rate algal ponds

APPENDICES

A thesis presented in partial fulfilment of the requirements for the degree of

Doctor of Philosophy

in Environmental Engineering

At Massey University, Palmerston North, New Zealand

Paul Chambonnière

2019

APPENDIX 1. VARIETY OF FAECAL INDICATOR AND LIMITATIONS ASSOCIATED TO THEIR USE

The most common indicator for faecal contamination is the group of coliforms, as reflected by their frequent use in the literature (see section 1.1.3.). However, the coliform group has shown limitations in the detection of faecal contamination. Outbreaks of cryptosporidiosis have been observed in the absence of coliforms in samples tested (Ashbolt et al., 2001) and Nelson et al. (2004) found faecal coliforms survival in sludge to be of several months while they found it to be of several years for some viruses meaning coliforms do not meet criteria 3 and 4 for an ideal indicator as given in Table 1 – 2.

Escherichia coli (*E. coli*), a member of the coliform group and the indicator preconized by New Zealand Ministry for the Environment to monitor microbiological quality of recreational waters (Ministry for the Environment, 2003), was found able to grow outside a host when conditions are favourable to it, notably in tropical water (Ashbolt et al., 2001) thus limiting its validity as a faecal contamination indicator (failing criterion 5 of Table 1 – 2). *Vibrio cholerae* was reported to have better persistence in stabilization ponds in warmer months while the opposite was found for *E. coli* (Maynard et al., 1999), again indicating *E. coli* is not a universal indicator (failing criterion 4 of Table 1 – 2).

Gram-positive bacteria such as faecal streptococci and enterococci are also widely used as they are present in high numbers in the excreta of humans being thus generally present in wastewater and polluted water (Ashbolt et al., 2001). Faecal enterococci are generally preferred over faecal streptococci (Ashbolt et al., 2001). Enterococci were however given up as the preferred indicator when testing microbial quality of recreational waters in New Zealand in 2003[186] due to their ability to multiply in natural water leading to important concentrations found in samples without any threat of faecal contamination. They are also thought to be mostly of animal origin in natural waters and thus not necessarily linked to human health risk (Ministry for the Environment, 2003).

Some anaerobes bacteria are sometimes used, principally *Clostridia perfringens*. The use of this bacteria is debated as it is thought to have a too high persistence in the environment compared with enteric pathogens (Ashbolt et al., 2001). Other anaerobes of interest include bifidobacteria which are known to be related to human faeces but are very sensitive to

[186] Status it had in the 1993 guidelines

environmental conditions (Ashbolt et al., 2001). *C. perfringens* has been mentioned as a suitable indicator for parasitic protozoa as it has, similarly to these organisms, a higher resistance to disinfection and it does not reproduce in aquatic sediment (Ashbolt et al., 2001).

Presence of bacteriophages have been correlated to faecal contamination in water and are mostly used as good models of viruses fate in water (Ashbolt et al., 2001). Coliphages, phages to the coliform group, are the preferred indicators of this group, mainly F-RNA and F-DNA phages (Ashbolt et al., 2001). However, data on phages presence in water are not consistent and the techniques for recovery of phages and subsequent enumeration are disputable (Ashbolt et al., 2001). In addition, non-alarming levels of phages in presence of viruses were reported in the past, since viruses are produced punctually by infected individuals while phages are constantly produced by all humans.

Other proposed challenge organisms for viral contamination are poliovirus and rotavirus. Poliovirus is known as a good and resistant indicator although it is weak against chlorine in which case Rotavirus is suggested as a complementary test (U.S. Environmental Protection Agency, 1987).

Protozoa removal can be tested through the counting of giardia cysts (U.S. Environmental Protection Agency, 1987) although only *E. coli* is suggested by New Zealand guidelines for wastewater monitoring (NZ Water Environment Research Foundation, 2002).

Other indicators of faecal contamination than micro-organisms can be used such as faecal sterol biomarkers. Coprostanol has been proposed as a marker of human faecal pollution. It rarely used in wastewater treatment technology as it is not directly associated to a health threat (Ashbolt et al., 2001).

As suggested by World Health Organization, (2011) and as the present paragraph suggests, the indicator should be chosen depending on the disinfection treatment used, since some treatments have been shown to remove more efficiently indicators commonly used than the actual pathogens. Hence, chlorination is known to be more efficient at coliforms removal than other common pathogens (NZ Water Environment Research Foundation, 2002). The U.S.EPA indicates that F2 coliphage is one of the most resistant species to chlorine but one of the most sensible to ozone treatment (U.S. Environmental Protection Agency, 1987).

Despite this wide panel of possible indicators for faecal contamination in wastewater, coliforms in general and *E. coli* in particular are the most commonly used and preconized indicators. Results given by this bacterial group have proven to be valuable, and our study therefore focused on *E. coli* removal in order to limit our scope.

APPENDIX 2. MIXING CONDITIONS HYPOTHESIS IN PILOT SCALE HRAPS AND IMPLICATIONS ON FINDINGS

In our study, results from the monitoring of the pilot scale HRAPs were analysed under the assumption that the ponds were well-mixed. The HRAP environmental model developed under well-mixed assumption in Chapter 6 was validated using data from pilot scale HRAP, therefore, the same assumption was also used during simulations assessing HRAP disinfection performance in varying conditions (Chapter 7). Because the well-mixed assumption was not verified during our study, its validity and implications is discussed in this Appendix.

VALIDITY OF THE WELL-MIXED ASSUMPTION FOR PILOT SCALE HRAPS

Due to the shape of the paddlewheel, the totality of the upper layer of the algal broth was recirculated to the bottom layer before the entire water cross section was turbulently pushed forward into the HRAP channel[187] (to quickly reach a laminar flow). It can therefore be assumed that the algal broth was fully-mixed directly downstream from the paddlewheel. Based on mean broth linear speed around the channel (22.2 $cm.s^{-1}$, see Chapter 3) and the HRAP channel length (approx. 2.5 m), a hypothetical water cross section moving through the channel would spend approx. 23 s between undergoing consecutive mixing. The complete mix hypothesis would not be valid if the timescale of the mechanisms governing variations of algal broth characteristics were significantly lower than 23 s (e.g. 100 fold i.e. 0.23 s). The timescales of mechanisms having most significant influence on *E. coli* decay according to our study are shown in Table S2 - 1. As can be seen, the time needed for a water column to circulate around the pilot scale HRAPs is shorter than the timescales of all listed mechanisms by several orders of magnitude. In addition, because chemical reactions involved in the conditions influencing *E. coli* decay are primarily governed by biological mechanisms (i.e. algae and heterotrophic growth) and physical parameters (temperature) which timescale are all over 100-fold higher than HRAPs mixing time-scale, it can be assumed concentrations in chemical species of interest in this study will no vary significantly across the pilot scale HRAP channel. Therefore, assuming pilot-scale HRAPs are well-mixed was concluded to be accurate under the conditions (scale) studied.

[187] Visual observation

Table S2 - 1: Timescale of the mechanisms governing physico-chemical conditions in pilot scale HRAPs

Mechanism	Timescale(s)	Source
Complete mix assumption limit	23	Experimental
Chemical reactions	0 – 86	Rate of reaction (Solimeno et al., 2017)
Algal growth	$8.6 \cdot 10^4$	Model[1]
Heterotrophic growth	$1.5 \cdot 10^4$	Specific growth rate (Metcalf and Eddy Inc., 2003)
Gas transfer at the air water interface	$8.4 \cdot 10^3$	Gas transfer rate experimentally determined
E. coli decay	$8.3 \cdot 10^3$	Median decay rate experimentally determined
Temperature variations	$7.6 \cdot 10^3$	Experimental[2]

[1] Computed as $\frac{HV \cdot V}{PE \cdot E} \cdot X^a$ (see Appendix 20) assuming $X^a = 0.15\ kg.m^{-3}$ and incident sunlight intensity is $1{,}000\ W.m^{-2}$

[2] Value shown is the average rate of 1°C change of HRAP broth observed during HRAP A monitoring (N = 1,039,081). The corresponding 1-percentile is $1.5 \cdot 10^3$ s.

In addition to the theoretical evidence exposed above, several experimental elements further evidence the validity of the well-mixed assumption:

1) Dr. Plouviez, who studied nitrous oxide (N_2O) emissions by algae cultures using HRAP A of the present study (Plouviez, 2017), demonstrated that nitrous oxide dissolved concentration did no vary significantly at different sampling location and depth.
2) When measuring the gas transfer coefficient at the air-water interface during this study (Appendix 9), dissolved oxygen was measured in opposite points of the pond. In the re-aeration phase, no discrepancies in dissolved oxygen concentration were observed (Figure S9 - 2) indicating gas transfer at the air water interface and diffusion in the broth are unlikely to limit our assumption.

Consequence on the choice of the sampling point: as shown in Figure 2 - 1, the sampling point used on pilot scale HRAP during our study were situated directly downstream of the paddlewheel. Our rationale was that the broth was always well mixed at that. Based on the theoretical and experimental consideration discussed above, the sampling point choice is not expected to influence results of our study. Nevertheless, we advise investigators to use sampling point situated closer to the outlet as it should provide samples that are the most representative to assess HRAP treatment.

VALIDITY OF WELL MIXED ASSUMPTION AT LARGER SCALE

Physico-chemical conditions in the HRAP: if we assume a 200 m channel length, the timescale limiting the well-mixed assumption would become 29 min ($2.0 \cdot 10^{-2}$ d). This timescale is in the same order of magnitude as gas transfer at the air water interface, *E. coli* decay, and temperature variations, and is significantly higher than the time scale of all

chemical reactions. Because chemical reactions of interest in our study are primarily influenced by biological reactions (10 – 100-fold higher timescale than mixing conditions) and to a lesser extent by temperature variations (same timescale as mixing conditions), it can be assumed that broth chemical characteristics would vary with the timescale of temperature[188] for low magnitude variations, and the timescale of biological reactions for significant variations. Therefore, in such full scale set-up, temperature and broth chemical characteristics are likely to vary through the length of the HRAP channel (albeit only at low magnitude for broth chemical characteristics). Since temperature has a critical impact on *E. coli* decay rate in HRAP, assessing the impact of channel length on *E. coli* removal performance is needed and results presented in Chapter 7 should be considered with caution. We suggest for later work that the environmental model should be adapted to plug-flow mixing conditions with high recirculation rate (Jupsin et al., 2003) and validated against data from full scale HRAP.

***E. coli* decay in full scale HRAP:** in a 200m long full-scale HRAP, the timescale of *E. coli* decay would become comparable with the timescale of mixing conditions meaning that the observed *E. coli* decay should be best represented by a plug-flow model with high circulation rate (Jupsin et al., 2003). The model developed in Chapter 6 and Chapter 7 should can be adapted (and validated) for these conditions to increase the reach of the conclusions drawn from our study. Consequently, results presented in Chapter 7 based on the model validated under well-mixed assumption are likely to be underestimating *E. coli* compared with full scale HRAP[189] since, as stated by Shilton and Sweeney (2005), plug-flow operation is the most effective to first order kinetics processes (therefore *E. coli* decay). Thus, results presented in Chapter 7 can be considered as conservative estimates of full-scale HRAP performance.

[188] Temperature variations within the algal broth could be expected due to incident sunlight radiation heating the algal broth from above, and natural thermal stratification enabled by the lack of mixing or turbulences through the channel.

[189] If the impact of mixing conditions on physico-chemical conditions in HRAPs presented in previous paragraph are neglected

APPENDIX 3. PILOT SCALE HRAP HYDRAULIC RETENTION TIME ANALYSIS

During routine monitoring of the pilot scale HRAPs, the influent flow rate was estimated using a volumetric column (see Chapter 2 section 2.2.1.1.). This method resulted in significant uncertainty of the inlet flowrate measurements, both due to the measurement inaccuracy and to the lack of information on changes in flow rate from one day of monitoring to the other. Hence, from November 2016 to June 2017, the flow was measured using a tipping bucket flowmeter (Model 6506G, Unidata Pty Ltd, O'Connor WA, Australia). The tipping bucket was carefully calibrated in the laboratory (cf. Appendix 4) prior to its installation on the HRAP A as shown in Figure S3 - 1.

Figure S3 - 1: Tipping bucket set up at the inlet of HRAP A for accurate wastewater flow rate monitoring

Since measurements obtained from the tipping bucket could be considered accurate, tipping bucket recordings were used to re-calibrate the measurements from the volumetric column obtained by comparing both data on the period of use of the tipping bucket.

CORRECTIONS OF INLET FLOWRATES MEASURED ONSITE

The results from the comparison between tipping bucket and volumetric column measurements from November 2016 to June 2017 are visible in Figure S3 - 2.

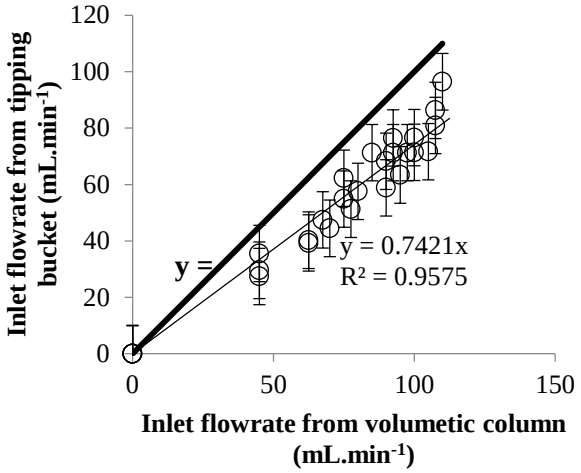

Figure S3 - 2: Comparison of the flowrate measured from on-site check with a volumetric column and tipping bucket recordings

Measurements performed on-site using the volumetric column were found consistently overestimated, which is likely due to a deformation of the volumetric column used. Since the ratio between the data measured with the volumetric column and the data gathered by the tipping bucket was found fairly constant equal to 0.74, the flow rate measured using the volumetric column was corrected accordingly.

SHIFTS IN THE INLET FLOWRATE

Because the pilot scale HRAPs were only visited for monitoring twice a week, the stability of the inlet flowrate was unknown but likely poor since flows were frequently found low or stopped on arrival. The profile of the HRT calculated based on the flowrate recorded by the tipping bucket over a week (15 – 23/02/2017, Figure S3 - 3) shows that the flowrate were indeed frequently interrupted either abruptly (16/02/2017) or following a period of gradually increasing flowrate (20 & 23/02/2017).

Due to the significant changes in inlet flowrate observed over short period of times, measurements carried out during the pilot scale HRAP study were relevant only in light of the inlet flow rate measured on site the day of the measurements. The HRT data used in the analyses presented in Chapter 3 were based on the flowrate measured prior to any flow correction action (see section 2.2.1.1.)

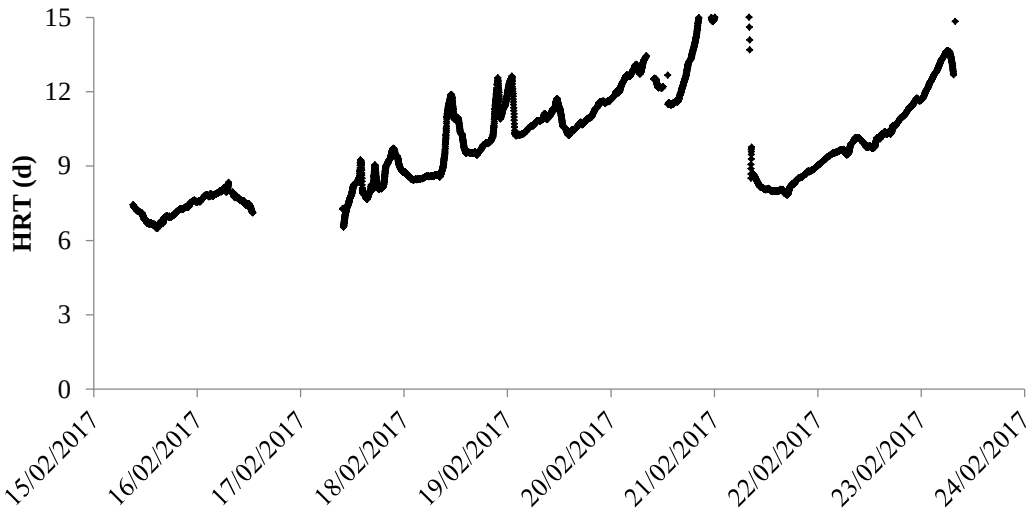

Figure S3 - 3: Example of the variations of pilot scale HRAP HRT calculated from flow rate measurements using tipping bucket data

APPENDIX 4. TIPPING BUCKET CALIBRATION

The tipping bucket set up at the inlet of the pilot scale HRAP A (see Appendix 3) was calibrated in the laboratory prior to its installation. The tipping bucket inlet was supplied with distilled using a variable speed peristaltic pump (Cole-Parmer Masterflex® L/S, motor model n°07557-02), allowing to calibrate the tipping bucket for varying flow rate. The pump speed was set on 4 different settings resulting in flow rates of 10, 50, 200, and 485 mL.min^{-1} thus encompassing the values regularly used on the pilot scale HRAP (typically 200 mL.min^{-1}). The different pump speeds were precisely adjusted to the desired flowrates by pumping water in a volumetric column for several minutes. For each flow rate tested, data from the tipping bucket was collected and the cumulated numbers of tipping counted by the bucket were plotted against time. The tipping frequency (min^{-1}) was determined through linear regression for each flowrate as shown in Figure S4 - 1

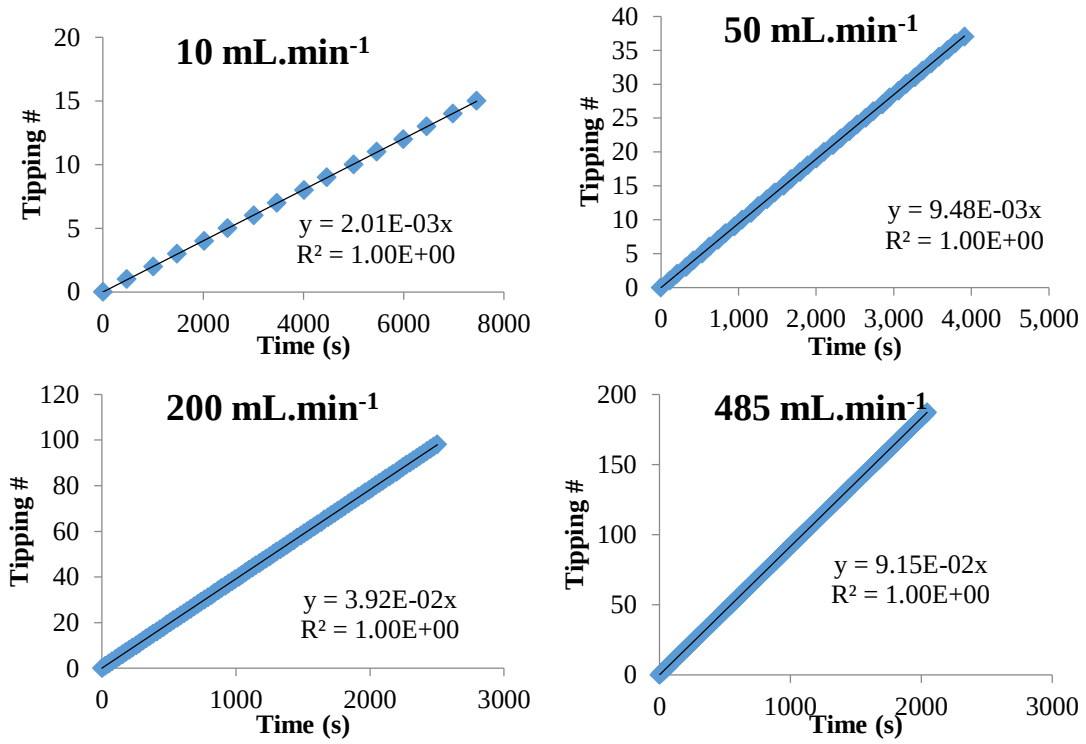

Figure S4 - 1: Cumulated number of tipping according to time for different flow rates tested, and associated linear regression

A linear relationship was found between the flow rate and the calculated tipping frequency (Figure S4 - 2), thus giving the final law between the flow rate and the tipping frequency

used when collecting data following the installation of the tipping bucket at pilot scale HRAP inlet. Practically, the tipping frequency at pilot scale HRAP was arbitrarily measured as 20 divided by the time separating 20 consecutive tipping. From this tipping frequency, the influent flowrate was calculated by multiplying the tipping frequency by the coefficient 87.67 mL.

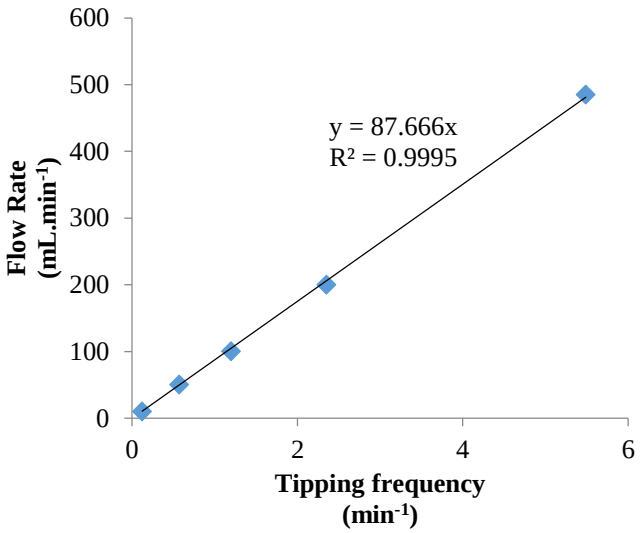

Figure S4 - 2: Variation of flow rate according to bucket tipping frequency

APPENDIX 5. IDEXX QUANTITRAY® COLILERT-18® PROCEDURE FOR THE COUNTING OF *E. COLI* CELLS IN HRAPS AND WASTEWATER SAMPLES

Total coliforms and *E. coli* counts in the pilot scale HRAP and during bench scale experiments were measured by IDEXX Quantitray® Colilert-18® method, according to the following procedure:

1. Samples were diluted in distilled water (dilution factor 20 000 and 1 000 for wastewater and HRAP samples respectively).
2. The content of one pack of Colilert-18® was added to 100 mL of the tested water samples in a 100 mL Durand bottle.
3. The Durand bottle was capped and shaken until the Colilert-18® powder was dissolved.
4. The sample was then poured into a Quanti-Tray® and sealed in an IDEXX Quanti-Tray® Sealer.
5. The sealed tray was incubated at 37±0.5°C for 24 hours (+/- 2 hours).
6. Yellow colour under normal light and fluorescence under UV-A light were quantified as shown in Figure S5 - 1 (on the right and on the left respectively).
7. The results of the counting was then obtained from the software IDEXX MPN Generator 1.4 provided by the constructor.

All the glassware used was cleaned with detergent and thoroughly rinsed with distilled water prior to the measurement.

Figure S5 - 1: Quanti-tray results example: readings under normal light for total coliforms counting (left) and fluorescence under UV-light for *E. coli* counting (right)

APPENDIX 6. SCHOTT® N-WG320

OPTICAL FILTER DATASHEET

N-WG320

Density	
ρ [g/cm³]	2.51

Notes
Base glass
Longpass filter

Reflection factor	
P_d	0.918

Bubble content	
Bubble class	1

Reference thickness	
d [mm]	2

Chemical Resistance	
FR class	0
SR class	1.0
AR class	2.0

Spectral values guaranteed		
λ_c (τ_i = 0.5) [nm]	=	320 ± 6
λ_s ($\tau_{i,U}$ = 10^{-5}) [nm]	=	280
λ_p ($\tau_{i,L}$ = 0.99) [nm]	=	470

Transformation temperature	
Tg [°C]	563

Thermal expansion	
$\alpha_{-30/+70°C}$ [10^{-6}/K]	7.1
$\alpha_{20/300°C}$ [10^{-6}/K]	8.4
$\alpha_{20/200°C}$ [10^{-6}/K]	

Refractive Index n
n_i (365.0 nm) = 1.540
n_d (587.6 nm) = 1.520
n_t (1014.0 nm) = 1.510

Temperature coefficient	
T_K [nm/°C]	0.06

All data wihout tolerances are to be understood to be reference values. Guaranteed values are only those values listed in the section "Spectral values guaranteed".

Colorimetric evaluation

Illuminant	A (Planck T = 2856 K)		
d [mm]	1	2	3
x			
y			
Y			
λ_d [nm]			
P_e			

Illuminant	Planck T = 3200 K		
d [mm]	1	2	3
x			
y			
Y			
λ_d [nm]			
P_e			

Illuminant	D65 (T_C = 6504 K)		
d [mm]	1	2	3
x			
y			
Y			
λ_d [nm]			
P_e			

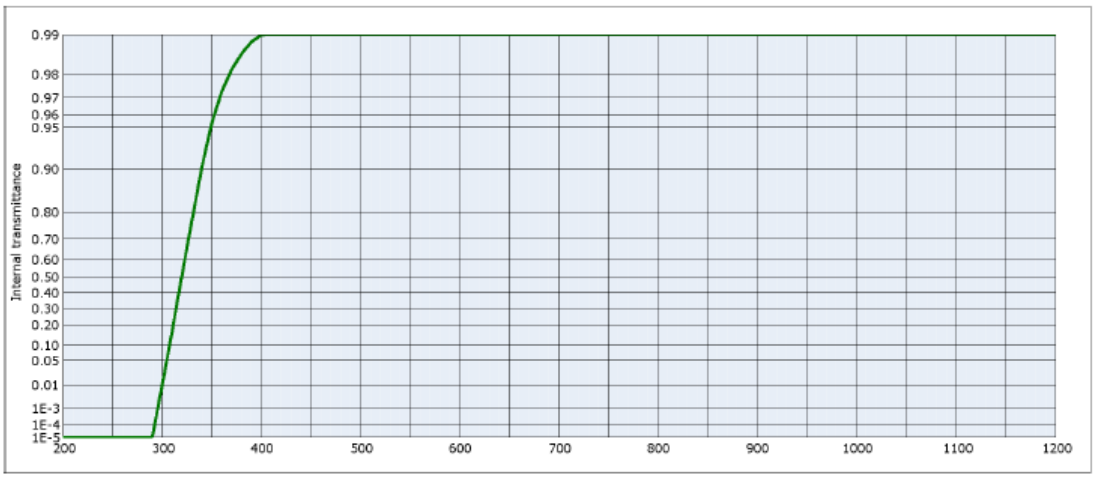

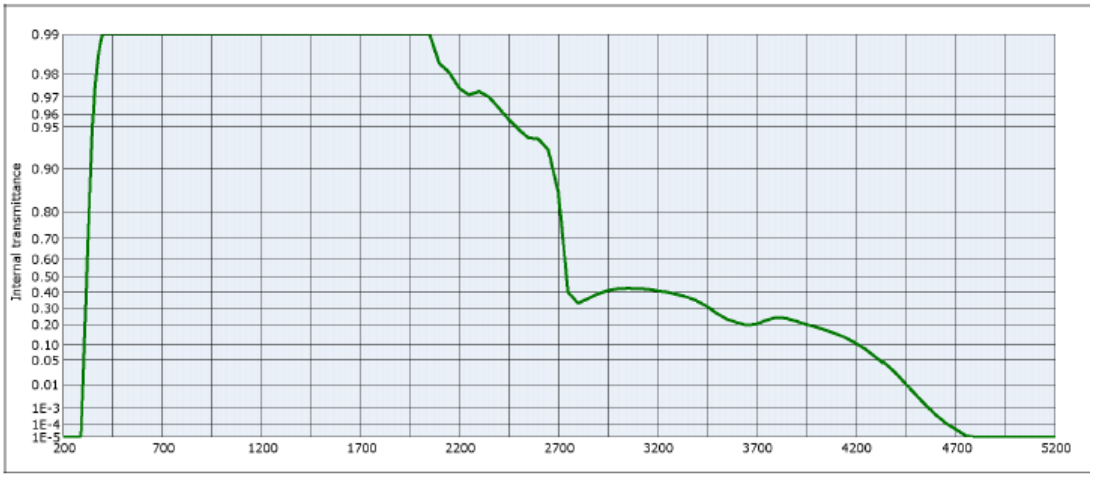

Internal transmittance τ_i at reference thickness d = 2 mm
The internal transmittance values, tabulated and graphically represented, are reference values only

λ [nm]	τ_i	λ [nm]	τ_i	λ [nm]	τ_i	λ [nm]	τ_i	λ [nm]	τ_i	λ [nm]	τ_i
200	$< 10^{-5}$	500	0.994	800	0.998	1100	1.000	2200	0.974	3700	0.202
210	$< 10^{-5}$	510	0.994	810	0.998	1110	1.000	2250	0.971	3750	0.225
220	$< 10^{-5}$	520	0.995	820	0.998	1120	1.000	2300	0.973	3800	0.240
230	$< 10^{-5}$	530	0.995	830	0.999	1130	1.000	2350	0.970	3850	0.236
240	$< 10^{-5}$	540	0.995	840	0.999	1140	1.000	2400	0.964	3900	0.220
250	$< 10^{-5}$	550	0.995	850	0.999	1150	1.000	2450	0.956	3950	0.201
260	$< 10^{-5}$	560	0.996	860	0.999	1160	1.000	2500	0.948	4000	0.186
270	$< 10^{-5}$	570	0.996	870	0.999	1170	1.000	2550	0.940	4050	0.169
280	$< 10^{-5}$	580	0.996	880	0.999	1180	1.000	2600	0.939	4100	0.152
290	$< 10^{-5}$	590	0.996	890	0.999	1190	1.000	2650	0.926	4150	0.132
300	$9.6 \cdot 10^{-3}$	600	0.996	900	0.999	1200	1.000	2700	0.854	4200	0.109
310	0.161	610	0.996	910	0.999	1250	1.000	2750	0.400	4250	$8.4 \cdot 10^{-2}$
320	0.507	620	0.997	920	0.999	1300	1.000	2800	0.330	4300	$6.0 \cdot 10^{-2}$
330	0.770	630	0.997	930	0.999	1350	1.000	2850	0.359	4350	$3.9 \cdot 10^{-2}$
340	0.901	640	0.997	940	0.999	1400	0.998	2900	0.390	4400	$2.2 \cdot 10^{-2}$
350	0.953	650	0.997	950	0.999	1450	1.000	2950	0.411	4450	$1.0 \cdot 10^{-2}$
360	0.973	660	0.997	960	0.999	1500	1.000	3000	0.422	4500	$4.0 \cdot 10^{-3}$
370	0.981	670	0.997	970	0.999	1550	1.000	3050	0.425	4550	$1.3 \cdot 10^{-3}$
380	0.986	680	0.997	980	0.999	1600	1.000	3100	0.424	4600	$4.1 \cdot 10^{-4}$
390	0.989	690	0.997	990	0.999	1650	1.000	3150	0.419	4650	$1.2 \cdot 10^{-4}$
400	0.990	700	0.997	1000	0.999	1700	1.000	3200	0.410	4700	$4.2 \cdot 10^{-5}$
410	0.991	710	0.998	1010	0.999	1750	0.999	3250	0.401	4750	$1.4 \cdot 10^{-5}$
420	0.991	720	0.998	1020	0.999	1800	0.998	3300	0.386	4800	$< 10^{-5}$
430	0.992	730	0.998	1030	0.999	1850	0.997	3350	0.370	4850	$< 10^{-5}$
440	0.992	740	0.998	1040	1.000	1900	0.996	3400	0.345	4900	$< 10^{-5}$
450	0.992	750	0.998	1050	1.000	1950	0.994	3450	0.309	4950	$< 10^{-5}$
460	0.993	760	0.998	1060	1.000	2000	0.993	3500	0.267	5000	$< 10^{-5}$
470	0.993	770	0.998	1070	1.000	2050	0.990	3550	0.231	5050	$< 10^{-5}$
480	0.993	780	0.998	1080	1.000	2100	0.983	3600	0.212	5100	$< 10^{-5}$
490	0.994	790	0.998	1090	1.000	2150	0.980	3650	0.196	5150	$< 10^{-5}$

APPENDIX 7. POUR PLATE COUNT DETAILED METHOD

The step by step methodology used for pour plate count analyses during laboratory scale experiments is described hereafter.

1. The shaker was stopped and a flask was removed and introduced in an aseptic space (i.e. in the vicinity of a flame) for sampling.
2. 1 mL of sample was pipetted into 9 mL of 5 $mg.L^{-1}$ buffered peptone water[190]. When the *E. coli* concentration was suspected to be low at the time of sampling, 1 mL was also pipetted directly into a petri dish.
3. The flask was brought back to the shaker and the shaker was restarted.
4. The sample was further diluted 10 folds in buffered peptone water and the procedure was repeated until achieving a cell density between 20 and 200 cells per mL (never exceeding a 10^7 fold dilution).
5. 1 mL from the dilutions was pipetted onto petri dishes.
6. Liquid standard count agar was poured over the 1 mL sample(s) and the petri dishes were gently swirled to spread the cells in the agar before solidification.
7. The agar was left to solidify and the dishes were then incubated for 48h at 37°C.
8. Counting was performed after incubation, and results from plates presenting between 20 and 200 colonies were henceforth reported when possible.

[190] The buffer is a made by adding 5 g of peptone to 1 L of water (Eaton et al., 1998, method 9050C)

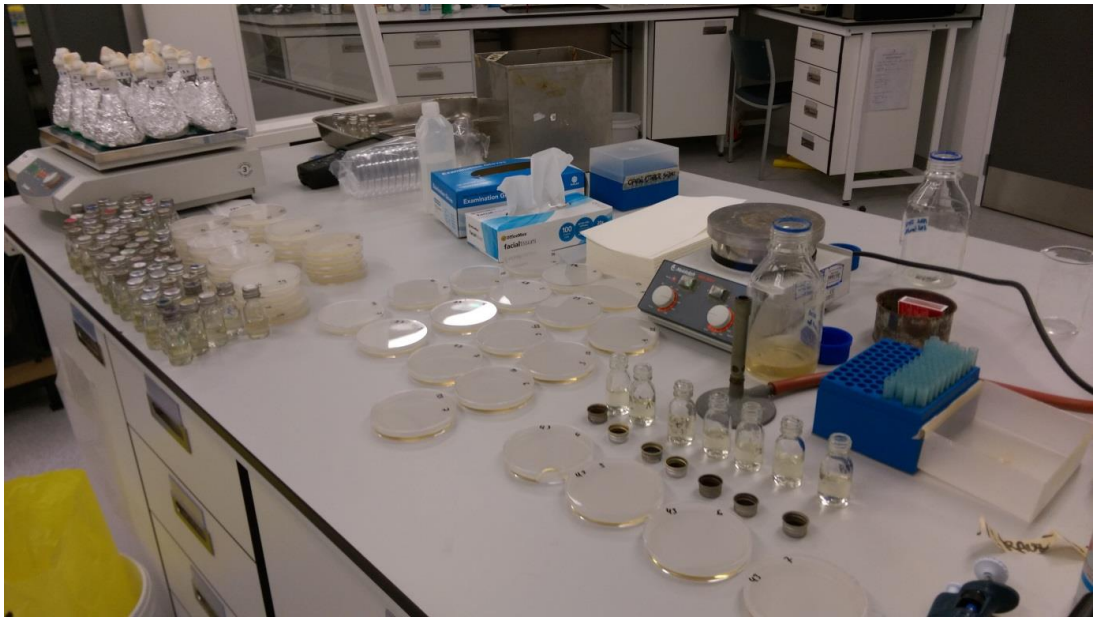

Figure S7 - 1: View of a laboratory scale experiment set up.
Shaker with experimental broth is visible on the top left next to the pour plate counting station as performed during this study

In the case of rooftop experiments, all the reactors were sampled at once near the shaker on the rooftop in non-aseptic conditions, by pipetting 1 mL of each sample in an adequately identified 9 mL peptone buffer vial. The vials were immediately taken to a fridge in the laboratory close to the manipulation point as the vials were undergoing one at a time the procedure described above from point 4, in the vicinity of a flame from that point.

APPENDIX 8. VARIATIONS OF *E. COLI* CELL COUNT IN THE WASTEWATER FEED DURING PILOT SCALE HRAPS MONITORING

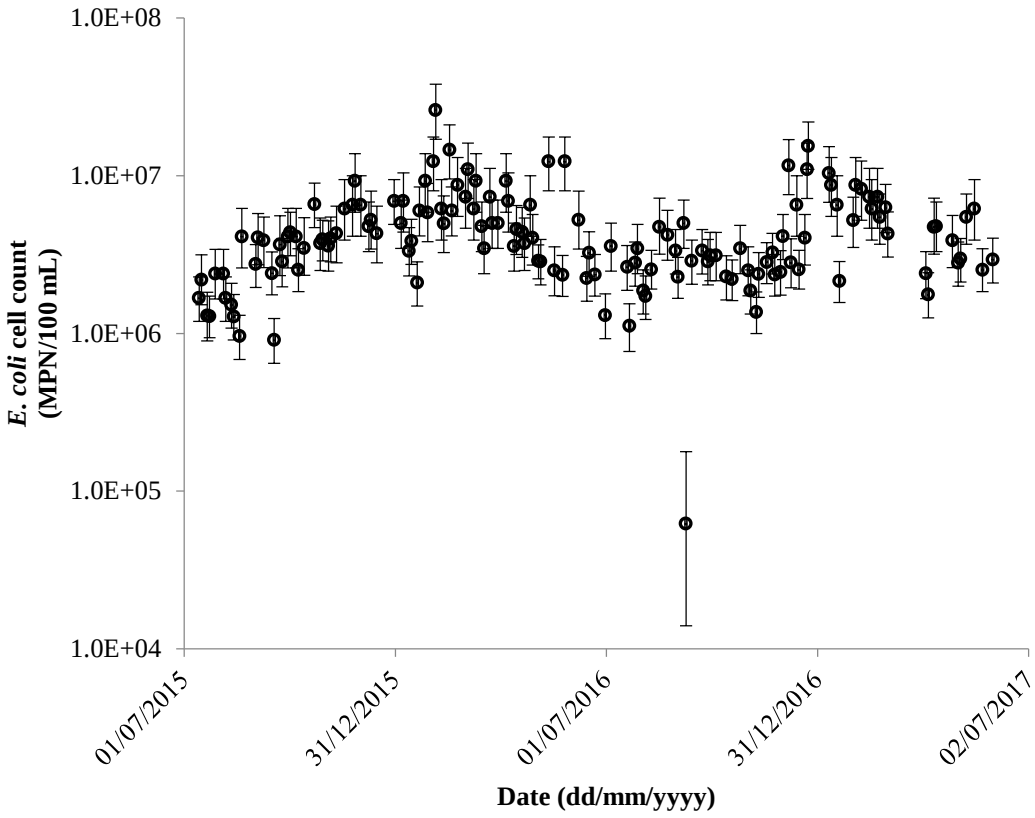

Figure S8 - 1: Variations of *E. coli* cell count in the wastewater feed during the study of pilot scale HRAPs

APPENDIX 9. MASS TRANSFER COEFFICIENT AT THE LIQUID-GAS INTERFACE OF PILOT SCALE HRAPS: DETERMINATION, AND RELATIONSHIP WITH ALGAL BROTH LINEAR SPEED

In order to better understand pilot scale HRAP behaviour (see Chapter 3), and having been identified as a critical parameter for pH and DO concentration predictions (see Chapter 6), the mass transfer coefficient of dioxygen at the liquid/gas interface (Kla_{O_2}) was measured experimentally on both pilot scale HRAPs (set-up described in section 2.2.1.1.). Following the determination of dioxygen mass transfer coefficient at the liquid/gas interface, this coefficient was theoretically calculated for ammonia and carbon dioxide.

MATERIALS AND METHODS

The mass transfer coefficient for dioxygen at the liquid/gas interface was determined experimentally following the dynamic oxygenation method (Gourich et al., 2008).

Experimental procedure

On the day of the experiment, the pilot scale HRAP was emptied and washed with a high pressure water blaster removing as much organic matter and living organisms as possible from the pond. The HRAP was then filled up with tap water, the paddlewheel being stopped.

Two electrodes measuring pH, dissolved oxygen (DO) concentration, and temperature were immersed in water (Multimeter Thermo Scientific™ Orion Star™ A326) at opposite sides of the pond and pH, DO, and temperature were recorded at one minute intervals during the experiment. N_2 gas was bubbled in the pond resulting in the rapid loss of the oxygen dissolved in the HRAP (visible in Figure S9 - 1 and Figure S9 - 3). When DO concentration was below 60% of the saturation value, the bubbling was stopped and the paddlewheel was started.

The experiment was performed once on HRAP A (18/11/2015) and once on HRAP B (06/07/2016).

Results analysis

O_2 concentration during the re-oxygenation period theoretically follows Equation S9 - 1 (Boogerd et al., 1990).

$$\frac{dO_2}{dt} = Kla_{O_2}.(O_2{}^* - O_2) \quad \text{(S9 - 1)}$$

Where O_2 is DO concentration (mg.L^{-1}), $O_2{}^*$ (mg.L^{-1}) is DO saturation concentration (temperature dependent), and Kla_{O_2} is the searched mass transfer coefficient for dioxygen at the liquid/gas interface (s^{-1}).

Assuming $O_2{}^*$ is constant during the experiment, (true for low variations of temperature), Equation S9 - 2 can be obtained by integrating Equation S9 - 1.

$$\ln\left(1 - \frac{O_2}{O_2{}^*}\right) = -Kla_{O_2}.t + \ln\left(1 - \frac{O_2(t=0)}{O_2{}^*}\right) \quad \text{(S9 - 2)}$$

Hence, plotting $\ln\left(1 - \frac{O_2}{O_2{}^*}\right)$ against time theoretically results in a linear law which slope is the searched mass transfer coefficient for dioxygen at the liquid/gas interface (Kla_{O_2}).

Effect of the paddlewheel speed

When repeated on the 06/07/2016 in HRAP B, the experiment was performed three times for three different paddlewheel speeds (10, 5, and 12 rpm by chronological order).

Relationship between paddlewheel speed and broth linear speed

On 23/02/2018, the broth linear speed was measured according to the three paddlewheel speed at which Kla_{O_2} was measured on 06/07/2016 (i.e. 5, 10, and 12 RPM). The linear speed of the broth was measured by dropping a floating cork stopper in the broth and measuring the time needed by the cap to go from one end to the other of the channel opposite to the paddlewheel (2.5 m long channel, as measured prior to the experiment). The procedure was repeated three times for each paddlewheel speed and results are given as the average of the three measurements.

RESULTS AND DISCUSSION

The recordings of O_2 concentration from the experiment performed on 18/11/2015 and 06/07/2016 are displayed in Figure S9 - 1 and Figure S9 - 3, respectively. The corresponding plots of $\ln\left(1 - \frac{O_2(t)}{O_2{}^*}\right)$ against time are shown in Figure S9 - 2 and Figure S9 - 4, respectively, which evidenced affine laws of time, the slope of which are the Kla_{O_2} coefficient, as previously explained.

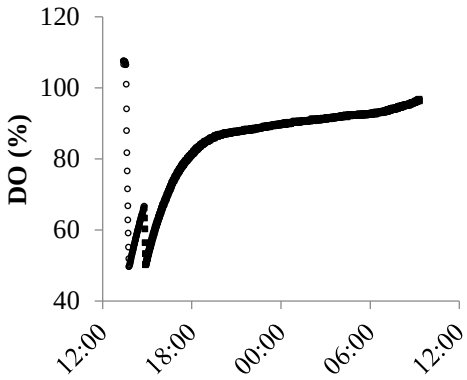

Figure S9 - 1: Variations of dissolved oxygen (% saturation) recorded during degassing and reaeration of pilot scale HRAP A for the measurement of gas transfer coefficient on 18/11/2015

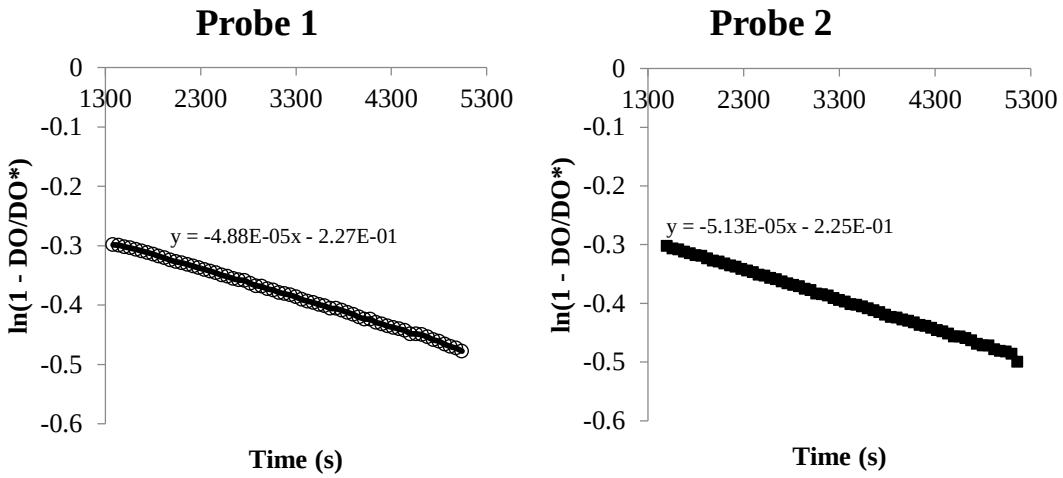

Figure S9 - 2: Variations of $ln\left(1-\frac{O_2}{O_2{}^*}\right)$ against time during gas transfer coefficient measurement experiment (18/11/2015, both DO probes), and associated linear regression

A Kla_{O_2} of $0.49 \cdot 10^{-4}$ s^{-1} was determined on 18/11/2015, against a value of $1.1 \cdot 10^{-4}$ s^{-1} on 06/07/2016. Because issues with the paddlewheel were experienced at the time the first experiment was performed, and the paddlewheel speed was well-known during the second experiment, the value $Kla_{O_2} = 1.0 \cdot 10^{-4}\, s^{-1}$ was kept for dioxygen in model base case scenario (see Chapter 6).

Effect of paddlewheel angular speed

The dissolved oxygen concentration recorded during the experiment testing the effect of the paddlewheel speed on the Kla coefficient is shown in Figure S9 - 3 while the plots of $\ln\left(1-\frac{O_2}{O_2{}^*}\right)$ versus time for each paddlewheel speeds are shown in Figure S9 - 4. Faster paddlewheel rotation was associated to higher dioxygen mass transfer coefficient.

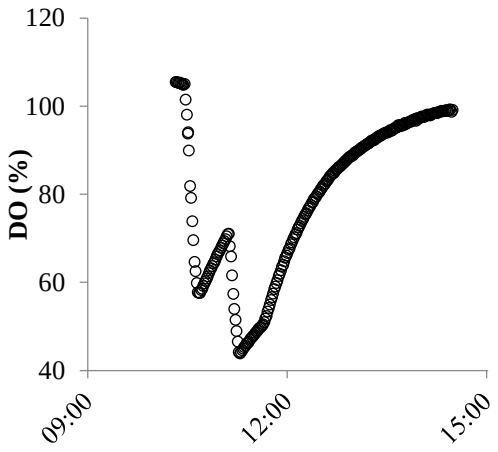

Figure S9 - 3: Recorded dissolved oxygen (% saturation) during O_2 mass transfer coefficient measurements on 06/07/2016.
3 phases for the different paddlewheel speed tested (10, 5 and 12 RPM) are visible

Gas transfer

The value of the mass transfer coefficient at the air/water interface for a species X can be calculated from Kla_{O_2} using Equation S9 - 3 (Boogerd et al., 1990).

$$Kla_X = \left\{\frac{D_{L_X}}{D_{L_{O_2}}}\right\}^{1/2} . Kla_{O_2} \qquad \text{(S9 - 3)}$$

Where D_{L_X} and $D_{L_{O_2}}$ are the diffusivity coefficients in water of the species X and dioxygen respectively. Based on the diffusivity coefficient at 25°C of $1.92 \cdot 10^{-5}$, $1.64 \cdot 10^{-5}$, and $2.10\ 10^{-5}$ $cm^2.s^{-1}$ for carbon dioxide, ammonia, and dioxygen respectively (Cussler, 2009), the following gas transfer coefficients $Kla_{CO_2} = 9.1 \cdot 10^{-5}\ s^{-1}$ and $Kla_{NH_3} = 8.6 \cdot 10^{-5}\ s^{-1}$ were calculated for carbon dioxide and ammonia respectively.

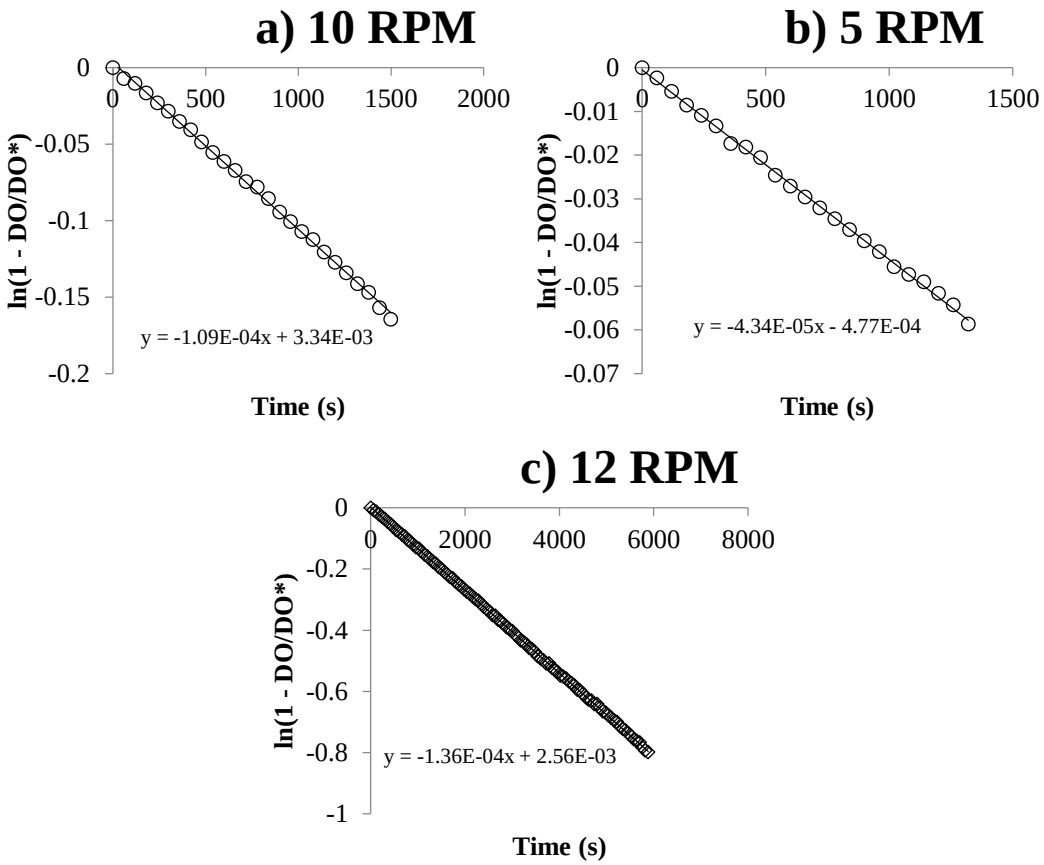

Figure S9 - 4: Calculated $ln\left(1-\frac{O_2}{O_2{}^*}\right)$ against time for different paddlewheel speed and associated linear regressions (a: 10 RPM, b: 5 RPM, c: 12 RPM)

Relationship between paddlewheel angular speed and algal broth linear speed

The measured algal broth linear speed according to the paddlewheel angular speed and the linear regression performed on the data are shown in Figure S9 - 5. The error of linear speed measurement was estimated based on the spread found between the three measurement performed while an error of 0.25 RPM was assumed for the reading of the paddlewheel angular speed[191].

A strong linear correlation was found between both variables (R^2 = 0.9986). The algal broth linear speeds shown in Table 3 - 2 were therefore computed assuming proportionality with the paddlewheel angular speed (by a factor 2.23 $cm.s^{-1}.RPM^{-1}$).

[191] The paddlewheel being 4-wheeled, 0.25 RPM is the max error possible from direct observation.

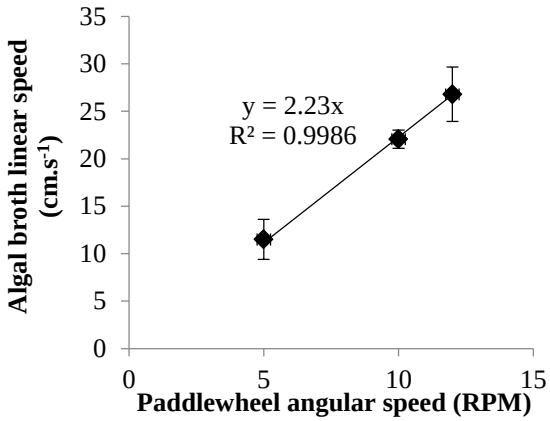

Figure S9 - 5: Variations of algal broth linear speed measured according to the paddlewheel angular speed

APPENDIX 10. CORRELATION ANALYSIS BETWEEN *E. COLI* DECAY COEFFICIENT AND PARAMETERS MEASURED IN PILOT SCALE HRAPS

Table S10 - 1: R^2, p-value[1], and number of data associated to the linear regressions between *E. coli* decay coefficient and different parameters monitored in pilot scale HRAPs

	R^2	p-value	N
Hydraulic retention time	2.04E-05	0.9600	126
Temperature at 9 AM	0.061	6.32E-03	122
pH at 9 AM	0.013	0.2221	119
DO concentration at 9 AM	2.57E-04	0.8619	120
HRAP TSS concentration	0.170	1.94E-06	124
HRAP TSS productivity	0.109	1.82E-04	124
WW TSS concentration	0.030	0.0539	123
WW COD concentration	0.132	0.0035	63
WW COD dissolved concentration	0.012	0.4163	59
HRAP COD concentration	0.015	0.3364	65
HRAP COD dissolved	5.43E-06	0.9857	62
WW N-NH_3 concentration	5.27E-04	0.8515	69
HRAP N-NH_3 concentration	8.26E-03	0.5093	55
HRAP Chloride concentration	0.192	5.43E-07	120
HRAP Nitrate concentration	0.026	0.0760	120
HRAP Nitrite concentration	1.01E-03	0.7315	119
HRAP Phosphate concentration	0.079	0.0018	120
HRAP Sulphate concentration	0.086	0.0011	120
HRAP TOC concentration	0.046	0.0181	121
HRAP TOC dissolved	6.34E-03	0.3893	119
HRAP TN concentration	9.40E-03	0.2962	118
HRAP TN dissolved	0.019	0.1665	105
WW *E. coli* cell count	0.124	5.38E-05	126
Maximum pH over previous 24h	0.056	0.0774	57
Minimum pH over previous 24h	4.45E-03	0.6218	57
Maximum DO concentration over previous 24h	0.064	0.0498	61
Minimum DO concentration over previous 24h	0.044	0.1042	61
Maximum temperature over previous 24h	0.081	0.0265	61
Minimum temperature over previous 24h	0.031	0.1759	61
Total incident sunlight energy over previous 24h	0.137	2.19E-05	125
Maximal hourly sunlight intensity over previous 24h	0.149	8.53E-06	125

[1] p-values were calculated using the function *fitlm* on MATLAB R2015a (MathWorks, Natick, Massachusetts, USA).

APPENDIX 11. DAILY VARIATIONS OF *E. COLI* CELL COUNT IN DOMESTIC WASTEWATER FEEDING PILOT SCALE HRAPS

Significant diurnal variations of domestic wastewater characteristics have been reported in the literature: for instance, the concentration of hormones and antibiotics were evidenced to peak in the morning, in the evening, or during high loads (Nelson et al., 2011; Plósz et al., 2010). With regards to pathogenicity indicators, Ekklesia et al. (2015) evidence higher faecal indicator bacteria (total coliform, *E. coli*, and enterococci) in tropical urban storm drain during the day than during the night. Farkas et al. (2018) however showed no significant diurnal variations in adenovirus, norovirus, and sapovirus counts in domestic wastewater.

In our study of pilot scale HRAP (Chapter 3), significant seasonal variations of *E. coli* cell count in the wastewater used to feed pilot scale HRAPs were experienced (see Figure S8 - 1). However, because the samples grabbed during routine monitoring of pilot scale HRAPs were always collected at 9 A.M. (see Chapter 2 section 2.2.1.2.), little was known about potentially significant variation of *E. coli* cell count in the wastewater over a 24h period. Because it may critically weaken the conclusions from daily profile experiments results (see Chapter 3 section 3.3.4.), daily variations of *E. coli* cell count in the wastewater were investigated.

MATERIALS AND METHODS

The refrigerated autosampler described in section 2.2.1.2. was connected to the wastewater channel (from which the wastewater feeding the pilot scale HRAPs was pumped, Figure 2 - 1). 200 mL wastewater samples were grabbed hourly by the autosampler over 24h from 26/11/2015 9 A.M. On 27/11/2015, shortly after 9 A.M., samples were brought to the laboratory for microbial analysis. The total cell count of *E. coli* were quantified using the IDEXX Quantitray® Colilert-18® method after 20,000 fold dilution in distilled water, following the procedure described in Appendix 5.

EXPERIMENTS RESULTS

The *E. coli* cell counts measurements obtained during this study are shown in Figure S11 - 1. As can be seen, no significant *E. coli* cell count variations were recorded during this experiment.

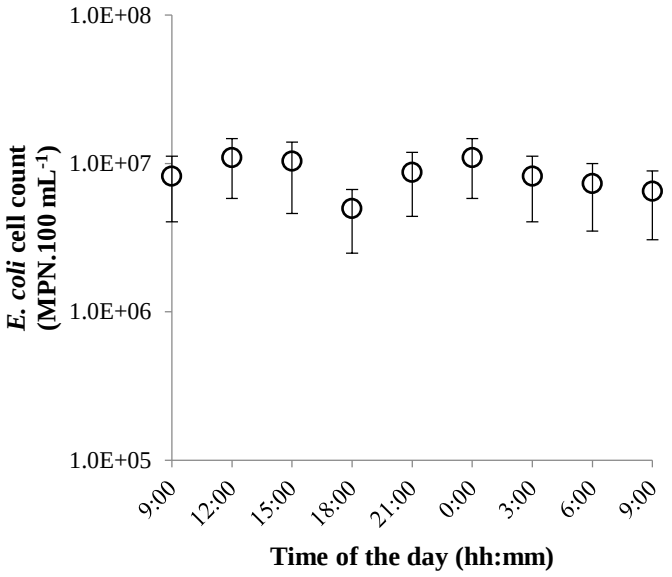

Figure S11 - 1: *E. coli* cell count variations over 24h (26 – 27/11/2015) in wastewater fed to the pilot scale HRAPs

CONCLUSION AND DISCUSSION

Although it is still uncertain if *E. coli* cell count in the wastewater varied during daily profile experiments since it was not monitored, the results presented in this section indicates that systematic variations are unlikely.

This is surprising considering this study was performed with real wastewater collected from Palmerston North domestic wastewater treatment plant: noticeable wastewater characteristics variations could be expected due to societal habits (Ekklesia et al., 2015). However, the wastewater feeding the pilot scale HRAPs was collected downstream from primary settler at Palmerston North wastewater treatment plant. This settler, of hydraulic retention time of 6 h may provide sufficient polishing of wastewater microbial characteristics over 24h to equalize *E. coli* cell count over 24h.

APPENDIX 12. POUR PLATE METHOD UNCERTAINTY ANALYSIS

Significant variability in the results was observed during laboratory scale experiments when assessing *E. coli* decay using pour plate method. It was therefore necessary to assess the uncertainty associated to countings obtained from pour plate method (method described in Appendix 7).

MATERIAL AND METHODS

All the decay rates obtained from reactors in the dark using distilled water or neutral pH buffer as experimental broth during laboratory scale experiments were gathered since it could be safely assumed that no decay was taking place in these reactors (see Chapter 4 section 4.1. 1. and section 4.1.3.3.). From such data, for each reactor, the deviation of the *E. coli* counts measured from each counting compared with the counting at the initial time (dev) was calculated using Equation S12 – 1.

$$dev = \frac{C_0 - C}{C_0} \quad \text{(S12 - 1)}$$

Where C_0 is the *E. coli* cell count measured at the beginning of the experiment (CFU.mL^{-1}) and C is the *E. coli* cell count measured at the time for which the deviation is looked for (CFU.mL^{-1}).

Since no decay is expected in the selected reactors, deviation dev is hypothesized to only be related to the uncertainty associated to the counting method.

The same analysis was performed over the log transformed concentrations.

RESULTS

The distribution of the deviations calculated over the raw counts (and the distribution of the deviations calculated over the log-transformed counts) are shown in Figure S12 - 1 (respectively a and b). The red curves represent the normal law $\mathcal{N}(0, \sigma)$ where sigma is the standard deviation calculated for the sample of calculated deviations.

As can be seen, both distributions follow a normal law, evidencing that the spread of the deviations is likely related to random errors as hypothesized.

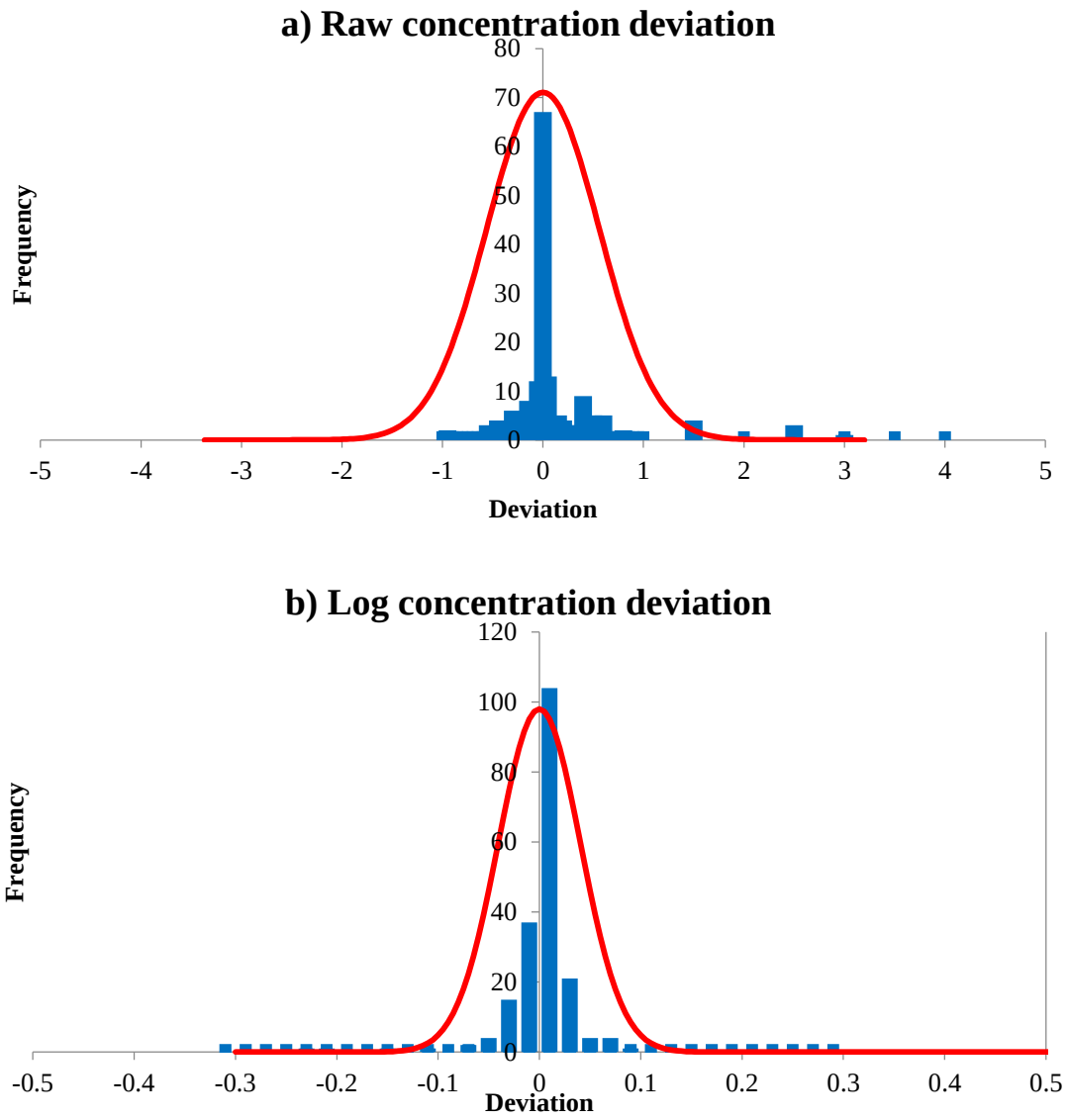

Figure S12 - 1: Distribution of the measured deviation in *E. coli* cell counts from initial counts in reactors presenting no mortality

While raw concentrations show a 95% confidence interval of about ±168 %, the same uncertainty for the log-transformed concentration was evaluated at ± 9.5% (rounded up to 10% uncertainty).

CONCLUSION

We concluded from this study that log transformed *E. coli* cell counts measured through pour plate method were accurate with 10% uncertainty at the 95% confidence level. Since measurements errors were found to trigger disproportionate relative uncertainty on the raw *E. coli* counts, this study led us to discuss the results from laboratory scale experiments in terms of log-transformed concentration.

APPENDIX 13. IMPACT OF TEMPERATURE ON *E. COLI* NATURAL DARK DECAY COEFFICIENT MEASURED AT LABORATORY SCALE

E. coli natural decay was demonstrated not to be significant during laboratory-scale assays (see Chapter 4 section 4.1.1.). This analysis took into account data from control reactors incubated at any temperature (in the range 5 – 35°C). However, temperature has a critical impact on known disinfection mechanism (e.g. high pH toxicity as shown in section 4.1.3.3.). We must therefore first demonstrate that temperature had no impact on the decay rates measured in control conditions in order to take into account the natural decay rates determined at varying temperature in the analysis presented in section 4.1.1.

To achieve that, the distribution of natural decay rates measured in control reactors was studied according to their incubation temperature (± 2°C). The results are shown in Figure S13 - 1. No relationship between natural decay coefficients and temperature are visible in Figure S13 - 1, as both positive and negative values were measured across the whole temperature range. The spread in the decay coefficients values increased with increasing temperature which was associated to the increase in measurements error due to shorter experiments at higher temperature (see discussion in section 4.1.1. for a more detailed explanation).

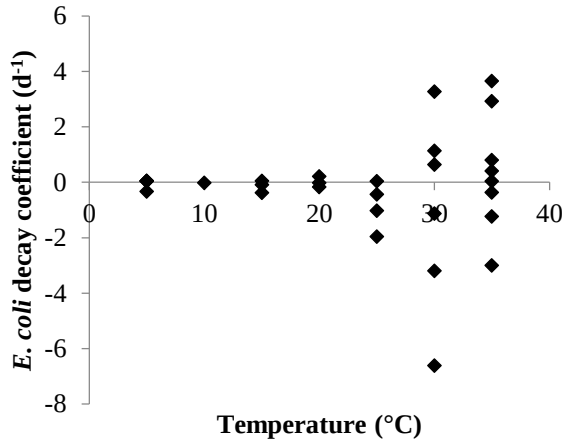

Figure S13 - 1: *E. coli* decay rates measured in dark control of all temperature-controlled experiments according to the incubation temperature

Taking into account decay coefficients measured in control reactors at varying incubation temperatures for natural decay coefficients analysis was therefore concluded to be valid.

APPENDIX 14. INITIAL *E. COLI* CELL COUNT DURING LABORATORY SCALE EXPERIMENTS SUPPORTED BY POUR PLATE METHOD

The procedure followed to grow and inoculate *E. coli* cells in experimental vials during laboratory experiments (as described in Chapter 2 section 2.2.2.2.) was developed in order to obtain a stable *E. coli* cell count for the initial sampling of each reactor in every experiments.

In this appendix, the success of this method to achieve a consistent initial count between 20 – $200 \cdot 10^6$ CFU.ml^{-1} as targeted[192] was investigated.

Initial *E. coli* cell counts from all the reactors when assessed by pour plate method were gathered and their distribution after log-transformation is shown in Figure S14 - 1. As can be seen, most initial *E. coli* cell counts were found within the targeted range (73.7 %). When adding to this range a 10% margin on the log concentration of *E. coli* accounting for pour plate method measurement uncertainty (see Appendix 12), 94.1% of the initial *E. coli* cell counts reported are within the tolerance interval (6.57 – 9.13 log units of CFU.ml^{-1}).

Hardly any reactors were found with higher *E. coli* than expected, and all of them correspond to early experiment when the method was not yet standardized[193]. However, ca. 5% of reactors were found with lower amount of *E. coli* cells than targeted. This could be expected since the manipulation comported several steps where loss of bacteria cells was possible (e.g. centrifugation supernatant discarding, resuspension of centrifugate). 5 flasks were even found with undetectable numbers of *E. coli* cells. All 5 of them corresponded to tests for pH 11 when the decay was fast enough to damage all *E. coli* cells before the first sampling was performed. Two experiments were found with consistently low numbers of *E. coli* cells in every reactor indicating an error was made in the experiment preparation, most likely during the centrifugation/resuspension step. Some of the errors also originate from early experiments, again prior to normalization of the experimental process. Finally, most flasks found to have relatively low starting *E. coli* count were testing high pH (> 10) at high temperature (30°C). Such reactors were therefore already experiencing significant decay prior to the first sampling.

[192] Corresponding to log transformed concentration between 7.30 and 8.30

[193] Such results are included in this analysis because they were considered in the discussion of this thesis.

Only 2 of all the reactors of this study (N = 157) had an abnormally low concentration that could not be related to any of the causes detailed above. Such reactors were most likely affected by an error during the inoculation or the serial dilution step.

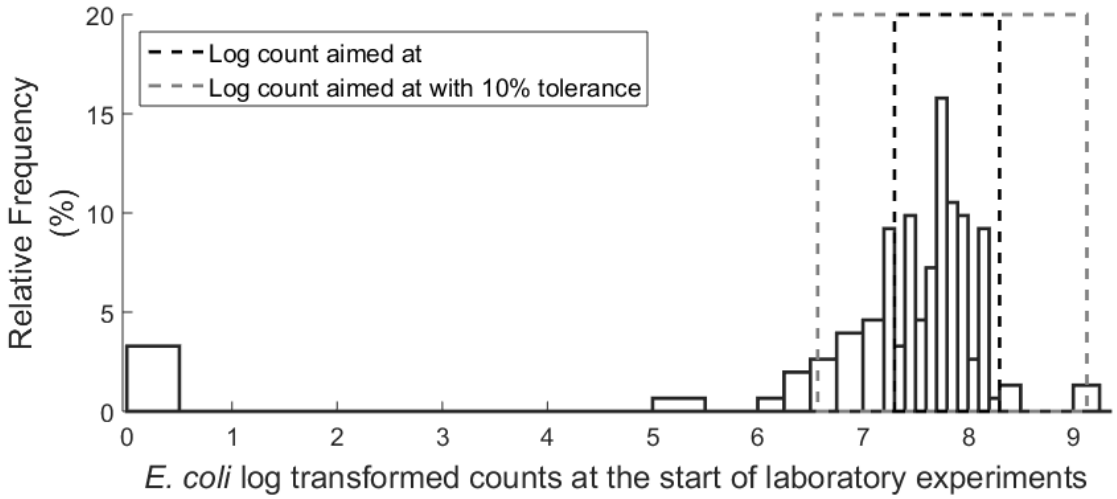

Figure S14 - 1: Repartition of the initial log transformed *E. coli* cell counts during laboratory scale experiments

CONCLUSION

As stated in the Chapter 2 section 2.2.2.1., a fairly constant initial count of *E. coli* cells was achieved during the laboratory experiment phase (within the 20 – 200 $x10^6$ $CFU.mL^{-1}$ range) ensuring decay coefficeints are recorded in the same range of concentrations and are therefore comparable between experiments.

APPENDIX 15. EVIDENCE OF HEIGHTENED RESISTANCE FROM WILD TYPE *E. COLI* STRAINS

In order to compare their respective decay coefficient, *E. coli* from the "domestic" strain ATCC 10536 and the two isolated "wild" strains (named #1 and #2) were tested in some of the harmful conditions identified by this study. Two comparative experiments were performed, one exposing the bacteria to sunlight, and one recording the decay of the bacteria at high pH in the dark.

MATERIAL AND METHODS

A rooftop experiment in RO water was performed following procedures as presented in Chapter 2 2.2.2.2. The experiment was carried out in Palmerston North, New Zealand (40°23'15"S 175°37'08"E) on the 7 of December 2016. The day was mostly overcast but significant sunlight energy was recorded at ground level as shown in Figure S15 - 1. 2x100 mL open beaker exposing bacteria to sunlight induced damage were prepared for each strain, as well as one foil covered E-flask used as dark control. The bacteria were exposed to sunlight from 12:30 to 15:30. Only two samplings were performed corresponding to the start of exposition and the end of exposition.

A typical pH experiment in the dark was conducted at ambient temperature on the 18 of November 2016 following the procedure described in Chapter 2 section 2.2.2. The three *E. coli* strains were all inoculated in one E-flask filled with 50 mL MQ water and one E-flask filled with pH 10 buffer. The reactors were sampled twice, once just after inoculation and once after a 4h incubation period.

RESULTS AND DISCUSSION

Sunlight exposition

The sunlight energy received at ground level on 7 December 2016 in Palmerston North[194] is shown in Figure S15 - 1.

[194] Data obtained from NIWA database (Palmerston North, station ID 21963)

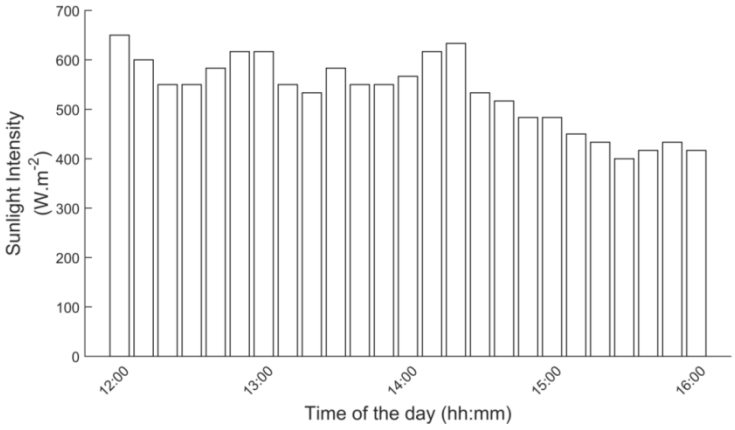

Figure S15 - 1: Sunlight intensity recorded on the 07/12/2016

Counting results

The results from the *E. coli* cell countings of the experiment investigating sunlight impact, respectively pH impact, are presented in Figure S15 - 2, respectively Figure S15 - 3.

While the initial cell counts are similar for all 3 strains, the decay coefficient of the 'laboratory' strain ATCC® 10536™ both when exposed to sunlight and to elevated pH was significantly higher than the decay coefficients of the wild strains exposed to the same conditions. For all strains, decay was insignificant under darkness at neutral pH (not shown).

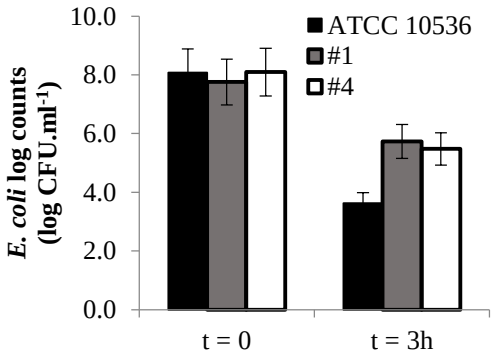

Figure S15 - 2: Log counts of the three *E. coli* strains (ATCC 10536 and wilds) prior and after exposition to sunlight

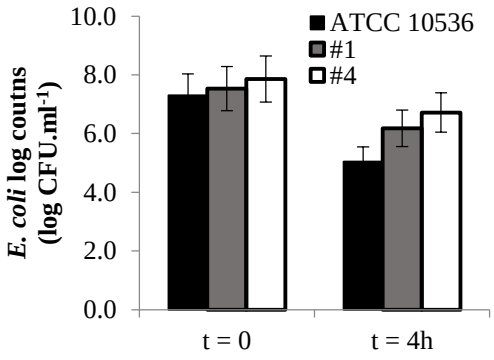

Figure S15 - 3: Log counts of the three different *E. coli* strains(ATCC 10536 and wilds) prior and after exposition to pH = 10

CONCLUSION

The higher sensitivity of the laboratory strain to conditions suspected to mediate disinfection in HRAPs was therefore confirmed for two well established mechanisms during laboratory scale experiment. This experiment validated the need to conduct experiments using wild strains of *E. coli*, as suggested by Fisher and Nelson (2014) and Silverman and Nelson

(2016)[195]. Hence, unless stated, experiments presented in this thesis were performed using *E. coli* #1 strain. Interestingly, no significant difference in mortality was found between both wild strains.

[195] We also gratefully thank Pr. Steve Flint (Massey University) for advising us caution when monitoring lab-cultured strain, thus initiating this investigation.

APPENDIX 16. ENVIRONMENTAL CONDITIONS EXPERIENCED BY ALGAL BROTH DURING BENCH SCALE EXPERIMENTS

In this paragraph, we present the environmental conditions (i.e. temperature, pH, DO concentration) recorded in algal broth, and sunlight intensities reported by NIWA (Palmerston North, station ID 21963) during bench scale experiments (results presented in Chapter 5). The conditions for the measurements of these parameters were presented in Chapter 2 section 2.2.3.

EXPERIMENT OF THE 02/11/2017 – LIGHT 1

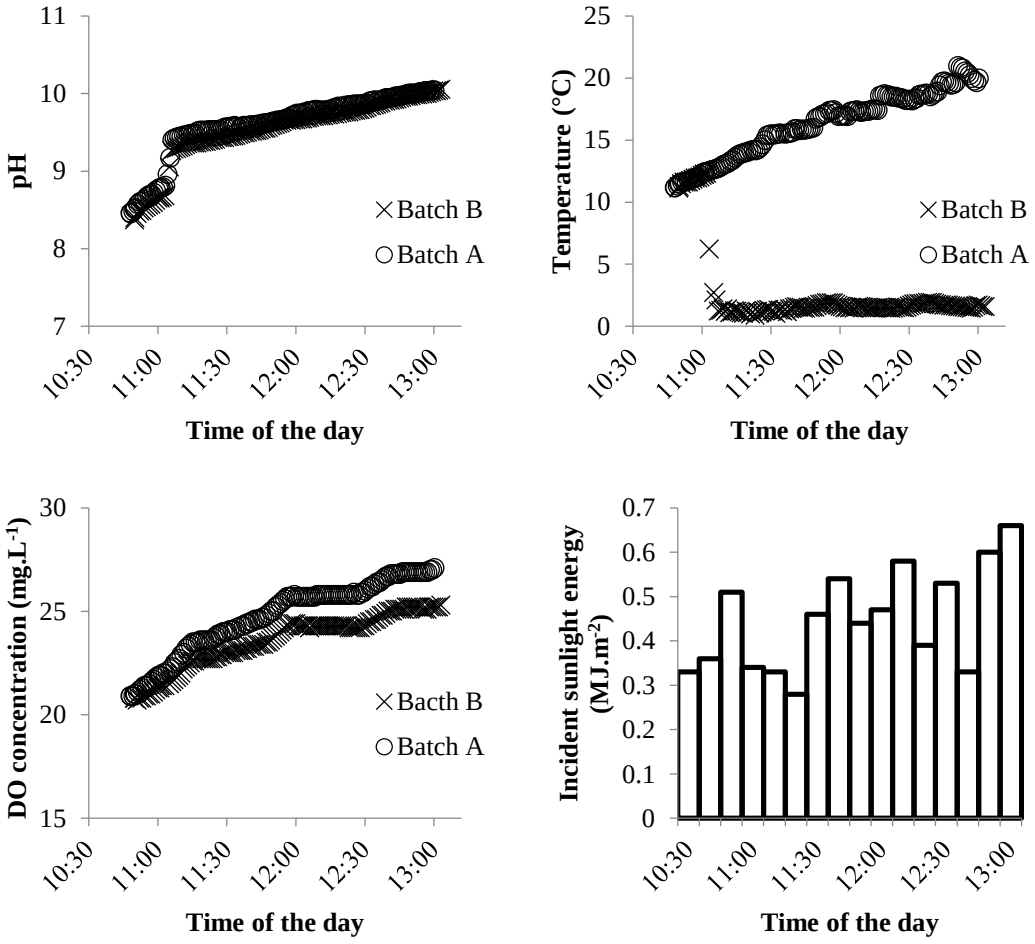

Figure S16 - 1: pH, temperature, DO concentration and incident sunlight energy variations during the first phase of bench-scale experiment carried out on 02/11/2017

EXPERIMENT OF THE 02/11/2017 – LIGHT 2

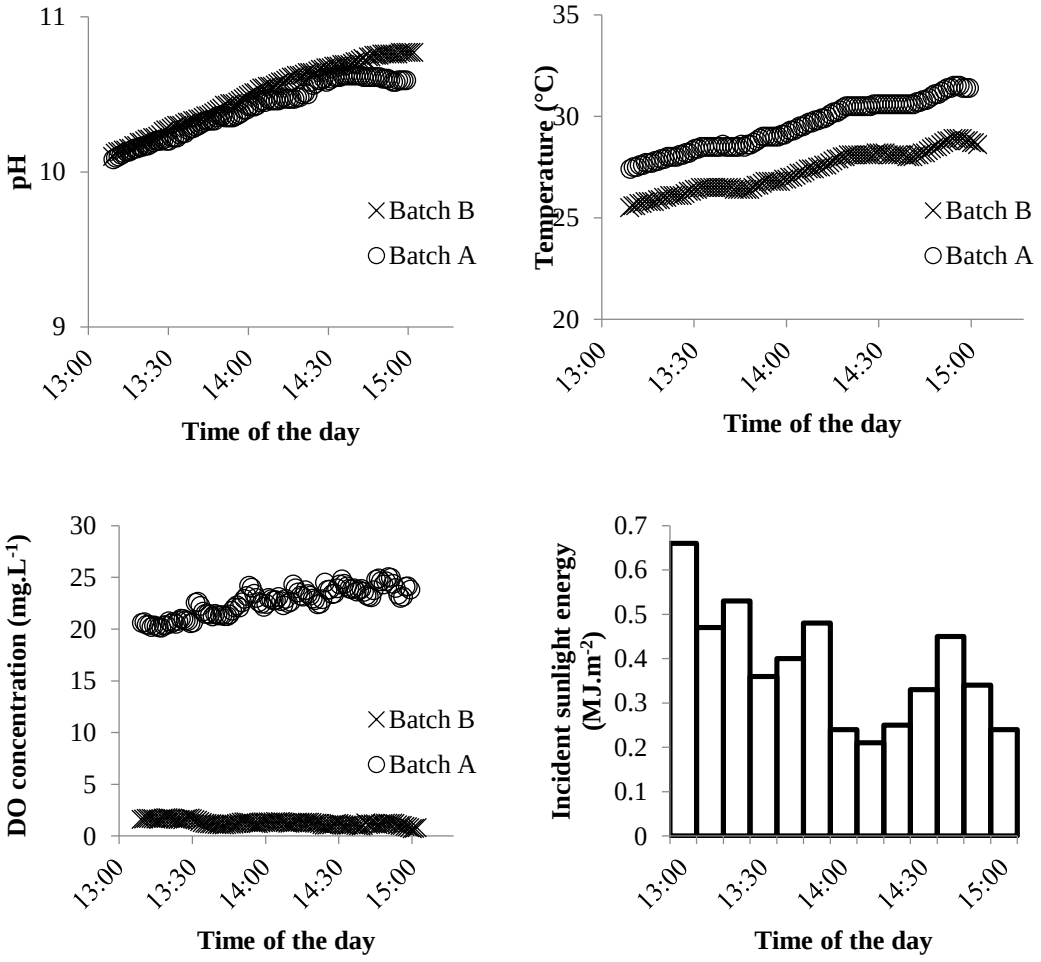

Figure S16 - 2: pH, temperature, DO concentration and incident sunlight energy variations during the second phase of bench-scale experiment carried out on 02/11/2017

EXPERIMENT OF THE 02/11/2017 – DARK

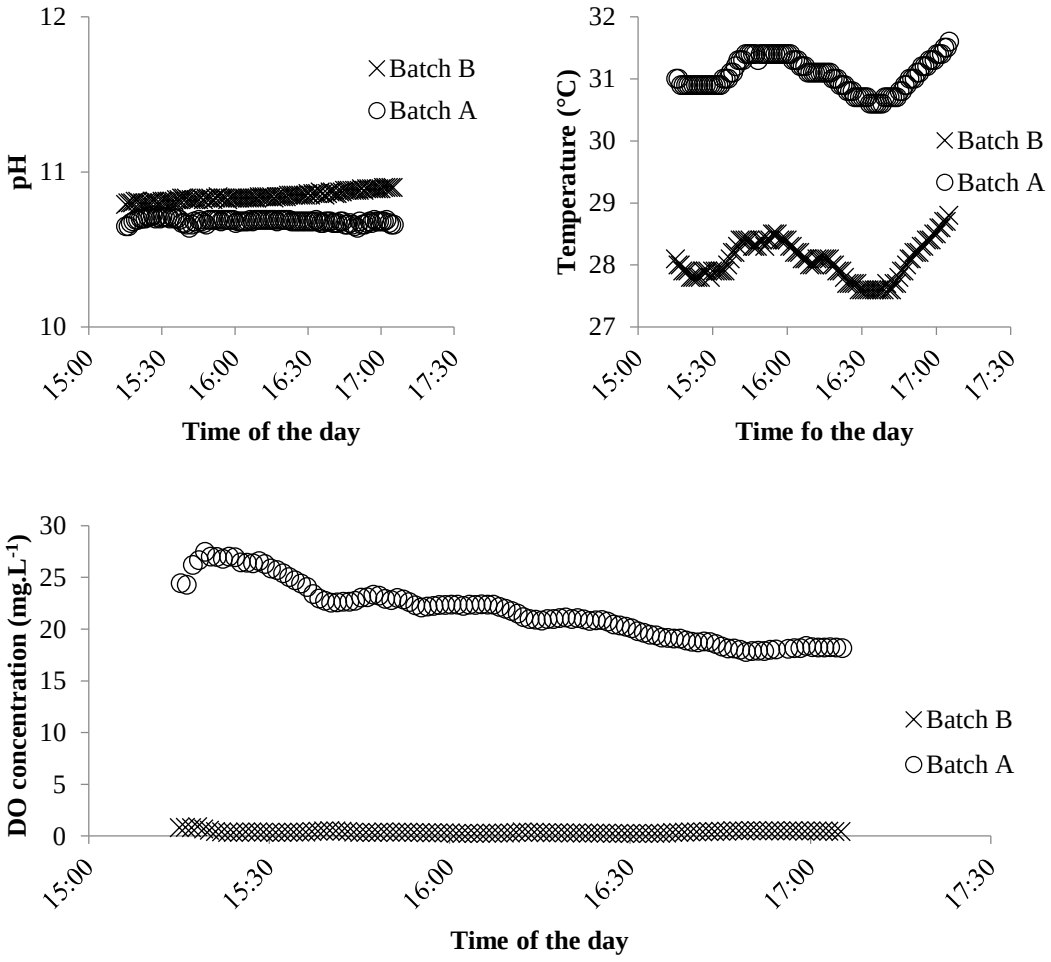

Figure S16 - 3: pH, temperature, and DO concentration variations during the third phase of bench-scale experiment carried out on 02/11/2017

EXPERIMENT OF THE 14/11/2017 – LIGHT 1

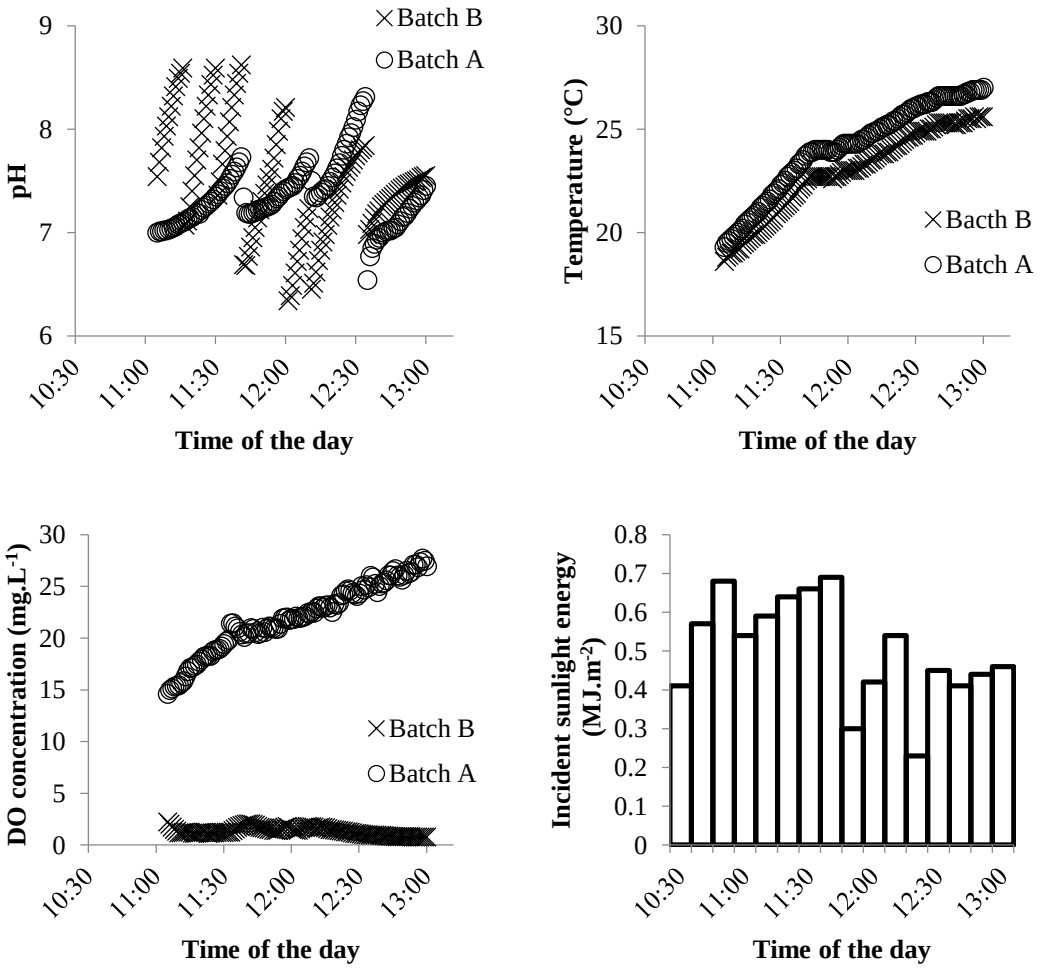

Figure S16 - 4: pH, temperature, DO concentration and incident sunlight energy variations during the first phase of bench-scale experiment carried out on 14/11/2017

EXPERIMENT OF THE 14/11/2017 – LIGHT 2

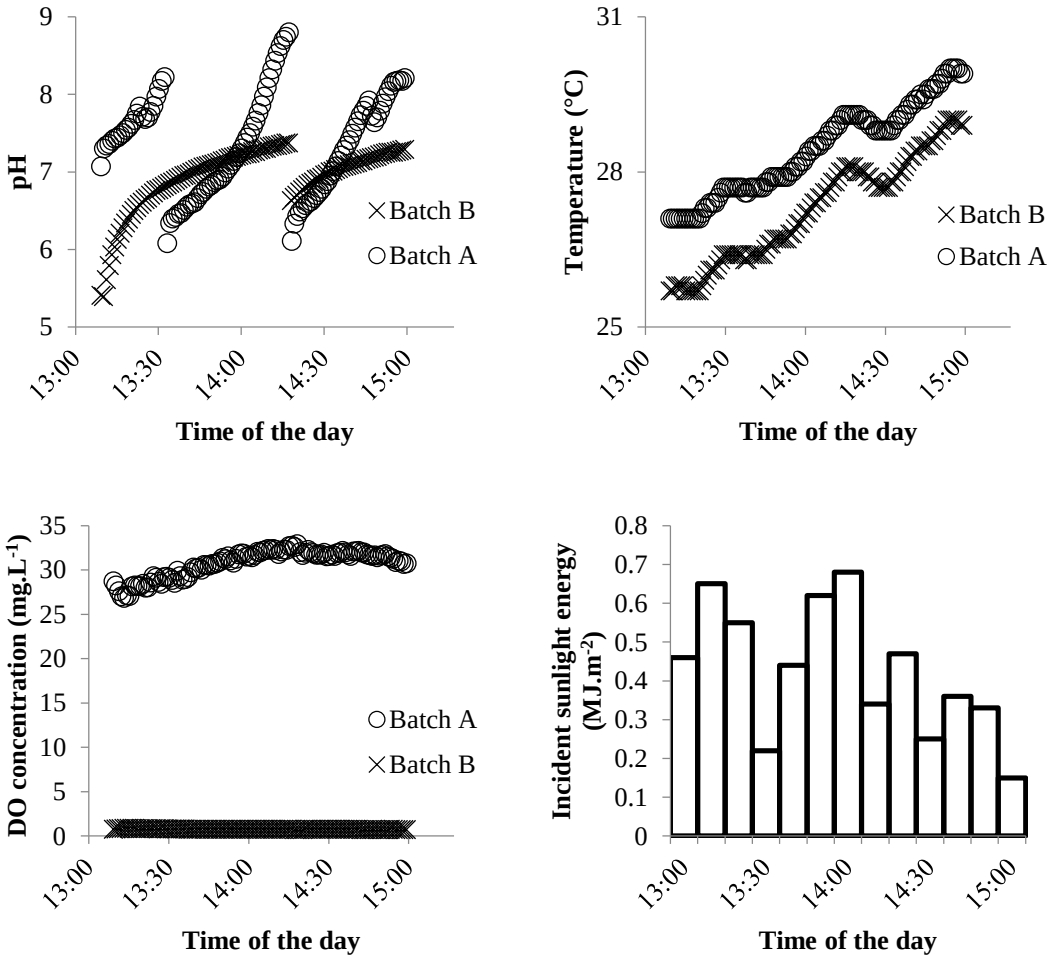

Figure S16 - 5: pH, temperature, DO concentration and incident sunlight energy variations during the second phase of bench-scale experiment carried out on 14/11/2017

EXPERIMENT OF THE 14/11/2017 – DARK

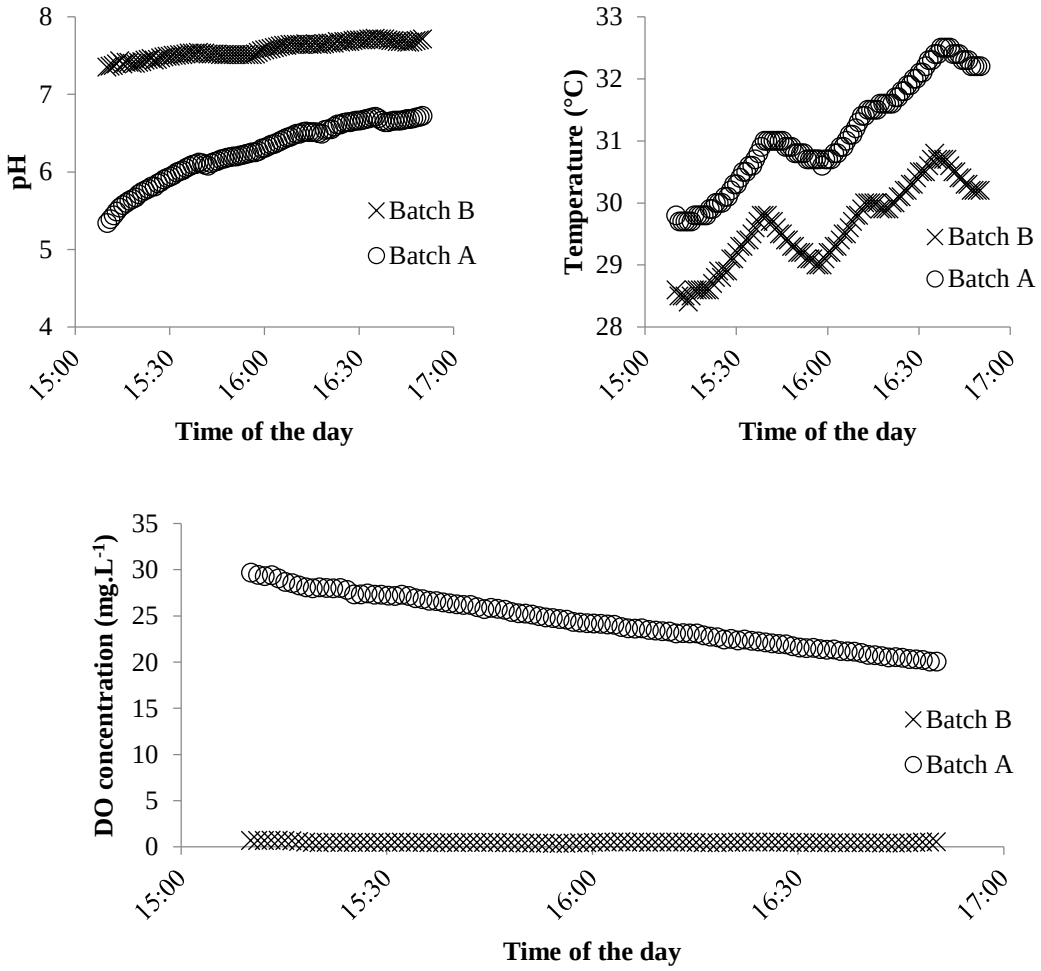

Figure S16 - 6: pH, temperature, and DO concentration variations during the third phase of bench-scale experiment carried out on 14/11/2017

EXPERIMENT OF THE 16/11/2017 – LIGHT 1

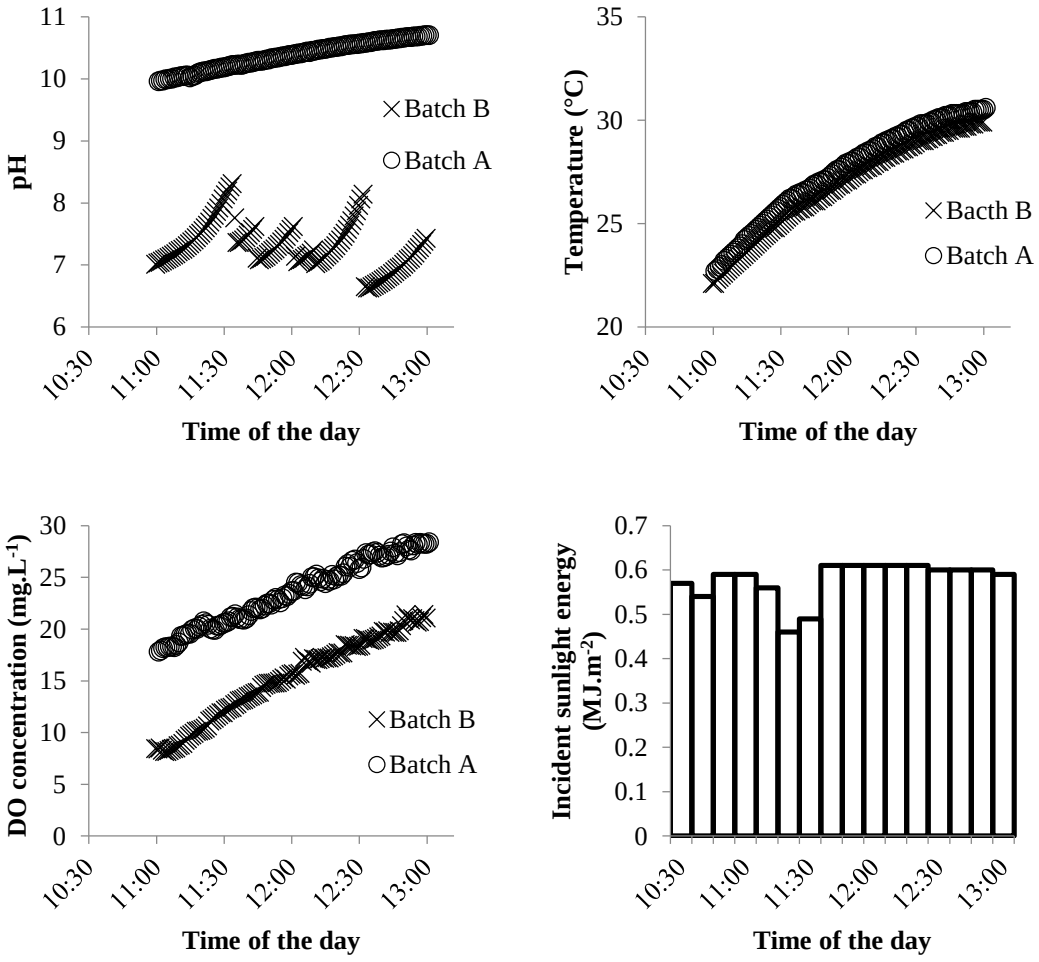

Figure S16 - 7: pH, temperature, DO concentration and incident sunlight energy variations during the first phase of bench-scale experiment carried out on 16/11/2017

EXPERIMENT OF THE 16/11/2017 – LIGHT 2

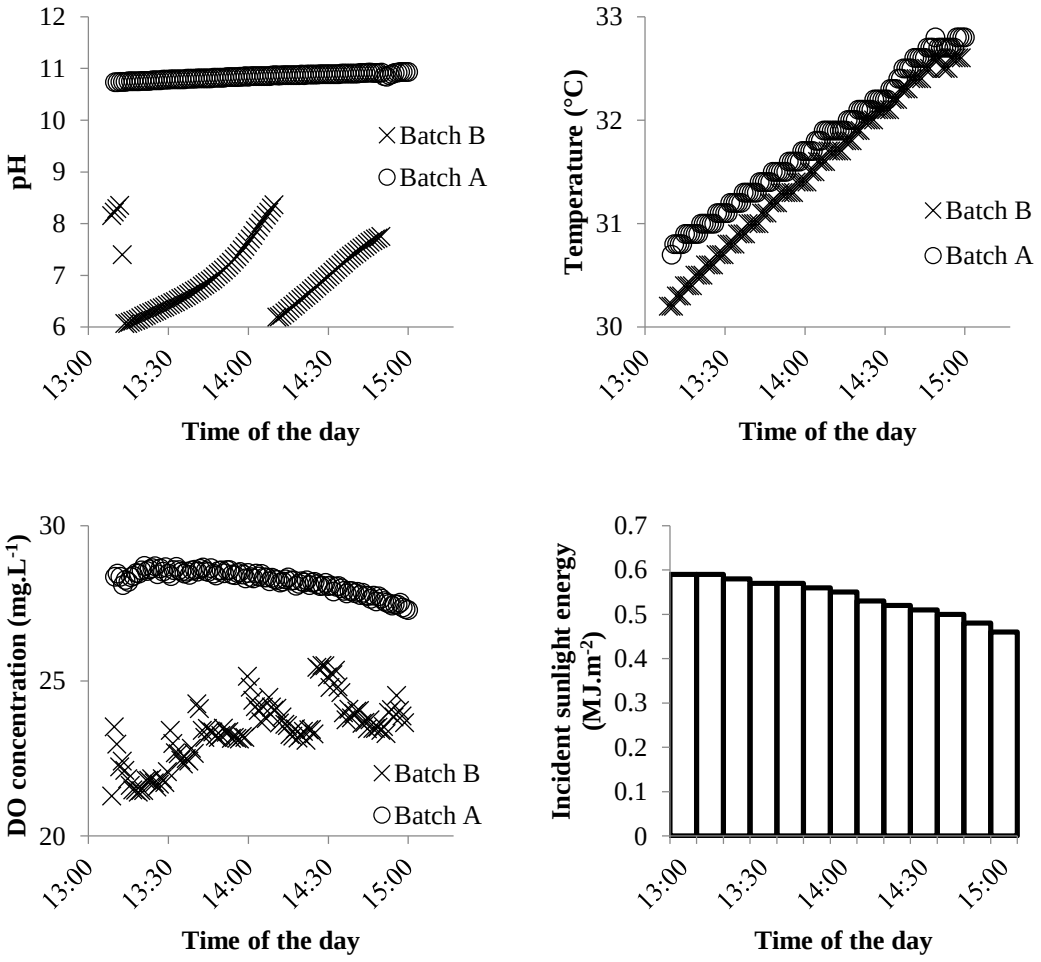

Figure S16 - 8: pH, temperature, DO concentration and incident sunlight energy variations during the second phase of bench-scale experiment carried out on 16/11/2017

EXPERIMENT OF THE 16/11/2017 – DARK

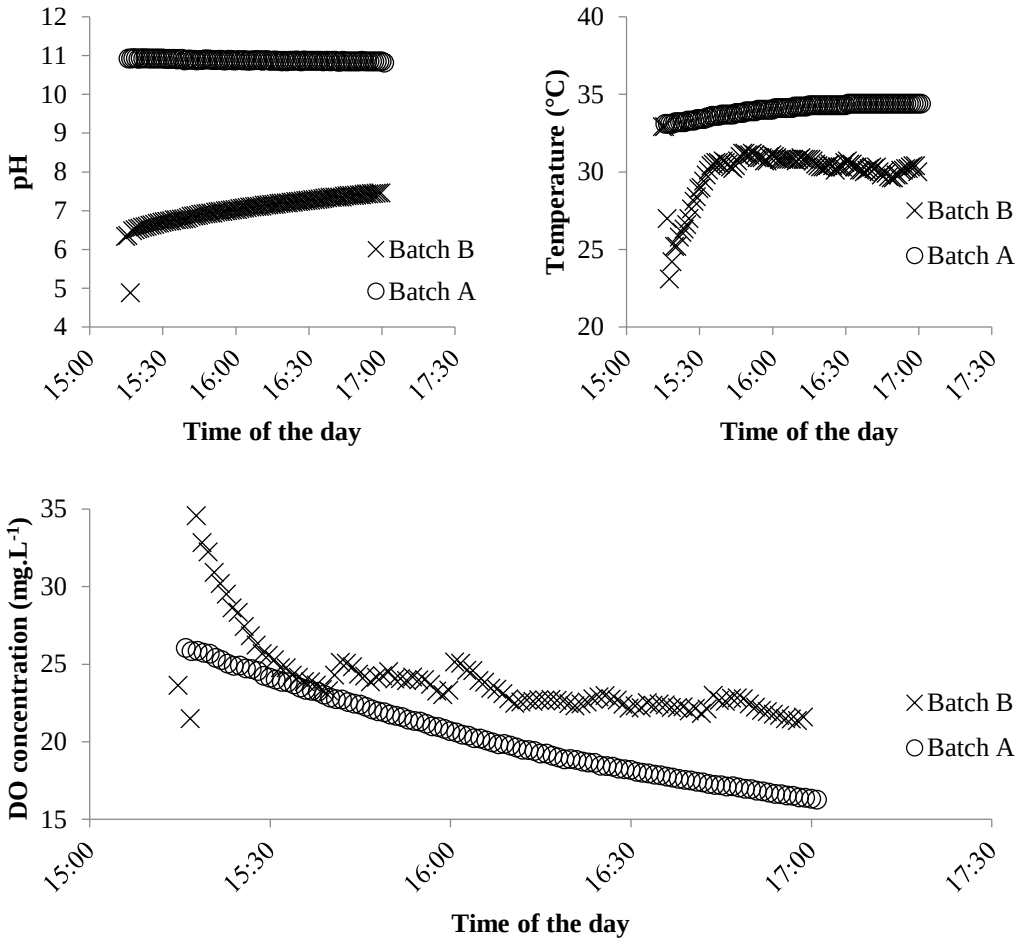

Figure S16 - 9: pH, temperature, and DO concentration variations during the third phase of bench-scale experiment carried out on 16/11/2017

EXPERIMENT OF THE 23/11/2017 – LIGHT 1

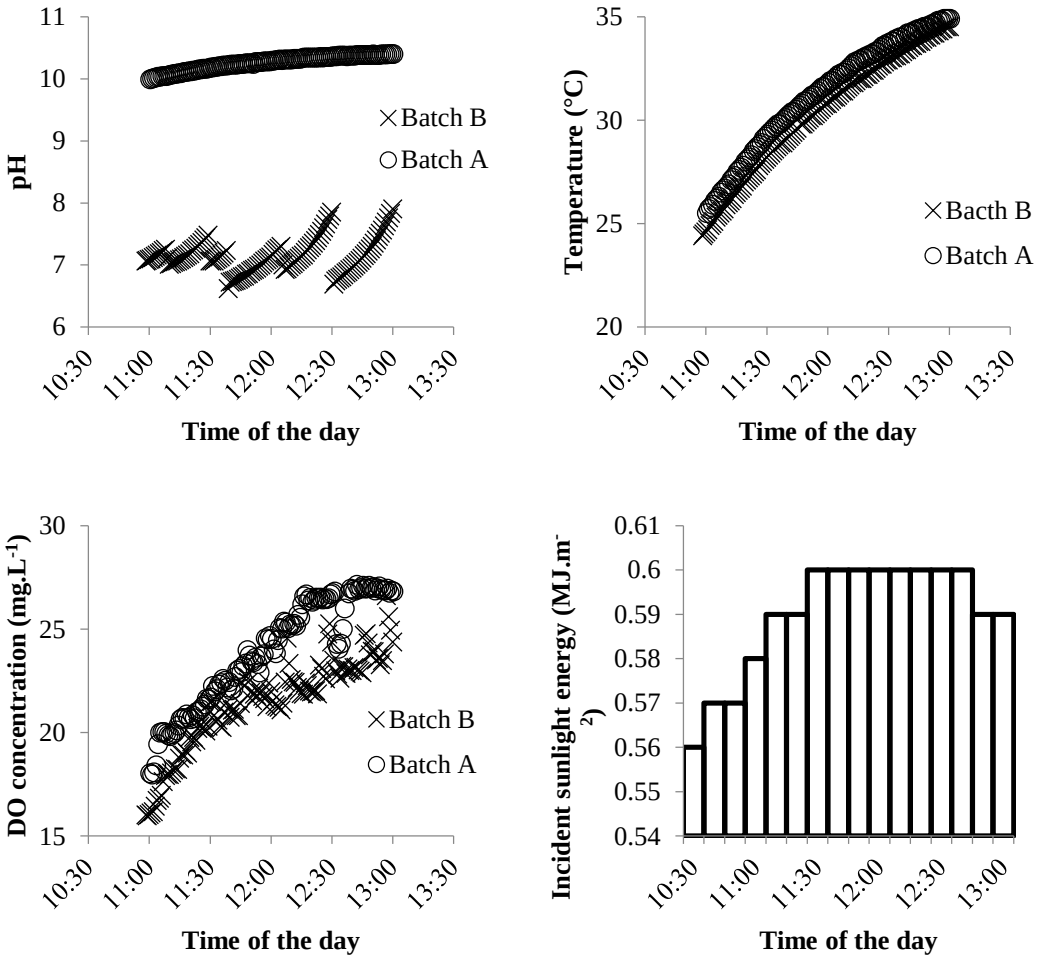

Figure S16 - 10: pH, temperature, DO concentration and incident sunlight energy variations during the first phase of bench-scale experiment carried out on 23/11/2017

EXPERIMENT OF THE 23/11/2017 – LIGHT 2

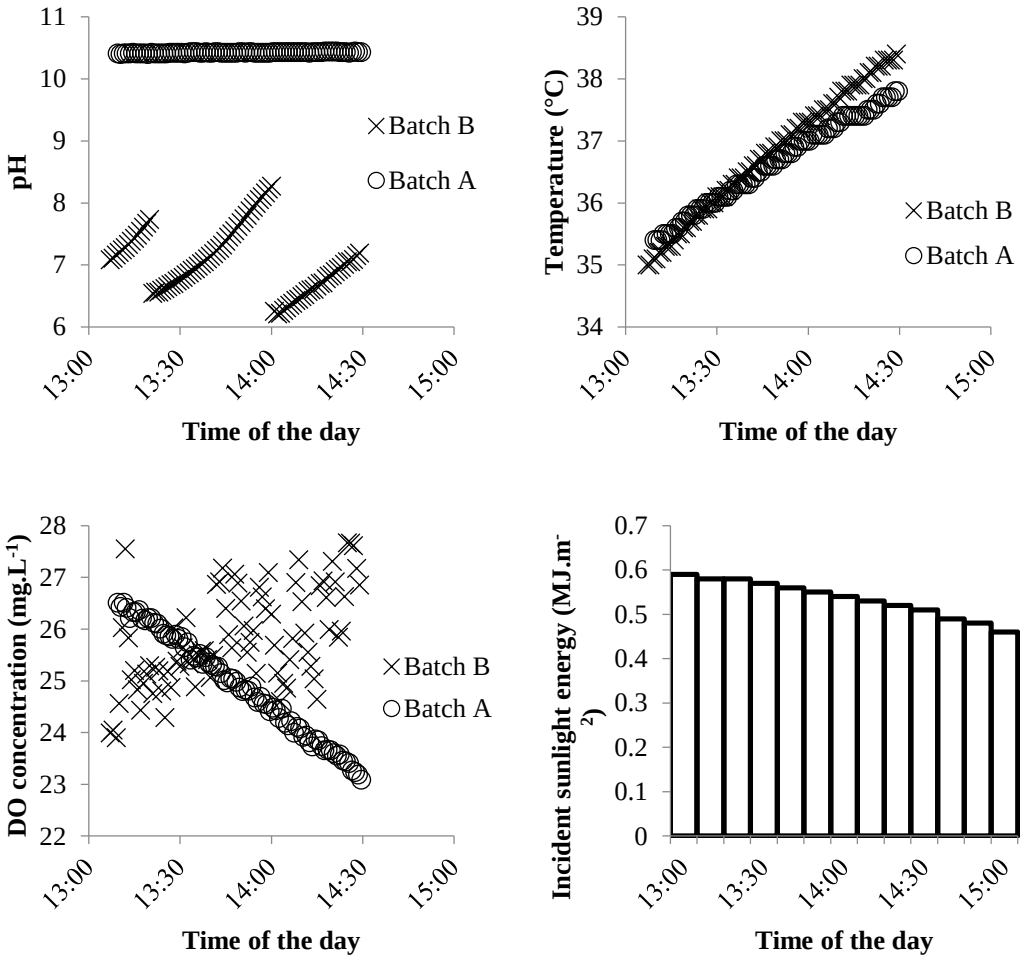

Figure S16 - 11: pH, temperature, DO concentration and incident sunlight energy variations during the second phase of bench-scale experiment carried out on 23/11/2017

EXPERIMENT OF THE 23/11/2017 – DARK

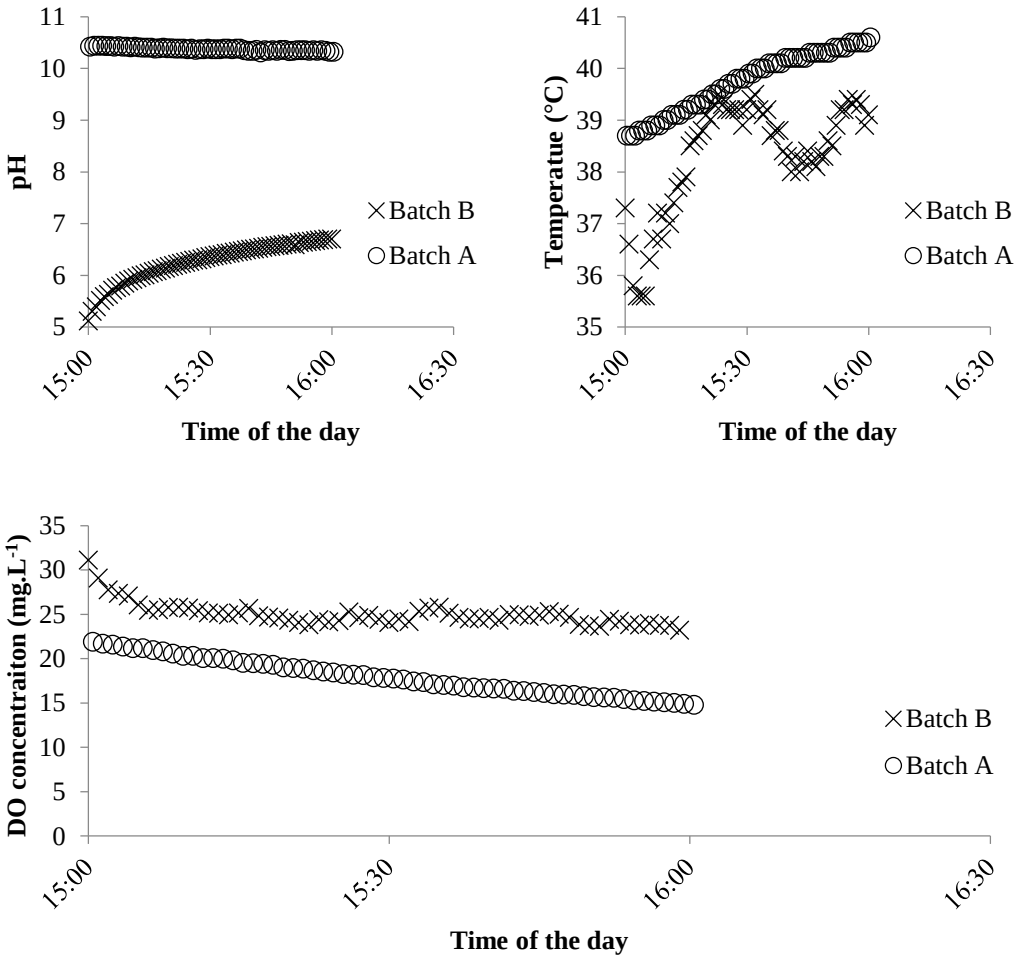

Figure S16 - 12: pH, temperature, and DO concentration variations during the third phase of bench-scale experiment carried out on 23/11/2017

APPENDIX 17. DIFFERENCES BETWEEN LABORATORY SCALE AND BENCH SCALE EXPERIMENTS POTENTIALLY EXPLAINING DISCREPANCIES IN THE OBSERVED MAGNITUDE OF *E. COLI* DECAY MECHANISMS

During laboratory scale experiments, *E. coli* decay was mainly caused by sunlight direct damage and pH toxicity, while natural decay (decay of *E. coli* in the absence of known harmful conditions) and algae toxicity were not significant. In contrast, *E. coli* dark decay was the most significant mechanism at bench scale while sunlight-mediated mechanisms had little impact on *E. coli* decay. pH toxicity was significant but substantially lower than at laboratory scale. Table S17 - 1 summarizes and compares experimental conditions used at laboratory and bench scales, in order to determine potential causes of discrepancies.

Table S17 - 1: Experimental conditions during laboratory and bench scale experiments and discussion on their respective impact for *E. coli* on the rates of natural and uncharacterized dark decay, sunlight direct damage, and pH toxicity

Experimental condition	Laboratory scale	Bench scale	Potential impact on characterized mechanisms of *E. coli* decay
Counting method	Pour plate method	Quanti-Tray method	In distilled water we found no difference between the two broadly used methods. It is however possible that in real effluents, *E. coli* viability (Quanti-Tray) could be higher than cultivability (pour plate). As the opposite is more unlikely, differences in counting methods unlikely explain why natural decay was higher at bench scale than at lab scale. Differences in methods may however explain the higher impact of pH recorded at laboratory scale.
Temperature	5 – 40°C	28 – 40°C	The ranges tested were similar during both experiments so this parameter unlikely explains the discrepancies observed.
pH	7 – 10	6 – 10.9	The ranges tested were similar during both experiments so this parameter unlikely explains the discrepancies observed.

Experimental condition	Laboratory scale	Bench scale	Potential impact on characterized mechanisms of *E. coli* decay
Light source **Light intensity** **Dissolved and suspended materials**	Natural sunlight 500 - 1,000 $W.m^{-2}$ RO water WW filtrates HRAP filtrates Phosphate buffer Carbonate buffer	Natural sunlight 400 - 1,000 $W.m^{-2}$ Comprehensive HRAP broth (following high light exposure) meaning presence of algae and algal products, chemicals originating from domestic wastewater, other micro-organisms	Different light conditions could lead to the release of different compounds (algae metabolites or others) with different antibiotic efficiencies in the dark. While the same light source and intensities were used on lab and bench assays, the presence of algae in the bench assay could therefore explain the higher natural decays reported. Light supply does not explain differences in the impact of sunlight-mediated disinfection which was probably caused by difference in light absorption. Differences in light supply also unlikely explained differences in pH toxicity, but the presence of suspended solids during bench scale experiments probably contributed to the formation of flocs of *E. coli* cells known to enhance bacterial survival at high pH, as observed in during bench scale experiments.
DO concentration	Aerobic (not measured, likely at saturation)	< 2 $mg.L^{-1}$ or > 16 $mg.L^{-1}$	High impact of sunlight intensity on *E. coli* decay was expected at high DO concentration but was not observed. Therefore, DO concentration was concluded not to explain the comparatively low sunlight mediated decay of *E. coli* at bench scale. In addition, no interference of DO concentration was expected with pH toxicity and natural decay.
Duration	Up to several days	~2h	Differences in duration may only explain difference in natural decays if *E coli* cells were able to recovery after a rapid and short phase of 'inactivation' (recorded by the Quanti-Tray method). This is however very unlikely as *E coli* is not known to grow in wastewater (in non-tropical environment) and as short-term tests during lab-scale never evidenced initial drop in cultivability followed by recovery. As decay from direct sunlight exposure and pH-toxicity were both consistently following first order kinetics, the duration of the experiment should not influence the decay rates measured.
History of *E. coli* cells	*E. coli* cells were inoculated from the resuspension of cells freshly cultivated under laboratory conditions, therefore probably still in exponential growth phase.	*E. coli* already present in the HRAP broth were mixed with *E. coli* cells freshly cultivated under laboratory conditions (likely still in exponential growth phase).	Lab-cultured *E. coli* cells could be fitter than the *E. coli* cells already present in the HRAP broth. The lab-cultured cells at the start of each bench scale assay accounted for at least 50% of the total *E. coli* cells. Lab-cultured cells have been shown to be less resistant to different sources of stress than 'wild' *E. coli* (e.g. pH and sunlight damage, see Appendix 15). However, the use of a strain of 'wild-type' *E. coli* isolated from wastewater samples at the beginning of this study mitigated this effect.

APPENDIX 18. CALCULATION OF FIRST ORDER *E. COLI* DECAY RATE DUE TO DIRECT SUNLIGHT DAMAGE IN FULL ALGAL BROTH

This paragraph shows how Equation 5 - 2 in Chapter 5 section 5.2.1. describing the decay of *E. coli* linked to direct sunlight exposition (i.e. including direct DNA damage and endogenous photo-oxidation in normal conditions[196]) was developed.

PROBLEM

We demonstrated in Chapter 4 section 4.2.2.1. that the decay of *E. coli* in a volume exposed to uniform sunlight intensity I ($W.m^{-2}$) follows a first order law which coefficient k_d (d^{-1}) is described by Equation S18 – 1.

$$k_d = 0.0678.I \quad \text{(S18 - 1)}$$

In the following, we aim at finding the apparent first order decay coefficient of *E. coli* in a full algal broth of optical density σ (m^{-1}), surface S (m^2), depth d (m), and exposed to incident sunlight intensity I_0 (assumed to reach the algal broth vertically).

CALCULATIONS

The sunlight intensity distribution in the algal broth is assumed to follow a Beer-Lambert law in the algal broth (Béchet et al., 2015; Bello et al., 2017; Dahl et al., 2017), i.e. the light intensity at a depth z[197] is calculated thanks to Equation S18 - 2.

$$I(z) = I_0.\exp(-\sigma.z) \quad \text{(S18 - 2)}$$

Sunlight intensity is therefore uniform at depth z and total *E. coli* decay can be calculated for a pond layer dz of given depth, the decay coefficient for a volume $S.dz$ between the depths z and $z + dz$ being given by Equation S18 - 3.

$$k_d(z) = 0.0678.I_0.\exp(-\sigma.z) \quad \text{(S18 - 3)}$$

The variation of *E. coli* cells counts $C(z,t)$ during an infinitesimal time step δt at depth z is found based on Equation S18 - 4, when assuming no *E. coli* cell enters or escapes from another layer of the broth (reasonable assumption for δt low enough).

$$C(z, t + \delta t) = C(z,t).[1 - 0.0678.I_0.\exp(-\sigma.z)] \quad \text{(S18 - 4)}$$

[196] I.e. at neutral pH and non-supersaturated DO concentration.
[197] Where $z = 0$ at the pond surface and $z > 0$ below the pond surface.

Since the total cell count in the volume is the mean of the concentration at every infinitesimal depth (as given by Equation S18 – 5) if the HRAP is assumed well mixed, the apparent cell count in the HRAP at the instant $t + \delta t$ is given by Equation S18 - 6, as a consequence of Equations S18 - 4 and S18 - 3.

$$C(t + \delta t) = \frac{1}{V} . \int_{z=0}^{d} C(z, t + \delta t) . S . dz \quad \text{(S18 - 5)}$$

$$C(t + \delta t) = C(t) . [\, 1 - \frac{0.0678 . I_0}{\sigma . d} . \exp(-\sigma . d) \, . \, \delta t] \quad \text{(S18 - 6)}$$

Equation S18 – 6 is analogous to a first order decay law[198] at a rate k_d described by.

$$k_d = \frac{0.0678 . I_0}{\sigma . d} . \exp(-\sigma . d) \quad \text{(S18 - 7)}$$

This decay rate is used directly from Chapter 5 to model the first order decay of *E. coli* due to direct sunlight exposition in the full HRAP broth.

[198] Neglecting any feed or loss of *E. coli* cells

APPENDIX 19. INFLUENCE OF ATTACHMENT TO SOLIDS ON THE QUANTIFICATION OF *E. COLI* CELL DENSITY IN WASTEWATER AND HRAP SAMPLES USING QUANTI-TRAY METHOD

The attachment of bacterial and viral pathogens to solids settling into ponds has been reported as a potentially significant mechanism of pathogens removal in the literature (Dias et al., 2017). As the settling of suspended solids is not expected to occur in HRAPs (continuous mixing), the attachment of pathogens to solids was not considered as removal mechanisms during this study.

However, because Quanti-Tray measurement accuracy relies on the isolation of single cells at known dilution, suspended materials which adsorbed several *E. coli* cells may be counted as one single cell during this procedure, and could therefore put at risk the accuracy of *E. coli* cell count obtained from this method. Therefore, attachment of *E. coli* cells to solids in HRAP samples was investigated.

Five wastewater and six HRAP A samples were collected in 1.5 mL Eppendorf tubes at PNCC wastewater treatment plant (site described in Chapter 2 section 2.2.1.1.), and subjected to the following procedures aiming at detaching potentially attached bacteria: two samples were vortexed in Eppendorf tubes (vortex mixer Scilogex® MX-S, set on maximal speed), two samples were 'forced' through a narrow syringe (TERUMO U-100 INSULIN 0.5 mL 29G x ½") as performed by Ansa et al. (2012), and two samples were kept untreated as controls (only one sample for wastewater). The wastewater and HRAP samples were then diluted by a factor 10^6 and 10^3 times respectively, and analyzed for total coliform and *E. coli* cell counts using the IDEXX Quantitray® Colilert-18® procedure as described in Appendix 5. This entire procedure was conducted within two hours after sample collection.

Results from the Quanti-Tray measurements are shown in Figure S19 - 1 for wastewater (a) and HRAP (b) samples. As can be seen, sample pre-treatment to separate bacteria from suspended solids did not significantly impact *E. coli* cell count (confirmed by one sample t-tests at the 5% significance level[199]).

[199] When testing that *E. coli* cell counts minus the average of control *E. coli* cell counts is of average 0. Confidence interval $[-2.72 \cdot 10^6 ; 2.72 \cdot 10^6]$ and $[-4.69 \cdot 10^3 ; 4.69 \cdot 10^3]$ MPN.100 mL^{-1}, p-value 1 and 0.999 for wastewater and HRAP *E. coli* counts respectively.

Cell attachment to solids was therefore not considered to impact measurement accuracy.

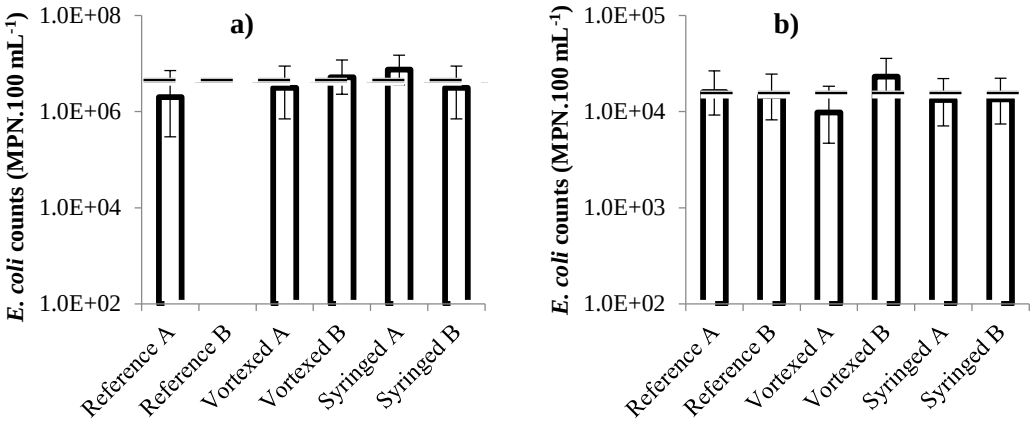

Figure S19 - 1: *E. coli* counts measured in wastewater (a) and HRAP (b) samples according to the different solids separation methods used.
Dashed lines represent the average *E. coli* counts measured for all samples, and uncertainty bars represent the uncertainty associated to the MPN method

APPENDIX 20. BIOLOGICAL REACTIONS CONTRIBUTING TO PH CHANGES IN HRAP AND ASSOCIATED STOICHIOMETRY

The stoichiometry of algal growth was determined assuming ammonium was used a nitrogen source (Béchet et al., 2015) and the algal biomass composition (both active and debris) was $C_{416}H_{749}O_{228}N_{29}$ (Illman et al., 2000):

$$416 \cdot CO_2 + 29 \cdot NH_4^+ + 331 \cdot H_2O \rightarrow C_{416}H_{749}O_{228}N_{29} + 467.5 \cdot O_2 + 29 \cdot H^+ \quad \text{(S20 - 1)}$$

The stoichiometry of algal decay was determined assuming N was released as ammonium:

$$C_{416}H_{749}O_{228}N_{29} + 467.5 \cdot O_2 + 29 \cdot H^+ \rightarrow 416 \cdot CO_2 + 29 \cdot NH_4^+ + 331 \cdot H_2O \quad \text{(S20 - 2)}$$

The stoichiometry of heterotrophic growth was determined assuming the molecular compositions of bCOD[200] and heterotrophic biomass were $C_{10}H_{19}NO_3$ and $C_5H_7NO_2$, respectively. Assuming a true synthetic yield of 0.40 g VSS/g bCOD (Metcalf and Eddy Inc., 2003) and a COD equivalent of 1.990 g bCOD/g $C_{10}H_{19}NO_3$[201], the synthetic yield was converted to 0.796 g VSS/g $C_{10}H_{19}NO_3$, yielding the following equation:

$$0.706 \cdot C_{10}H_{19}NO_3 + 3.83 \cdot O_2 + 0.294 \cdot NH_4^+ \rightarrow C_5H_7NO_2 + 0.294 \cdot H^+ + 2.06 \cdot CO_2 + 3.65 \cdot H_2O \quad \text{(S20 - 3)}$$

Heterotrophic decay can then be described as (Metcalf and Eddy Inc., 2003):

$$C_5H_7NO_2 + 5\ O_2 + H^+ \rightarrow NH_4^+ + 2\ H_2O + 5\ CO_2 \quad \text{(S20 - 4)}$$

The stoichiometry of nitrification was represented as (Metcalf and Eddy Inc., 2003):

$$95.1 \cdot O_2 + 5 \cdot CO_2 + 51.0 \cdot NH_4^+ \rightarrow C_5H_7NO_2 + 50 \cdot NO_3^- + 48.1 \cdot H_2O + 101 \cdot H^+ \quad \text{(S20 - 5)}$$

[200] Assumed to be the only carbon source for heterotrophs growth in the wastewater.
[201] $C_{10}H_{19}NO_3 + 17 \cdot H_2O \rightarrow 10 \cdot CO_2 + NH_4^+ + 49 \cdot H^+ + 50 \cdot e^-$ meaning 12.5 moles of O_2 are required for the oxidation of 1 mole of $C_{10}H_{19}NO_3$.

Nitrifier decay was considered to have a negligible impact on total nitrifier biomass formation.

ALGAL GROWTH

The net volumetric rate of algae growth (r^a, kg VSS·m^{-3}·s^{-1}) was calculated as the difference between the photosynthesis (r_g^a, kg VSS·m^{-3}·s^{-1}) and decay (r_d^a, kg VSS·m^{-3}·s^{-1}) volumetric rates:

$$r^a = r_g^a - r_d^a \quad \text{(S20 - 6)}$$

Where the rate of photosynthesis was predicted based on the model of Béchet et al. (2013) as:

$$r_g^a = \frac{IC}{K_C^a + IC} \cdot \frac{PE \cdot E}{HV \cdot V} \quad \text{(S20 - 7)}$$

Where X_{act}^a (g·m^{-3}) is the active algae concentration in the HRAP, IC (kg C·m^{-3}) is the total concentration of inorganic carbon, K_C^a (kg C·m^{-3}) the saturation constant for *IC*, HV the algae heat value (MJ·kg VSS^{-1}), V (m^3) the HRAP volume, PE the photosynthetic efficiency, and E (W) the amount of Photosynthetically Active Radiation (PAR) received by the algae. As can be seen, the impact of *IC* was estimated using a Monod function added to the original model of Béchet et al. (2013), based on the literature (Bai et al., 2015; Costache et al., 2013; Lee and Zhang, 2016; Malek et al., 2016). E was calculated assuming the HRAP broth was completely opaque resulting in the following equation:

$$E = 0.47 \cdot Hs \cdot S \quad \text{(S20 - 8)}$$

Where 0.47 is the PAR fraction of the total solar spectrum, Hs the total incident sunlight radiations (W·m^{-2}), and S the HRAP surface (m^2).

The rate of algae decay was computed as:

$$r_d^a = \frac{DO}{K_{DO}^a + DO} \cdot k^a \cdot X_{act}^a(t) \quad \text{(S20 - 9)}$$

Where DO (kg O_2·m^{-3}) is the dissolved O_2 concentration, K_{DO}^a (kg O_2·m^{-3}) the saturation constant of algae for DO, and k_a (s^{-1}) the specific algal decay rate. The impact of DO concentration was therefore modelled using a Monod function according to Solimeno et al. (2015) and k^a was computed based on the approach used by Metcalf and Eddy Inc. (2003) for heterotrophic biomass:

$$k^a = k_{20}^a \cdot \theta_{k_d}^{(T_p - 293.15)} \quad \text{(S20 - 10)}$$

where k_{20}^a (s^{-1}) is the algae endogenous decay rate at 20°C, θ_{k_d} the correction factor for temperature, and T_p the pond temperature (K).

The active algae concentration in the HRAP (X_{act}^a, $g \cdot m^{-3}$) was predicted using a mass balance as:

$$X_{act}^a(t + dt) = X_{act}^a(t) - \rho_s \cdot \frac{q_{out}}{V} \cdot X_{act}^a \cdot dt + r^a \cdot dt \quad \text{(S20 - 11)}$$

Where ρ_s is the fraction of suspended materials effectively washed out (see Appendix 21 for experimental determination), q_{out} ($m^3 \cdot s^{-1}$) is the outlet flow, and dt (s) is the time-step of the calculation.

The algal biomass debris concentration (X_{deb}^a, $g \cdot m^{-3}$) was determined by mass balance analysis:

$$X_{deb}^a(t + dt) = X_{deb}^a(t) + f_d \cdot r_d^a \cdot dt - \rho_s \cdot \frac{q_{out}}{V} \cdot X_{deb}^a(t) \quad \text{(S20 - 12)}$$

Where f_d represents the fraction of biomass decayed (either algal or bacterial) that is converted into inert solids. The total algae concentration (X_T^a, $g \cdot m^{-3}$) is calculated as the sum of the active and debris algae concentrations.

HETEROTROPHS GROWTH

The net volumetric rate of heterotrophic growth (r^h, kg $VSS \cdot m^{-3} \cdot s^{-1}$) was calculated as the difference between the growth (r_g^h, kg $VSS \cdot m^{-3} \cdot s^{-1}$) and decay ($r_d^h$, kg $VSS \cdot m^{-3} \cdot s^{-1}$) volumetric rates as:

$$r^h = r_g^h - r_d^h \quad \text{(S20 - 13)}$$

The growth volumetric rate was predicted using Monod growth kinetic (Metcalf and Eddy Inc., 2003):

$$r_g^h = \frac{DO}{K_{DO}^h + DO} \cdot X_{act}^h \cdot \left(\frac{\mu \cdot bCOD}{K_S^h + bCOD} \right) \quad \text{(S20 - 14)}$$

Where DO (kg $O_2 \cdot m^{-3}$) is the dissolved O_2 concentration, K_{DO}^h (kg $O_2 \cdot m^{-3}$) the saturation constant of heterotroph for DO, X_{act}^h (kg VSS m^{-3}) the concentration of active heterotrophs, μ (s^{-1}) the heterotrophic specific growth rate, $bCOD$ the bCOD concentration (kg $COD \cdot m^{-3}$), and K_S the saturation constant for bCOD (kg $COD \cdot m^{-3}$).

The decay volumetric rate was predicted using first order kinetics (Metcalf and Eddy Inc., 2003):

$$r_d^h = \frac{DO}{K_{DO}^h + DO} \cdot X_{act}^h \cdot k^h \quad \text{(S20 - 15)}$$

Where k^h (s^{-1}) is the heterotroph decay rate. The kinetic constants were adjusted for temperature[202] based on Metcalf and Eddy Inc. (2003). K_{DO}^h, which variability's impact on model predicitons was determined negligible during sensitivity analysis (see Section 6.3.) was not adjusted for temperature.

$$\mu = \mu_{20} \cdot \theta_\mu^{(T_p - 293.15)} \quad \text{(S20 - 16)}$$

$$K_S^h = K_{S_{20}}^h \cdot \theta_{K_S}^{(T_p - 293.15)} \quad \text{(S20 - 17)}$$

$$k^h = k_{d_{20}}^h \cdot \theta_{k_d}^{(T_p - 293.15)} \quad \text{(S20 - 18)}$$

Changes in X_{act}^h were then computed based on the mass balance as:

$$X_{act}^h(t + dt) = X_{act}^h(t) + \frac{q_{in}}{V} \cdot X_{in}^h \cdot dt - \rho_s \cdot \frac{q_{out}}{V} \cdot X_{act}^h \cdot dt + r^h \cdot dt \quad \text{(S20 - 19)}$$

Where X_{in}^h (kg VSS·m^{-3}) is the active heterotroph concentration in the inlet. Changes in associated debris concentration (X_{deb}^h, kg VSS·m^{-3}) were computed using the following mass balance:

$$X_{deb}^h(t + dt) = X_{ded}^h(t) - \rho_s \cdot \frac{q_{out}}{V} * X_{deb}^h(t) \cdot dt + f_d \cdot r_d^h \cdot dt \quad \text{(S20 - 20)}$$

Changes in bCOD concentration were computed using the following mass balance for substrate:

$$bCOD(t + dt) = bCOD(t) + \frac{q_{in}}{V} \cdot bCOD_{in} \cdot dt - \frac{q_{out}}{V} \cdot bCOD(t) \cdot dt - \frac{1}{Y} \cdot r_g^h \cdot dt \quad \text{(S20 - 21)}$$

Where $bCOD_{in}$ is the bCOD concentration in the inlet (kg COD·m^{-3}).

[202] K_{DO}^h was assumed independent of temperature. Although low variations of K_{DO}^h with temperature could be expected, the sensitivity analysis showed that small variations of K_{DO}^h had a minor impact on the model outputs.

NITRIFICATION

The volumetric rate of growth of nitrifying bacteria (r^n, kg VSS·s^{-1}) was calculated by assuming a constant yield of nitrification[203] (Y_{nit}, kg VSS·kg NO_3^-) and a negligible production of debris:

$$r^n = Y^n \cdot [NO_3^-] \cdot \frac{q_{out}}{V} \quad \text{(S20 - 22)}$$

Where $[NO_3^-]$ (kg NO_3^-·m^{-3}) is the concentration of nitrate in the HRAP. Changes in nitrifier concentration were computed by mass balance assuming no nitrifying bacteria is present in the inlet.

$$X^n(t+dt) = X^n(t) - \rho_s \cdot \frac{q_{OUT}}{V} \cdot X^n(t) \cdot dt + r^n \cdot dt \quad \text{(S20 - 23)}$$

[203] As nitrite concentration was generally negligible in the HRAP (median concentration 0.38 mg.L^{-1}, N = 184), the nitrifying activity was assumed to oxidize ammonium in nitrate only

APPENDIX 21. SOLIDS SEDIMENTATION RATE IN PILOT SCALE HRAPS

Due to non-turbulent laminar flow in the loop of the pilot scale HRAPs, suspended materials were suspected to experience settling when flowing from the paddlewheel. Because the outlet of the pilot scale HRAPs collected water directly from the surface of the ponds, such settling could have led to an accumulation of suspended solids compared with a true well-mixed system, as hypothesized in the model developed in this study (Chapter 6). In situ investigations were thus performed to determine the extent of settling experienced by suspended solids in pilot scale HRAPs.

MATERIAL AND METHODS

Two 100 mL samples of the pilot scale HRAPs were grabbed (experiment performed on 16/04/2018). One sample was collected from the water top layer, by dipping the sampling flasks just below the surface, and one sample was collected from the bottom layer, by maintaining the sampling flask upside down until reaching the HRAP bottom, then flipping the flask, and leaving it at the bottom of the water column to fill up with algal both before bringing it back to the surface. Samples were collected on both pilot scale HRAPs of the study.

TSS for the 4 samples were measured in triplicates, quantified via dry weights measurements following the standard method 2540.D using GF/C™ grade (General Electric®) fiberglass filters (Eaton et al., 1998).

RESULTS AND CONCLUSION

9 estimates of the sedimentation rate were obtained from each pond. The average sedimentation rate[204] measured in HRAP A was 0.814 (std = 0.029) and in HRAP B was 0.783 (std = 0.064) for an average TSS concentration in the upper layer of 207.8 and 240.0 $mg.L^{-1}$ respectively.

A sedimentation rate of 0.8 was concluded from this study, and used during simulations (Chapter 6 and Chapter 7).

[204] Calculated as the ratio of TSS in the upper layer by TSS in the lower layer of HRAP broth.

APPENDIX 22. COEFFICIENTS OF THE POLYNOMIAL SOLVING pH IN THE HRAP

The coefficients of the polynomial used in model simulations to solve $[H^+]$ equilibrium (see Chapter 6 section 6.2.1.3.) are shown in Table S22 - 1. These coefficients are calculated from the values for equilibrium constants presented in Table 6 - 7, and the values for the total ammoniacal nitrogen IN, the total inorganic phosphorous IP, the total inorganic carbon IC, and the wastewater electroneutrality Σ as defined in Chapter 6 section 6.2.1.3.

Table S22 - 1: Coefficients of the polynomial used for solving of $[H^+]$

$\boldsymbol{a_0} =$	1
$\boldsymbol{a_1} =$	$\Sigma + K_{C1} + K_{P2} + K_N + IN - IP$
$\boldsymbol{a_2} =$	$K_{C1} \cdot K_{P2} + K_{C1} \cdot K_N + K_{C1} \cdot K_{C2} + K_{P2} \cdot K_N + K_{P2} \cdot K_{P3} + \Sigma \cdot (K_{C1} + K_{P2} + K_N) - K_w + IN \cdot (K_{C1} + K_{P2}) - IP \cdot (K_{C1} + K_N) - 2 \cdot IP \cdot K_{P2} - K_{C1} \cdot IC$
$\boldsymbol{a_3} =$	$K_{C1} \cdot K_{C2} \cdot K_{P2} + K_{C1} \cdot K_{C2} \cdot K_N + K_{C1} \cdot K_N \cdot K_{P2} + K_{P2} \cdot K_{P3} \cdot K_N + K_{P2} \cdot K_{P3} \cdot K_{C1} + \Sigma \cdot (K_{C1} \cdot K_{P2} + K_{C1} \cdot K_N + K_{C1} \cdot K_{C2} + K_{P2} \cdot K_N + K_{P2} \cdot K_{P3}) - K_w \cdot (K_{C1} + K_{P2} + K_N) + IN \cdot (K_{C1} \cdot K_{P2} + K_{C1} \cdot K_{C2} + K_{P2} \cdot K_{P3}) - IP \cdot (K_{C1} \cdot K_{C2} + K_{C1} \cdot K_N) - 2 \cdot IP \cdot K_{P2} \cdot (K_{C1} + K_N) - 3 \cdot IP \cdot K_{P2} \cdot K_{P3} - K_{C1} \cdot IC \cdot (K_{P2} + K_N) - 2 \cdot K_{C1} \cdot K_{C2} \cdot IC$
$\boldsymbol{a_4} =$	$K_{C1} \cdot K_{C2} \cdot K_{P2} \cdot K_N + K_{C1} \cdot K_{C2} \cdot K_{P2} \cdot K_{P3} + K_{C1} \cdot K_N \cdot K_{P2} \cdot K_{P3} + \Sigma \cdot (K_{C1} \cdot K_{C2} \cdot K_{P2} + K_{C1} \cdot K_{C2} \cdot K_N + K_{C1} \cdot K_N \cdot K_{P2} + K_{P2} \cdot K_{P3} \cdot K_N + K_{P2} \cdot K_{P3} \cdot K_{C1}) - K_w \cdot (K_{C1} \cdot K_{P2} + K_{C1} \cdot K_N + K_{C1} \cdot K_{C2} + K_{P2} \cdot K_N + K_{P2} \cdot K_{P3}) + IN \cdot (K_{C1} \cdot K_{C2} \cdot K_{P2} + +K_{P2} \cdot K_{P3} \cdot K_{C1}) - IP \cdot K_{C1} \cdot K_{C2} \cdot K_N - 2 \cdot IP \cdot K_{P2} \cdot (K_{C1} \cdot K_{C2} + K_{C1} \cdot K_N) - 3 \cdot IP \cdot K_{P2} \cdot K_{P3} \cdot (K_{C1} + K_N) - K_{C1} \cdot IC \cdot (K_N \cdot K_{P2} + K_{P2} \cdot K_{P3}) - 2 \cdot K_{C1} \cdot K_{C2} \cdot IC \cdot (K_{P2} + K_N)$
$\boldsymbol{a_5} =$	$K_{C1} \cdot K_{C2} \cdot K_N \cdot K_{P2} \cdot K_{P3} + \Sigma \cdot (K_{C1} \cdot K_{C2} \cdot K_{P2} \cdot K_N + K_{C1} \cdot K_{C2} \cdot K_{P2} \cdot K_{P3} + K_{C1} \cdot K_N \cdot K_{P2} \cdot K_{P3}) - K_w \cdot (K_{C1} \cdot K_{C2} \cdot K_{P2} + K_{C1} \cdot K_{C2} \cdot K_N + K_{C1} \cdot K_N \cdot K_{P2} + K_{P2} \cdot K_{P3} \cdot K_N + K_{P2} \cdot K_{P3} \cdot K_{C1}) + IN \cdot K_{C1} \cdot K_{C2} \cdot K_{P2} \cdot K_{P3} - 2 \cdot IP \cdot K_{P2} \cdot K_{C1} \cdot K_{C2} \cdot K_N - 3 \cdot IP \cdot K_{P2} \cdot K_{P3} \cdot (K_{C1} \cdot K_{C2} + K_{C1} \cdot K_N) - K_{C1} \cdot IC \cdot K_N \cdot K_{P2} \cdot K_{P3} - 2 \cdot K_{C1} \cdot K_{C2} \cdot IC \cdot (K_N \cdot K_{P2} + K_{P2} \cdot K_{P3})$
$\boldsymbol{a_6} =$	$\Sigma \cdot (K_{C1} \cdot K_{C2} \cdot K_N \cdot K_{P2} \cdot K_{P3}) - K_w \cdot (K_{C1} \cdot K_{C2} \cdot K_{P2} \cdot K_N + K_{C1} \cdot K_{C2} \cdot K_{P2} \cdot K_{P3} + K_{C1} \cdot K_N \cdot K_{P2} \cdot K_{P3}) - 3 \cdot IP \cdot K_{P2} \cdot K_{P3} \cdot K_{C1} \cdot K_{C2} \cdot K_N - 2 \cdot K_{C1} \cdot K_{C2} \cdot IC \cdot K_N \cdot K_{P2} \cdot K_{P3}$
$\boldsymbol{a_7} =$	$-K_w \cdot K_{C1} \cdot K_{C2} \cdot K_N \cdot K_{P2} \cdot K_{P3}$

APPENDIX 23. VALUES USED FOR THE INITIALIZATION OF THE SIMULATIONS OF PH DURING MODEL VALIDATION

Table S23 - 1: Values used for variable initialization during model validation

Parameter	Base value	Justification
HRAP temperature	7.0 °C	Measured value
Algae concentration	50 $g.m^{-3}$	Realistic value as shown by the modelling
***E. coli* concentration**	$1.3 \cdot 10^{9}$ $MPN.m^{-3}$	Average of monitored data
DO concentration	7.8 $mg.L^{-1}$	Measured value
Total inorganic carbon concentration	22 mg $C.L^{-1}$	Realistic value as shown by the modelling
Total inorganic phosphate concentration	0.8 mg $P.L^{-1}$	Realistic value as shown by the modelling
Total ammoniacal nitrogen	4 mg $N.m^{-3}$	Realistic value as shown by the modelling
bCOD concentration	1.5 $mg.L^{-1}$	Realistic value as shown by the modelling
Heterotrophic bacteria concentration	85 $g.m^{-3}$	Realistic value as shown by the modelling
HRAP inert charge balance	1.4 $mol.m^{-3}$	Realistic value as shown by the modelling
Algal debris concentration	0	-
Nitrifying bacteria concentration	2.64 $mg.L^{-1}$	Realistic value as shown by the modelling
Bacterial debris concentration	0	-

APPENDIX 24. MODELLING SENSITIVITY STUDY: RANGE OF VARIATIONS FOR TESTED PARAMETERS

The ranges of each parameter for which the model sensitivity was evaluated are shown in Table S24 - 1, alongside it justification. The corresponding results were discussed in section 6.3.

Table S24 - 1: Range tested for each parameter during sensitivity analysis of the environmental model developed during this study (Chapter 6)

Parameter/Input variable (Units)	Base case value	-	+	Justification
Solar radiation ($W.m^{-2}$)	Var.[1]		10%	Exploratory[1]
Dry bulb temperature (K)	Var.[1]		10%	Exploratory[1]
Dew point temperature (K)	Var.[1]		10%	Exploratory[1]
Surface wind speed ($m.s^{-1}$)	Var.[1]		10%	Exploratory[1]
Air emissivity (-)	0.8	0.75	0.95	Béchet et al. (2011)
Soil thermal conductivity ($W.m^{-1}.K^{-1}$)	1.7	0.2	4	Béchet et al. (2011)
Water emissivity (-)	0.97	0.95	0.99	Davies et al. (1971)
Air kinematic viscosity ($m^2.s^{-1}$)	$1.5 \cdot 10^{-5}$	$1.35 \cdot 10^{-5}$	$1.65 \cdot 10^{-5}$	Exploratory[2]
Air thermal diffusivity ($m^2.s^{-1}$)	$2.20 \cdot 10^{-5}$	$1.98 \cdot 10^{-5}$	$2.42 \cdot 10^{-5}$	Exploratory[2]
Soil specific heat capacity ($J.kg^{-1}.K^{-1}$)	1,250	1,125	1,375	Exploratory[2]
Soil temperature at reference depth (°C)	13.6	12.2	13.5	Exploratory[2]
Algae photosynthetic efficiency (-)	0.02	0.01	0.05	Béchet et al. (2011)
Inlet temperature (°C)	15	10	20	Exploratory[2]
HRAP depth (m)	0.25	0.225	0.275	Exploratory[3]
HRAP surface (m^2)	3.42		10%	Exploratory[3]
Hydraulic retention time (d)	7.9	6	10	± 25%[4]
Aeration rate (s^{-1})	$1.0 \cdot 10^{-4}$	$5.0 \cdot 10^{-5}$	$1.2 \cdot 10^{-4}$	Range measured on pilot scale HRAP (see Appendix 9)

Parameter/Input variable (Units)	Base case value	-	+	Justification
Sedimentation rate (-)	0.8	0.6	1	Exploratory[2]
NO_3 concentration in the effluent (g NO_3^-.m^{-3})	58	0	70	Range commonly measured on pilot scale HRAP
Wastewater COD concentration (g O_2.m^{-3})	300	120	500	5 – 95 percentile observed during pilot scale HRAP study
Wastewater inorganic carbon (g C.m^{-3})	50	35	60	5 – 95 percentile based on PNCC wastewater treatment plant data
Wastewater charge balance (mol.m^{-3})	2.4	1.6	3.1	5 – 95 percentile based on PNCC wastewater treatment plant data
Wastewater inorganic phosphorous concentration (g P.m^{-3})	2	0.69	3.15	5 – 95 percentile based on PNCC wastewater treatment plant data
Wastewater ammoniacal N concentration (g N.m^{-3})	28.4	7.07	37.4	5 – 95 percentile based on PNCC wastewater treatment plant data
Wastewater heterotrophic bacteria concentration (g.m^{-3})	0	-	20	Exploratory[2]
Algae affinity for inorganic carbon (g C.m^{-3})	0.00432	0	0.0084	Novak and Brune, (1985), range for *Chlorella spp.*
Algae affinity for DO during decay (g DO.m^{-3})	0.02	0.008	0.022	Exploratory[2]
Algae heat value (kJ.g^{-1})	24.7	23.2	28.5	Béchet et al. (2013)[5]
Algae decay rate at 20°C in light (d^{-1})	0.12	0.06	0.2	Same range as heterotrophic decay
Algae decay rate at 20°C in darkness (d^{-1})	0.144	0.072	0.24	Based on algae decay rate in light (see Table 6 – 6)
DO yield by algae growth ($g\ O_{2produced} \cdot g\ VSS_{produced}^{-1}$)	1.53	1.377	1.683	Exploratory[2]
DO yield by algae growth ($g\ O_{2consumed} \cdot g\ VSS_{decayed}^{-1}$)	1.53	1.377	1.683	Exploratory[2]
IC yield by algae growth ($g\ C_{uptaken} \cdot g\ VSS_{produced}^{-1}$)	0.510	0.459	0.561	Exploratory[2]
IC yield by algae decay ($g\ C_{produced} \cdot g\ VSS_{decayed}^{-1}$)	0.510	0.459	0.561	Exploratory[2]
Ammoniacal N yield by algae growth ($g\ N_{uptaken} \cdot g\ VSS_{produced}^{-1}$)	0.0415	0.0374	0.0457	Exploratory[2]
IC yield by algae decay ($g\ N_{produced} \cdot g\ VSS_{decayed}^{-1}$)	0.0415	0.0374	0.0457	Exploratory[2]

Parameter/Input variable (Units)	Base case value	-	+	Justification
Heterotroph maximal specific growth at 20°C (d^{-1})	6	3	13.2	Metcalf and Eddy Inc. (2003)
Heterotroph affinity for bCOD at 20°C (d^{-1})	20	5	40	Metcalf and Eddy Inc. (2003)
Heterotroph decay rate at 20°C (d^{-1})	0.12	0.06	0.2	Metcalf and Eddy Inc. (2003)
Specific heterotroph growth rate temperature correction factor (-)	1.07	1.03	1.08	Metcalf and Eddy Inc. (2003)
Heterotroph decay rate temperature correction factor (-)	1.04	1.03	1.08	Metcalf and Eddy Inc. (2003)
Heterotroph affinity for DO ($g\ bCOD.m^{-3}$)	0.2	0.18	0.22	Exploratory[2]
Debris production fraction for algae and bacteria (-)	0.15	0.08	0.2	Metcalf and Eddy Inc. (2003)
DO yield by bacteria growth ($g\ O_{2uptaken} \cdot g\ VSS_{produced}^{-1}$)	1.08	0.972	1.19	Exploratory[2]
IC yield by bacteria growth ($g\ C_{produced} \cdot g\ VSS_{produced}^{-1}$)	0.219	0.197	0.241	Exploratory[2]
Ammoniacal N yield by bacteria growth ($g\ N_{uptaken} \cdot g\ VSS_{produced}^{-1}$)	0.0364	0.0328	0.400	Exploratory[2]
DO yield by bacteria decay ($g\ O_{2produced} \cdot g\ VSS_{decayed}^{-1}$)	1.42	1.28	1.56	Exploratory[2]
IC yield by bacteria decay ($g\ C_{produced} \cdot g\ VSS_{produced}^{-1}$)	0.531	0.478	0.584	Exploratory[2]
Ammoniacal N yield by bacteria decay ($g\ N_{produced} \cdot g\ VSS_{produced}^{-1}$)	0.124	0.112	0.136	Exploratory[2]
DO yield by nitrifier growth ($g\ O_{2uptaken} \cdot g\ VSS_{produced}^{-1}$)	26.9	24.2	29.6	Exploratory[2]
IC yield by nitrifier growth ($g\ C_{uptaken} \cdot g\ VSS_{produced}^{-1}$)	0.531	0.478	0.584	Exploratory[2]
Ammoniacal N yield by nitrifier growth ($g\ N_{uptaken} \cdot g\ VSS_{produced}^{-1}$)	6.32	5.69	6.95	Exploratory[2]
Inert charge yield by nitrifier growth ($mol\ e^{-}\ produced \cdot g\ VSS_{produced}^{-1}$)	0.442	0.398	0.486	Exploratory[2]

[1] Input variables which measurements uncertainty was unknown;
[2] Parameters associated with poorly known uncertainty/variability. The influence of the variations of these parameters on the model predictions was assessed based on the ranges listed in the present table, and not investigated further due to the low impact estimated (see Chapter 6 section 6.3.);
[3] Design parameter with no associated uncertainty, but which impact on model sensitivity was tested for model performance assessment.
[4] Observed standard deviation of the HRT measured on the pilot scale algal ponds used in this thesis;
[5] The range of algae heat value was given in this publication per gram of dry weight (TSS). It was corrected in this study by a factor 0.9 to obtain algae heat value per gram of volatile suspended solids (VSS);

References

Ansa EDO, Lubberding HJ, Gijzen HJ. 2012a. The effect of algal biomass on the removal of faecal coliform from domestic wastewater. *Appl. Water Sci.* **2**:87–94. http://dx.doi.org/10.1007/s13201-011-0025-y.

Ansa EDO, Lubberding HJ, Ampofo JA, Amegbe GB, Gijzen HJ. 2012b. Attachment of faecal coliform and macro-invertebrate activity in the removal of faecal coliform in domestic wastewater treatment pond systems. *Ecol. Eng.* **42**:35–41. http://dx.doi.org/10.1016/j.ecoleng.2012.01.018.

Ansa EDO, Lubberding HJ, Gijen HJ. 2008. Fecal coliform removal in algal-based domestic wastewater treatment systems. In: . *Sess. 5 UCOWR Conf.*, p. Paper 37.

Araki S, Martín-Gomez S, Bécares E, De Luis-Calabuig E, Rojo-Vazquez F. 2001. Effect of high-rate algal ponds on viability of *Cryptosporidium parvum* oocysts. *Appl. Environ. Microbiol.* **67**:3322–3324. http://dx.doi.org/10.1128/AEM.67.7.3322-3324.2001.

Arbib Z, Ruiz J, Álvarez-Díaz P, Garrido-Pérez C, Barragan J, Perales JA. 2013a. Long term outdoor operation of a tubular airlift pilot photobioreactor and a high rate algal pond as tertiary treatment of urban wastewater. *Ecol. Eng.* **52**:143–153. http://dx.doi.org/10.1016/j.ecoleng.2012.12.089.

Arbib Z, Ruiz J, Álvarez-Díaz P, Garrido-Pérez C, Barragan J, Perales JA. 2013b. Effect of pH control by means of flue gas addition on three different photo-bioreactors treating urban wastewater in long-term operation. *Ecol. Eng.* **57**:226–235. http://dx.doi.org/10.1016/j.ecoleng.2013.04.040.

Archer HE, Mara DD. 2003. Waste stabilisation pond developments in New Zealand. *Water Sci. Technol.* **48**:9–15.

Ashbolt NJ, Grabow WOK, Snozzi M. 2001. Indicators of microbial water quality. In: Fewtrell, L, Bartram, J, editors. *Water Qual. Guidel. Stand. Heal.* London, UK: IWA Publishing, pp. 289–316. www.who.int/water_sanitation_health/dwq/whoiwa/en/.

Auer MT, Niehaus SL. 1993. Modeling fecal coliform bacteria—I. Field and laboratory determination of loss kinetics. *Water Res.* **27**:693–701. http://dx.doi.org/10.1016/0043-1354(93)90179-L.

Babauta JT, Nguyen HD, Harrington TD, Renslow R, Beyenal H. 2012. pH, redox potential and local biofilm potential microenvironments within *Geobacter sulfurreducens*

biofilms and their roles in electron transfer. *Biotechnol. Bioeng.* **109**:2651–2662. http://dx.doi.org/10.1002/bit.24538.

Bahlaoui MA, Baleux B, Troussellier M. 1997. Dynamics of pollution-indicator and pathogenic bacteria in high-rate oxidation wastewater treatment ponds. *Water Res.* **31**:630–638. http://dx.doi.org/10.1016/S0043-1354(96)00299-0.

Bahlaoui MA, Baleux B, Frouji MA. 1998. The effect of environmental factors on bacterial populations and community dynamics in high rate oxidation ponds. *Water Environ. Fed.* **70**:1186–1197.

Bai X, Lant P, Pratt S. 2015. The contribution of bacteria to algal growth by carbon cycling. *Biotechnol. Bioeng.* **112**:688–695. http://dx.doi.org/10.1002/bit.25475.

Banat I, Puskas K, Esen I, Al-Daher R. 1990. Wastewater treatment and algal productivity in an integrated ponding system. *Biol. Wastes* **32**:265–275. http://dx.doi.org/10.1016/0269-7483(90)90058-Z.

Barcina I, Lebaron P, Vives-Rego J. 1997. Survival of allochtonous bacteria in aquatic systems: a biological approach. *Fed. Eur. Microbiol. Soc.* **23**:1–9. http://dx.doi.org/10.1007/s13398-014-0173-7.2.

Bayles KW. 2014. Making sense of a paradox. *Nat. Rev. Microbiol.* **12**:63–69. http://dx.doi.org/10.1038/nrmicro3136.

Béchet Q, Chambonnière P, Shilton A, Guizard G, Guieysse B. 2015. Algal productivity modeling: A step toward accurate assessments of full-scale algal cultivation. *Biotechnol. Bioeng.* **112**:987–996. http://dx.doi.org/10.1002/bit.25517.

Béchet Q, Muñoz R, Shilton A, Guieysse B. 2013. Outdoor cultivation of temperature-tolerant *Chlorella sorokiniana* in a column photobioreactor under low power-input. *Biotechnol. Bioeng.* **110**:118–126. http://dx.doi.org/10.1002/bit.24603.

Béchet Q, Shilton A, Fringer OB, Munoz R, Guieysse B. 2010. Mechanistic modeling of broth temperature in outdoor photobioreactors. *Environ. Sci. Technol.* **44**:2197–2203. http://dx.doi.org/10.1021/es903214u.

Béchet Q, Shilton A, Guieysse B. 2016. Maximizing productivity and reducing environmental impacts of full-scale algal production through optimization of open pond depth and hydraulic retention time. *Environ. Sci. Technol.* **50**:4102–4110. http://dx.doi.org/10.1021/acs.est.5b05412.

Béchet Q, Shilton A, Park JBK, Craggs RJ, Guieysse B. 2011. Universal temperature model

for shallow algal ponds provides improved accuracy. *Environ. Sci. Technol.* **45**:3702–3709. http://dx.doi.org/10.1021/es1040706.

Bello M, Ranganathan P, Brennan F. 2017. Dynamic modelling of microalgae cultivation process in high rate algal wastewater pond. *Algal Res.* **24**:457–466. http://dx.doi.org/10.1016/j.algal.2016.10.016.

Benchokroun S, Imziln B, Hassani L. 2003. Solar inactivation of mesophilic *Aeromonas* by exogenous photooxidation in high-rate algal pond treating wastewater. *J. Appl. Microbiol.* **94**:531–538. http://dx.doi.org/10.1046/j.1365-2672.2003.01867.x.

Berdahl P, Martin M. 1984. Emissivity of clear skies. *Sol. Energy* **32**:663–664. http://dx.doi.org/https://doi.org/10.1016/0038-092X(84)90144-0.

Bitton G. 2014. Microbiology of drinking water production and distribution. *Microbiol. Drink. Water Prod. Distrib.* Hoboken, New Jersey : Wiley Blackwell, [2014] 1–298 p. http://dx.doi.org/10.1002/9781118743942.

Blaustein RA, Pachepsky Y, Hill RL, Shelton DR, Whelan G. 2013. *Escherichia coli* survival in waters: Temperature dependence. *Water Res.* **47**:569–578. http://dx.doi.org/10.1016/j.watres.2012.10.027.

Boehm AB, Yamahara KM, Love DC, Peterson BM, Mcneill K, Nelson KL. 2009. Covariation and photoinactivation of traditional and novel indicator organisms and human viruses at a sewage-impacted marine beach. *Environ. Sci. Technol.* **43**:8046–8052. http://dx.doi.org/10.1021/es9015124.

De Boer JP, Cronenberg CCH, De Beer D, Van den Heuvel JC, De Mattos MJT, Neijssel OM. 1993. pH and glucose profiles in aggregates of *Bacillus laevolacticus*. *Appl. Environ. Microbiol.* **59**:2474–2478.

Boogerd, P B, Kuenen JG, Heijnen JJ, Van der Lans RGJM. 1990. Oxygen and carbon dioxide mass transfer and the aerobic, autotrophic cultivation of moderate and extreme thermophiles: A case study related to the microbial desulfurization of coal. *Biotechnol. Bioeng.* **35**:1111–1119. http://dx.doi.org/10.1002/bit.260351106.

Buchanan AN. 2014. Comparing the performance of a high rate algal pond with a waste stabilisation pond in rural South Australia; Flinders University.

Buhr HO, Miller SB. 1983. A dynamic model of the high-rate algal-bacterial wastewater treatment pond. *Water Res.* **17**:29–37. http://dx.doi.org/10.1016/0043-1354(83)90283-X.

Canale RP, Auer MT, Owens EM, Heidtke TM, Effler SW. 1993. Modeling fecal coliform bacteria—II. Model development and application. *Water Res.* **27**:703–714. http://dx.doi.org/10.1016/0043-1354(93)90180-P.

Castro-Alférez M, Polo-López MI, Fernández-Ibáñez P. 2016. Intracellular mechanisms of solar water disinfection. *Sci. Rep.* **6**:38145. http://dx.doi.org/10.1038/srep38145.

Charles CJ, Rout SP, Patel KA, Akbar S, Laws AP, Jackson BR, Boxall SA, Humphreys PN. 2017. Floc formation reduces the pH stress experienced by microorganisms living in alkaline environments. *Appl. Environ. Microbiol.* **83**. http://dx.doi.org/10.1128/AEM.02985-16.

Cho D-H, Choi J-W, Kang Z, Kim B-H, Oh H-M, Kim H, Ramanan R. 2017. Microalgal diversity fosters stable biomass productivity in open ponds treating wastewater. *Sci. Rep.* **7**. http://dx.doi.org/10.1038/s41598-017-02139-8.

Christensen ER, Li A. 2014. Water Chemistry. In: . *Phys. Chem. Process. Aquat. Environ.* Hoboken: Wiley, pp. 113–137.

Cook KL, Bolster CH. 2007. Survival of *Campylobacter jejuni* and *Escherichia coli* in groundwater during prolonged starvation at low temperatures. *J. Appl. Microbiol.* **103**:573–583. http://dx.doi.org/10.1111/j.1365-2672.2006.03285.x.

Costache TA, Acien Fernandez FG, Morales MM, Fernandez-Sevilla JM, Stamatin I, Molina E. 2013. Comprehensive model of microalgae photosynthesis rate as a function of culture conditions in photobioreactors. *Appl. Microbiol. Biotechnol.* **97**:7627–7637. http://dx.doi.org/10.1007/s00253-013-5035-2.

Craggs RJ, Davies-Colley RJ, Tanner CC, Sukias JP. 2003. Advanced pond system: Performance with high rate ponds of different depths and areas. *Water Sci. Technol.* **48**:259–267.

Craggs R, Park J, Heubeck S, Sutherland D. 2014. High rate algal pond systems for low-energy wastewater treatment, nutrient recovery and energy production. *New Zeal. J. Bot.* **52**:60–73. http://dx.doi.org/10.1080/0028825X.2013.861855.

Craggs RJ, Zwart A, Nagels JW, Davies-Colley RJ. 2004. Modelling sunlight disinfection in a high rate pond. *Ecol. Eng.* **22**:113–122. http://dx.doi.org/10.1016/j.ecoleng.2004.03.001.

Craggs R, Sutherland D, Campbell H. 2012. Hectare-scale demonstration of high rate algal ponds for enhanced wastewater treatment and biofuel production. *J. Appl. Phycol.*

24:329–337. http://dx.doi.org/10.1007/s10811-012-9810-8.

Curtis TP, Mara DD, Silva SA. 1992. Influence of pH, oxygen, and humic substances on ability of sunlight to damage fecal coliforms in waste stabilization pond water. *Appl. Environ. Microbiol.* **58**:1335–1343.

Cussler EL. 2009. Diffusion: mass transfer in fluid systems. Cambridge university press.

Dahl NW, Woodfield PL, Lemckert CJ, Stratton H, Roiko A. 2017. A practical model for sunlight disinfection of a subtropical maturation pond. *Water Res.* **108**:151–159. http://dx.doi.org/10.1016/j.watres.2016.10.072.

Davies-Colley RJ, Bell RG, Donnison AM. 1994. Sunlight inactivation of enterococci and fecal coliforms in sewage effluent diluted in seawater. *Appl. Environ. Microbiol.* **60**:2049–2058.

Davies-Colley RJ, Donnison AM, Speed DJ, Ross CM, Nagels JW. 1999. Inactivation of faecal indicator micro-organisms in waste stabilisation ponds: Interactions of environmental factors with sunlight. *Water Res.* **33**:1220–1230. http://dx.doi.org/10.1016/S0043-1354(98)00321-2.

Davies-Colley RJ. 2005. Pond disinfection. In: Shilton, A, editor. *Pond Treat. Technol.* London, UK: IWA Publishing, pp. 100–136.

Davies JA, Robinson PJ, Nunez M. 1971. Field determinations of surface emissivity and temperature for Lake Ontario. *J. Appl. Meteorol.* **10**:811–819.

Dawson RMC, Elliott DC, Elliott WH, Jones KM. 1986. Data for biochemical research 3rd ed. Oxford Science Publ.

Deal PH, Souza KA, Mack HM. 1975. High pH, ammonia, toxicity, and the search for life on the Jovian planets. *Orig. Life* **6**:561–573.

Decamp O, Warren A. 1998. Bacterivory in ciliates isolated from constructed wetlands (reed beds) used for wastewater treatment. *Water Res.* **32**:1989–1996. http://dx.doi.org/10.1016/S0043-1354(97)00461-2.

Delgadillo-Mirquez L, Lopes F, Taidi B, Pareau D. 2016. Nitrogen and phosphate removal from wastewater with a mixed microalgae and bacteria culture. *Biotechnol. Reports* **11**:18–26. http://dx.doi.org/10.1016/j.btre.2016.04.003.

Dias DFC, Passos RG, Von Sperling M. 2017. A review of bacterial indicator disinfection mechanisms in waste stabilisation ponds. *Rev. Environ. Sci. Biotechnol.* **16**:517–539.

http://dx.doi.org/10.1007/s11157-017-9433-2.

Dias DFC, Von Sperling M. 2018. Vertical profiling and modelling of *Escherichia coli* decay in a shallow maturation pond operating in a tropical climate. *Environ. Technol.* **39**:759–769. http://dx.doi.org/10.1080/09593330.2017.1310936.

Dias DFC, Von Sperling M. 2017. Solar radiation (PAR, UV-A, UV-B) penetration in a shallow maturation pond operating in a tropical climate. *Water Sci. Technol.* **76**:182–191. http://dx.doi.org/10.2166/wst.2017.203.

Eaton AD, Clesceri LS, Greenberg AE, Franson MAH, Association. APH, Association. AWW, Federation. WE. 1998. Standard methods for the examination of water and wastewater. Washington, DC: American Public Health Association.

Edberg SC, Rice EW, Karlin RJ, Allen MJ. 2000. *Escherichia coli*: the best biological drinking water indicator for public health protection. *J. Appl. Microbiol.* **88**:106S-116S. http://dx.doi.org/10.1111/j.1365-2672.2000.tb05338.x.

Ekklesia E, Shanahan P, Chua LHC, Eikaas HS. 2015. Temporal variation of faecal indicator bacteria in tropical urban storm drains. *Water Res.* **68**:171–181. http://dx.doi.org/10.1016/j.watres.2014.09.049.

Fallowfield HJ, Young P, Taylor MJ, Buchanan N, Cromar N, Keegan A, Monis P. 2018. Independent validation and regulatory agency approval for high rate algal ponds to treat wastewater from rural communities. *Environ. Sci. Water Res. Technol.* **4**:195–205. http://dx.doi.org/10.1039/c7ew00228a.

Fallowfield HJ, Cromar NJ, Evison LM. 1996. Coliform die-off rate constants in a high rate algal pond and the effect of operational and environmental variables. *Water Sci. Technol.* **34**:141–147.

Farkas K, Marshall M, Cooper D, McDonald JE, Malham SK, Peters DE, Maloney JD, Jones DL. 2018. Seasonal and diurnal surveillance of treated and untreated wastewater for human enteric viruses. *Environ. Sci. Pollut. Res.* **25**:33391–33401. http://dx.doi.org/10.1007/s11356-018-3261-y.

Fernandez A, Tejedor C, Chordi A. 1992. Effect of different factors on the die-off of fecal bacteria in a stabilization pond purification plant. *Water Res.* **26**:1093–1098. http://dx.doi.org/10.1016/0043-1354(92)90145-T.

Fisher MB, Iriarte M, Nelson KL. 2012. Solar water disinfection (SODIS) of *Escherichia coli*, *Enterococcus spp.*, and MS2 coliphage: Effects of additives and alternative

container materials. *Water Res.* **46**:1745–1754. http://dx.doi.org/10.1016/j.watres.2011.12.048.

Fisher MB, Nelson KL. 2014. Inactivation of *Escherichia coli* by polychromatic simulated sunlight: Evidence for and implications of a fenton mechanism involving iron, hydrogen peroxide, and superoxide. *Appl. Environ. Microbiol.* **80**:935–942. http://dx.doi.org/10.1128/AEM.02419-13.

García J, Green BF, Lundquist T, Mujeriego R, Hernández-Mariné M, Oswald WJ. 2006. Long term diurnal variations in contaminant removal in high rate ponds treating urban wastewater. *Bioresour. Technol.* **97**:1709–1715. http://dx.doi.org/10.1016/j.biortech.2005.07.019.

García J, Mujeriego R, Hernández-Mariné M. 2000. High rate algal pond operating strategies for urban wastewater nitrogen removal. *Appl. Phycol.* **12**:331–339. http://dx.doi.org/10.1023/a:1008146421368.

García M, Soto F, González JM, Bécares E. 2008. A comparison of bacterial removal efficiencies in constructed wetlands and algae-based systems. *Ecol. Eng.* **32**:238–243. http://dx.doi.org/10.1016/j.ecoleng.2007.11.012.

de Godos I, Blanco S, García-Encina PA, Becares E, Muñoz R. 2009. Long-term operation of high rate algal ponds for the bioremediation of piggery wastewaters at high loading rates. *Bioresour. Technol.* **100**:4332–4339. http://dx.doi.org/10.1016/j.biortech.2009.04.016.

de Godos I, Blanco S, García-Encina PA, Becares E, Muñoz R. 2010. Influence of flue gas sparging on the performance of high rate algae ponds treating agro-industrial wastewaters. *J. Hazard. Mater.* **179**:1049–1054. http://dx.doi.org/10.1016/j.jhazmat.2010.03.112.

Gotaas HB, Oswald WJ, Ludwig HF. 1954. Photosynthetic reclamation of organic wastes. *Sci. Mon.* **79**:368–378.

Gourich B, Vial C, El Azher N, Belhaj Soulami M, Ziyad M. 2008. Influence of hydrodynamics and probe response on oxygen mass transfer measurements in a high aspect ratio bubble column reactor: Effect of the coalescence behaviour of the liquid phase. *Biochem. Eng. J.* http://dx.doi.org/10.1016/j.bej.2007.08.011.

Guieysse B, Béchet Q, Shilton A. 2013. Variability and uncertainty in water demand and water footprint assessments of fresh algae cultivation based on case studies from five climatic regions. *Bioresour. Technol.* **128**:317–323.

http://dx.doi.org/10.1016/j.biortech.2012.10.096.

Hadiyanto H, Elmore S, Van Gerven T, Stankiewicz A. 2013. Hydrodynamic evaluations in high rate algae pond (HRAP) design. *Chem. Eng. J.* **217**:231–239. http://dx.doi.org/10.1016/j.cej.2012.12.015.

El Hamouri B, Rami A, Vasel J-L. 2003. The reasons behind the performance superiority of a high rate algal pond over three facultative ponds in series. *Water Sci. Technol.* **48**:269–276.

El Hamouri B. 2009. Rethinking natural, extensive systems for tertiary treatment purposes: The high-rate algae pond as an example. *Desalin. Water Treat.* **4**:128–134. http://dx.doi.org/10.5004/dwt.2009.367.

Hickey CW, Quinn JM, Davies-Colley RJ. 1989. Effluent characteristics of dairy shed oxidation ponds and their potential impacts on rivers. *New Zeal. J. Mar. Freshw. Res.* **23**:569–684. http://dx.doi.org/10.1080/00288330.1989.9516394.

Hoffmann JP. 1998. Wastewater treatment with suspended and nonsuspended algae. *J. Phycol.* **34**:757–763. http://dx.doi.org/10.1046/j.1529-8817.1998.340757.x.

Hom-Diaz A, Norvill ZN, Blánquez P, Vicent T, Guieysse B. 2017. Ciprofloxacin removal during secondary domestic wastewater treatment in high rate algal ponds. *Chemosphere* **180**:33–41. http://dx.doi.org/10.1016/j.chemosphere.2017.03.125.

Huang Y, Truelstrup Hansen L, Ragush CM, Jamieson RC. 2018. Disinfection and removal of human pathogenic bacteria in arctic waste stabilization ponds. *Environ. Sci. Pollut. Res.* **25**:32881–32893. http://dx.doi.org/10.1007/s11356-017-8816-9.

Hunter RC, Beveridge TJ. 2005. Application of a pH-sensitive fluoroprobe (C-SNARF-4) for pH microenvironment analysis in *Pseudomonas aeruginosa* biofilms. *Appl. Environ. Microbiol.* **71**:2501–2510. http://dx.doi.org/10.1128/AEM.71.5.2501.

Illman AM, Scragg AH, Shales SW. 2000. Increase in *Chlorella* strains calorific values when grown in low nitrogen medium. *Enzyme Microb. Technol.* **27**:631–635. http://dx.doi.org/10.1016/S0141-0229(00)00266-0.

Imlay JA. 2013. The molecular mechanisms and physiological consequences of oxidative stress: Lessons from a model bacterium. *Nat. Rev. Microbiol.* **11**:443–454. http://dx.doi.org/10.1038/nrmicro3032.

John DE, Rose JB. 2005. Review of factors affecting microbial survival in groundwater. *Environ. Sci. Technol.* **39**:7345–7356. http://dx.doi.org/10.1021/es047995w.

Jupsin H, Praet E, Vasel J. 2003. Dynamic mathematical model of high rate algal ponds (HRAP). *Water Sci. Technol.* **48**:197–204. http://dx.doi.org/10.2166/wst.2003.0120.

Kadir K, Nelson KL. 2014. Sunlight mediated inactivation mechanisms of *Enterococcus faecalis* and *Escherichia coli* in clear water versus waste stabilization pond water. *Water Res.* **50**:307–317. http://dx.doi.org/10.1016/j.watres.2013.10.046.

Kapuscinski RB, Mitchell R. 1983. Sunlight-induced mortality of viruses and *Escherichia coli* in coastal seawater. *Environ. Sci. Technol.* **17**:1–6.

Katharios-Lanwermeyer S, Xi C, Jakubovics NS, Rickard AH. 2014. Mini-review: Microbial coaggregation: ubiquity and implications for biofilm development. *Biofouling* **30**:1235–1251. http://dx.doi.org/10.1080/08927014.2014.976206.

Khaengraeng R, Reed RH. 2005. Oxygen and photoinactivation of *Escherichia coli* in UVA and sunlight. *J. Appl. Microbiol.* **99**:39–50. http://dx.doi.org/10.1111/j.1365-2672.2005.02606.x.

Kohn T, Nelson KL. 2007. Sunlight-mediated inactivation of MS2 coliphage via exogenous singlet oxygen produced by sensitizers in natural waters. *Environ. Sci. Technol.* **41**:192–197. http://dx.doi.org/10.1021/es061716i.

Krulwhich TA, Sachs G, Padan E. 2011. Molecular aspects of bacterial pH sensing and homeostasis. *Nat. Rev. Microbiol.* **9**:330–343. http://dx.doi.org/10.1038/nrmicro2549.Molecular.

Lee E, Zhang Q. 2016. Integrated co-limitation kinetic model for microalgae growth in anaerobically digested municipal sludge centrate. *Algal Res.* **18**:15–24. http://dx.doi.org/10.1016/j.algal.2016.05.019.

Lisle JT, Broadaway SC, Prescott AM, Pyle BH, Fricker C, Mcfeters GA. 1998. Effects of starvation on physiological activity and chlorine disinfection resistance in *Escherichia coli* O157:H7. *Appl. Environ. Microbiol.* **64**:4658–4662.

Madigan MT, Martinko JM. 2006. Brock Biology of Microorganisms 11th ed. Pearson Education, Inc.

Maïga Y, Denyigba K, Wethe J, Ouattara AS. 2009a. Sunlight inactivation of *Escherichia coli* in waste stabilization microcosms in a sahelian region (Ouagadougou, Burkina Faso). *J. Photochem. Photobiol. B Biol.* **94**:113–119. http://dx.doi.org/10.1016/j.jphotobiol.2008.10.008.

Maïga Y, Wethe J, Denyigba K, Ouattara AS. 2009b. The impact of pond depth and

environmental conditions on sunlight inactivation of *Escherichia coli* and enterococci in wastewater in a warm climate. *Can. J. Microbiol.* **55**:1364–1374. http://dx.doi.org/10.1139/W09-104.

Maiga Y, Wethé J, Ouattara AS, Traoré AS. 2017. Predicting attenuation of solar radiation (UV-B, UV-A and PAR) in waste stabilization ponds under Sahelian climatic conditions. *Environ. Sci. Pollut. Res.* **25**:21341–21349. http://dx.doi.org/10.1007/s11356-017-9668-z.

Malek A, Zullo LC, Daoutidis P. 2016. Modeling and dynamic optimization of microalgae cultivation in outdoor open ponds. *Ind. Eng. Chem. Res.* **55**:3327–3337. http://dx.doi.org/10.1021/acs.iecr.5b03209.

Mancini JL. 1978. Numerical estimates of coliform mortality rates under various conditions. *Water Pollut. Control Fed.* **50**:2477–2484.

Mara DD. 2005. Pond process design - a practical guide. In: Shilton, AN, editor. *Pond Treat. Technol.* London, UK: IWA Publishing, pp. 168–187.

Maraccini PA, Wenk J, Boehm AB. 2016a. Exogenous indirect photoinactivation of bacterial pathogens and indicators in water with natural and synthetic photosensitizers in simulated sunlight with reduced UVB. *J. Appl. Microbiol.* **121**:587–597. http://dx.doi.org/10.1111/jam.13183.

Maraccini PA, Mattioli MCM, Sassoubre LM, Cao Y, Griffith JF, Ervin JS, Van De Werfhorst LC, Boehm AB. 2016b. Solar inactivation of enterococci and *Escherichia coli* in natural waters: Effects of water absorbance and depth. *Environ. Sci. Technol.* **50**:5068–5076. http://dx.doi.org/10.1021/acs.est.6b00505.

Maraccini PA, Wenk J, Boehm AB. 2016c. Photoinactivation of eight health-relevant bacterial species: Determining the importance of the exogenous indirect mechanism. *Environ. Sci. Technol.* **50**:5050–5059. http://dx.doi.org/10.1021/acs.est.6b00074.

Marais GVR, Shaw VA. 1961. A rational theory for the design of sewage stabilization ponds in Central and South Africa. *Trans. South African Inst. Civ. Eng.* **3**:205–227.

Marais GVR. 1974. Fecal bacterial kinetics in stabilization ponds. *J. Environ. Eng. Div.* **100**:119–139.

Matamoros V, Gutiérrez R, Ferrer I, García J, Bayona JM. 2015. Capability of microalgae-based wastewater treatment systems to remove emerging organic contaminants: A pilot-scale study. *J. Hazard. Mater.* **288**:34–42.

http://dx.doi.org/10.1016/j.jhazmat.2015.02.002.

Maynard HE, Ouki SK, Williams SC. 1999. Tertiary lagoons: A review of removal mechanisms and performance. *Water Res.* **33**:1–13. http://dx.doi.org/10.1016/S0043-1354(98)00198-5.

Mayo AW. 1995. Modeling coliform mortality in waste stabilization ponds. *J. Environ. Eng.* **121**:140–152.

Mayo AW, Noike T. 1996. Effects of temperature and pH on the growth of heterotrophic bacteria in waste stabilization ponds. *Water Res.* **30**:447–455.

Mendonca AF, Amoroso TL, Knabel SJ. 1994. Destruction of gram-negaive food-borne pathogens by high pH involves disruption of the cytoplasmic membrane. *Appl. Environ. Microbiol.* **60**:4009–4014.

Metcalf and Eddy Inc. 2003. Wastewater engineering: Treatment and reuse. Ed. George Tchobanoglous, Franklin L Burton, H David Stensel 4th ed. New York: Mc. Graw-Hill.

Mezrioui N, Oudra B, Oufdou K, Hassani L, Loudiki M, Darley J. 1994. Effect of microalgae growing on wastewater batch culture on *Escherichia coli* and *Vibrio cholerae* survival. *Water Sci. Technol.* **30**:295–302.

Ministry for the Environment. 2003. Microbiological water quality guidelines for marine and freshwater recreational areas. Wellington, New Zealand: Ministry for the Environment 159 p.

Moeller JR, Calkins J. 1980. Bactericidal agents in wastewater lagoons and lagoon design. *J. Water Pollut. Control Fed.* **52**:2442–2451.

Montgomery DC, Runger GC. 2003. Simple linear regression and correlation. In: . *Appl. Stat. Probab. Eng.*, pp. 372–409.

Moreira JF, Cabral AR, Oliveira R, Silva SA. 2009. Causal model to describe the variation of faecal coliform concentrations in a pilot-scale test consisting of ponds aligned in series. *Ecol. Eng.* **35**:791–799. http://dx.doi.org/10.1016/j.ecoleng.2008.12.002.

Mostafa S, Rubinato M, Rosario-Ortiz FL, Linden KG. 2016. Impact of light screening and photosensitization by surface water organic matter on *Enterococcus faecalis* inactivation. *Environ. Eng. Sci.* **33**:365–373. http://dx.doi.org/10.1089/ees.2016.0041.

Muela A, García-Bringas JM, Seco C, Arana I, Barcina I. 2002. Participation of oxygen and

role of exogenous and endogenous sensitizers in the photoinactivation of *Escherichia coli* by photosynthetically active radiation, UV-A and UV-B. *Microb. Ecol.* **44**:354–364. http://dx.doi.org/10.1007/s00248-002-1027-y.

Müller T, Walter B, Wirtz A, Burkovski A. 2006. Ammonium toxicity in bacteria. *Curr. Microbiol.* **52**:400–406. http://dx.doi.org/10.1007/s00284-005-0370-x.

Muñoz R, Gonzalez-Fernandez C. 2017. Microalgae-based biofuels and bioproducts: from feedstock cultivation to end-products. Elsevier Science. Woodhead Publishing Series in Energy.

Muñoz R, Guieysse B. 2006. Algal-bacterial processes for the treatment of hazardous contaminants: A review. *Water Res.* **40**:2799–2815. http://dx.doi.org/10.1016/j.watres.2006.06.011.

Nelson ED, Do H, Lewis RS, Carr SA. 2011. Diurnal variability of pharmaceutical, personal care product, estrogen and alkylphenol concentrations in effluent from a tertiary wastewater treatment facility. *Environ. Sci. Technol.* **45**:1228–1234. http://dx.doi.org/10.1021/es102452f.

Nelson KL, Boehm AB, Davies-Colley RJ, Dodd MC, Kohn T, Linden KG, Liu Y, Maraccini PA, McNeill K, Mitch WA, Nguyen TH, Parker KM, Rodriguez RA, Sassoubre LM, Silverman AI, Wigginton KR, Zepp RG. 2018. Sunlight-mediated inactivation of health-relevant microorganisms in water: A review of mechanisms and modeling approaches. *Environ. Sci. Process. Impacts*:1089–1122. http://xlink.rsc.org/?DOI=C8EM00047F. http://dx.doi.org/10.1039/C8EM00047F.

Nelson KL, Cisneros BJ, Tchobanoglous G, Darby JL. 2004. Sludge accumulation, characteristics, and pathogen inactivation in four primary waste stabilization ponds in central Mexico. *Water Res.* **38**:111–127. http://dx.doi.org/10.1016/j.watres.2003.09.013.

Nguyen MT, Jasper JT, Boehm AB, Nelson KL. 2015. Sunlight inactivation of fecal indicator bacteria in open-water unit process treatment wetlands: Modeling endogenous and exogenous inactivation rates. *Water Res.* **83**:282–292. http://dx.doi.org/10.1016/j.watres.2015.06.043.

NIWA National Climate Center. 2017. A cool summer for most but dry in the north and east 10 p. https://www.niwa.co.nz/sites/niwa.co.nz/files/Climate_Summary_Summer_2017_Final.pdf.

Nørgaard LS, Roslev P. 2016. Effects of ammonia and density on filtering of commensal and pathogenic *Escherichia coli* by the cladoceran *Daphnia magna*. *Bull. Environ. Contam. Toxicol.* **97**:848–854. http://dx.doi.org/10.1007/s00128-016-1963-8.

Novak JT, Brune DE. 1985. Inorganic carbon limited growth kinetics of some freshwater algae. *Water Res.* **19**:215–225. http://dx.doi.org/10.1016/0043-1354(85)90203-9.

NZ Water Environment Research Foundation. 2002. New Zealand municipal wastewater monitoring guidelines. Wellington, New Zealand 319 p.

Oladeinde A, Lipp E, Chen C-Y, Muirhead R, Glenn T, Cook K, Molina M. 2018. Transcriptome changes of *Escherichia coli*, *Enterococcus faecalis*, and *Escherichia coli* O157:H7 laboratory strains in response to photo-degraded DOM. *Front. Microbiol.* **9**. http://dx.doi.org/10.3389/fmicb.2018.00882.

Ouali A, Jupsin H, Vasel JL, Ghrabi A. 2015. Removal of *E. coli* and enterococci in maturation pond and kinetic modelling under sunlight conditions. *Desalin. Water Treat.* **53**:1068–1074. http://dx.doi.org/10.1080/19443994.2013.856350.

Pachepsky YA, Blaustein RA, Whelan G, Shelton DR. 2014. Comparing temperature effects on *Escherichia coli*, salmonella, and enterococcus survival in surface waters. *Lett. Appl. Microbiol.* **59**:278–283. http://dx.doi.org/10.1111/lam.12272.

Papadopoulos FH, Metaxa EG, Iatrou MN, Papadopoulos AH. 2014. Evaluation of performance of full-scale duckweed and algal ponds receiving septage. *Water Environ. Res.* **86**:2309–2316. http://dx.doi.org/10.2175/106143014X14062131178754.

Parhad NM, Rao NU. 1974. Effect of pH on survival of *Escherichia coli*. *Water Pollut. Control Fed.* **46**:980–986.

Park JBK, Craggs RJ, Shilton AN. 2011. Wastewater treatment high rate algal ponds for biofuel production. *Bioresour. Technol.* **102**:35–42. http://dx.doi.org/10.1016/j.biortech.2010.06.158.

Park JBK, Craggs RJ, Shilton AN. 2013. Enhancing biomass energy yield from pilot-scale high rate algal ponds with recycling. *Water Res.* **47**:4422–4432. http://dx.doi.org/10.1016/j.watres.2013.04.001.

Park Talaro K. 2008. Foundation in microbiology: Basic principles. Mc. Graw-Hill, New York.

Parker JA, Darby JL. 1995. Particle-associated coliform in secondary effluents: Shielding from ultraviolet light disinfection. *Water Environ. Res.* **67**:1065–1075.

Paterson C, Curtis TP. 2005. Physical and chemical environments. In: Shilton, AN, editor. *Pond Treat. Technol*. London, UK: IWA Publishing, pp. 49–65.

Pearson H. 2005. Microbiology of waste stabilization ponds. *Pond Treat. Technol*.:14–43.

Plósz BG, Leknes H, Liltved H, Thomas K V. 2010. Diurnal variations in the occurrence and the fate of hormones and antibiotics in activated sludge wastewater treatment in Oslo, Norway. *Sci. Total Environ.* **408**:1915–1924. http://dx.doi.org/10.1016/j.scitotenv.2010.01.042.

Plouviez M. 2017. N_2O synthesis by microalgae : pathways, significance and mitigations : a thesis presented in partial fulfilment of the requirement for the degree of Doctor of Philosophy in Environmental Engineering at Massey University, Palmerston North, New Zealand; Massey University. http://hdl.handle.net/10179/12657.

Polprasert C, Dissanayake MG, Tranh NC. 1983. Bacterial die-off kinetics in waste stabilization ponds. *Water Pollut. Control Fed.* **55**:285–296.

Posadas E, Morales MDM, Gomez C, Acién FG, Muñoz R. 2015a. Influence of pH and CO2 source on the performance of microalgae-based secondary domestic wastewater treatment in outdoors pilot raceways. *Chem. Eng. J.* **265**:239–248. http://dx.doi.org/10.1016/j.cej.2014.12.059.

Posadas E, Muñoz A, García-González MC, Muñoz R, García-Encina PA. 2015b. A case study of a pilot high rate algal pond for the treatment of fish farm and domestic wastewaters. *J. Chem. Technol. Biotechnol.* **90**:1094–1101. http://dx.doi.org/10.1002/jctb.4417.

Qualls RG, Flynn MP, Johnson JD. 1983. The role of suspended particles in ultraviolet disinfection. *Water Pollut. Control Fed.* **55**:1280–1285.

Reinoso R, Torres LA, Bécares E. 2008. Efficiency of natural systems for removal of bacteria and pathogenic parasites from wastewater. *Sci. Total Environ.* **395**:80–86. http://dx.doi.org/10.1016/j.scitotenv.2008.02.039.

Ruas G, Serejo ML, Paulo PL, Boncz MÁ. 2017. Evaluation of domestic wastewater treatment using microalgal-bacterial processes: effect of CO2 addition on pathogen removal. *J. Appl. Phycol.* **30**:921–929. http://dx.doi.org/10.1007/s10811-017-1280-6.

Schuler AJ, Jenkins D. 2003. Enhanced biological phosphorus removal from wastewater by biomass with different phosphorus contents , Part I : Experimental results and comparison with metabolic models. *Water Environ. Res.* **75**:485–498.

Schultz-Fademrecht C, Wichern M, Horn H. 2008. The impact of sunlight on inactivation of indicator microorganisms both in river water and benthic biofilms. *Water Res.* **42**:4771–4779. http://dx.doi.org/10.1016/j.watres.2008.08.022.

Sheludchenko M, Padovan A, Katouli M, Stratton H. 2016. Removal of fecal indicators, pathogenic bacteria, adenovirus, *Cryptosporidium* and *Giardia* (oo)cysts in waste stabilization ponds in Northern and Eastern Australia. *Int. J. Environ. Res. Public Health* **13**:96. http://dx.doi.org/10.3390/ijerph13010096.

Shilton AN, Walmsley N. 2005. Introduction to pond treatment technology. In: Shilton, AN, editor. *Pond Treat. Technol.* London, UK: IWA Publishing, London-Seattle, pp. 1–13. http://dx.doi.org/10.1104/pp.104.900191.Plant.

Shilton A, Sweeney D. 2005. Hydraulic design. In: Shilton, A, editor. *Pond Treat. Technol.* London, UK: IWA Publishing, pp. 188–209.

Silverman AI, Nelson KL. 2016. Modeling the endogenous sunlight inactivation rates of laboratory strain and wastewater *E. coli* and enterococci using biological weighting functions. *Environ. Sci. Technol.* **50**:12292–12301. http://dx.doi.org/10.1021/acs.est.6b03721.

Silverman AI, Peterson BM, Boehm AB, McNeill K, Nelson KL. 2013. Sunlight inactivation of human viruses and bacteriophages in coastal waters containing natural photosensitizers. *Environ. Sci. Technol.* **47**:1870–1878. http://dx.doi.org/10.1021/es3036913.

Sinclair RG, Rose JB, Hashsham SA, Gerba CP, Haas CN. 2012. Criteria for selection of surrogates used to study the sate and control of pathogens in the environment. *Appl. Environ. Microbiol.* **78**:1969–1977. http://dx.doi.org/10.1128/AEM.06582-11.

Sinton LW, Hall CH, Lynch PA, Davies-Colley RJ. 2002. Sunlight inactivation of fecal indicator bacteria and bacteriophages from waste stabilization pond effluent in fresh and saline waters. *Appl. Environ. Microbiol.* **68**:1122–1131. http://dx.doi.org/10.1128/AEM.68.3.1122.

Sobsey MD, Cooper RC. 1973. Enteric virus survival in algal-bacterial wastewater treatment systems—I. Laboratory studies. *Water Res.* **7**:669–685. http://dx.doi.org/10.1016/0043-1354(73)90085-7.

Solimeno A, Parker L, Lundquist T, García J. 2017. Integral microalgae-bacteria model (BIO_ALGAE): Application to wastewater high rate algal ponds. *Sci. Total Environ.* **601**–**602**:646–657. http://dx.doi.org/10.1016/j.scitotenv.2017.05.215.

Solimeno A, Samsó R, Uggetti E, Sialve B, Steyer JP, Gabarró A, García J. 2015. New mechanistic model to simulate microalgae growth. *Algal Res.* **12**:350–358. http://dx.doi.org/10.1016/j.algal.2015.09.008.

Von Sperling M. 1999. Performance evaluation and mathematical modelling of coliform die-off in tropical and subtropical waste stabilization ponds. *Water Res.* **33**:1435–1448. http://dx.doi.org/10.1016/S0043-1354(98)00331-5.

Von Sperling M. 2005. Modelling of coliform removal in 186 facultative and maturation ponds around the world. *Water Res.* **39**:5261–5273. http://dx.doi.org/10.1016/j.watres.2005.10.016.

Sukias JPS, Tanner CC, Davies-Colley RJ, Nagels JW, Wolters R. 2001. Algal abundance, organic matter, and physico-chemical characteristics of dairy farm facultative ponds: Implications for treatment performance. *New Zeal. J. Agric. Res.* **44**:279–296. http://dx.doi.org/10.1080/00288233.2001.9513485.

Sutherland DL, Howard-Williams C, Turnbull MH, Broady PA, Craggs RJ. 2014a. Seasonal variation in light utilisation, biomass production and nutrient removal by wastewater microalgae in a full-scale high-rate algal pond. *J. Appl. Phycol.* **26**:1317–1329. http://dx.doi.org/10.1007/s10811-013-0142-0.

Sutherland DL, Turnbull MH, Craggs RJ. 2014b. Increased pond depth improves algal productivity and nutrient removal in wastewater treatment high rate algal ponds. *Water Res.* **53**:271–281. http://dx.doi.org/10.1016/j.watres.2014.01.025.

U.S. Environmental Protection Agency. 1986. Design manual: Municipal wastewater disinfection. Cincinnati 264 p. http://nepis.epa.gov/Exe/ZyPURL.cgi?

U.S. Environmental Protection Agency. 1987. Guide standard and protocol for testing microbiological water purifiers. United States of America: Registration Division, Office of Pesticide Program, Criteria and Standards Division, Office of Drinking Water 34 p.

U.S. Environmental Protection Agency. 2010. UV radiation. *Epa 430-F-10-025*. http://www.epa.gov/sunwise/doc/uvradiation.html.

Wada A, Kono M, Kawauchi S, Takagi Y, Morikawa T, Funakoshi K. 2012. Rapid discrimination of gram-positive and gram-negative bacteria in liquid samples by using NaOH-sodium dodecyl sulfate solution and flow cytometry. *PLoS One* **7**:e47093. http://dx.doi.org/10.1371/journal.pone.0047093.

World Health Organization. 2011. Guidelines for drinking-water quality - 4th Ed. Geneva 564 p. http://dx.doi.org/10.1016/S1462-0758(00)00006-6.

Xu P, Brissaud F, Fazio A. 2002. Non-steady-state modelling of faecal coliform removal in deep tertiary lagoons. *Water Res.* **36**:3074–3082. http://dx.doi.org/10.1016/S0043-1354(01)00534-6.

Young P, Taylor M, Fallowfield HJ. 2017. Mini-review: high rate algal ponds, flexible systems for sustainable wastewater treatment. *World J. Microbiol. Biotechnol.* **33**:117. http://dx.doi.org/10.1007/s11274-017-2282-x.

Young P, Buchanan N, Fallowfield H. 2016. Inactivation of indicator organisms in wastewater treated by a high rate algal pond system. *J. Appl. Microbiol.* **121**:577–586. http://dx.doi.org/10.1111/jam.13180.

Young TC, King DL. 1980. Interacting limits to algal growth: light, phosphorous, and carbon dioxide availability. *Water Res.* **14**:409–412.

Zhang S, Ye C, Lin H, Lv L, Yu X. 2015. UV disinfection induces a vbnc state in *Escherichia coli* and *Pseudomonas aeruginosa*. *Environ. Sci. Technol.* **49**:1721–1728. http://dx.doi.org/10.1021/acs.est.5b01681.